

**The impact of mouse placental endocrine
function on fetal resource allocation and adult
offspring health**

Efthimia Rafaelia Christoforou

This thesis is submitted for the degree of

Doctor of Philosophy



**UNIVERSITY OF
CAMBRIDGE**

Department of Physiology, Development and Neuroscience

Peterhouse

March 2021

Declaration

This thesis is the result of my own work and includes nothing which is the outcome of work done in collaboration except as declared in the Preface and specified in the text. I further state that no substantial part of my thesis has already been submitted, or is being concurrently submitted for any such degree, diploma or other qualification at the University of Cambridge or any other University or similar institution except as declared in the Preface and specified in the text. It does not exceed the prescribed word limit for the Faculty of Biology Degree Committee.

Efthimia Rafaelia Christoforou

30th March 2021

The impact of mouse placental endocrine function on fetal resource allocation and adult offspring health

Efthimia Rafaelia Christoforou

Abstract

During pregnancy, optimum maternal and fetal outcomes are determined by adequate nutrient partitioning between the mother and fetus. In turn, the placenta plays a critical role in nutrient partitioning during pregnancy, as it is responsible for secreting hormones that induce maternal insulin resistance and transports the nutrients available to support fetal growth and metabolic demand. Disturbances in placental endocrine function may lead to pregnancy complications such as gestational diabetes mellitus (GDM) and intrauterine growth restriction (IUGR) with immediate negative impacts on fetal outcomes. Moreover, as postulated by the Developmental Origins of Health and Disease (DOHaD) hypothesis, abnormalities in fetal nutrient supply and growth can programme the offspring to develop altered metabolic health in later life. Despite this, little is known about the role of the endocrine placenta in fetal nutrient supply, growth and the programming of adult metabolism. To study this, we conditionally disrupted the imprinting of the *H19-Igf2* locus in the mouse placental endocrine zone (junctional zone, Jz; maternally inherited Jz-ICR1 Δ). This is because this locus is important in controlling the formation and function of placental endocrine cells. Thus, the aims of this study were 1) to assess the impact of Jz-ICR1 Δ on placental morphology and materno-fetal nutrient supply and fetus growth 2) to evaluate how Jz-ICR1 Δ impacts offspring metabolic health, both with a chow and an obesogenic postnatal diet 3) to determine the effect of Jz-ICR1 Δ on the fetal hepatic transcriptome and evaluate whether these perturbations persist in the adult liver and relate to offspring metabolic phenotype. Fetal nutrient supply was determined *in vivo* and *in vitro* via placental substrate transport assays and quantifying nutrient transporter expression by qPCR respectively, whilst placental morphology was evaluated using histology and stereology techniques. Offspring metabolic health was evaluated via insulin and glucose tolerance tests, by examining pancreas morphology and insulin content, and by determining the abundance of proteins involved in

gluconeogenesis, insulin signalling and lipid metabolism in the liver, skeletal muscle and white adipose tissue using Western blotting. RNA sequencing and bioinformatic analysis was used to assess changes in gene expression/functional pathways in fetal livers and select differentially expressed genes were quantified in adult offspring liver using qPCR.

The Jz-ICR1 Δ mutation increased Jz volume at embryonic day (E) 16 (term ~E20), alongside an increase in Jz insulin-like growth factor 2 (*Igf2*) expression. Moreover, in response to Jz-ICR1 Δ fetal growth was unaltered at E16 but reduced at E19. This was associated with a reduction in placental glucose transport to the fetus and a decrease in the surface area of the placenta for exchange on E16. Postnatally, Jz-ICR1 Δ offspring displayed alterations in growth, adiposity, glucose and insulin handling and pancreatic function and morphology. This was also accompanied by changes in the abundance of proteins involved in gluconeogenesis, insulin signalling and lipid metabolism in offspring liver, skeletal muscle and white adipose tissue. However, these alterations were largely dependent on offspring sex and the postnatal diet consumed, with male offspring showing detrimental metabolic changes which were largely not present in females. In part, sex-dependent programmed changes in adult offspring metabolic phenotype appeared to be linked to sex-specific alterations in the fetal hepatic transcriptome on E19 in response to Jz-ICR1 Δ , with a portion of genes displaying altered expression in the female fetus (*G6pc*, *Rgs16*) also tending to be altered in adult livers.

Overall, this study highlights the importance of the endocrine placenta in determining fetal nutrient supply and growth. Furthermore, defects in placental endocrine capacity programme changes in adult metabolic health in a sex-dependent manner that appear to link to alterations in the fetal hepatic transcriptome. By improving our understanding of how the endocrine placenta leads to adverse fetal outcomes and the programming of offspring health, in future we may consequently lessen the burden of metabolic disease associated with gestational origins.

Acknowledgements

First and foremost, I would like to thank my supervisors. I am infinitely grateful to my primary supervisor, Dr Amanda Sferruzzi-Perri, for giving me the opportunity to work on this project. Amanda's constant support, encouragement and patience throughout have been most invaluable, and I am privileged to have been a part of the Sferruzzi-Perri lab. I would also like to express my sincere gratitude to my secondary supervisor, Dr Alison Forhead for her support and advice throughout my studies and for editing this thesis. I also thank Dr Miguel Constancia and Dr Ionel Sandovici for their seminal work in this mouse model. I am further grateful to my PhD advisor Professor Dino Giussani, for his constructive comments throughout our meetings.

Furthermore, I am indebted to the Cambridge Trust and the Rutherford Foundation for the award of a Cambridge-Rutherford Memorial PhD Scholarship, during the tenure of which this work was carried out.

Throughout my studies I have been fortunate to learn from and work alongside several talented scientists. Dr Jorge Lopez-Tello played an integral role in helping with animal work and teaching me various techniques needed for this project. For that, and day to day help in the laboratory I will always be extremely thankful. I would also like to express my sincere gratitude to Dr Hannah Yong who also taught me so much in the lab and for her friendly and positive disposition. I am thankful to Dr Tina Napso, for her help and encouragement. Furthermore, I am very thankful to Panayiotis Laouris for his meticulous stereology work in this project, and his support and friendship throughout. I would like to thank Dr Russell Hamilton and Marta Ibanez Lligona for assistance in RNA sequencing data analysis and Erica Ferrarri Trecate for help during animal dissections. Furthermore, I would like to thank Dr Marcella Ma for her patience in guiding me through the library preparation protocol. Thank you also to Edina Gulacsi, for assistance in sectioning samples, and for doing such a great job at keeping the lab running smoothly. I am also grateful to all of the staff at the animal facility for looking after the animals used in this project so well.

I would like to thank all the members of the department of Physiology, Development and Neuroscience (PDN) and the Centre for Trophoblast Research (CTR). In particular, I

would like to thank all the past and current members of the Sferruzzi-Perri lab for making my PhD studies such a memorable experience.

It was my privilege to have been a part of the Peterhouse MCR community during my studies, and I would like to thank all my friends that I met along the way for their encouragement. Thank you to my family in Greece, my aunts, uncles and cousins for their constant support. Finally, I wish to express my gratitude to my parents, Maria and Demetrius, for their encouragement from the other side of the world.

Abbreviations

^3H – radioactive isotope of hydrogen (tritium)

^{14}C – radioactive isotope of carbon

AAC – area above the curve

AUC – area under the curve

ANOVA – analysis of variance

BAT – brown adipose tissue

BCA – bicinchoninic acid

BSA – bovine serum albumin

BWS – Beckwith Wiedemann syndrome

C57Bl/6 – C57 black 6; an inbred strain of laboratory mouse

cDNA – complementary DNA

db – decidua basalis

DEGs – differentially expressed genes

DOHaD – Developmental Origins of Health and Disease

DMR – differentially methylated region

DPX – dibutyl phthalate polystyrene xylene

E – embryonic day

ECL – enhanced chemiluminescence

ELISA – enzyme-linked immunosorbent assay

FABP – fatty acid binding protein

FAS – fatty acid synthase

FAT – fatty acid translocase

FATP – fatty acid transport protein

FC – fetal capillaries

FFA – free fatty acid

G6Pase – glucose-6 phosphatase

GDM – gestational diabetes mellitus

GLUT – glucose transporter

GlyT – glycogen trophoblast cell

GSK3 – glycogen synthase kinase 3

GTT – glucose tolerance test
H&E – haematoxylin and eosin
ICR – imprinting control region
IGF – insulin-like growth factor
IGF1R – insulin-like growth factor 1 receptor
InsR – insulin receptor
ITT – insulin tolerance test
IUGR – intrauterine growth restriction
Jz – junctional zone
Lz – labyrinth zone
LPL – lipoprotein lipase
MAPK – mitogen activated protein kinase
MBS – maternal blood space
mTOR – mammalian target of rapamycin
NEFA – non-esterified fatty acid
O/N – overnight
p – phosphorylated
p110 – catalytic subunit of PI3K
p85 – regulatory subunit of PI3K
PBS – phosphate buffered saline
PCR – polymerase chain reaction
PEPCK – phosphoenolpyruvate carboxykinase
PI3K – phosphoinositide 3-kinase
PPAR – peroxisome proliferator-activated receptor
PTA – placental transport assay
RM – repeated measure
RT – room temperature
RT-qPCR – real-time quantitative polymerase chain reaction
S6K – ribosomal S6 kinase
SDS – sodium dodecyl sulphate
SDS-PAGE – SDS-polyacrylamide gel electrophoresis
SEM – standard error of the mean
SpT – spongiotrophoblast cell
SRS – Silver-Russell syndrome

S-TGC – sinusoidal trophoblast giant cell
SynT-I – syncytiotrophoblast cell layer I
SynT-II – syncytiotrophoblast cell layer II
SynT-III – syncytiotrophoblast cell layer III
TBST – tris-Buffered Saline and Tween 20
TG – triglyceride
Tpbpa – trophoblast-specific protein alpha
WAT – white adipose tissue

List of units:

Bq	becquerel
DPM	decay per minute
g	gram
hr	hour
L	litre
m	metre
min	minute
s	second

Abstract.....	i
Acknowledgements	iii
Abbreviations	v
Chapter 1: Introduction	1
1.1 Placental structure.....	1
1.1.1 The human and rodent placenta.....	1
1.1.2 Murine placental development.....	2
1.1.3 Murine placental structure	3
1.2 <i>H19</i> and Insulin-like growth factor 2 (<i>Igf2</i>).....	5
1.2.1 Imprinted genes and feto-placental growth	5
1.2.2 <i>H19</i> and <i>Igf2</i> imprinting mechanisms.....	6
1.2.3 Fetoplacental <i>H19</i> and <i>Igf2</i> expression.....	7
1.2.4 <i>H19</i> and <i>Igf2</i> in fetoplacental growth and resource allocation	8
1.3 Placental endocrine function.....	11
1.3.1 Placental steroidogenesis	12
1.3.2 Placental corticosterone metabolism	14
1.3.3 Placental endocrine function and maternal physiology	14
1.3.4 The effect of placental endocrine function on pregnancy outcomes	16
1.4 Nutrient transport across the placenta.....	17
1.4.1 Amino acid transport	19
1.4.2 Glucose transport	19
1.4.3 Fatty acid transport	20
1.4.4 Alterations in nutrient transport in response to pregnancy complications..	21
1.5 The Developmental Origins of Health and Disease.....	22
1.5.1 Mouse models in developmental programming.....	23
1.5.2 Metabolic outcomes in mouse models of maternal hyperglycaemia	24
1.5.3 Pancreatic morphology and insulin production in type 2 diabetes and mouse models of a high-nutrient environment <i>in utero</i>	31
1.6 Insulin signalling pathway	32
1.6.1 Insulin receptor (InsR) and insulin-like growth factor 1 receptor (IGF1R).....	33
1.6.2 Insulin receptor substrate (IRS1/2).....	33
1.6.3 Phosphatidylinositol 3-kinase (PI3K).....	34
1.6.4 AKT and glycogen synthesis	34
1.6.5 AKT and protein synthesis	35
1.7 Lipid metabolism	36
1.8 Hepatic gluconeogenesis and lipid synthesis.....	37
1.9 Insulin resistance.....	38
1.10 Molecular alterations in mouse models of developmental programming...38	
1.11 Sexual dimorphism in developmental programming.....	39
1.11.1 Sexual dimorphism in adulthood in developmental programming.....	40
1.11.2 Sexual dimorphism in prenatal mechanisms of developmental programming.....	40

1.12	Epigenetic mechanisms in developmental programming	41
1.13	Overall Objectives and Aims	42
1.13.1	Background	42
1.13.2	Study Aims	44
Chapter 2: General materials and methods		45
2.1	Animals	45
2.2	Experimental procedures I: The effect of Jz-ICR1 Δ on placental morphology and nutrient transport capacity	46
2.2.1	Breeding study design	46
2.2.2	Placental transport assay	48
2.2.3	SRX sexing	50
2.2.4	Placental histological preparation	50
2.2.5	Placental immunohistochemistry	51
2.2.6	Placental stereological analysis	52
2.2.6.1	Placental compartment volumes	52
2.2.6.2	Junctional zone morphology	52
2.2.6.3	Labyrinth zone morphology	53
2.2.7	Glycogen assay	55
2.2.8	mRNA quantification	56
2.2.8.1	RNA extraction	56
2.2.8.2	Reverse transcription	57
2.2.8.3	Quantitative polymerase chain reaction (qPCR)	57
2.3	Experimental procedures II: The effect of Jz-ICR1 Δ on adult offspring metabolic health outcomes	61
2.3.1	Study design	61
2.3.2	Diet optimisation	62
2.3.3	Glucose and insulin tolerance tests	63
2.3.4	Biometry	64
2.3.5	Biochemical composition	64
2.3.5.1	Fat content assay	64
2.3.5.2	Protein assay	64
2.3.5.3	Hormone and metabolite assays	65
2.3.5.4	Pancreatic insulin assay	66
2.3.6	Tissue morphology	67
2.3.6.1	Pancreatic islet immunohistochemistry and area analysis	67
2.3.6.2	Adipocyte stereology	68
2.3.7	Western blotting	68
2.3.7.1	Protein extraction	68
2.3.7.2	SDS PAGE gel preparation and electrophoresis	69
2.3.7.3	SDS PAGE gel transfer	69
2.3.7.4	Antibody detection	70
2.3.7.5	Antibody stripping	72
2.3.7.6	Western blot analysis	72
2.4	Experimental procedures III: The effect of Jz-ICR1 Δ on the hepatic transcriptome in male and female fetuses	73
2.4.1	RNA sequencing	73
2.4.1.1	Sample preparation	73

2.4.1.2	RNA quality control.....	73
2.4.1.3	Illumina TruSeq Stranded mRNA library preparation.....	74
2.4.1.4	Validation of library quality and library normalisation	76
2.4.1.5	Sequencing	77
2.4.1.6	Data processing	77
2.4.1.7	RNA sequencing validation	77
2.4.1.8	Data analysis	79
2.5	Statistical analysis.....	79
Chapter 3: The effect of Jz-ICR1Δ on placental morphology and nutrient transport capacity		81
3.1	Introduction.....	81
3.2	Materials and methods	83
3.3	Results.....	86
3.3.1	Litter size and resorptions.....	86
3.3.2	Fetal and placental weights.....	86
3.3.3	<i>Igf2</i> and <i>H19</i> expression	89
3.3.4	<i>Igf2</i> receptor expression.....	90
3.3.5	Placental zone volume and glycogen content	91
3.3.6	Junctional zone cell volume and marker expression	93
3.3.7	Junctional zone steroidogenic gene expression	95
3.3.8	Labyrinth zone morphology.....	96
3.3.9	Placental MeG and MeAIB clearance	99
3.3.10	Nutrient transporter expression in the labyrinth zone.....	101
3.3.11	Corticosterone handling in the labyrinth zone.....	102
3.4	Discussion.....	103
3.4.1	The effect of <i>Igf2</i> and <i>H19</i> expression on Jz-ICR1Δ placental morphology..	104
3.4.2	Placental endocrine capacity in response to Jz-ICR1Δ.....	107
3.4.3	Placental Lz morphology and nutrient transport capacity in response to Jz-ICR1Δ	108
3.4.4	Maternal physiology and Jz-ICR1Δ placental morphology and nutrient transport capacity	111
3.4.5	Placental corticosterone handling in response to Jz-ICR1Δ	113
Chapter 4: The effect of Jz-ICR1Δ on adult offspring metabolic health outcomes.		117
4.1	Introduction.....	117
4.2	Materials and methods	120
4.3	Results.....	123
4.3.1	Gestation and delivery	123
4.3.2	Postnatal day 3 biometry.....	124
4.3.3	Offspring growth trajectory	126
4.3.4	Offspring biometry	128
4.3.5	Offspring adiposity	130
4.3.6	Offspring glucose and insulin handling <i>in vivo</i>	132
4.3.7	Offspring pancreas biometry and morphology	135
4.3.8	Offspring tissue biochemical composition	137
4.3.9	Offspring plasma hormone and metabolite concentrations	139

4.3.10	Hepatic gluconeogenesis	142
4.3.11	Insulin signalling	143
4.3.11.1	Liver insulin signalling	143
4.3.11.2	Skeletal muscle insulin signalling.....	146
4.3.11.3	White adipose tissue insulin signalling.....	149
4.3.12	Lipid metabolism	152
4.3.12.1	Liver lipid metabolism.....	152
4.3.12.2	Skeletal muscle lipid metabolism	153
4.3.12.3	White adipose tissue lipid metabolism	154
4.4	Discussion.....	157
4.4.1	Adult offspring adiposity and adipose morphology in response to Jz-ICR1Δ	160
4.4.2	Adult offspring insulin production and pancreas morphology in response to Jz-ICR1Δ	161
4.4.3	Adult offspring insulin and glucose handling in response to Jz-ICR1Δ.....	163
4.4.4	Adult offspring hepatic biochemical composition and gluconeogenesis in response to Jz-ICR1Δ	166
4.4.5	Adult offspring biometry in response to Jz-ICR1Δ	167
3.4.6	Limitations in study design and mechanisms of offspring programming	168
Chapter 5: The effect of Jz-ICR1Δ on the hepatic transcriptome in male and female fetuses.....		171
5.1	Introduction.....	171
5.2	Materials and methods.....	174
5.3	Results.....	177
5.3.1	Biometry of E19 fetuses	177
5.3.2	Differentially expressed genes (DEGs) in response to Jz-ICR1Δ and fetal sex	178
5.3.3	Differentially expressed gene (DEG) analysis in male and fetal fetuses in response to Jz-ICR1Δ	179
5.3.4	DEG knockout phenotypes	184
5.3.5	The expression of fetal DEGs in adult Jz-ICR1Δ livers.....	192
5.4	Discussion.....	193
5.4.1	Sex differences in DEGs in response to Jz-ICR1Δ.....	195
5.4.2	Common DEGs in males and females in response to Jz-ICR1Δ	198
5.4.3	Association of fetal DEGs in response to Jz-ICR1Δ with adult offspring phenotypes	199
Chapter 6: General discussion.....		201
6.1	The maternal environment in offspring programming	202
6.2	The gestational period in offspring programming	203
6.3	The post-gestational period in offspring programming	206
6.4	Limitations and future directions.....	207
6.5	Concluding remarks.....	210
Appendices.....		212
Appendix 1: Supplementary data.....		212

A1.1:	Offspring diet optimisation.....	212
A1.2.	The effect of gestational age on placental parameters.....	214
A1.2.1.	Jz <i>Igf2</i> expression over time.....	214
A1.2.2.	Glycogen cell volume over time.....	215
A1.2.3.	Glycogen content over time.....	216
A1.3:	Western blot images.....	217
A1.3.1.	Liver western blot images.....	217
A1.3.2.	Skeletal muscle western blot images.....	221
A1.3.3.	Adipose western blot images.....	225
A1.4:	Supplementary RNA sequencing data.....	229
A1.4.1.	Enrichment analyses.....	229
A1.4.2.	The effect of sex on fetal liver DEGs.....	230
Appendix 2:	Reagents.....	233
A2.1.	Reagents.....	233
Appendix 3:	Stock solutions and reagents.....	235
A3.1.	Solutions and primers for SRY sexing.....	235
A3.2.	Solutions for Immunohistochemistry and insulin content assay.....	236
A3.3.	Solutions for Western blots.....	237
Bibliography	240

Chapter 1: Introduction

The placenta is a transient organ present during gestation which is the interface between the mother and fetus. Its roles include immunological functions, secretion of hormones, and nutrient and waste transport (Burton and Fowden, 2015). Of these, its nutrient transport function has been comparatively most studied in relation to fetal growth outcomes (Fowden et al., 2006, Dimasuay et al., 2016). Nutrient distribution can be altered either via changes in placental function and morphology or through influences on maternal metabolism which alter the capacity of placental nutrient transport (Fowden and Moore, 2012). Moreover, the placenta secretes a milieu of hormones, which exert local effects within the uterus promoting blood flow and also adapt maternal physiology by systemic actions to support pregnancy (Burton and Fowden, 2015, Napso et al., 2018, Sferruzzi-Perri et al., 2020). Thus, alterations in placental nutrient transport via changes in maternal metabolism are ultimately a consequence of placental endocrine capacity. Moreover, alterations in fetal nutrient acquisition are known to programme adult offspring to develop metabolic dysfunction later in life, with the placenta playing a critical role in this fetal nutrient allocation (Wu et al., 2004). Fetal programming also occurs alongside changes in fetal growth governed by hormones such as insulin-like growth factors (IGF) and glucocorticoids, which the placenta also plays an important role in regulating (Fowden and Forhead, 2004). Thus, by mediating maternal insults imposed on the fetus, the placenta itself is a major contributor to the programming of offspring metabolic disease (Burton et al., 2016, Sferruzzi-Perri and Camm, 2016, Myatt and Thornburg, 2018).

1.1 Placental structure

1.1.1 The human and rodent placenta

Both primate and rodent placentas are haemochorial, whereby erosion of the endometrium allows maternal blood to directly bathe the trophoblast surface (Rossant and Cross, 2001). The placentas of both species are also chorioallantoic, with allantoic vessels connecting the chorionic membrane to the fetal circulation (Leiser and Kaufmann, 1994). In the human placenta, both endocrine and transport functions are performed by the syncytiotrophoblast (Georgiades et al., 2002). However, the mouse differs in this manner, with its placenta comprised of discernible zones: the endocrine junctional zone

(Jz) and the transport labyrinth zone (Lz; Figure 1.1; Muntener and Hsu, 1977). This makes the mouse placenta an excellent model in the study of placental endocrine and transport functions.

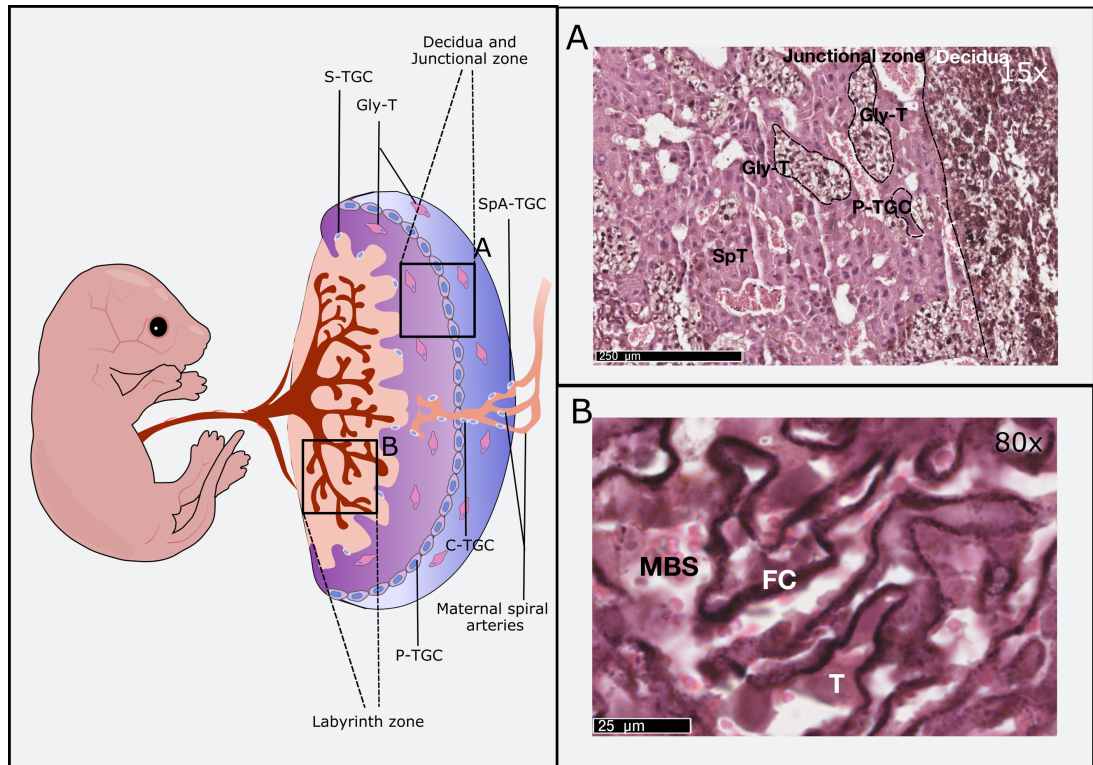


Figure 1.1. A schematic diagram of the mouse fetus connected to the placenta and representative photomicrographs of the mature placenta stained with lectin and cytokeratin to show the junctional zone and decidua (A) and labyrinth zone (B). Images/photos represent embryonic day 16 (term is day 20). C-TGC, canal-associated trophoblast giant cell; FC, fetal capillaries; Gly-T, glycogen trophoblast cell; MBS, maternal blood space, SpA-TGC, spiral artery-associated trophoblast giant cell; SpT, spongiotrophoblast; S-TGC, sinusoidal trophoblast giant cell; P-TGC, parietal trophoblast giant cell; T, trophoblast. Scale bars 250 μ m (A) and 25 μ m (B).

1.1.2 Murine placental development

Murine placental development commences at embryonic day (E) 3.5 with formation of a separate trophoblast layer and inner cell mass (Watson and Cross, 2005). At E4.5, when implantation occurs, trophoblast cells proliferate giving rise to the extra-embryonic ectoderm and the ectoplacental cone. The extraembryonic ectoderm develops into the trophoblast cells of the placental chorion and subsequently into the labyrinth zone (Rossant and Cross, 2001, Watson and Cross, 2005). The ectoplacental cone differentiates into five distinct populations of trophoblast cell types, namely the spongiotrophoblast cells (SpT), glycogen trophoblast cells (GlyT), secondary parietal trophoblast giant cells

(P-TGC), spiral artery-associated trophoblast giant cells (SpA-TGC) and canal-associated trophoblast giant cells (C-TGC; Simmons et al., 2007). *Tpbpa* is a trophoblast-specific gene with its expression observed first in the ectoplacental cone cells beginning at E7.5 (Hasan et al., 2015). Thus, trophoblast subtypes such as glycogen trophoblast cells and giant cells arise from *Tpbpa*-positive progenitor cells, with *Tpbpa* expression observed in the spongiotrophoblast layer (Carney et al., 1993, Adamson et al., 2002, Simmons et al., 2007). However, several giant cell subtypes arise from *Tpbpa*-negative progenitor cells (Simmons et al., 2007). For instance, whilst all Spa-TGCs arise from *Tpbpa*⁺ precursors, none of the sinusoidal trophoblast giant cells (S-TGC) in the labyrinth layer arise from *Tpbpa*⁺ precursors (Simmons et al., 2007). Moreover, approximately half of P-TGCs and C-TGCs originate from *Tpbpa*⁺ precursors, whilst both SpT and GlyT arise from *Tpbpa*⁺ progenitors (Simmons and Cross, 2005, Simmons et al., 2007, Simmons et al., 2008). The *Tpbpa*-positive cell lineage plays a crucial role in placental function, since ablation of these precursors leads to defects in maternal spiral artery remodelling, and conceptus death at approximately E11.5 (Hu and Cross, 2011).

1.1.3 Murine placental structure

The definitive murine placenta forms between E10.5 and E12.5 when maternal blood spaces (MBS) and fetal capillaries (FC) in the Lz can be observed, respectively (Figure 1.1B). (Müntener and Hsu, 1977). The mouse placenta is connected to the decidua basalis (Db), which is formed by decidualisation of endometrial stroma and is regulated by oestrogen and progesterone (Ramathal et al., 2010). The Db is comprised of invading trophoblast cells, spiral arteries, immune cells and stromal cells. It produces cytokines and growth factors at the materno-fetal interface, regulates trophoblast invasion, supports maternal blood vessel formation and also has an immunoregulatory role (Stewart and Peel, 1978, Guzeloglu-Kayisli et al., 2009, Vacca et al., 2019).

In the mature mouse placenta, the Jz is comprised of three main cell populations: spongiotrophoblast cells, glycogen cells and giant cells (Figure 1.1A).

Spongiotrophoblast cells are present between the outer secondary trophoblast giant cells and the labyrinth zone (Simmons and Cross, 2005). The Jz is largely comprised of spongiotrophoblast cells and their volume doubles between E12.5 and E16.5 (Coan et al., 2006). The function of spongiotrophoblast cells is predominantly to maintain the

structural integrity of the Jz and to secrete hormones that ensure maternal support of fetal growth during pregnancy (Rossant and Cross, 2001).

There are four subtypes of trophoblast giant cells, with classification dependent on localisation within the placenta and patterns of gene expression. Despite different gene expression between subtypes, the formation of all giant cells is regulated by *Hand1* (Simmons et al., 2007). Parietal giant cells are found between the Jz and Db, whilst spiral artery giant cells are located in the Db, and likely regulate maternal angiogenesis via the production of proliferin and vascular endothelial growth factor (VEGF; Adamson et al., 2002, Simmons et al., 2007). Canal and sinusoidal giant cells are also found lining the maternal blood supply entering the labyrinth and lining maternal sinusoids in the labyrinth, respectively. The importance of giant cells in placental vascular development has been demonstrated in mice with knockdown of the giant cell-specific transcription factor *Gata2*, which show a reduction in neo-vascularisation of the decidua *in vivo* and overall reduced angiogenic activity *in vitro* (Ma et al., 1997). Moreover, giant cells and spongiotrophoblasts are also important in modulating maternal metabolism, secreting hormones such as progesterone, prolactin-like hormones and placental lactogens that are known to induce insulin resistance in the mother (Soares et al., 1996).

Glycogen cells are formed at E7.5, originating from the central portion of the ectoplacental cone and begin to accumulate glycogen from E12.5 (Bouillot et al., 2006, Coan et al., 2006). An 80-fold increase in glycogen cell number is observed from E12.5 to E16.5, followed by a reduction by E18.5, as the glycogen cells accumulate in the Db and then undergo lysis to form large glycogen filled lacunae (Coan et al., 2006). The presence of glycogen may act as a store of energy for the placenta and a rapidly mobilisable source of energy during the latter stages of gestation and parturition (Bouillot et al., 2006, Coan et al., 2006, Tunster et al., 2020). Indeed, a reduction in glycogen cell number is accompanied by a concomitant reduction in placental glycogen content from E15 to E18 (Lopez et al., 1996).

The LZ is commonly described as the transport zone, providing the main site for haemotrophic exchange. The syncytiotrophoblast surrounds the endothelium of fetal capillaries and provides a surface for materno-fetal nutrient transfer (Watson and Cross, 2005, Lager and Powell, 2012). The mouse placenta is haemotrichorial, consisting of three trophoblast layers, assigned SynT-I, SynT-II and SynT-III. Comparatively, the

human placenta is haemomonochorial, consisting of one trophoblast layer (King and Hastings, 1977). In humans, the syncytiotrophoblast is comprised of two polarised plasma membranes, the microvillous plasma membrane (MVM) and basal plasma membrane (BM; (Lager and Powell, 2012). FC and MBS allow the independent circulation of maternal and fetal blood. In mice, a fenestrated S-TGC layer lines the maternal blood sinusoid, allowing access of the maternal blood to the SynT-I layer, whilst the SynT-II layer is adjacent to the fetal vascular endothelium (Georgiades et al., 2002, Coan et al., 2006). Moreover, unlike the villous-type structure of the human placenta, the placenta of the mouse is labyrinthine (Georgiades et al., 2002). However, the human chorionic villi and mouse labyrinth are considered to be homologous (Leiser and Kaufmann, 1994, Rinkenberger and Werb, 2000). The labyrinthine structure in the mouse placenta has extensive branching and allows the flow of maternal and fetal blood in a counter current manner (Adamson et al., 2002). During placental development, the growth of the placenta is determined by several factors, namely hormones and metabolites derived from the mother, placenta and fetus, as well as the placenta's own genetic drive for growth.

1.2 *H19* and Insulin-like growth factor 2 (*Igf2*)

1.2.1 Imprinted genes and feto-placental growth

Placental and fetal growth are in part governed by imprinted genes (Coan et al., 2005). Genomic imprinting refers to epigenetic modifications, including the methylation of cytosines in imprinting control regions (ICR), resulting in monoallelic parent-of-origin expression (Fowden et al., 2011). In the placenta, paternally expressed insulin-like growth factor 2 (*Igf2*), mesoderm-specific transcript (*Peg1*) and paternally expressed 3 (*Peg3*) genes induce feto-placental growth whilst maternally expressed *H19*, insulin-like growth factor 2 receptor (*Igf2r*), pleckstrin homology-like domain family A member 2 (*Phlda2*), growth factor receptor-bound protein 10 (*Grb10*) and cyclin dependent kinase inhibitor 1c (*Cdkn1c*) genes reduce feto-placental growth (Reik et al., 2003, Coan et al., 2005). The kinship theory hypothesises that paternally expressed imprinted genes in the placenta maximise maternal resources for offspring growth, whilst maternally expressed imprinted genes in the placenta act to limit fetal nutrient provision allowing equal distribution of maternal resources to all offspring, and ensuring maternal survival (Moore, 2001). Moreover, restricting placental growth and nutrient transport function offers an indirect way of limiting fetal growth and use of maternal resources. According to the kinship

theory, therefore, it is perhaps not surprising that most of the identified imprinted genes in the mouse are expressed in the placenta (Reik and Walter, 2001). Of the aforementioned paternally expressed imprinted genes, *Igf2* was one of the first discovered (Salmon and Daughaday, 1957, DeChiara et al., 1991). Conversely, *H19* is a maternally expressed long non-coding RNA, flanking *Igf2* on the 3' side (Bartolomei et al., 1991, DeChiara et al., 1991).

1.2.2 *H19* and *Igf2* imprinting mechanisms

H19 transcription from the paternal allele is suppressed as a result of DNA methylation of a 7- to 9-kb domain that surrounds *H19* and its promoter, the ICR. The ICR and *H19* itself maintain the monoallelic expression of *Igf2* (Figure 1.2). For instance, targeted deletion of the ICR or *H19* on the maternal allele disrupts *Igf2* imprinting leading to expression of the normally silent copy of *Igf2*. Conversely, a paternally inherited deletion of the ICR activates *H19* and leads to loss of *Igf2* expression (Bartolomei et al., 1993, Leighton et al., 1995, Thorvaldsen et al., 1998). On the maternal chromosome, CCCTC-binding factor (CTCF) binds within the unmethylated *H19* ICR, regulating the interaction of the ICR with matrix attachment region 3 (MAR3) and differentially methylated region 1 (DMR1) at *Igf2*. This may contribute to *Igf2* silencing on the maternal chromosome due to the formation of a tight loop around the maternal *Igf2* locus. Conversely on the paternal allele, enhancers can interact with *Igf2* promoters, so that *Igf2* is expressed (Kurukuti et al., 2006). The imprinting mechanism of *Igf2* and *H19* is shown in Figure 1.2 (Bartolomei et al., 1993, Thorvaldsen et al., 1998). In addition to being critical in maintaining the genomic imprinting of *Igf2*, *H19* is also a microRNA (miRNA) precursor (Cai and Cullen, 2007). *miR-675* is derived from *H19* and one of its targets is the gene encoding the insulin-like growth factor 1 receptor (*Igf1r*), whose expression is increased upon *H19* deletion (Keniry et al., 2012).

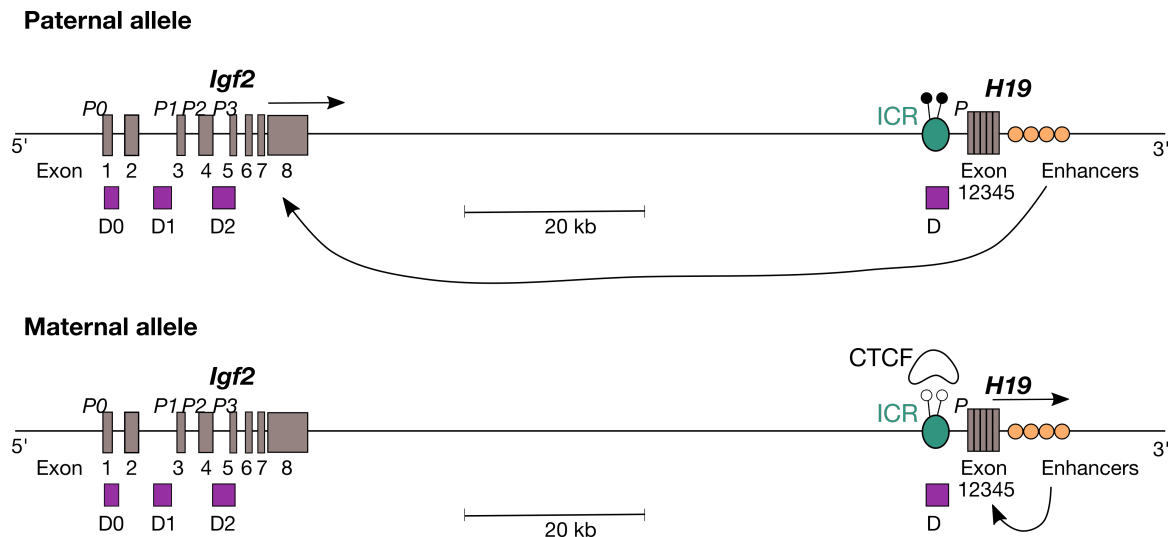


Figure 1.2. Imprinting mechanism in *Igf2* and *H19* expression. Arrows represent gene expression on the maternal (bottom) or paternal (top) alleles. Shaded and unshaded lollipops represent methylated and unmethylated regions, respectively. The unmethylated imprinting control region (ICR) on the maternal allele is able to bind CCCTC-binding factor (CTCF) so that enhancers interact with *H19* to induce expression. On the paternal allele, the methylated ICR prevents CTCF binding so that *H19* is not expressed. Purple rectangles represent differentially methylated regions; *Igf2DMR0* (D0), *Igf2DMR1* (D1), *Igf2DMR2* (D2) and *H19DMR* (D). The *H19DMR* is coincident with the ICR. Shared enhancers for *H19* and *Igf2* expression are located downstream of *H19*. Exons are shown as grey rectangles. P, promoter.

1.2.3 Fetoplacental *H19* and *Igf2* expression

In the mouse, *Igf2* expression is first detected at E5.5 in the extraembryonic ectoderm and ectoplacental cone and thereafter, in subsequent stages of placental development. At E9.5, *Igf2* is expressed in the undifferentiated cells morphologically resembling the subsequently formed spongiotrophoblast layer, and in the yolk sac placenta (Redline et al., 1993, Cindrova-Davies et al., 2017). Once distinct junctional and labyrinth zones form in the mouse placenta, 10% of *Igf2* expression is driven by the extra-embryonic-specific promoter (P0) present exclusively in the labyrinth zone, whilst the remaining *Igf2* transcripts derive from fetal promoters (P1, P2, P3) in the junctional zone, decidua and fetal endothelial cells (Redline et al., 1993, Constância et al., 2000). Utilising in situ hybridisation or RNA scope would enable the detection of different *Igf2* transcripts and identify subcellular expression by the placenta. *Igf2* expression occurs via fetal promoters in the Jz. In the Jz, between E12.5 and E15.5 of pregnancy, glycogen cells are the cell type with the greatest expression of *Igf2*, with spongiotrophoblast cells having the strongest expression earlier in gestation (Redline et al., 1993). Expression of *Igf2* in the embryo proper begins at the primitive streak/neural plate stage (Lee et al., 1990). In the

placenta, the effects of IGF2 are elicited via its receptors IGF1R, IGF2R and insulin receptor (InsR) and the downstream phosphatidylinositol 3-kinase (PI3K) signalling pathway (will be described in section 1.6). IGF1R is also expressed in the extraembryonic ectoderm, ectoplacental cone and developing embryo from E5.5 (Pringle and Roberts, 2007) and IGF2R and InsR are expressed from the two cell stage and eight cell stage, respectively (Rappolee et al., 1992). Overall, IGF2 and its receptors are expressed from an early stage of fetal and placental development, as well as throughout pregnancy (Sferruzzi-Perri, 2018b). Moreover, IGF2 signalling in the placenta may act through a distinct tissue-specific receptor, as interaction of IGF2 with an unknown receptor in the placenta has been described (DeChiara et al., 1991, Baker et al., 1993). *IGF2* is also important in the context of human pregnancy, with a high level of placental *IGF2* and *H19* expression observed throughout gestation (Goshen et al., 1993).

1.2.4 *H19* and *Igf2* in fetoplacental growth and resource allocation

The *IGF2/H19* locus regulates fetal growth in humans, with associations between *IGF2* (DMR0 and DMR2) methylation levels and fetal growth observed (St-Pierre et al., 2012). Hyper and hypomethylation at the *H19*-ICR in gametes leads to the development of Beckwith-Wiedemann syndrome (BWS) and Silver-Russell syndrome (SRS) respectively. Whilst BWS is associated with fetal overgrowth and increased *IGF2* expression, SRS is associated with fetal growth restriction and reduced *IGF2* expression (Gicquel et al., 2005, Weksberg et al., 2010). Moreover, in the placenta specifically, hypomethylation of *H19*-DMR and concomitant biallelic expression of *H19* are observed in cases of pregnancy-induced hypertension and fetal growth restriction (Yamaguchi et al., 2019). Studies also indicate that maternal stressors cause dysregulation in *H19/Igf2* ICR methylation and expression of these genes in samples of cord blood. Indeed, maternal anxiety is associated with a reduction in *H19/IGF2* ICR methylation in cord blood (Mansell et al., 2016). Furthermore, in the cord blood of infants born to mothers with gestational diabetes mellitus (GDM), *IGF2* and *H19* expression is increased and decreased respectively and placental *IGF2* expression is also increased (Su et al., 2016a). Overall, in humans, the *H19/IGF2* locus plays an important role in fetal growth, and adverse pregnancy environments cause dysregulation in its methylation and expression.

Whilst clinical studies show the importance of the *IGF2/H19* locus in fetal growth outcomes and pregnancy complications, mouse models offer the advantage of genetic

manipulation in distinct placental endocrine and transport zones, resulting in either global (fetoplacental) over-expression or under-expression, as well as Lz-specific (*P0*) under-expression of *Igf2*. Together these gene manipulation experiments illustrate the importance of *Igf2* in fetoplacental growth, fetal nutrient provision and placental structure and morphology (Figure 1.3). In particular, *Igf2* over-expression (via *H19* and *H19-ICR* deletion) and *Igf2* under-expression increase and decrease fetoplacental growth, respectively (Constancia et al., 2005, Angiolini et al., 2011) as indeed IGF2 signalling leads to the induction of trophoblast proliferation *in vitro* (Chen et al., 2016). Interestingly, specific ablation of *H19* and miR-675, with unaltered placental *Igf2* expression, results in placental overgrowth, with fetal overgrowth occurring to a lesser degree (Keniry et al., 2012), indicating that *H19* and *miR-675* are themselves regulators of placental size.

IGF2 also plays a critical role in regulating the structure of the Lz. In response to constitutive and *Igf2P0* under-expression, MBS, FC and trophoblast volume are decreased, along with the surface area of the trophoblast membrane (Sibley et al., 2004, Coan et al., 2008b). Conversely, global over-expression of *Igf2* leads to increased MBS, FC and T volumes and surface area of the trophoblast membrane at both E16 and E19 (Angiolini et al., 2011). An increase in surface area in the *Igf2* over-expression model is also associated with an increase in the Lz theoretical diffusion capacity for oxygen on both gestational days (Angiolini et al., 2011). Barrier thickness is increased by both *Igf2* global and Lz-specific knockout, whilst it remains unaltered by global over-expression of *Igf2* (Coan et al., 2008b, Angiolini et al., 2011). Overall, changes in Lz structure via manipulation of *Igf2* expression may influence fetal oxygen and nutrient provision.

The importance of placental *Igf2* expression in regulating placental nutrient transfer has also been shown via studies *in vivo*, and by quantifying nutrient transporter gene expression. For instance, placental amino acid transport is decreased in the global *Igf2* knockout mouse towards the end of gestation (Constancia et al., 2005). In the *Igf2P0* model however, where *Igf2* under-expression occurs exclusively in the Lz, the placenta increases glucose, amino acid and calcium transport so that growth restriction of the fetus is only observed near term (Constancia et al., 2005, Dilworth et al., 2010). This upregulation in placental glucose and amino acid transport is not observed when fetal growth demand is reduced via a reduction in fetal *Igf2* expression in the global *Igf2* null

and is correlated to a greater decrease in fetal weight when compared to the *Igf2P0* null (Constancia et al., 2005). In the global *Igf2* over-expression model, the placenta transports less glucose and amino acids, and fetuses are less growth enhanced than the placenta (Angiolini et al., 2011). These reductions in glucose and amino acid transport are associated with decreased placental glucose and amino acid transporter gene expression (Angiolini et al., 2011).

Igf2 is also critical in Jz formation, with *Igf2* loss and gain impacting glycogen cells in the Jz. In particular, deletion of *Igf2* results in a decrease in glycogen cell number, whilst *Igf2* over-expression (via *H19* deletion) increases glycogen cell number (Lopez et al., 1996, Esquiliano et al., 2009). However, spongiotrophoblast and giant cell number remain unaltered in response to *Igf2* over-expression (Esquiliano et al., 2009). Interestingly, in the *P0* knockout model, Jz and glycogen cell volumes are decreased, indicating that paracrine signalling can occur between the two placental zones (Sferruzzi-Perri et al., 2011). *Igf2* deletion in the Jz increased cytochrome P450 family 17 subfamily A member 1 (*Cyp17a1*) and reduced prolactin-3b1 (*Prl3b1*) expression in both male and female placentas, whilst 3-hydroxy-3-methylglutaryl-CoA reductase (*Hmgcr1*) and steroidogenic acute regulatory protein (*Stard1*) expression was reduced in male placentas, indicating an alteration in the placental capacity to produce hormones in this model (Aykroyd et al., 2020). Moreover, spongiotrophoblast and glycogen cell volume are decreased in female, but not male placentas upon *Igf2* deletion in the Jz (Aykroyd et al., 2020). Despite the importance of *Igf2* in Jz formation, specific Jz-*Igf2* over-expression has not been described to date but would offer a means to study the effect of increased placental endocrine size and capacity on fetal outcomes.

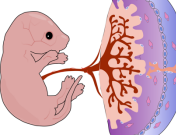
Genotype	Fetal and placental phenotype	Placental structure	Placental function
<i>Igf2</i> (Global knockout)	↓ 52% ↓ 40% 	↓ MBS, FC, T ↓ SA ↑ BT ↓ GlyT	↔ Gluc and ↓ AA transport ↓ Placental efficiency
<i>Igf2 P0</i> (Placental specific knockout)	↓ 35% ↓ 24% 	↓ MBS, FC, T ↓ SA ↑ BT ↓ GlyT	↑ Gluc and AA transport ↑ Placental efficiency
<i>H19</i> (Global overexpression)	↑ 45% ↑ 23% 	↑ MBS, FC, T ↑ SA ↔ BT ↑ GlyT	↓ Gluc and AA transport ↓ Placental efficiency

Figure 1.3. The effects of *Igf2* placental and global knockout and global over-expression on fetal and placental phenotype, placental structure and function. Phenotypes are from E19 of pregnancy, aside from GlyT number (E15 or E16). Figure adapted from (Sferruzzi-Perri, 2018b). Data displayed are from references Lopez et al., 1996, Constancia et al., 2002, Sibley et al., 2004, Constancia et al., 2005, Coan et al., 2008b, Esquiliano et al., 2009, Angiolini et al., 2011, Sferruzzi-Perri et al., 2011. AA, amino acid; BT, interhaemal membrane barrier thickness; FC, fetal capillaries; Glu, glucose; GlyT, glycogen trophoblast cells; Lz, labyrinth zone; MBS, maternal blood spaces; SA, surface area; T, trophoblast.

1.3 Placental endocrine function

During pregnancy, fetal and maternal outcomes are in part determined by the endocrine function of the placenta, which secretes a milieu of hormones into the maternal circulation and to a lesser extent in the fetal circulation. In humans, these include steroid hormones (oestrogen and progesterone), the prolactin-growth hormone family, neuro-active peptides (melatonin, serotonin, oxytocin, kisspeptin, thyrotropin-releasing hormone and corticotropin-releasing hormone), in addition to activin, relaxin, leptin, chorionic gonadotropin, and parathyroid hormone-related protein (Napso et al., 2018, Sferruzzi-Perri et al., 2020). Importantly, species differences are evident in the hormones secreted by the murine and human placenta. For instance, regarding the prolactin-growth hormone family, the mouse expresses prolactin, but not growth hormone. Conversely, in humans,

the decidua and trophoblast are sources of prolactin and growth hormone, respectively (Soares, 2004). Moreover, whilst the human placenta produces leptin, the mouse placenta does not (Malik et al., 2005, Noguez et al., 2019). The placenta also produces growth factors, namely IGF1 and IGF2, which play a critical role in fetoplacental growth (Sferruzzi-Perri et al., 2013a, Sferruzzi-Perri et al., 2017, Sferruzzi-Perri, 2018b). Overall, placental hormones are also able to act in a local manner on the uterus to maintain pregnancy and prevent pre-term birth (Daya, 1989).

1.3.1 Placental steroidogenesis

The placenta produces steroid hormones via the steroidogenic pathway as depicted in Figure 1.4. Steroidogenic acute regulatory protein (StAR) is strongly expressed in the rodent trophoblast giant cells between E11 and E13 of pregnancy (Koh et al., 2002). In mouse trophoblast giant cells, LDL in the maternal circulation is delivered from the outer to the inner mitochondrial membrane by StAR, which is the rate-limiting step of steroidogenesis (Gwynne and Strauss, 1982, Arakane et al., 1998). Whilst in the rodent placenta expresses StAR, the human placenta does not (Strauss et al., 1996, Ben-Zimra et al., 2002). In humans, it is thought that the protein StAR related lipid transfer domain containing 3 (StARD3) subserves StAR's role for steroidogenesis in the placenta, with its expression being observed in human placental cell extracts (Strauss et al., 2003). Moreover, the trophoblast giant cells express high levels of both cytochrome P450 cholesterol side-chain cleavage (P450_{scc}) enzyme and 3 β -hydroxysteroid dehydrogenase/ Δ 5- Δ 4 isomerase (3 β HSD (Schiff et al., 1993, Peng and Payne, 2002). Cholesterol is converted to pregnenolone by P450_{scc}, encoded by the cytochrome P450 family 11 subfamily A member 1 (*CYP11A1*) gene. 3 β HSD, encoded by the *HSD3B* gene, then metabolises pregnenolone to progesterone (Payne and Hales, 2004). Androgens are synthesised from pregnenolone by *Cyp17a1* in a two-stage reaction involving 17 α -hydroxylase and 17, 20-lyase activities (Payne and Hales, 2004). In the rat placenta after E12, 17 α -hydroxylase and 17,20-lyase activities are observed, and the placenta can produce androgens. Whilst the rodent placenta expresses *Cyp17a1*, its expression is absent in the human placenta (Voutilainen and Miller, 1986, Johnson and Sen, 1990). Indeed, in the human placenta oestrogen synthesis is dependent on androgen precursors from the fetal and maternal adrenal gland (Malassiné et al., 2003). Thereafter, the conversion of testosterone to oestradiol and androstenedione to oestrone is catalysed

by cytochrome P450 family 19 subfamily A member 1 (*Cyp19a1*; Payne and Hales, 2004).

StAR and P450_{scc} proteins decline in the mouse placenta from E10.5-14.5 (Arensburg et al., 1999). Indeed in rodents, despite placental capacity for progesterone synthesis from early gestation, ovarian progesterone synthesis occurs throughout gestation (Murr et al., 1974). Moreover, in the rat, crosstalk between the ovaries and placenta occurs, whereby placental hypertrophy is observed upon ovariectomy (Csapo and Wiest, 1973). It is hypothesised that in rodents, progesterone from the corpus luteum is converted to androgens in the placenta which are used as substrates by the corpus luteum to produce oestrogen (Jackson and Albrecht, 1985). In humans during early pregnancy, chorionic gonadotrophin maintains the synthesis of progesterone by the corpus luteum. After the luteo-placental shift at 4-5 weeks post-conception, the placenta takes over progesterone production and can support the pregnancy even in the absence of ovarian function (Csapo et al., 1972, Csapo et al., 1973, Costea et al., 2000).

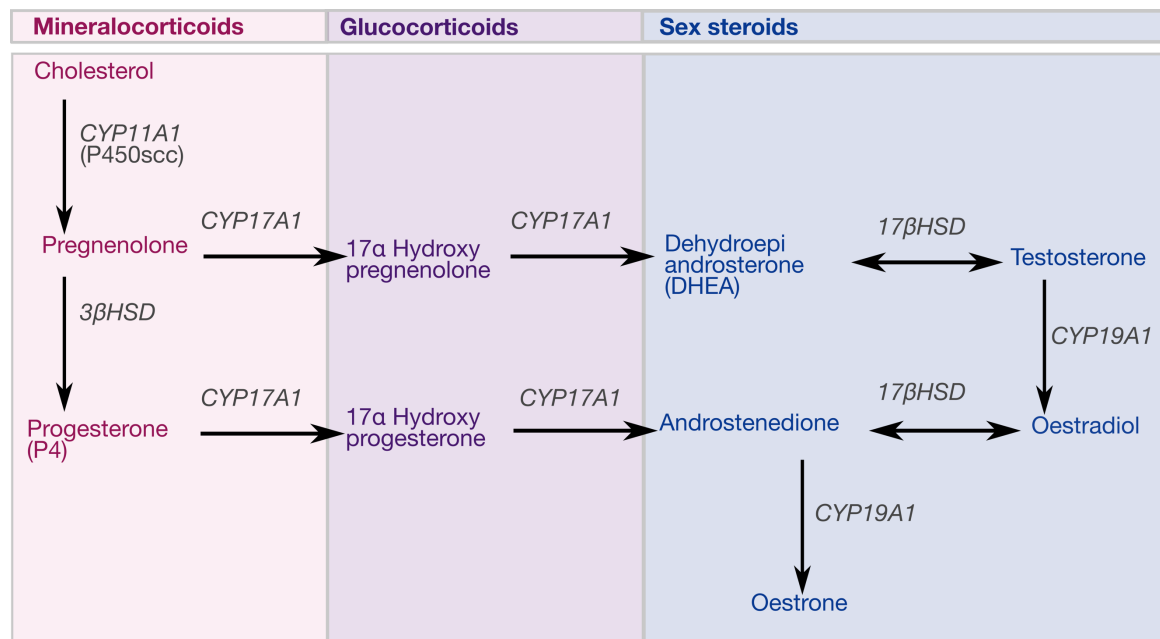


Figure 1.4. Steroidogenesis pathway. 3βHSD, 3β-hydroxysteroid dehydrogenase/Δ5-Δ4 isomerase; 17βHSD, CYP11A1, Cytochrome P450 family 11 subfamily A member 1; CYP17A1, Cytochrome P450 family 17 subfamily A member 1; CYP19A1, Cytochrome P450 family 19 subfamily A member 1; StAR, Steroidogenic acute regulatory protein' P450_{scc}, P450 cholesterol side-chain cleavage

1.3.2 Placental corticosterone metabolism

Exposure of the placenta to glucocorticoids via the maternal circulation plays an important role in its regulation of fetal nutrient supply (De Courcy et al., 1952, Berliner et al., 1956, Vaughan et al., 2012). The placenta has high levels of 11 β HSD activity, which is involved in the interconversion between bioactive glucocorticoids such as cortisol and corticosterone and their inactive metabolites, 11-dehydrocorticosterone and cortisone (Osinski, 1960, Monder and Shackleton, 1984). 11 β HSD2 inactivates glucocorticoids and is localised in the syncytiotrophoblast in both rodents and humans, with expression observed in the Lz in the mouse (Krozowski et al., 1995, Roland and Funder, 1996). Thus, it has been proposed that 11 β HSD2 protects the developing fetus from excessive exposure to maternal glucocorticoids, which are known to reduce fetal growth (Lindsay et al., 1996). Indeed, a decrease in 11 β HSD2 activity in the placenta is associated with IUGR in humans and rodents (Shams et al., 1998, Sloboda et al., 2000, Thompson et al., 2002). 11 β HSD1 is also localised in the murine Lz and is conversely involved in catalysing the regeneration of active glucocorticoids (Thompson et al., 2002). Glucocorticoids exert their effects via the glucocorticoid receptor (GR) and mineralocorticoid receptor (MR), both of which are intracellular receptors that regulate the transcription of several target genes (Groeneweg et al., 2012). MR is expressed in the murine fetal central nervous system from E15.5 (Diaz et al., 1998), whilst GR is ubiquitously expressed in the murine placenta and the fetal nervous system (Thompson et al., 2002). Indeed, GR is required for the maturation of several fetal organs including the lungs, heart and liver (Cole et al., 1995, Opherk et al., 2004, Rog-Zielinska et al., 2013).

1.3.3 Placental endocrine function and maternal physiology

Both placentally derived and maternally produced hormones influence maternal physiology, aiding in its adaptation throughout pregnancy. During early pregnancy, known as the “anabolic phase”, increased glycogen and lipid stores in peripheral tissues and an overall increase in insulin sensitivity is observed in the mother (Bustamante et al., 2010, Sferruzzi-Perri et al., 2020). Moreover, maternal hyperphagia, central leptin resistance and increased plasma insulin levels all contribute to increased lipid synthesis. Maternal adipocyte hypertrophy also occurs to increase the storage of lipids (Knopp et al., 1973, Ramos et al., 2003, Trujillo et al., 2011). An increase in maternal pancreatic β -cell mass is also associated with an increase in pancreatic insulin production (Ackermann and

Gannon, 2007, Rieck and Kaestner, 2010). Increased pancreatic islet mass is also observed in the latter phase of pregnancy to balance maternal insulin resistance and is achieved through both hypertrophy and hyperplasia of the pancreatic islets (Kalhan et al., 1997, Sorenson and Brelje, 1997, Rieck and Kaestner, 2010). In both cases, several placental hormones have been shown to be involved in the expansion of β -cell mass. Studies in mice where prolactin was knocked out *in vivo* or added to islet cultures *in vitro*, indicate its importance in inducing β -cell expansion via increased proliferation and reduced apoptosis (Brelje et al., 1993, Huang et al., 2009). Moreover, other placental hormones, namely growth hormone, IGF2, placental growth factor, progesterone, oestrogen and parathyroid hormone-related protein have all been shown to alter pancreatic β -cell mass, proliferation and insulin secretion (Costrini and Kalkhoff, 1971, Brelje et al., 1993, Vasavada et al., 1996, Li et al., 2015a, Modi et al., 2015). For instance, the administration of progesterone or oestradiol in pregnant rats enhances insulin secretion (Costrini and Kalkhoff, 1971). Conversely, studies in non-pregnant rodents indicate that leptin inhibits glucose-induced pancreatic insulin secretion (Emilsson et al., 1997, Roduit and Thorens, 1997).

The “catabolic phase” during late gestation is characterised by increased fetal growth and demand, with several hormones produced by the placenta inducing systemic effects in the mother to promote insulin resistance (King et al., 2001, Newbern and Freemark, 2011, Sferruzzi-Perri et al., 2020). Prolactin, placental lactogen and growth hormone are all important mediators in maternal insulin resistance (Kelly et al., 1991). In the mouse, placental lactogen and prolactin alter maternal glucose homeostasis, as shown in an adipocyte culture system whereby treatment with these hormones *in vitro* reduced glucose uptake, whilst insulin binding remained unaltered (Ryan and Enns, 1988). Growth hormone is also important in inducing insulin resistance in the mother in the case of normal pregnancy, to increase nutrient provision to the fetus. Studies indicate that growth hormone decreases insulin sensitivity in the peripheral tissues of non-pregnant mice, such as skeletal muscle and the liver, as indicated by a reduction in glucose transporter 4 (GLUT4) and InsR expression (Dominici et al., 1999, Barbour et al., 2004). In mouse white adipose tissue, growth hormone excess also decreases insulin stimulated PI3K activity and inhibits lipid deposition (del Rincon et al., 2007). The production of placental progesterone, as well as adipokines such as resistin and leptin, all act to induce insulin resistance in the mother during pregnancy (Sutter-Dub et al., 1981, Zavalza-Gomez et al.,

2008). For instance, progesterone inhibits the PI3K pathway in adipocyte cell culture (Wada et al., 2010). Conversely, knockout of the progesterone receptor in non-pregnant mice improves glucose tolerance and concomitantly increases β -cell proliferation and insulin secretion (Picard et al., 2002). Overall, maternal insulin resistance enhances lipolysis and reduces lipoprotein lipase in adipocytes, thus reducing fatty acid uptake and fat storage (Knopp et al., 1973, Ramos et al., 2003).

Conversely, oestrogen produced by the placenta appears to increase insulin sensitivity by increasing insulin binding in adipocytes (Ryan and Enns, 1988). The ability of oestrogen to increase insulin sensitivity is however dependent on its concentration and the presence or absence of other hormones, such as progesterone (Ahmed-Sorour and Bailey, 1981, González et al., 2002). Near term in mice, there are improvements in maternal insulin sensitivity, which may act to conserve glucose and lipids for the mother in preparation for delivery and the lactation period (Musial et al., 2016).

1.3.4 The effect of placental endocrine function on pregnancy outcomes

As the maternal hormonal environment is critical in the adaptation of maternal insulin sensitivity during pregnancy, endocrine dysfunction during pregnancy contributes to several adverse pregnancy outcomes. Indeed, maternal serum and urinary oestriol and placental lactogen concentrations are used to monitor fetal growth, as IUGR is often associated with reductions in the levels of these hormones (Gardner et al., 1997).

Moreover, exposure to endocrine disruptors is also associated with changes in fetoplacental weight and pregnancy complications (Gingrich et al., 2020). In pregnant women with endocrine disorders, such as in polycystic ovarian syndrome (PCOS), which is frequently diagnosed in part by hyperandrogenism, pregnancy complications such as GDM, preeclampsia, preterm birth and either macrosomia or IUGR are more commonly observed (Boomsma et al., 2008), alluding to the importance of the maternal hormonal environment in pregnancy outcomes.

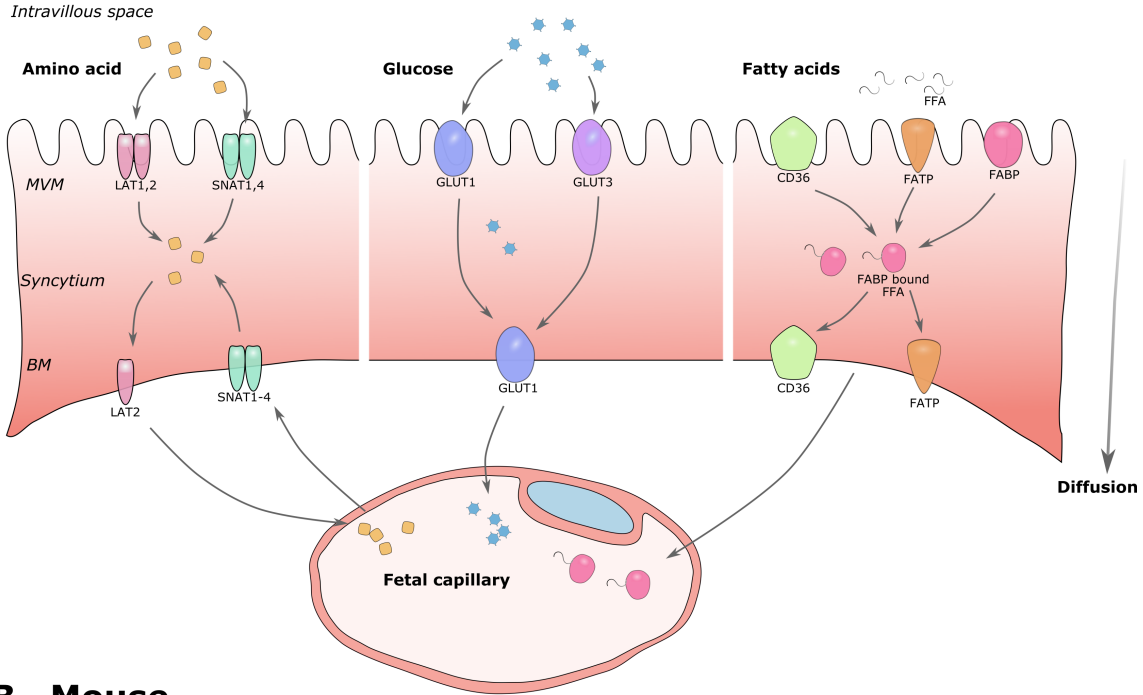
Several aforementioned hormones induce insulin resistance in normal pregnancy, whilst a diagnosis of GDM in women involves an impairment of glucose tolerance with onset during pregnancy (Riskin-Mashiah et al., 2010). Indeed, in the placentas of GDM patients, dysregulation of the expression of several hormones such as leptin, placental growth hormone variant and human placental lactogen has been observed alongside

increased placental progesterone production (Hu et al., 1999, Lea et al., 2000, Fisher et al., 2020), which is indicative of dysregulated placental endocrine function in GDM. Obesity during pregnancy also increases the risk of developing GDM and is similarly associated with hyperglycaemia during pregnancy (Catalano et al., 2012). Interestingly, in a mouse model of maternal obesity showing GDM-like symptoms, a reduction in placental prolactin expression was observed, indirectly implicating placental endocrine capacity in the maternal metabolic consequences of obesity (Musial et al., 2017). In obese pregnancies fetal outcomes differ, with both macrosomia and IUGR being observed (Ehrenberg et al., 2004, Radulescu et al., 2013). Mothers with GDM are more likely to give birth to babies with macrosomia who are predisposed to hypoglycaemia in early fetal life, due to exposure to a hyperglycaemic environment *in utero* stimulating greater pancreatic insulin production in the fetus (Esakoff et al., 2009, He et al., 2015). Conversely, IUGR births reportedly occur primarily in individuals with diabetes of extended duration or vasculopathy (Lucas et al., 1989). Thus, high-nutrient environments *in utero* (i.e., hyperglycaemia) alter fetal growth outcomes, and may in part be influenced by placental endocrine function. Nonetheless, such alterations in birth weight are also likely influenced by changes in placental nutrient transport function.

1.4 Nutrient transport across the placenta

Materno-fetal nutrient transport is facilitated across the syncytiotrophoblast by several transporters. In humans, nutrient transport from the mother to the fetus across the trophoblast membrane involves the uptake of nutrients from the maternal circulation across the MVM, passage through the cytoplasm of the trophoblast and then across the BM. As the mouse placenta is haemotrichorial, nutrients must pass through a fenestrated sinusoidal trophoblast giant cell layer and two syncytiotrophoblast layers to the fetal capillary (Figure 1.5). Changes in the rate of materno-fetal nutrient transport are governed by several factors including trophoblast surface area, uteroplacental and umbilical blood flows and placental metabolism (Lager and Powell, 2012). Moreover, nutrient transporter abundance on the syncytiotrophoblast is a critical determinant of placental capacity for nutrient transfer (Constancia et al., 2005, Angiolini et al., 2011). These transporters are involved in the uptake of several nutrients crucial for fetal growth, such as amino acids, glucose and fatty acids.

A Human



B Mouse

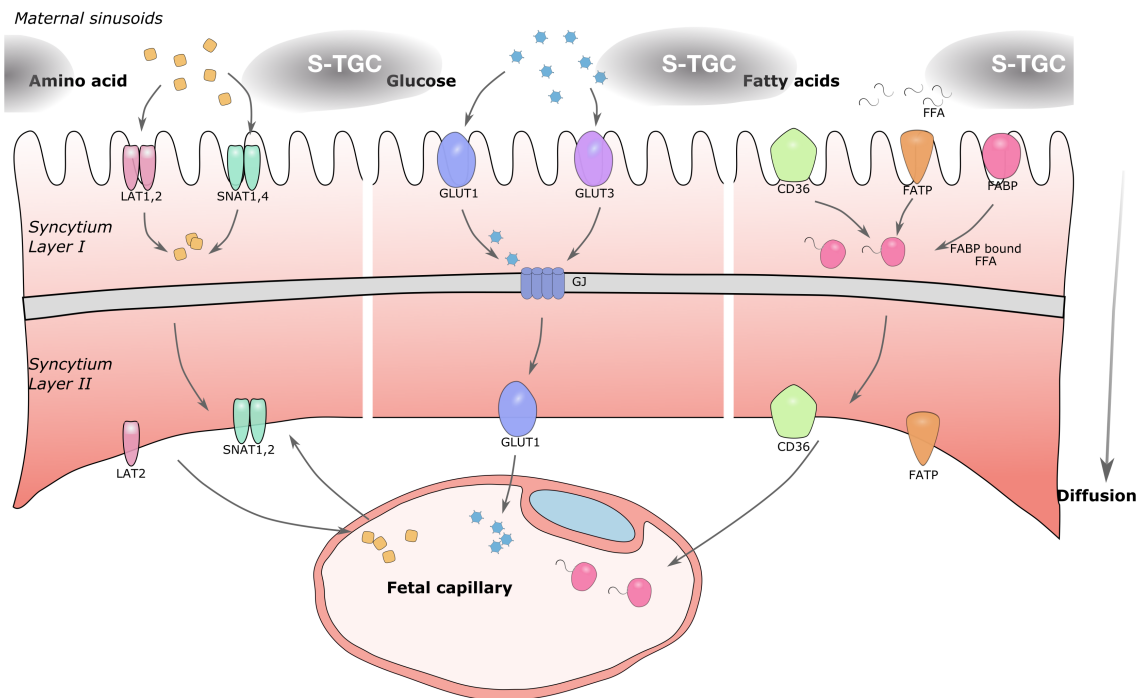


Figure 1.5. Amino acid, glucose and fatty acid transport across the syncytiotrophoblast in the human (A) and mouse (B). Figure adapted from Winterhager and Gellhaus, 2017. BM, basal membrane; FFA, free fatty acids; FABP, fatty acid binding protein; FATP, fatty acid transporter protein; GJ, gap junction; GLUT, glucose transporter, LAT, the light chain-type amino acid transporter; MVM, microvillous membrane; SNAT, sodium-coupled neutral amino acid transporters, S-TGC, sinusoidal trophoblast giant cell.

1.4.1 Amino acid transport

Amino acids provide the building blocks required for net protein synthesis in all mammalian species, with fetal whole body protein synthesis occurring at approximately 13 g/day per kg of fetus in humans (Chien et al., 1993). In addition to their importance in protein synthesis, amino acids also serve as metabolic fuel for fetal growth. As the fetus is incapable of amino acid synthesis, the uptake of amino acids occurs from the maternal circulation via the placenta. Amino acid transporter proteins, which are localised on both the MVM and BM, actively transfer amino acids across the syncytiotrophoblast. Amino acid transporters can be classified as accumulative transporters, exchangers or facilitated transporters (Cleal et al., 2011). Several systems of amino acid transporters have been identified, with A, ASC, B⁰, L, N and Gly systems mediating the uptake of neutral amino acids (Palacin et al., 1998, Fukasawa et al., 2000, Regnault et al., 2002). The systems y⁺, y⁺L, b⁰⁺ mediate the transport of cationic amino acids and the systems X-AG and β mediate the transport of anionic amino acids (Malandro et al., 1996, Ayuk et al., 2002, Radaelli et al., 2002, Regnault et al., 2002, Noorlander et al., 2004).

System A contains the sodium-coupled neutral amino acid transporters (SNAT). SNATs are members of the SLC38 family and, as their name suggests, are involved in the transport of small neutral amino acids, namely small aliphatic amino acids (Cramer et al., 2002, Mackenzie and Erickson, 2004). Human and rodent placentas express *Slc38a1*, *Slc38a2* and *Slc38a4* isoforms (Jansson, 2001, Jansson et al., 2002, Coan et al., 2008b). In both rats and humans, SNAT1 is the main contributor to system A mediated amino acid uptake, whilst SNAT2 and SNAT4 primarily mediate the remaining uptake in rats and humans, respectively (Takahashi et al., 2017). Sodium independent amino acid transporters include the light chain-type amino acid transporter 1 (LAT-1) system, which has two isoforms (LAT1, LAT2), and are also critical in the exchange of amino acids in the placenta (Gaccioli et al., 2015).

1.4.2 Glucose transport

During pregnancy, glucose metabolism increases to meet fetal requirements, with glucose being the major fetal energy source (Catalano et al., 1992, Rao et al., 2013). The fetus is largely dependent on the placental supply of glucose via the maternal circulation (Warnes et al., 1977, Hay et al., 1984), with placental glycogen being a potential additional source

(Bouillot et al., 2006, Coan et al., 2006, Tunster et al., 2020). Due to the limited permeability of the syncytiotrophoblast, placental glucose transport is facilitated by sodium-independent transporters, namely by members of the GLUT family of glucose transporter proteins (Johnson and Smith, 1980, Johnson and Smith, 1985, Bain et al., 1988). The GLUT transporters are transmembrane proteins, divided into three subfamilies consisting of 13 isoforms (GLUT1-12, HMIT1; Joost et al., 2002). The expression of these transporters is tissue-specific (Joost and Thorens, 2001), with only a proportion of GLUT transporters expressed in the placenta. GLUT1 mRNA and protein are abundant in the human syncytiotrophoblast (Jansson et al., 1993, Jansson et al., 1995). Furthermore, GLUT1 density is higher in the syncytiotrophoblast MVM compared to BM isolates, suggesting a higher capacity for glucose transport by the MVM. In contrast, *GLUT3* mRNA is evenly dispersed across several placental cell types in the villus and GLUT3 protein is not present in the syncytiotrophoblast (Jansson et al., 1993). Thus, it can be concluded that in humans, GLUT1 is the predominant glucose transporter protein involved in placental glucose transport (Jansson et al., 1993). In rodents, GLUT1 and GLUT3 are present on the maternal side of syncytiotrophoblast layer I, whilst layer II is immuno-positive for only GLUT1 (Takata et al., 1994, Shin et al., 1997). It has been proposed that gap junctions facilitate the transport of glucose between syncytiotrophoblast layer I and layer II (Takata et al., 1994).

1.4.3 Fatty acid transport

During gestation, lipids provide an energy source for fetal growth and development, and fetal lipid supply increases throughout the course of pregnancy concomitant with increasing fetal caloric demands (Friedman et al., 1978). Long-chain polyunsaturated fatty acids (LC-PUFA) are critical in fetal development, acting as metabolic fuel and precursors of prostaglandins, prostacyclins, thromboxanes and leukotrienes. However, due to the limited ability of the placenta and fetus for LC-PUFA synthesis, placental transfer of maternally supplied fatty acids to the fetus is essential (Chambaz et al., 1985). Thus, the placenta preferentially transfers LC-PUFAs to the fetus, illustrated *in vivo* by the presence of high LC-PUFA levels in the fetal compared to maternal circulation (Friedman et al., 1978, Berghaus et al., 2000) and *in vitro* through placental perfusion studies (Haggarty et al., 1997, Haggarty et al., 1999).

Compared to glucose and amino acids, the transport of fatty acids across the syncytiotrophoblast is comparatively less well characterised. However, a variety of fatty acid binding and transport proteins have been characterised and are present on the plasma membrane or intracellularly in the placenta and are involved in materno-fetal fatty acid transport (Figure 1.5). For instance, fatty acid transport proteins (FATPs) are localised on the plasma membrane of trophoblast and are involved in the transfer of fatty acids (Schaffer and Lodish, 1994, Larque et al., 2006b), with multiple isoforms identified (Jia et al., 2007). In primary human trophoblast at term, *FATP2*, *FATP4*, and *FATP6* expression is observed, whilst *FATP1* and *FATP3* are more weakly expressed (Mishima et al., 2011). FAT/CD36 binds and transports free fatty acids and is expressed on both the MVM and BM of the human placenta (Abumrad et al., 1993, Campbell et al., 1998). The trafficking of fatty acids is also facilitated by fatty acid binding proteins (FABPs). In humans, FABP1, FABP3, and FABP4 have been localised to the trophoblast of the placenta (Campbell et al., 1998, Knipp et al., 2000, Larque et al., 2006a, Scifres et al., 2011, Islam et al., 2014, Makkar et al., 2014). In addition, FABP5 is not detected in the trophoblast but rather localised in the endothelium of the microvasculature in the human placenta (Masouye et al., 1997). Moreover, results indicating FABP7 expression in human trophoblast have been conflicting to date (Larque et al., 2006b, Biron-Shental et al., 2007).

In the rodent placenta, the fatty acid transport system has not yet been precisely localised. However, *Fatp1*, *Fatp3*, *Fatp4* and *Fatp6* are primarily expressed in the mouse placenta near term, with *Fatp2* expression mainly limited to the amnion (Mishima et al., 2011). Furthermore, *Fat/Cd36* expression has been observed in the Lz (Knipp et al., 2000). Like humans, the trophoblast in the rodent placenta also shows *Fabp1*, *Fabp3*, and *Fabp4* expression (Campbell et al., 1998, Knipp et al., 2000, Larque et al., 2006a, Scifres et al., 2011, Islam et al., 2014, Makkar et al., 2014).

1.4.4 Alterations in nutrient transport in response to pregnancy complications

Fetal growth is associated with placental nutrient transporter abundance and activity. Indeed, a positive correlation between birth weight and placental system A amino acid transporter activity is evident (Jansson et al., 2013), whilst in IUGR, there is a reduction in system A transporter activity in the MVM (Mahendran et al., 1993, Glazier et al., 1997). However, plasticity in the form of alterations in placental transport function have

also been shown in response to environmental challenges such as hypoxia, undernutrition, maternal anaemia and obesity (Jansson et al., 2002, Jauniaux and Burton, 2007, Sferruzzi-Perri et al., 2011, Sferruzzi-Perri et al., 2013b, Higgins et al., 2016). For instance, an increase in GLUT3 expression in human placentas from IUGR pregnancies may be a form of placental adaptation in an attempt to maintain appropriate fetal growth (Janzen et al., 2013). In GDM pregnancies placental transport capacity is altered with increased GLUT1 expression and uptake of D-glucose across the basal membrane, increased system A activity in the trophoblast MVM, and higher expression of FABP1, FABP4 and FABP5 (Gaither et al., 1999, Jansson et al., 2002, Magnusson et al., 2004, Radaelli et al., 2009). These increases in placental nutrient transporter expression may contribute to the fetal macrosomia frequently reported in women with GDM (He et al., 2015). Maternal obesity may also lead to fetal overgrowth, with a correlation between birth weight and BM GLUT1 transporter expression being reported (Acosta et al., 2015). Modifications in nutrient transporter expression are also observed in rodent models of maternal high fat diet including increases in placental *Glut1*, *Glut3* and *Snat2* expression (Jones et al., 2009, Lin et al., 2011, Sferruzzi-Perri et al., 2013b, Aye et al., 2015, Rosario et al., 2015). Such alterations in placental nutrient transport and accompanying changes in fetal nutrient acquisition in response to adverse gestational environments are known to programme offspring to poor metabolic health in later life (Sferruzzi-Perri and Camm, 2016).

1.5 The Developmental Origins of Health and Disease

The concept that an adverse environment during gestation is associated with an increased propensity to develop non-communicable disease in later life is known as the Developmental Origins of Health and Disease (DOHaD) hypothesis and was first described using epidemiological data. For instance, David Barker made an association between poor fetal nutrient acquisition, using low birth weight as a surrogate marker, and an increased rate of adult mortality from ischaemic heart disease in a cohort of English men (Barker and Osmond, 1986). Barker and colleagues then extended such associations of poor nutrition during gestation with the development of type 2 diabetes and glucose intolerance in adulthood (Hales et al., 1991). Traditionally, the concept of programming was formulated using evidence from gestational malnutrition and reduced fetal weight. Data from other epidemiological studies evaluating the impact of fetal malnutrition in the

Dutch famine of 1944-1945 on the incidence of obesity and reduced glucose tolerance in adult life further corroborated this concept (Ravelli et al., 1976, Ravelli et al., 1998, Roseboom et al., 2001). However, more recently it has been shown that programming of poor metabolic health in adulthood can also be linked to other conditions *in utero* where birth weight is unaltered or increased, such as in pregnancies associated with GDM (Dabelea, 2007). Moreover, studies have linked a variety of other pregnancy complications or environments, such as maternal obesity, smoking, alcohol consumption and living in areas with high pollution or high altitude to poor offspring health even in the absence of a change in birthweight (Wright et al., 1983, Jauniaux and Burton, 2007, Rich et al., 2009, Moore et al., 2011, Chandler-Laney et al., 2012, Tan et al., 2015).

The periods prior to and after fetal development may also programme offspring metabolism in the longer term. For instance, it has been shown in mice that a compromised maternal or paternal environment may alter DNA methylation in oocytes and sperm associated with negative metabolic consequences for adult offspring (Ge et al., 2014b, Watkins et al., 2018). Moreover, the environment during the lactational period and onwards can also influence offspring metabolism. Indeed, unhealthy diet including the consumption of a calorie dense diet postnatally in humans may exacerbate or expose the vulnerability of the offspring for adverse health outcomes as a result of developmental programming (Li et al., 2015b, Li et al., 2015c). An additive interaction between low birthweight and unhealthy diet was observed in these offspring for the development of type 2 diabetes (Li et al., 2015b). This has also been indicated in rodent models of developmental programming, where poor conditions *in utero*, such as maternal diabetes or obesity, with the superimposition of a calorie dense diet after the lactational period exacerbate glucose intolerance and insulin resistance and accelerates their onset (Kamel et al., 2014, Yokomizo et al., 2014). Overall, these studies emphasise the importance of both prenatal and postnatal environments in offspring metabolic outcomes.

1.5.1 Mouse models in developmental programming

Despite epidemiological studies demonstrating how an adverse pregnancy environment can programme offspring to metabolic dysfunction in later life, it is difficult to study the molecular mechanisms of the DOHaD hypothesis in the clinic, due to increased difficulties in accessing metabolic tissues and the length of lifespan in humans. Rodents are frequently used to study the molecular mechanisms underlying DOHaD due to their

short gestation and lifespan, accessibility to metabolic tissues for molecular analysis, and ease of maternal manipulation, including gene manipulation (Theys et al., 2011, Desai et al., 2015, Lecoutre et al., 2016 and Table 1.1). Several rodent models of developmental programming with clinical relevance have been studied, including the impact of maternal nutrient imbalance (total caloric restriction, high fat diet and protein restriction), inhalation hypoxia, synthetic glucocorticoid treatment (dexamethasone), uterine ligation, diabetes (streptozotocin treatment) and alcohol intake (Rueda-Clausen et al., 2011, Somm et al., 2012, Fante et al., 2016, Campisano et al., 2017) and reviewed in (Christoforou and Sferruzzi-Perri, 2020). Of these, maternal high calorie diets (high fat diet, high sugar, high fat and sugar; often accompanied with elevated maternal adiposity) and diabetes are considered models of maternal hyperglycaemia (Kamel et al., 2014, Yokomizo et al., 2014, Inoguchi et al., 2019). These rodent models also impact offspring metabolism and molecular pathways in metabolic tissues (Table 1.1, taken from (Christoforou and Sferruzzi-Perri, 2020).

1.5.2 Metabolic outcomes in mouse models of maternal hyperglycaemia

A high nutrient environment during gestation in rodents causes maternal obesity and is associated with increased adiposity in the offspring during adulthood suggesting metabolic programming (Yang et al., 2013, Latouche et al., 2014, Desai et al., 2015, Seet et al., 2015, Fante et al., 2016). An increase in adipocyte diameter is also observed in the offspring of streptozotocin treated mothers (Oliveira et al., 2015). The expansion of adipose stores in these offspring is frequently accompanied by an increase in leptin, triacylglycerol (TAG) and cholesterol in the circulation (Zhang et al., 2011b, Khalyfa et al., 2013, Zheng et al., 2014, Seet et al., 2015). Alterations in offspring adipose morphology in response to maternal obesity may begin *in utero*, with fetuses displaying increased adipocyte differentiation and elevated adipose expression of the zinc finger protein 423 (*Zfp423*), a transcription factor which commits cells to the adipogenic lineage (Yang et al., 2013). Offspring born to diabetic or obese dams also display reduced insulin sensitivity and glucose tolerance in adulthood, as well as hyperglycaemia and hyperinsulinemia (as summarised in Table 1.1). Moreover, changes in pancreatic morphology and insulin secreting capacity are a common aetiology in the development of type 2 diabetes contributing to changes in insulin sensitivity and hyperglycaemia.

Table 1.1. The effects of a high-nutrient environment *in utero* on molecular pathways in relation to offspring metabolic outcomes

Model (maternal manipulation)	Species	Sex studied	Treatment period	Alterations in gene expression and protein abundance in metabolic tissues *unless otherwise stated, alterations occur in the sex studied	Metabolic outcomes	Reference
High calorie diet						
High calorie diet (23% fat, 40% sugars)	Rat	M&F	D1-23	3 months (pancreas): ↓ <i>Ucp2, Gck, Glut2</i> (females)	↑ β-cell mass (females), ↓ ROS, ATP content in islets	(Theys et al., 2011)
High calorie diet (24% fat, 20% sugars)	Rat	M	3 weeks prior, D1- PD21	12 months (skeletal muscle): ↓ p-AKT ↑ total AKT, ↓ mitochondrial complexes I, II, and V protein	↑ adiposity, plasma insulin	(Latouche et al., 2014)
High calorie diet (45%, 35% sugars)	Rat	M	D1-PD21	3 months (liver): ↓ <i>Gpx1, Sod1, Pon1, Pon2,</i> <i>Pon3, p16, ↑ Cox2</i> 5 months (liver): ↓ <i>Igfbp1</i>	↑ plasma insulin, leptin, IGF-1, IGFBP3, LDL, HDL, lipase, triglycerides, TBARS, hepatic lipid droplets	(Zhang et al., 2011b, Smith et al., 2014)
High calorie diet (45% fat, 35% sugars)	Rat	M&F	D1-PD21	2 days (liver): ↑ <i>Cdkn1a, Pmp22, ↓ Tbl1, Ccnf,</i> <i>Pena, Ccna2, Mki67</i> 1 week (liver): ↓ <i>Wnt1</i>	↓ transition from G1 to S-phase in liver ↓ liver mass,	(Dudley et al., 2011)
High calorie diet (45% fat, 35% sugars)	Rat	M	D1-PD21	1 week (liver): ↓ <i>Wnt1</i>	↑ hepatic triglycerides	(Yang et al., 2012)

High calorie diet (45% fat, 35% sugars)	Mouse	M&F	8 weeks prior to mating	D14.5 (adipose): ↑ <i>Zfp423</i>	↑ adipogenic differentiation	(Yang et al., 2013)
High calorie diet (49% fat, 32% sugars)	Mouse	M	3 months prior, D1- PD21	6 months (pancreas): ↑ FOXO1, Insulin ↓ IRS1, PI3K, pAKT, PDX-1, GLUT2	↑ plasma insulin, leptin, cholesterol, triacylglycerol adiposity, mass of pancreatic β and α-cells, ↓ glucose tolerance	(Bringhenti et al., 2016)
High calorie diet (45% fat, 35% sugars)	Rat	M	6 weeks prior, D1- PD21	4 months (pancreas): ↑ <i>Il1-1a, Csf3, Slfn4,</i> <i>Cxcl6, Gabrp, Cldn2, Mx2</i> 4 months (liver): ↓ InsRβ	↑ plasma glucose, ↓ insulin sensitivity	(Pereira et al., 2015, Agarwal et al., 2019)
High calorie diet (45% fat, 35% sugars) with postnatal HFD challenge	Rat	M		4 months (pancreas): ↓ <i>Cd69, Csf1, Tnfaip2</i> 4 months (liver): ↓ p-AKT	↑ plasma insulin, ↓ glucose tolerance, ↓↓ insulin sensitivity	(Pereira et al., 2015, Agarwal et al., 2019)
High calorie diet (45% fat, 35% sugars)	Mouse	M	3 weeks prior, D1- PD21	1 month (muscle): ↑ p-JNK, p-IKK, PTP1B 1 month (adipose): ↑ p-JNK, p-IKK, PTP1B, ↓ α7nAChR, pJAK2, pSTAT3 1 month (liver): ↑ pJNK1, ↓ α7nAChR, pJAK2, pSTAT3, pCREB/β 2.5 months (liver): ↑ PEPCK 2.5 months (muscle): ↑ PEPCK, p-JNK, p-IKK 2.5 months (adipose): ↑ p-JNK, ↓ <i>Pparγ</i>	↑ adiposity, inflammatory markers ↓ hepatic glycogen, insulin sensitivity	(Fante et al., 2016, Payolla et al., 2016)

High calorie diet (45% fat, 35% sugar) with postnatal HFD challenge	Mouse	M		2.5 months (liver): \leftrightarrow PEPCK, \downarrow p-JNK 2.5 months (muscle): \uparrow PEPCK, p-IKK, PTP1B 2.5 months (adipose): \uparrow PTP1B, \downarrow <i>Cidec</i> , <i>Pparγ</i>	$\uparrow\uparrow$ adiposity \downarrow hepatic glycogen, glucose tolerance, \uparrow plasma leptin	(Fante et al., 2016, Payolla et al., 2016)
High calorie diet (58% fat, 26% sugar)	Mouse	M&F	D1-PD21	3 weeks (liver): \uparrow <i>Cd36</i> , <i>Aqp7</i> , <i>Cpt1b</i> , <i>Fabp2</i> , <i>Ppara</i> , <i>Pparγ</i> (males for all genes)	\downarrow glucose tolerance, insulin sensitivity \uparrow serum cholesterol, hepatic steatosis (males for all parameters)	(Zheng et al., 2014)
High calorie diet (59% fat, 20% sugar)	Rat	M	4 weeks prior, D1-23	3 months (liver): \downarrow InsR β , IRS1, \uparrow PKC ζ 3 months (muscle): \uparrow InsR β , p85	\uparrow hepatic triglyceride content, adiposity \leftrightarrow glucose tolerance, insulin resistance	(Buckley et al., 2005)
High calorie diet (60% fat, 20% sugar)	Mouse	M&F	D12-PD21	5 months (adipose): \uparrow <i>leptin</i> , <i>Gcg</i> \downarrow <i>Lepr</i> , <i>AdipoQ</i>	\uparrow plasma cholesterol, LDL cholesterol, triglyceride, FFA, leptin \downarrow HDL cholesterol, adiponectin, insulin sensitivity	(Khalyfa et al., 2013)
High calorie diet (60% fat, 20% sugar)	Rat	M	8 wks prior, D1-PD21	6 months (liver): \uparrow SCD-1	\uparrow adiposity, plasma TAG	(Seet et al., 2015)
High calorie diet (60% fat, 20% sugar)	Rat	M or M&F	14 weeks prior, D1-PD21	3 weeks (adipose): \downarrow <i>Pparγ</i> , <i>Srebp1</i> , \uparrow <i>Lpl</i> 9 months (adipose): \uparrow <i>leptin</i> , <i>Fas</i> , <i>Srebp1</i> and \downarrow <i>Pparγ</i> , <i>11βHsd1</i> , <i>Ob-Rb</i> (males), \uparrow <i>C/Ebpa</i> and \downarrow <i>Adipoq</i> , <i>Gr</i> (females)	\uparrow adiposity, plasma leptin, adipocyte hypertrophy and hyperplasia, plasma corticosterone and \downarrow insulin sensitivity, glucose	(Lecoutre et al., 2016, Lecoutre et al., 2018)

					tolerance (males), ↓ brown adipose (females)	
High calorie diet (60% fat, 20% sugar)	Rat	M	8 weeks prior, D1-PD21	1 day (adipose): ↑ C/EBPβ, PPARγ, SREBP1, FAS, HSL, ↓C/EBPα, SIRT1, NCoR, SMRT, SRC1 9 months (adipose): ↑ C/EBPβ, PPARγ, SREBP1, FAS, SRC1, TIF2 ↓ C/EBPα, HSL, LPL, SIRT1, NCoR, SMRT	↑ plasma glucose, insulin, triglycerides, adiposity	(Desai et al., 2015)
High calorie diet (62% fat, 20% sugar)	Mouse	M&F	D1-PD21	20 weeks (pancreas): ↓ <i>Pdx-1</i> (males) ↑ <i>Pdx-1</i> (females)	↓ insulin secretion in response to glucose, pancreatic insulin content, islet area and ↑ islet oxidative stress (males), ↑ insulin secretion in response to glucose, pancreatic insulin content, islet area (females)	(Yokomizo et al., 2014)
High calorie diet (62% fat, 20% sugar) with postnatal HFD challenge	Mouse	M&F			↑ hepatic triacylglycerol content, adipocyte area, markers of inflammation in adipose	(Yokomizo et al., 2014)
Streptozotocin injection to induce maternal diabetes						
Streptozotocin injection	Rat	M or M&F	Prior to mating	3 months (adipose): ↑ GLUT4, INSRβ, ACC	↑ plasma glucose, insulin, adipocyte diameter, adipose	(Kamel et al., 2014, Oliveira et

				5 months (liver): ↑ <i>G6pc</i> & <i>Pck1</i> (FOXO1 pathway) and <i>Pdk4</i> , <i>Cdkn1a</i> , <i>Gadd45a</i> , <i>Igfbp1</i> , <i>Hmox1</i> , ↓ <i>Srebf1</i> 2-7 months (muscle): ↓ INSR 2-7 months (adipose): ↓ INSR 4.5 months (muscle): ↓ GLUT4 (males) 4.5 months (adipose): ↓ GLUT4	glucose uptake ↓ glucose tolerance, insulin sensitivity	al., 2015, Dong et al., 2017, Inoguchi et al., 2019)
Streptozotocin injection with postnatal HFD challenge	Rat	M&F		4.5-7 months (adipose): ↓ GLUT4 7 months (adipose): ↑ <i>mTFA</i> 7 months (muscle): ↑ <i>mTFA</i>	↑↑ plasma glucose	(Kamel et al., 2014)
Streptozotocin injection	Rat	NS	D0	3 months (pancreas): ↓ <i>Kir6.1</i> , <i>Cdk4</i> , <i>E2f1</i>	↑ plasma glucose	(Nazari et al., 2017)
Streptozotocin injection	Rat	F	D0.5	7 months (adipose): ↑ <i>Tnfa</i>	↓ pancreatic islet area, glucose tolerance, ↑ plasma glucose	(Su et al., 2016b)
Streptozotocin injection with postnatal HFD challenge	Rat	F			↓↓ glucose tolerance	(Su et al., 2016b)
Streptozotocin injection	Rat	M	D6 and D12	4.5 months (pancreas): ↓ <i>Abcc8</i> , <i>Cav1.2</i> , <i>Cav2.3</i>	↓ insulin sensitivity, glucose tolerance, ↑ plasma insulin	(Zhu et al., 2019)
Streptozotocin injection with	Rat	M		4.5 months (pancreas): ↓↓ <i>Cav1.2</i>	↓↓ insulin sensitivity, glucose tolerance	(Zhu et al., 2019)

postnatal HFD

challenge

Table modified from Christoforou and Sferruzzi-Perri, (2020). Alterations in gene expression are indicated by italicisation, and alterations in protein abundance is not italicised. *Gestational age: mouse 20 days, rats 23 days* 11 β HSD1, 11 β -hydroxysteroid dehydrogenase type 1; A7nAChR, nicotinic acetylcholine receptor alpha7 subunit; Abcc8, ATP binding cassette subfamily C member 8; Acc, acetyl-coenzyme A carboxylase; AdipoQ, adiponectin; Akt, protein kinase B; Aqp7, aquaporin 7; ATP, adenosine triphosphate; C/Ebpa, CCAAT-enhancer-binding protein alpha; C/Ebpb, CCAAT-enhancer-binding protein beta; Cav1.2, calcium voltage-gated channel subunit alpha1 C; Cav2.3, calcium voltage-gated channel subunit alpha1 E; Ccna2, cyclin A2; Ccnf, cyclin F; Cd36, Cd36 molecule; Cd69, Cd69 molecule; Cdk4, cyclin dependent kinase 4; Cdkn1a, cyclin dependent kinase inhibitor 1A; Cidec, cell death inducing DFFA like effector C; Cldn2, Claudin 2; Cox2, cytochrome c oxidase subunit 2; Cpt1b, carnitine palmitoyltransferase 1B; CREB/ β , cyclic AMP-responsive element binding protein beta; Csf1, colony stimulating factor 1; Csf3, colony stimulating factor 3; Cxcl6, C-X-C motif chemokine ligand 6; E2f1, E2F transcription factor 1; F, females; Fabp2, fatty acid binding protein 2; Fas, fatty acid synthase; FFA, free fatty acid; FoxO1, forkhead box protein O1; G6pc, glucose-6-phosphatase catalytic subunit; Gabrp, gamma-aminobutyric acid type A receptor subunit Pi; Gadd45a, growth arrest and DNA damage inducible alpha; Gcg, glucagon; Gck, glucokinase; Glut, glucose transporter; Gpx1, glutathione peroxidase 1; Gr, glucocorticoid receptor; HDL, high density lipoprotein; HFD, high fat diet; Hmox1, heme oxygenase 1; HSL, hormone-sensitive lipase ortholog; Igf1, insulin-like growth factor 1; Igfbp1, insulin-like growth factor binding protein 1; Igfbp3, insulin-like growth factor binding protein 3; Ikk, I kappa B kinase; Il1-1a, interleukin 1-1a; InsR β , insulin receptor beta; Irs1, insulin receptor substrate 1; Jak2, janus kinase 2; Jnk, c-jun N-terminal kinase; Kir6.1, potassium inwardly rectifying channel subfamily J member 8; LDL, low density lipoprotein; Leptr, leptin receptor; Lpl, lipoprotein lipase; M, males; Mki67, marker of proliferation Ki-67; mTFA, mitochondrial transcription factor A; Mx2, Mx dynamin like GTPase 2; NCoR, nuclear receptor corepressor; NS, not specified; Ob-Rb, leptin receptor (long); PD, postnatal day; p16, cyclin dependent kinase inhibitor 2A; p85, phosphoinositide-3-kinase regulatory subunit; Pck1, phosphoenolpyruvate carboxykinase; PcnA, proliferating cell nuclear antigen; Pdk4, pyruvate dehydrogenase kinase 1; Pdx-1, pancreatic and duodenal homeobox 1; PEPCK, phosphoenolpyruvate carboxykinase; PI3K, phosphatidylinositol 3-kinase; Pkc ζ , protein kinase C zeta; Pmp22, peripheral myelin protein 22; Pon1, paraoxonase 1; Pon2 paraoxonase 2; Pon3 paraoxonase 3; Ppara, peroxisome proliferator-activated receptor alpha; Pparg, peroxisome proliferator-activated receptor gamma; Ptp1b, protein tyrosine phosphatase 1B; ROS, reactive oxygen species; Scd-1, stearoyl-CoA desaturase-1; Sirt1, sirtuin 1; Sln4, Schlafen 4; Smrt, silencing mediator for retinoid and thyroid hormone receptor; Sod1, superoxide dismutase 1; Src1, steroid receptor co-activator 1; Srebf1, sterol regulatory element-binding factor 1; Srebp1, sterol regulatory element-binding protein 1; Stat3, signal transducer and activator of transcription 3; TBARS, thiobarbituric acid reactive substance; Tbl1, transducing beta like 1 X-linked; Tif2, transcriptional intermediary factor 1; Tnfaip2, TNF alpha induced protein 2; Tnf α , tumour necrosis factor alpha; Ucp2, mitochondrial uncoupling protein; Wnt1, Wnt family member; Zfp423, zinc finger protein 423

1.5.3 Pancreatic morphology and insulin production in type 2 diabetes and mouse models of a high-nutrient environment *in utero*

In a normal adult human insulin is secreted from pancreatic β -cells in response to increased glucose levels and enhances the uptake of glucose into the skeletal muscle and adipose tissue whilst inhibiting hepatic glucose output. Conversely, pancreatic α -cells secrete glucagon, which increases blood glucose levels (Roder et al., 2016). In a healthy state, there is debate regarding the extent of β -cell neogenesis during adulthood, however studies in mice show that new β -cells form primarily through proliferation, rather than neogenesis (Dor et al., 2004, Georgia and Bhushan, 2004). During the development of type 2 diabetes, perturbances in pancreatic endocrine capacity and morphology occur (Ackermann and Gannon, 2007). In a pathological state, a compensatory increase in pancreatic β -cell mass and insulin secretion are observed in response to peripheral insulin resistance to maintain normoglycemia. However, when β -cell compensation fails, hyperglycaemia and type 2 diabetes are induced (Steil et al., 2001, Ackermann and Gannon, 2007). Indeed, approximately half of patients with type 2 diabetes mellitus also have endocrine pancreatic insufficiency (Hardt and Ewald, 2011). Although the mechanisms underlying β -cell compensation are incompletely understood, rodent models indicate an increase in β -cell mass occurs through a combination of increased neogenesis, survival and a transient increase in proliferation (Jetton et al., 2005). Moreover, compensatory hyperinsulinaemia is also observed with an increase in glucokinase activity in islets (Chen et al., 1994). In diabetic Zucker rats, hyperglycaemia precedes β -cell exhaustion, apoptosis and resultant insulin deficiency (Pick et al., 1998). Conversely, some clinical data support the onset of β -cell dysfunction prior to the development of hyperglycaemia in type 2 diabetes patients (Holman, 1998), albeit there is much debate regarding the chronological order and contribution of β -cell dysfunction and insulin resistance in the pathophysiology of type 2 diabetes.

Rodent models of a high-nutrient gestational environment also programme pancreatic morphology and insulin secretion capacity in offspring. Indeed, the hyperinsulinemia observed in these rodent offspring is also often accompanied by an increase in pancreatic islet mass (Theys et al., 2011, Brighenti et al., 2016) and may be a compensatory mechanism for the aforementioned insulin resistance. There are also changes in pancreatic insulin secretion and content in offspring of diabetic or high fat diet fed dams,

but these may be dependent on sex. For instance, in offspring from mothers fed a high fat diet, during gestation and lactation, female offspring display increased insulin secretion in response to glucose and increased pancreatic insulin content, whilst these measurements were reduced in male offspring (Yokomizo et al., 2014). Moreover, alterations in pancreatic insulin secretion likely influence the handling of insulin in peripheral tissues and may cause perturbations in glucose homeostasis.

1.6 Insulin signalling pathway

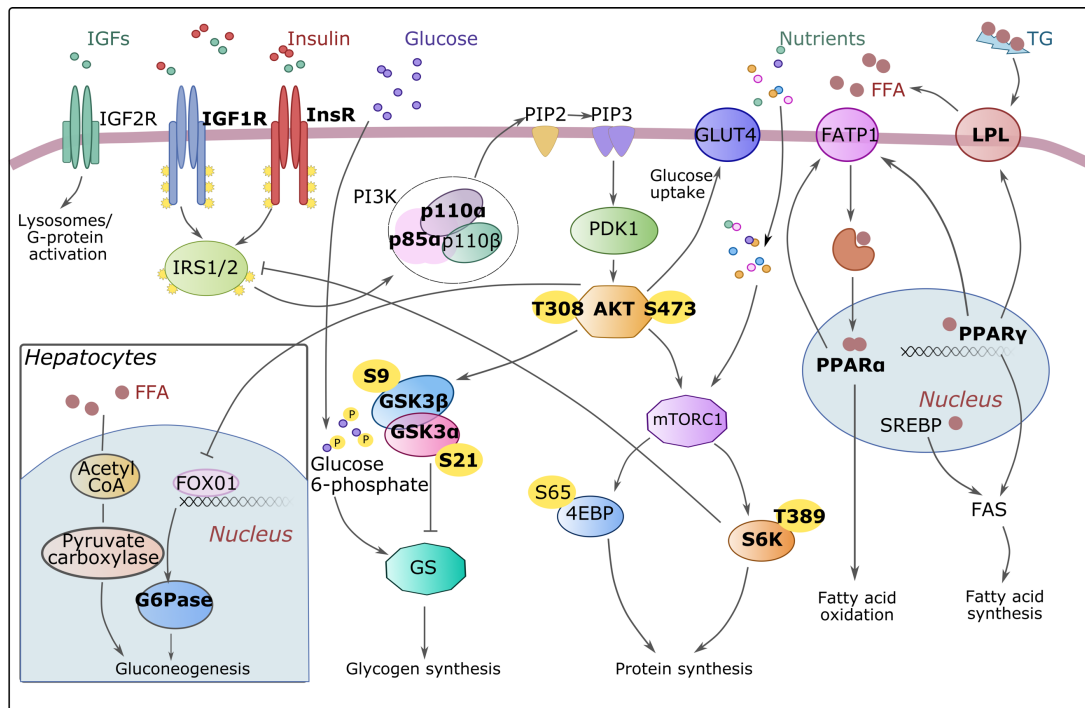


Figure 1.6. A schematic diagram of the insulin signalling pathway and cross talk between lipid metabolism and hepatic gluconeogenesis. Proteins in bold were measured in this study. 4EBP, eukaryotic translation initiation factor 4E binding protein; AKT, protein kinase AKT (kinase B); FABP, fatty acid binding protein; FAS, fatty acid synthase; FATP1, fatty acid transport protein 1; FFA, free fatty acids; FOXO1, forkhead box protein O1; G6Pase, glucose-6-phosphatase; GLUT4, glucose transporter 4; GS, glycogen synthase; GSK3, glycogen synthase kinase 3; IGF, insulin-like growth factor; IGF1R, insulin-like growth receptor 1; InsR, insulin receptor; IRS, insulin receptor substrate; LPL, lipoprotein lipase; ; mTORC1, mammalian target of rapamycin kinase complex 1; p85 α , PDK, phosphoinositol -dependent kinase -1; PI3K regulatory subunit; p110, PI3K catalytic subunit; PI3K, phosphoinositide 3-kinase; PIP2, phosphatidylinositol 4, 5 -biphosphate; PIP3, phosphatidylinositol 3, 4, 5 -phosphate; PPAR α , peroxisome proliferator activated receptor alpha; PPAR γ , peroxisome proliferator activated receptor gamma; S21, serine residue 21 of isoform GSK α ; S473, serine residue 473 of kinase AKT; S65, serine residue of 4EBP; S9, serine residue of isoform GSK3 β ; S6K, ribosomal S6 kinase; T308, threonine residue 308 of kinase AKT; SREBP, sterol regulatory element binding protein; T389, threonine residue of S6K; TG, triglycerides.

1.6.1 Insulin receptor (InsR) and insulin-like growth factor 1 receptor (IGF1R)

Insulin controls glucose homeostasis via the PI3K pathway (Figure 1.6). IGF1 and IGF2 signalling also occurs via the PI3K pathway. Insulin and IGFs act through InsR, a tetrameric transmembrane glycoprotein receptor belonging to the tyrosine kinase receptor family (White and Kahn, 1994). Insulin and IGFs also bind IGF1R, which has approximately 60% homology to InsR depending on the receptor domain studied (Belfiore et al., 2009). Both receptors are comprised of two α and two β subunits linked by a disulphide bond to form a crosslinked transmembrane receptor. Whilst the α subunit is primarily extracellular, the β subunit spans the plasma membrane. The α subunit contains the insulin binding domain, whereby insulin binding activates the enzymatic activity of the receptor and subsequent tyrosine phosphorylation of the β subunit, thus initiating the signalling cascade (Rosen, 1987, Seino et al., 1989, Tatulian, 2015). InsR and IGF1R can also form hybrid receptors, which have similar affinity for insulin as their homotypic receptor counterparts (Frattali and Pessin, 1993). Moreover, IGF2 also binds to IGF2R which either leads to its lysosomal degradation or G-protein coupled receptor signalling activation (Okamoto et al., 1990, Hawkes and Kar, 2004). The mechanisms that determine the outcome of this IGF2-IGF2R interaction remain unknown.

1.6.2 Insulin receptor substrate (IRS1/2)

Activation of InsR and IGF1R leads to the phosphorylation of several downstream protein mediators of the insulin signalling cascade (Figure 1.6). For instance, InsR phosphorylates a multitude of proteins, with data from adipocyte cultures *in vitro* indicating the phosphorylation of 122 tyrosine phosphorylation sites on 89 proteins upon insulin stimulation (Schmelzle et al., 2006). Of these, insulin receptor substrate 1 (IRS1) and IRS2 are required for the downstream responses induced by insulin and IGF1, with insulin resistance observed in IRS-knockout mice (Withers et al., 1999, Previs et al., 2000). Moreover, phosphorylation of IRS1 and IRS2 also occurs downstream of IGF1R (Cheng et al., 2010). Knockout studies indicate that IRS1 and IRS2 also mediate changes in lipid and carbohydrate metabolism downstream of insulin. This occurs, however, in a tissue-specific manner with IRS2 having a major role in the liver, skeletal muscle and adipose tissue whilst IRS1 is primarily involved in muscle (Previs et al., 2000). Protein

tyrosine kinases activate protein-protein interactions in the insulin signalling pathway via SH2 domains. For instance, IRS1 binds multiple SH2 proteins at several phosphotyrosine-containing sequences (Eck et al., 1993, Schlessinger, 1994).

1.6.3 Phosphatidylinositol 3-kinase (PI3K)

PI3K is composed of p110, a 110 kDa catalytic subunit, and p85 α , an 85 kDa regulatory subunit with two SH2 domains. Both the SH2 domains of p85 α are able to associate with IRS1 in its phosphorylated state (Sun et al., 1993). The p85 α gene can generate three protein products (p85 α , p55 α and p50 α) with tissue-specific distribution (Inukai et al., 1997). Whilst all isoforms can bind to the p110 catalytic subunit, p85 α and p50 α display a higher affinity for binding IRS protein compared to p55 α (Ueki et al., 2000). p85 α may act as a negative regulator of PI3K signalling, with free p85 α forming a complex with phosphorylated IRS so that IRS1 signalling via PI3K activation is downregulated (Luo et al., 2005). The catalytic subunit p110 also has several isoforms, namely, p110 α , p110 β and p110 δ , with p110 α and p110 β being the ubiquitous isoforms (Thorpe et al., 2015). In the insulin signalling pathway, PI3K increases the amounts of phosphatidylinositol 4,5-bisphosphate (PIP₂) and phosphatidylinositol 3, 4, 5 phosphate (PIP₃) which are formed on intracellular membranes. Subsequently, phosphoinositide-dependent kinase-1 (PDK1) activates AKT1 via phosphorylation at threonine 308 (T308; (Carpenter and Cantley, 1996, Alessi et al., 1997).

1.6.4 AKT and glycogen synthesis

Protein kinase B (AKT) is a serine threonine protein kinase and the central hub of the PI3K signalling pathway, with its activation leading to several pathways involved in cell proliferation, survival, differentiation, and glucose, carbohydrate and lipid metabolism (Figure 1.6; Manning and Cantley, 2007). Several isoforms of this protein kinase exist, namely AKT1, AKT2 and AKT3. Whilst AKT1 is expressed in all tissues, AKT2 is predominantly expressed in tissues sensitive to insulin, whilst AKT3 is expressed mainly in the brain and testes (Huang et al., 2018). AKT activation occurs at two sites: one site in the activation loop (T308) and one site in the hydrophobic motif (S473) through phosphorylation by PDK1 and mechanistic target of rapamycin complex 2 (mTORC2), respectively (Alessi et al., 1997, Sarbassov et al., 2005). AKT is critical in controlling glycogen synthesis, with insulin stimulating glucose uptake in tissues such as the liver

and muscle, and adipose tissue (Cusin et al., 1990, Crosson et al., 2003). Stimulation of glycogen synthesis occurs via phosphorylation and inactivation of GSK3, so that it is unable to inhibit glycogen synthase (GS), the enzyme required for glycogen synthesis (Cross et al., 1995). GSK3 has two isoforms which are closely related (GSK3 α and GSK3 β) and inhibition by AKT is a result of phosphorylation at an N-terminal serine residue, namely S21 in GSK3 α and S9 in GSK3 β (Woodgett, 1990, Cross et al., 1995). However, as phosphorylation of GSK3 by AKT2 is not essential for glycogen synthesis, it is evident that other pathways are also implicated (Wan et al., 2013). Indeed, GS is activated via interaction with glucose-6-phosphate, with this pathway critical in maintaining glycogen synthesis (von Wilamowitz-Moellendorff et al., 2013). Insulin stimulated phosphorylation of AKT2 also increases the translocation of glucose transporter 4 (GLUT4) to the plasma membrane by phosphorylation of the 160-kDa protein AS160 (Sano et al., 2003).

1.6.5 AKT and protein synthesis

AKT is important in cell growth and protein synthesis by activation of the mTORC1, which regulates the initiation of translation and is critical in ribosome biogenesis. Ribosomal S6 kinase (S6K) and eukaryotic translation initiation factor 4E binding protein (4EBP) are translation regulators that are targets of mTORC1 (Wullschleger et al., 2006). Whilst phosphorylation of AKT at T308 is essential for mTORC1 activation, phosphorylation at S473 is not (Rodrik-Outmezguine et al., 2011). mTORC1 activation inhibits 4EBP, leading to the activation of eIF4E which promotes the translation of a subset of mRNAs (Mamane et al., 2004). Activation of S6K by mTOR1 also leads to phosphorylation of the 40S ribosomal protein S6 and a subsequent increase in the translation of several mRNAs (Magnuson et al., 2012). Moreover, a negative feedback loop exists between IRS and the mTORC1-S6K pathway (Harrington et al., 2004). Indeed, S6K1 deficient mice have enhanced insulin sensitivity and are protected against diet-induced obesity (Um et al., 2004). Activation of AKT is also critical in the downstream activation of c-Jun N-terminal kinases (JNK)/p38, mitogen-activated protein kinase (MAPK), and B-cell lymphoma 2 (BCL-2)/BCL2 associated X, apoptosis regulator (BAX) which are involved in inflammation, proliferation and apoptosis, respectively (Sawatzky et al., 2006, Ola et al., 2011, Zhou et al., 2015b).

1.7 Lipid metabolism

Insulin, acting via mTORC1, is a key regulator of lipid metabolism. The synthesis of triglycerides and formation of fatty acids from acetyl-CoA, known as lipogenesis, is stimulated by, and dependent on, the levels of circulating insulin (Kersten, 2001). The sterol regulatory element binding proteins (SREBPs) are a family of basic helix-loop-helix leucine zipper transcription factors (Horton et al., 2002). The SREBPs exist in three isoforms, namely SREBP1a, SREBP1c and SREBP2. SREBP2 and SREBP1c activate genes involved in the cholesterol pathway and fatty acid synthesis, respectively. Furthermore, over-expression of SREBP1a enhances fatty acid synthesis/secretion in mice and produces fatty liver and adipocyte hypertrophy (Horton et al., 2002, Horton et al., 2003). Indeed, SREBP and the nuclear receptor peroxisome proliferator-activated receptor gamma (PPAR γ) stimulate transcription of the enzyme fatty acid synthase (FAS; Schadinger et al., 2005, Choi et al., 2008).

The PPARs are a group of closely related nuclear receptors which have been implicated in lipogenesis and fatty acid oxidation and thus are critical in maintaining whole body lipid homeostasis (Schoonjans et al., 1996b). PPARs form heterodimers with the retinoid X receptor (RXR) and after ligand binding, can bind the promoter and activate transcription. Ligands include polyunsaturated fatty acids, oxidised fatty acids, long-chain unsaturated fatty acids and eicosanoids (Tontonoz et al., 1994, Krey et al., 1997). The PPARs exist in three isoforms, namely PPAR α , PPAR δ (β) and PPAR γ . The expression of PPAR α is highest in brown adipose tissue, liver and skeletal muscle whilst PPAR δ (β) is expressed in almost all tissues abundantly. In contrast, PPAR γ expression is highest in white adipose tissue (Desvergne and Wahli, 1999, Evans et al., 2004). PPAR δ (β) has been comparatively less studied, however, it may be involved in lipid metabolism, as shown by its ability to transcriptionally regulate acyl-CoA synthetase 2 (ACS2; Basu-Modak et al., 1999). In fasted PPAR α null mice, plasma free fatty acid levels are elevated, due to inhibition of fatty acid uptake and oxidation. Thus, PPAR α is implicated in the stimulation of fatty acid oxidation to acetyl-CoA and thereafter, to ketone bodies in the liver (Kersten et al., 1999).

PPAR γ plays an important role in adipogenesis, controlling the terminal differentiation of adipocytes (Rosen et al., 1999). C/EBP α is another transcription factor involved in the differentiation of adipocytes and participates with PPAR γ in a single pathway of

adipocyte differentiation. C/EBP α induces the expression of PPAR γ and maintains the differentiated state in the mature adipocyte (Wu et al., 1999). Moreover, both PPAR γ and C/EBP α are key in maintaining insulin sensitivity. This has been shown by the presence of insulin resistance in mice deficient in PPAR γ , whilst knockout of C/EBP α in adipocyte culture prevents insulin-stimulated glucose transport and reduces IRS1 and insulin receptor phosphorylation (Wu et al., 1999, He et al., 2003). Activation of both PPAR α and PPAR γ via ligand binding positively regulates the expression of FATP1, which is critical in the delivery of FFA to PPARs, as well as to lipoprotein lipase (LPL; Schoonjans et al., 1996a, Martin et al., 2000). LPL is involved in the hydrolysis of triglycerides from very-low density lipoprotein (VLDL) and chylomicrons to generate free fatty acids (Goldberg et al., 1988). Moreover, in hepatocytes, LPL also increases the selective uptake of high-density lipoprotein (HDL) cholesterol esters (Rinninger et al., 1998). Physiological regulators of LPL include glucocorticoids, insulin, growth hormone, and prolactin which induce LPL enzyme activity (Enerback and Gimble, 1993).

1.8 Hepatic gluconeogenesis and lipid synthesis

Hepatocytes are a site of glucose and lipid uptake, and glucose production and metabolism. Thus, the liver is critical in maintaining whole body glucose homeostasis. In a normal physiological state, insulin acts on the liver to increase glycolysis and lipid synthesis. Activation of AKT by insulin leads to phosphorylation and inactivation of the transcription factor, FOXO1 (Figure 1.6; (Gross et al., 2008). FOXO1 regulates the expression of glucose-6-phosphatase (G6Pase) and phosphoenolpyruvate carboxykinase (PEPCK), two rate limiting enzymes involved in gluconeogenesis (Barthel and Schmolz, 2003). In addition to insulin, hepatic gluconeogenesis can also be regulated by the action of FFAs on the liver. For instance, endogenous fatty acid oxidation regulates hepatic gluconeogenesis through the formation of acetyl-CoA, an activator of pyruvate carboxylase (Ferre et al., 1979).

In the liver, FOXO1 also acts to inhibit lipogenesis by suppressing the expression of SREBP-1c via the reduction of the transcriptional activity of SREBP-1c and SP1 (Zhang et al., 2006, Deng et al., 2012). Moreover, insulin stimulates *de novo* hepatic lipogenesis through the SREBP-1 pathway. Subsequently this leads to the secretion of triacylglycerol (TAG) via the export of VLDL-TAG (Rui, 2014). However, it has also been proposed that hepatic triglyceride synthesis may occur independent of insulin and its signalling

pathway, requiring only fatty acids. Indeed, a study has shown the rate of fatty acid esterification into hepatic triglyceride is independent of plasma insulin concentration (Vatner et al., 2015). Thus, in a pathological state, in individuals who are insulin resistant, hepatic gluconeogenesis is not inhibited and hepatic lipid synthesis is increased so that concomitant hyperglycaemia and hyperlipidaemia are observed.

1.9 Insulin resistance

Insulin resistance refers to a state in which a reduction in the usual biological response to insulin is observed, in the presence of normal or elevated insulin concentrations. In the liver, insulin resistance leads to increased hepatic glucose production resulting in glucose intolerance and hyperglycaemia. In peripheral tissues such as skeletal muscle and adipose tissue, insulin resistance leads to a decreased ability of insulin to mediate glucose uptake via GLUT4 translocation (Wilcox, 2005). Insulin sensitivity can be studied both *in vivo* and *in vitro*. In humans, hyperinsulinemic-euglycaemic clamp studies, (which involves infusing a known constant concentration of insulin while infusing in a variable amount of glucose to maintain normal glucose concentrations) are considered the gold standard and are frequently used in a research setting. In a clinical setting, fasting plasma insulin levels are routinely measured, alongside mathematical modelling such as the Homeostasis Assessment Model (HOMA), using simultaneous measurements of fasting insulin and glucose (Wilcox, 2005, Kim, 2009). Moreover, identification of individuals at high risk for type 2 diabetes also involves the use of oral glucose tolerance tests (Stern et al., 2002). In rodent models of diabetes, insulin and glucose tolerance tests are frequently employed (Oliveira et al., 2015, Inoguchi et al., 2019), however diagnostic criteria to grade the stages of diabetes do not exist for rodent species.

1.10 Molecular alterations in mouse models of developmental programming

Insulin resistance can also be used to describe alterations at a molecular level, with the downregulation of the insulin receptor and several insulin-receptor substrates and signalling components dampening the ability of insulin to activate its pathway (Bruning et al., 1998, Dong et al., 2008, Kubota et al., 2016). Indeed, alterations in the aforementioned genes and proteins involved in insulin signalling, glucose and lipid metabolism occur in rodent offspring exposed to a high-nutrient, hyperglycaemic environment during gestation (i.e., maternal obesity and diabetes) and are associated with

previously discussed metabolic perturbations (Table 1.1). Reductions in the expression of receptors of the insulin signalling pathway (InsR, IGF1R) are observed in the liver of offspring exposed to a maternal high fat diet (Buckley et al., 2005, Pereira et al., 2015). Generally, decreases in the downstream signalling proteins of the insulin signalling pathway are also observed in offspring from diet-induced obese mothers, with decreased pAKT S473 in skeletal muscle and liver (Latouche et al., 2014, Pereira et al., 2015). However, in the muscle of these offspring, increases in InsR and p85 protein abundance are observed, which may be indicative of tissue-specific compensation for the hepatic insulin resistance present in these offspring (Buckley et al., 2005). Moreover, in the adult offspring born to dams with diabetes (streptozotocin treatment), a decrease in InsR in the muscle and adipose is observed, and a reduction in GLUT4 in these tissues is indicative of a reduced capacity to store glucose (Kamel et al., 2014). Overall, a reduction in the protein components in the insulin signalling pathway is indicative of insulin resistance at a molecular level, however alterations in protein abundance may be tissue-specific and vary with the specific maternal manipulation.

The hyperglycaemia observed in offspring from mouse dams given a high fat diet occurs with a concomitant increase in the protein abundance of PEPCK, the rate limiting enzyme involved in gluconeogenesis, in the liver (Fante et al., 2016). Moreover, hyperlipidaemia in these offspring is associated with increases in *Leptin*, CEBP β , PPAR γ , SREBP1, FAS and hormone sensitive lipase (HSL) expression in adipose tissue (Khalyfa et al., 2013, Desai et al., 2015). The abundance of genes and proteins involved in inflammation (tumour necrosis factor alpha, *Tnfa*, phosphorylated-JNK), growth and development (cyclin dependent kinase inhibitor 1A, *Cdkn1a*, *Wnt*), mitochondrial metabolism (uncoupling protein 2, *Ucp2*, mitochondrial complexes) and ion transport (calcium voltage-gated channel subunit alpha1 C, *Cav1.2*, calcium voltage-gated channel subunit alpha1 E, *Cav2.3*) are also altered in metabolic organs (pancreas, liver, skeletal muscle and adipose tissue) of rodent offspring exposed to maternal obesity and diabetes (Theys et al., 2011, Latouche et al., 2014, Zhu et al., 2019).

1.11 Sexual dimorphism in developmental programming

Rodent models of maternal diabetes and obesity indicate that in general, male offspring are programmed to have more negative metabolic consequences compared to female offspring (Ornellas et al., 2013, Lecoutre et al., 2016, Inoguchi et al., 2019). Indeed, both

animal models and epidemiological studies show that sex differences are evident in the prevalence, pathophysiology and outcomes of metabolic syndrome and type 2 diabetes mellitus. For instance, men are diagnosed with diabetes at a lower body mass index (BMI) and younger age compared to women in European populations (Logue et al., 2011). Moreover, GDM is a risk factor for childhood obesity in male, but not female offspring (Li et al., 2017, Le Moullec et al., 2018). The molecular mechanisms underlying these sexual disparities are poorly understood, and as most studies in rodent models of programming study only male offspring, this makes it more difficult to address this phenomenon.

1.11.1 Sexual dimorphism in adulthood in developmental programming

During adulthood, sex steroids may contribute to the sexual discrepancies observed in the severity and pathophysiology of type 2 diabetes developed in programmed offspring. For instance, oestrogen, and its associated signalling pathway, has protective effects on the development of metabolic syndrome and type 2 diabetes. This has been shown in male mice with aromatase (CYP19) deficiency displaying insulin resistance, and in humans where pharmacological inhibition of aromatase decreases insulin sensitivity in healthy men (Takeda et al., 2003, Gibb et al., 2016). The oestrogen receptor α (ER α) has also been implicated in the pathology of metabolic disease, with its activation preventing insulin resistance, liver steatosis and obesity in mice (Guillaume et al., 2017, Guillaume et al., 2019). In contrast, androgens such as testosterone enhance the development of metabolic syndrome and type 2 diabetes. For instance, insulin resistance induced by glucocorticoids is potentiated by androgens in mice (Gasparini et al., 2019). Moreover, in female mice, hyperandrogenaemia leads to concomitant insulin resistance (Skarra et al., 2017), whilst women with PCOS associated with hyperandrogenaemia have a higher propensity to develop insulin resistance when obese (Al-Jefout et al., 2017).

1.11.2 Sexual dimorphism in prenatal mechanisms of developmental programming

Several differences in the temporal and hormonal development of male and female fetuses *in utero* may also underlie the sexual disparity observed in developmental programming outcomes. Temporal sex differences are evident during gestation in mice, with male embryos developing at a faster rate compared to female embryos (Tsunoda et al., 1985, Valdivia et al., 1993). Moreover, in mice, sex differences are also evident in

fetal circulating corticosterone levels, with higher corticosterone levels in female compared to male fetuses due to greater transport from the maternal circulation across the placenta (Montano et al., 1993). Corticosterone levels are also altered in a sex-specific manner in response to maternal stressors such as a high fat diet during pregnancy (Chin et al., 2017). Prenatal stress in mice also alters placental gene expression in a sex-dependent manner, with specific sex-chromosome genes playing an important role. For instance, expression of the X-linked gene encoding O-GlcNAc transferase (OGT) is lower in male placentas and reduced further in response to maternal chronic variable psychological stress (Howerton et al., 2013). OGT also determines sex differences in placental H3K27me3, a repressive histone marker (Nugent et al., 2018). Furthermore, H3K27me3 regulates sex-specific trophoblast gene expression in response to prenatal chronic variable psychological stress (Nugent et al., 2018). Thus, sexual dimorphism in gene expression in response to stressors during gestation may be controlled in an epigenetic manner.

1.12 Epigenetic mechanisms in developmental programming

Epigenetics has been described as “the structural adaptation of chromosomal regions so as to register, signal or perpetuate altered activity states” (Bird, 2007). Such epigenetic modifications can be categorised as alterations in DNA methylation, histone modifications and alterations in small non-coding RNAs (Gibney and Nolan, 2010). In the context of rodent models of developmental programming, changes in the expression of metabolic genes may be altered in an epigenetic manner. For instance, offspring exposed to a maternal high fat diet display altered methylation at the promoters of genes involved in lipid metabolism (*Ppar γ* , *Fas* and *Leptin*) which is linked to changes in the expression of these genes, as well as increases in adipose expansion and circulating triglycerides (Khalyfa et al., 2013, Jiao et al., 2016, Lecoutre et al., 2018). Moreover, histone modifications at the promoter of genes involved in lipid metabolism (*Ppar γ 2*, *Leptin*) and glucose metabolism (*Pepck*, *Pck1*, *Gck*) in the liver and adipose of these offspring has also been observed (Strakovsky et al., 2011, Masuyama et al., 2015, Zhou et al., 2015a, Panchenko et al., 2016, Lecoutre et al., 2018). Alterations in the abundance of several miRNAs have been indicated in rodent offspring from obese dams in key metabolic organs such as the liver (*miR-122*, *miR-370*, *miR-615*, *miR-143*) and adipose tissue (*miR-126*, *miR-204*; Benatti et al., 2014, Fernandez-Twinn et al., 2014, Zheng et al., 2016, de Paula Simino et al., 2017, Wang et al., 2019a). In addition to these

epigenetic alterations, developmental programming may also be attributed to many other mechanisms including *de novo* point mutations, the maternal transmission of microorganisms to offspring or modifications to mitochondrial DNA (Simmons et al., 2005, Jia et al., 2013, Turner and Robker, 2015, Calatayud et al., 2019).

1.13 Overall Objectives and Aims

1.13.1 Background

Exposure to stressors *in utero* can change gene expression in key metabolic organs in offspring via epigenetic processes and lead to alterations in the morphology and function of these tissues resulting in metabolic disturbances in adulthood (Fernandez-Twinn et al., 2019). Maternal insults during gestation are mediated by the placenta, which provides a feto-maternal interface and can adapt morphologically and functionally to improve fetal outcomes (Fowden and Moore, 2012). The placenta also secretes hormones, which adapt maternal physiology (Napso et al., 2018). Thus, placental endocrine malfunction may negatively influence offspring outcomes (both directly through altered endocrine output and indirectly via changes in maternal metabolism), implicating the placenta as both a mediator and a cause of offspring programming. Indeed, via *Igf2P0* knockout, the placenta has been directly shown to programme offspring emotional behaviour (Mikaelsson et al., 2013), however the consequences of placental manipulation and subsequent programming of offspring metabolism has not yet been described. Moreover, despite *Igf2* also being critical in the development of placental endocrine cells in the mouse (Lopez et al., 1996, Esquiliano et al., 2009, Aykroyd et al., 2020), this paternally expressed gene has not been used as a tool to modify the development of the placental endocrine layer and study in depth, consequent fetal and adult offspring outcomes. To address this, a new mouse model has been developed, whereby the two reciprocally expressed imprinted genes *H19* and *Igf2* are misexpressed only in the Jz of the placenta. This is achieved through the manipulation of the *H19/Igf2* imprinting control region (ICR) using the Jz-specific *Cre* line, *Tpbpa-Cre* (Jz-ICR1 Δ). In the following studies, placentas, dams and offspring will be referred to as Jz-ICR1 Δ for ease, however it is important to note that only the placental Jz (and not the mother or fetus) has been genetically manipulated.

Experimental work in our laboratory has previously illustrated that in this mouse model of placental endocrine region manipulation, overgrowth of the placental Jz occurs (Lopez-Tello et al. unpublished) and there are perturbations in maternal metabolism, as summarised in Table 1.13.1. In particular, dams have increased circulating levels of insulin, glucose and leptin on E16 and E19. Moreover, plasma lipid concentrations are altered, however this is dependent on gestational age. These changes in maternal metabolic state due to Jz-ICR1 Δ resemble features of GDM in women (Carpenter and Coustan, 1982, Kautzky-Willer et al., 2001, Riskin-Mashiah et al., 2010, Bao et al., 2018). Despite placental endocrine zone expansion and alterations in the maternal metabolic environment, fetal weight is unaltered at E16. However, nothing is known about the impact of Jz-ICR1 Δ on nutrient supply capacity in relation to fetal development in the lead up to term. Moreover, the consequences of endocrine zone manipulation and altered gestational environment due to Jz-ICR1 Δ on the metabolic health of female or male offspring on a chow or high sugar and fat (HSHF) diet postnatally also remain unknown.

Table 1.13.1. Summary of changes to metabolism in Jz-ICR1 Δ dams on day 16 and day 19 of pregnancy.

E16	E19
↑ glucose, insulin, leptin	↑ glucose, insulin, leptin
↑ progesterone, oestradiol	↔ progesterone, oestradiol
↑ LDL-C, ↔triglycerides, ↓NEFA	↔ LDL-C, ↑ triglycerides, ↑NEFA
↑ corticosterone	↔ corticosterone
↔ AAs	↓ AAs
↔ IGF2	↔ IGF2

Data collected by Dr Jorge Lopez-Tello and Dr Amanda Sferruzzi-Perri. AAs, amino acids; E16, embryonic day 16; E19, embryonic day 19; IGF2, insulin-like growth factor 2; LDL-C, low density lipoprotein cholesterol; NEFA, non-esterified fatty acids

1.13.2 Study Aims

The overall objective of this project is to assess the effect of placental endocrine zone manipulation (via Jz-ICR1 Δ) on placental morphology, hormone production, nutrient supply capacity and fetal growth, and in the programming of metabolic health outcomes in adult offspring. It also seeks to understand whether programmed metabolic health outcomes may relate to changes in the transcriptome of a key metabolic organ, the liver of the fetus. This study hypothesises that the altered maternal gestational environment induced by Jz-ICR1 Δ dams has consequences for fetal nutrient supply, growth and hepatic transcriptome and as a result, programmes alterations in the metabolic health of adult offspring.

The specific aims of this study are as follows:

- To determine the effect of placental endocrine zone manipulation (Jz-ICR1 Δ) on placental morphology, hormone production and nutrient transport capacity in relation to fetal growth (Chapter 3).
- To assess the impact of Jz-ICR1 Δ on the metabolic outcomes of adult offspring on a postnatal chow or HSHF diet (Chapter 4).
- To evaluate the effect of Jz-ICR1 Δ on the transcriptome of the fetal liver and examine whether gene expression changes may persist into adult life (Chapter 5).

Chapter 2: General materials and methods

2.1 Animals

Experiments were performed under the UK Home Office Animals (Scientific Procedures) Act 1986, approved by the Animal Welfare and Ethical Review Body at the University of Cambridge. The Home Office project licence number is 70/7645. Mice were group housed prior to mating in open cages and given *ad libitum* access to tap water and standard chow diet (RM3, SDS diets; Table 2.3). The temperature of the animal room was maintained at 22 °C and the lighting was under a 12:12 h dark/light photocycle. All mice were bred on a C57BL/6N (Charles River) background for at least 10 generations. Female mice carried a mutation on chromosome 7, upstream of the *H19* gene to delete the ICR1. The mutation was achieved using a targeting vector carrying a *loxP* site at the -0.8-kb *XbaI* site and a neomycin resistance gene flanked by *loxP* sites at the -7.0-kb *HindIII* site (distances are relative to the transcriptional start of *H19*; (Srivastava et al., 2000). Female mice were mated with males expressing *Cre* recombinase under the promoter of the Jz-specific gene, *Tpbpa* (*Tpbpa-Cre*). The reverse parental cross was utilised as a control in all experiments (Figure 2.1). Mouse lines for this study were kindly provided by Dr Miguel Constancia and Dr Ionel Sandovici. The specificity of the *Tpbpa-Cre* line has been previously demonstrated by others (Simmons et al., 2007, Hu and Cross, 2011), including in the Sferruzzi-Perri lab by using the tdTomato reporter mouse line to verify *Tpbpa-Cre* activity in just the placental Jz (leaving the placental Lz, fetus and maternal tissues unaltered; data not shown). Furthermore, the efficiency of the *Tpbpa-Cre* mouse line for altering the expression of *Igf2* specifically in the Jz has been demonstrated in litters of mixed genotype by others in the laboratory (Aykroyd et al., 2020, Aykroyd et al., 2021).

A Breeding strategy



B Reverse parental cross

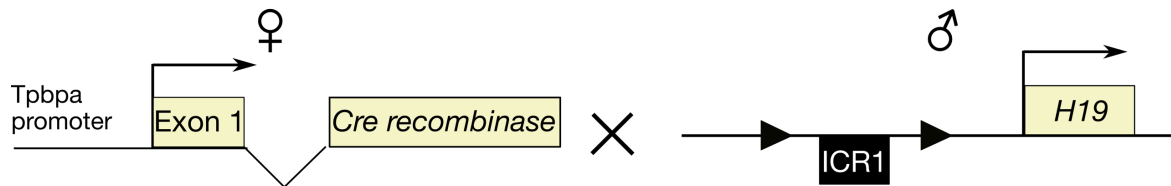


Figure 2.1 Mouse breeding strategy. Triangles represent excision sites. *LoxP* sites are 34 base pairs long. Arrows represent gene expression. ICR1, imprinting control region 1; Tpbpa, trophoblast-specific protein alpha

2.2 Experimental procedures I: The effect of Jz-ICR1 Δ on placental morphology and nutrient transport capacity

2.2.1 Breeding study design

Female mice (six to eight weeks old, >20 g) were placed in cages with a male stud in the afternoon and left overnight. The presence of a vaginal copulatory plug the following morning was defined as E1 of pregnancy. Dam weights were recorded on E1 and E16 or E19 (where term is E20). On E16 or E19, dams underwent a placental transport assay (PTA) and/or were killed by cervical dislocation and placentas taken for morphological assessment or separated into Jz and Lz and snap frozen. Placentas chosen for analysis were those closest to the mean placental weight of each litter. The time-points E16 and E19 were chosen as these are the gestational periods representing maximal placental and fetal growth, respectively (Coan et al., 2004). The number of mice used for pregnancy and offspring studies are shown in Table 2.1. Offspring procedures are described in section 2.3.

Table 2.1. Number of mice used for pregnancy and offspring studies. The number of animals (pregnancy and adult offspring) used for biometry represents the total number of animals used. Additional procedures were carried out in a proportion of these animals prior to biometry. A portion of animals during pregnancy were used for studies external to the ones currently described (i.e., maternal studies). A portion of animals at E19 were also utilised for fetal liver RNA sequencing/qPCR validation (Chapter 5). The composition of diets is detailed in Table 2.3.

Study	Diet	Genotype	Age	Procedure	Number	Chapter
Pregnancy	Chow	Control	E16	PTA	6	3
	Chow	Jz-ICR1 Δ	E16	PTA	6	3
	Chow	Control	E19	PTA	8	3 and 5
	Chow	Jz-ICR1 Δ	E19	PTA	8	3 and 5
	Chow	Control	E16	Biometry	31	3
	Chow	Jz-ICR1 Δ	E16	Biometry	29	3
	Chow	Control	E19	Biometry	30	3 and 5
	Chow	Jz-ICR1 Δ	E19	Biometry	29	3 and 5
Offspring	Chow	Control	16 weeks	GTT	10	4
	Chow	Jz-ICR1 Δ	16 weeks	GTT	14	4
	Chow	Control	16 weeks	ITT	12	4
	Chow	Jz-ICR1 Δ	16 weeks	ITT	12	4
	Chow	Control	3 days	Biometry	19	4
	Chow	Jz-ICR1 Δ	3 days	Biometry	30	4
	Chow	Control	17 weeks	Biometry	45	4 and 5
	Chow	Jz-ICR1 Δ	17 weeks	Biometry	46	4 and 5
	Diet A	Control	16 weeks	ITT	8	Appendix
	Diet A	Jz-ICR1 Δ	16 weeks	ITT	10	Appendix
	Diet B	Control	16 weeks	GTT	13	4
	Diet B	Jz-ICR1 Δ	16 weeks	GTT	14	4
	Diet B	Control	16 weeks	ITT	12	4
	Diet B	Jz-ICR1 Δ	16 weeks	ITT	10	4
	Diet B	Control	17 weeks	Biometry	46	4
	Diet B	Jz-ICR1 Δ	17 weeks	Biometry	41	4

E, embryonic day; GTT, glucose tolerance test; ITT, insulin tolerance test; PTA placental transport assay

2.2.2 Placental transport assay

Jz-ICR1Δ and control dams underwent a PTA on either E16 or E19, as described previously (Sferruzzi-Perri, 2018a). An intraperitoneal injection containing 10μg/mL fentanyl-fluanisone, midazolam and water in a 1:1:2 ratio (Janssen Animal Health, High Wycombe, UK) was administered to dams to induce anaesthesia. The mouse was placed on its back on a heat pad to maintain an appropriate body temperature and the depth of anaesthesia was confirmed by squeezing the foot to check for reflexes. To dampen down fur, the mouse neck was doused with 70% ethanol prior to making a ~ 2 cm incision to expose the jugular vein. A catheter, with a 25-gauge needle attached was weighed before and after the addition of 200 μL bolus of ³H-MeG (MeGlu; NEN NEC-377; specific activity 2.1 GBq/mmol; Perkin-Elmer) and ¹⁴C-MeAIB (MeAIB; NEN NEC-671; specific activity 1.86 GBq/mmol), prepared in a 1:1 ratio. MeAIB is a non-metabolisable amino acid analogue that is transported utilising the System A amino acid transport system. Pressure was applied to the distal end of the jugular vein with a cotton tip and the catheter was inserted at a shallow angle. Thereafter, the needle was held in place with forceps whilst the radioactive isotope was slowly infused into the mouse. As the catheter was withdrawn, pressure was applied with a cotton tip to the injection site. The experiment was terminated between 1- and 4-minutes post isotope infusion by using operating scissors to open the chest cavity and cutting the top of the heart to exsanguinate the blood. Maternal blood was collected with a syringe and placed in a pre-chilled ethylenediaminetetraacetic acid (EDTA) tube stored on ice. Cervical dislocation was used to ensure the dam was euthanised and the time allowed for the tracer to enter the circulation was recorded. The peritoneal cavity was opened and the number of viable and resorbed fetuses counted in the left and right uterine horns prior to removal of the uterus. Upon removal of the uterus, the dam carcass weight was recorded, and the fetuses were separated from their respective placentas and fetal membranes. Placentas and fetuses were dried and weighed and the fetuses were decapitated. Placentas near the average weight were selected for stereology and qPCR analysis. Fetal tails were collected in labelled Eppendorf tubes and placed on ice to allow for fetal sexing at a later date. Fetuses were thoroughly minced with a scalpel blade and placed into 15 mL screw cap tubes containing either 2 mL (for E16) or 4 mL (for E19) Biosol (National Diagnostics) and shaken. Maternal blood was centrifuged at 3,000 x g for 10 minutes at 4°C. Maternal plasma was transferred to an Eppendorf tube and stored at -20°C for analysis at a later date. Maternal

plasma samples were prepared in triplicate, with 2 μL plasma, 198 μL Biosol and 4 mL AS ScintLogic scintillation liquid (LabLogic). Fetal samples, immersed in Biosol, were incubated for one week at 55 $^{\circ}\text{C}$ prior to determining fetal radioactive counts. Fetal samples were prepared in duplicate, with 250 μL or 500 μL lysate (for E16 or E19 respectively) and 4 mL AS ScintLogic scintillation liquid (LabLogic). Samples were placed into a Hidex 200 SL Liquid Scintillation Counter (LabLogic) with ^3H and ^{14}C standards and β particle emissions recorded in disintegrations per minute (DPM).

The average DPM counts from the fetal and maternal samples were calculated and corrected for the dilution used. Background value counts (with no sample) from each run were subtracted from fetal and maternal sample counts. MeGlu (glucose) and MeAIB (system A amino acid) clearance curves were generated, plotting maternal plasma DPM/ μL and time points (Figure 2.2). The area under curve (AUC) values of MeGlu and MeAIB clearance were used to determine placental glucose and amino acid clearance per gram of placenta or divided by the average value of the trophoblast membrane surface area per genotype (described in section 2.2.6.3). The placental transport assay procedure was performed by Dr Amanda Sferruzzi-Perri and Dr Jorge Lopez-Tello.

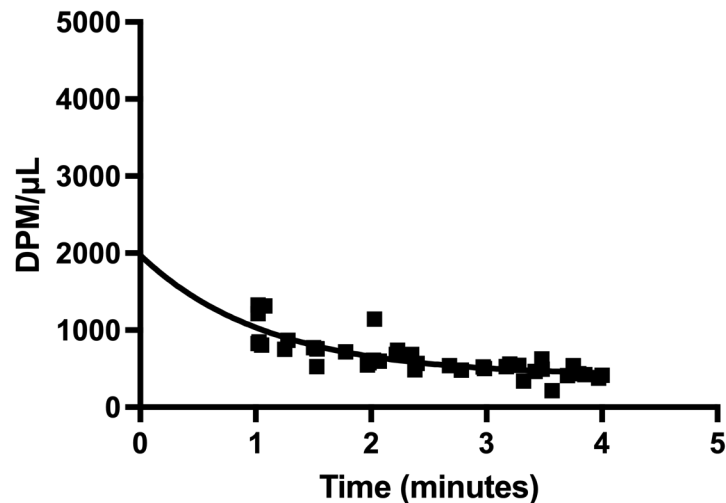


Figure 2.2. One-phase exponential decay curve for MeAIB. Each data point represents DPM counts in a plasma sample from a single dam on either E16 or E19 of pregnancy.

2.2.3 SRY sexing

Fetal tails were immersed in 200 μ L lysis buffer (Appendix 3.1, Table A3.1.1) and incubated at 55 $^{\circ}$ C overnight. The following day, fetal tail mixtures were incubated at 95 $^{\circ}$ C for 15 minutes and stored at 4 $^{\circ}$ C. Fetal sex was determined using the sex determining region Y (SRY) detection method. Briefly, reaction mixes containing 0.5 μ L each of primers (see Appendix 3.1, Table A3.1.2 for sequences), 9.5 μ L nuclease free water and 12.5 μ L RedTaq Mix (Sigma-Aldrich) were prepared with 1 μ L fetal tail DNA (\sim 50ng) in 200 μ L strip tubes with a no-template negative control and known female and male positive controls. Reaction mixes were subjected to the following conditions on a MiniAmp Plus Thermal Cycler (Applied Biosystems, Thermofisher): five cycles of 94 $^{\circ}$ C for 30 seconds, 60 $^{\circ}$ C for 1 minute, 72 $^{\circ}$ C for one minute and thereafter 72 $^{\circ}$ C for 10 minutes. PCR products were loaded on a 2% agarose gel (Appendix 3.1) with a DNA ladder (New England BioLabs) and underwent electrophoresis at 120V for 20-30 minutes. Bands were visualised on an iBright 1500 Imaging System (Invitrogen, Thermofisher).

2.2.4 Placental histological preparation

Bisected mouse placentas (E16 and E19) were fixed in 4% paraformaldehyde (PFA; Sigma-Aldrich) overnight at 4 $^{\circ}$ C and then transferred to a 70% ethanol solution. Tissue was processed using a Benchtop Tissue Processor (Leica Biosystems; 1 hour in 90% ethanol, three hours in 100% ethanol, 2 hours in HistoClear solution and 4 hours in wax) and then embedded in paraffin wax. Using a manual rotary Leica RM2235 microtome, a placental half was exhaustively sectioned at 8 μ m with the theoretical horizontal plane indicated by the chorionic plate. The placental mid-line was identified by the presence of all placental layers alongside a complete chorion, at which point the first 20 mid-line placental sections were kept for analysis. Thereafter, every 20th section throughout the placental half was stained with haematoxylin and eosin (H&E; Sigma-Aldrich) using a standard protocol. Slides were dehydrated through an ethanol series, placed in xylene and coverslip-mounted using dibutylphthalate polystyrene xylene (DPX; Sigma, Life Science) and analysed for gross placental structure.

2.2.5 Placental immunohistochemistry

One placental section (E16 and E19) close to the midline was immuno-stained to detect both fetal capillaries (FC) and trophoblast (T) with lectin and cytokeratin, respectively. Lectin I from the African legume plant *Griffonia simplicifolia* (GS-I) specifically binds monosaccharides, α -linked 2-acetamido-2-deoxy-d-galactopyranose (DGalNAc) and α -linked d-galactose (DGal) glycans across different species (Wood et al., 1979, Lescar et al., 2002) and in this instance, was utilised to bind to endothelial glycans of the FC. All trophoblast lineages in the mouse placenta were detected by immuno-staining for cytokeratin, which belongs to a subfamily of intermediate filament proteins and are unique to epithelial cells (Coulombe and Omary, 2002).

Placental sections were deparaffinised in xylene and progressively rehydrated through an ethanol series. Slides were heated in sodium citrate buffer (Appendix 3.2, Table A3.2.1) for antigen retrieval at 80 °C for 20 minutes. Endogenous peroxidases were blocked with 3% hydrogen peroxide (Fisher Chemical) in methanol for 10 minutes at room temperature. To prevent non-specific binding of antibodies, the sections were blocked with 1% bovine serum albumin (BSA; Sigma, Life Science) in phosphate buffered saline (PBS) for one hour at room temperature. To stain for lectin, the sections were incubated with primary antibody (Biotinulated *Griffonia Simplicifolia* Lectin I (GSL I) isolectin B4; Vector, B-12-5) diluted 1:200 in PBS with 1% BSA (Sigma, Life Science). Thereafter, the slides were washed in PBS and were incubated with streptavidin-horse radish peroxidase complex (Rockland) and stained with 3,3'-diaminobenzidine (DAB; Abcam) and ammonium nickel (II) sulphate hexahydrate (Aldrich Chemistry) solutions.

Sections were re-blocked for one hour at room temperature with 10% goat serum (Abcam) in 1% BSA in PBS and then incubated with a rabbit-raised polyclonal primary antibody against cytokeratin (Life Technologies) diluted 1:100 in 10% goat serum in 1% BSA in PBS overnight at 4 °C in a humid chamber. Slides were washed in PBS and incubated with a goat anti-rabbit secondary antibody (Abcam, Ab6720) for one hour at room temperature. Thereafter, sections were washed in PBS and stained with DAB. The reaction was quenched by rinsing in PBS and slides were counterstained with H&E using standard protocol. Eosin staining aided in the visualisation of maternal and fetal blood

cells. Thereafter, slides were dehydrated through an ethanol series, placed in xylene and coverslip-mounted using DPX.

2.2.6 Placental stereological analysis

2.2.6.1 Placental compartment volumes

Placental compartment volumes were obtained by means of the Cavalieri principle, using the Computer Assisted Stereological Toolbox (CAST v2.0, Olympus) according to Coan et al, (2004). In particular, point sampling on placental sections was used to determine volume densities as a fraction of placental components, with the assumption that test points hit these components with probabilities relative to their volumes (Mayhew, 2006). A 16-point grid was superimposed at 10x magnification on each H&E-stained placental section and each point was assigned as either Lz, Jz or Db. The total points in each section were summed and the volume density of each zone, VD_Z , was calculated as follows:

$$VD_Z = \frac{N_Z}{N_T}$$

Where N_Z = the sum of points in a placental zone per placenta and N_T = the sum of all points in a placenta

Absolute volumes were determined by multiplying volume densities by the placental mass (assuming that mass is equal to volume). Stereological analysis was performed blind, without knowledge of the group (placental genotype and sex).

2.2.6.2 Junctional zone morphology

Junctional zone cell type volumes were determined by using a high-throughput slide scanner NanoZoomer 2.0-RS (Hamamatsu Photonics, Japan) to scan slides. An 81-point grid was superimposed at 10x magnification on the first complete mid-line placental section. Each point was assigned as a different Jz and Db cell, namely spongiotrophoblast cell, glycogen cell, trophoblast giant cell, decidual stromal cells, decidual glycogen cells and decidual vessels. Each cell type was quantified as a proportion, which was converted to a cell volume by multiplying with either the Jz or Db volume (depending on cell

location). The whole area of each placental section was analysed. The volume of Jz clusters in the LZ was determined by manually drawing around each cluster using NanoZoomer Digital Pathology view software (version 2.7, Hamamatsu Photonics, Japan).

2.2.6.3 Labyrinth zone morphology

Labyrinth zone analyses were also performed according to Coan et al, (2004) with the only modification being the use of bright-field microscopy with the high-throughput slide scanner Nanozoomer 2.0-RS (Hamamatsu Photonics, Japan) to scan slides and using NanoZoomer Digital Pathology view software (version 2.7, Hamamatsu Photonics, Japan) to make measurements.

The volume fraction densities of MBS, FC and T present in the labyrinth zone were determined by identifying these components on sixteen equidistant random, non-overlapping fields at 40x magnification (Figure 2.3A). The number of points hitting the labyrinth component of interest was divided by the sum of points hitting all components. Absolute component volumes were determined by multiplying volume fraction densities by labyrinth zone volume.

Vascular surface densities were determined by the superimposition of randomly positioned cycloids on placental sections. The number of times lines encounter fetal membranes correlate to the membrane surface density (Mayhew, 2006). Thus, vascular surface densities were determined using a cycloid arcs grid and counting the number of intersections between cycloid arcs and MBS and FC surfaces of the interhaemal membrane in 20 randomly selected fields at 80x magnification (Figure 2.3B). The following equation was employed to convert MBS and FC vascular surface densities to vascular surface area:

$$Surface\ area = \frac{2 \times \Sigma I_{(struct)}}{I_{(p)} \times \Sigma P_{(ref)}} \times V_{(Lz)}$$

Where $\Sigma I_{(struct)}$ = total number of intersections of cycloid arcs with the structure; $\Sigma P_{(ref)}$ = total number of points that hit the reference space; $I_{(p)}$ = length of cycloid arc and $V_{(Lz)}$ = labyrinth zone volume.

The average of the MBS and FC surface area values was calculated to determine the mean surface area of the placental labyrinth.

Barrier thickness was determined by making 200 measurements of the interhaemal trophoblast membrane. Measurements of the shortest distance between FC and MBS were taken using orthogonal intercept lengths as a guide in randomly selected fields. The harmonic interhaemal trophoblast membrane thickness was determined by calculating the reciprocal of each measure, averaging these values, and determining its reciprocal. Values were multiplied by a correction factor of $(8/3)\pi$ to correct for the plane of sectioning. Capillary length density was determined by counting the number of fetal capillaries within a counting frame comprised of two contiguous forbidden lines in 20 randomly selected fields. Absolute capillary length was determined by multiplying capillary length density by labyrinth zone volume. The following equation was used to determine capillary diameter:

$$diameter = 2 \left(\frac{mean\ area}{\pi} \right)^{1/2}$$

The theoretical diffusion capacity was determined by multiplying the surface area by Krogh's constant for oxygen diffusion ($17.3 \times 10^{-8} \text{ cm}^2 \text{ min}^{-1} \text{ kPa}^{-1}$) and dividing by barrier thickness. Specific theoretical diffusion was calculated as a proportion of fetal weight.

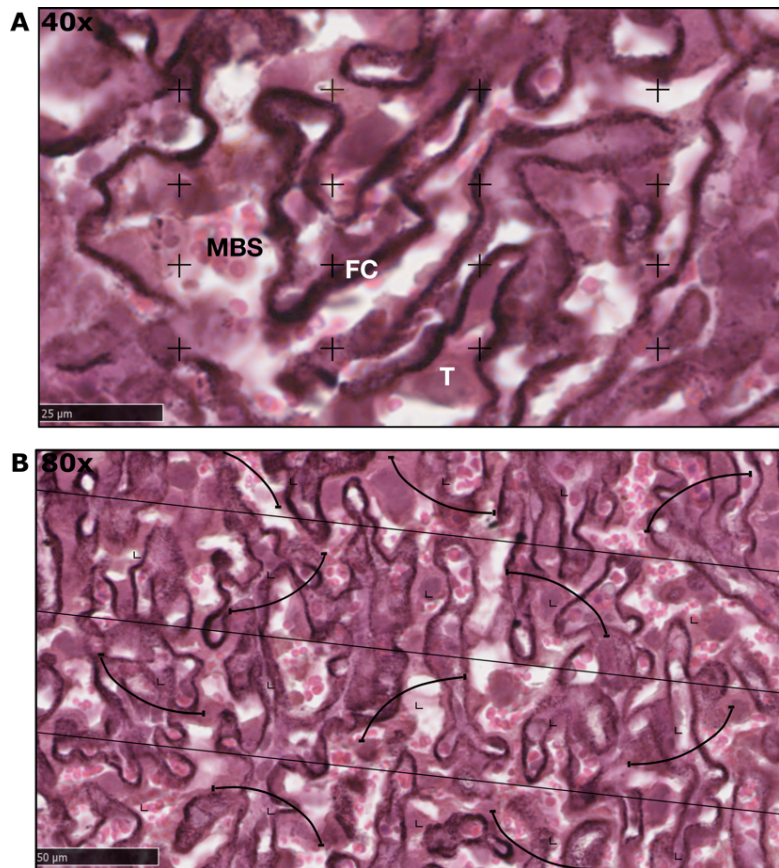


Figure 2.3. Representative photomicrographs of the placental labyrinth zone stained with lectin and cytokeratin to visualise fetal capillaries and trophoblast respectively. Photomicrographs have an overlay of the grids used to determine maternal blood space (MBS), fetal capillary (FC) and trophoblast (T) volume (A) and vascular surface density (B). Images represent gestational day 16 (term is day 20). Scale bars are 25 μm (A) and 50 μm (B).

2.2.7 Glycogen assay

Glycogen content was measured indirectly in E16 and E19 placentas and adult offspring livers using an amyloglucosidase enzymatic assay. Briefly, 40-100 mg tissue was homogenised in ice-cold deionised water (1 mL per 100 mg of tissue) using either a glass tube and plunger for placental tissue or with ribolyser tubes containing lysing matrix D ceramic beads (MP Biomedicals) on a Magna ribolyser (LifeScience, Roche) for liver tissue. Homogenates were prepared in duplicate in glass tubes with 0.1 mL deionised water, 0.1 mL acetate buffer (0.05M, pH 4.5) and 0.1 mL homogenate. Tubes were incubated at 55 $^{\circ}\text{C}$ for 10 minutes and 0.1 mL amyloglucosidase (70U; Sigma Life Science) or the same volume of water (no enzyme control) were added. To deproteinise samples, 0.3 mL each of zinc sulphate (Sigma, Life Science) and barium hydroxide (0.3

M; Sigma, Life Science) were added and the samples centrifuged at 3,000 x g for 10 minutes. The supernatant was removed, and glucose levels were analysed using a glucose analyser (VML 2300 Stat Plus). To determine glycogen concentration, the no enzyme control sample was subtracted from each sample containing enzyme. Glucose levels in the final volume were determined and multiplied by the molar mass of glucose (180 g/mol), assuming that all glycogen is broken down to glucose during the reaction. Total glycogen content as well as glycogen content (mg) per g of tissue were calculated.

2.2.8 mRNA quantification

2.2.8.1 RNA extraction

Mouse placental Jz and Lz samples (E16 and E19) and fetal livers (only on E19) were flash frozen in liquid nitrogen and stored at -80 °C until analysed. Prior to RNA extraction, placental samples were cut in half on dry ice. Total RNA was isolated from one half of the previously dissected placental Jz or Lz using a RNeasy Plus Mini Kit (Qiagen, UK), following the manufacturer's instructions. All samples were weighed and placed into pre-weighed ribolyser tubes, containing lysing matrix D ceramic beads. A 1:10 dilution of β -mercapthoethanol: RNeasy lysis (RLT) buffer was prepared and 600 μ L was added per 20-30 mg sample or 350 μ L per <20 mg sample. Samples were disrupted on a Magna ribolyser machine (LifeScience, Roche) at 4,500 x g three times for 20 s increments. The tissue disruption process was repeated twice. Thereafter the lysate was centrifuged at 16,200 x g for three minutes at 4 °C and the supernatant was removed and transferred to a gDNA eliminator spin column placed in a 2 mL collection tube. Samples were centrifuged at 9,600 x g for 30s and the column discarded. Depending on the sample size, 600 μ L or 350 μ L of 70% ethanol was added to the flow-through and thoroughly mixed by pipetting. The sample (700 μ L) was transferred to a RNeasy column in a 2 mL collection tube and centrifuged at 9,600 x g for 30s, discarding the flow-through. This was repeated with any remaining sample. RNeasy wash (RW1) buffer (700 μ L) was added to the spin column and centrifuged at 9,600 x g for 30s and the flow-through was discarded. RPE wash buffer (500 μ L) was then added and samples centrifuged at 9,600 x g for 30s. After discarding the flow-through, a further 500 μ L RPE buffer was added to each sample and centrifuged at 9,600 x g for two minutes. The collection tube was replaced with a new 2 mL collection tube and centrifuged at 16,200 x

g for one minute. Thereafter, the column was placed in a 1.5 mL collection tube and RNA eluted by adding 50 μ L RNase-free water and centrifuging at 9,600 x g for 1 minute. The RNA samples were either frozen at -80 °C or RNA concentration determined before carrying on immediately with the reverse transcription. RNA concentration of each sample was determined using a NanoDrop 1000 (Thermo Scientific). A A_{260}/A_{280} value of approximately 2 was considered acceptable, to indicate a lack of protein contamination. RNA samples were diluted to 50 ng/ μ L in 50 μ L RNase free water.

2.2.8.2 Reverse transcription

Complementary DNA (cDNA) was synthesised from placental RNA using the High-Capacity cDNA Reverse Transcription Kit (Applied Biosystems, Thermofisher, UK) following the manufacturer's instructions. Briefly, in 200 μ L PCR tubes, 5 μ L 10X RT buffer, 2 μ L 25X dNTP mix, 5 μ L 10X random primers, 2.5 μ L reverse transcriptase, 10.5 μ L RNase-free water and 25 μ L diluted RNA were added and mixed thoroughly. The synthesis of cDNA was performed on a MiniAmp Plus Thermal Cycler (Applied Biosystems, Thermofisher) under the following conditions: 25 °C for 10 minutes, 37 °C for 120 minutes and 85 °C for 5 seconds. cDNA was stored at -20 °C prior to further use.

2.2.8.3 Quantitative polymerase chain reaction (qPCR)

Primer sequences were either obtained from published literature or designed using NCBI Primer-BLAST and were synthesised by Sigma-Aldrich Company Ltd (UK) and diluted to 10 μ M for use in all subsequent experiments. Primer sequences for housekeeping genes and genes assessed in the placenta are shown in Table 2.2. SYBR Green qPCR chemistry was utilised for all gene expression analysis. qPCR efficiencies were determined for each target gene using serial dilutions (1 to 1: 1025) of pooled cDNA. Reaction mixes containing 6.5 μ L SYBR Green qPCR master mix (Applied Biosystems, Thermofisher), 0.25 μ L of forward and reverse primers (Table 2.2), 5 μ L UltraPure distilled water (Invitrogen, Thermofisher Scientific) and 3 μ L cDNA were prepared in 96 well plates. qPCR preparations were loaded onto a MiniAmp Plus Thermal Cycler (Applied Biosystems, Thermofisher) and subjected to the following conditions: 95 °C for 3 minutes, and then 40 cycles of 95 °C for 60 seconds, 95 °C for 15 seconds, and 60 °C for 60 seconds. Serial dilutions were conducted with three technical replicates, and the mean threshold cycle (Ct) value was plotted against the log dilution to generate a linear

standard curve. The efficiency value (E) of each reaction was calculated using the slope of the linear standard curve and the following equation:

$$E = 10^{\frac{-1}{\text{slope}}}$$

An example of a linear standard curve for primer optimisation is depicted in Figure 2.4. All primers were verified by serial dilution to have an efficiency >80%. For all primers, the PCR product was run on a 2% agarose gel (Appendix 3.1) and verified to have the correct size. Following optimisation of all gene sets, gene expression levels were measured in cDNA samples by qPCR. cDNA samples were diluted 1:10 for further use. Similar reaction mixes were prepared as described above, in two technical replicates and subjected to the same thermal cycling conditions. *Polr2a*, *Ubc*, *Gapdh* and *Ywhaz* were used as reference genes for sample normalisation for Jz or Lz samples. *Hprt* with *Polr2a* or *Hprt* alone were used as reference genes for sample normalisation for fetal and adult liver samples respectively. The expression of all reference genes, or combination of reference genes chosen, was not affected by genotype or sex. Negative controls included reactions with the sample omitted (no template control) or where the reverse transcriptase was omitted (no reverse transcriptase control). The Ct value of the reference gene, or geometric mean of several reference genes was subtracted from the Ct value for each gene to obtain a ΔCt value for every sample. Where sexes were combined for analysis, to account for possible sex effects on the calculated $\Delta\Delta\text{Ct}$ value, the average ΔCt value for only the male control samples was subtracted from each sample for each gene resulting in the $\Delta\Delta\text{Ct}$ value. Where sexes were separated for analysis, the average ΔCt from control males or control females were subtracted from each sample. To deduce the relative difference in mRNA expression levels for each gene between placental samples, the equation of $2^{(-\Delta\Delta\text{CT})}$ was calculated (Livak and Schmittgen, 2001).

Table 2.2. Nucleotide sequences for forward and reverse primers for reference and target genes

Gene	Primers	Product size	Reference
<i>Reference genes</i>			
<i>Polr2a</i>	F- CACTGTCATCACCCCTGACC R- ATRACTGGCTGTTTCCCCTGC	148	-
<i>Ubc</i>	F- GGAGTCGCCCCGAGGTCA R- AAAGATCTGCATCGTCTCTCTCAC	100	-
<i>YWhaz</i>	F- AAACAGCTTTCGATGAAGCCA R- CATCTCCTTGGGTATCCGATGT	129	-
<i>Gapdh</i>	F- GGGAAATGAGAGAGGCCAG R- GAACAGGGAGGAGCAGAGAG	188	-
<i>Hprt</i>	F- CAGGCCAGACTTTGTTGGAT R- TTGCGCTCATCTTAGGCTTT	147	-
<i>Experimental model genes</i>			
<i>H19</i>	F- CATTCTAGGCTGGGGTCAAA R- GCCCTTCTTTTCCATTCTCC	112	(Keniry et al., 2012)
<i>Igf2</i>	F- CTTGTTGACACGCTTCAGTTTG R- GGGTGGCACAGTATGTCTCC	151	-
<i>Transporter genes</i>			
<i>Slc2a1</i>	F- GCTTATGGGCTTCTCCAAACT R- GGTGACACCTCTCCCACATAC	123	(Chen et al., 2015)
<i>Slc2a3</i>	F- GA TCGGCTCTTTCCAGTTTG R- CAATCATGCCACCAACAGAG	176	-
<i>Slc38a1</i>	F- CCTTCACAAGTACCAGAGCAC R- GGCCAGCTCAAATAACGATGAT	127	(Chen et al., 2015)
<i>Slc38a2</i>	F- TAATCTGAGCAATGCGATTGTGG R- AGATGGACGGAGTATAGCGAAAA	129	(Chen et al., 2015)
<i>Slc38a4</i>	F- GCGGGGACAGTATTCAGGAC R- GGAACTTCTGACTTTTCGGCAT	102	(Chen et al., 2015)
<i>Cd36</i>	F-ATGGGCTGTGATCGGAACTG R- GTCTTCCCAATAAGCATGTCTCC	100	(Schaiff et al., 2007)

<i>Fatp1</i>	F- GGCTCCTGGAGCAGGAACA R- ACGGAAGTCCCAGAAACCAA	65	(Mishima et al., 2011)
<i>Fatp3</i>	F- GAGAAGTTGCCACCGTATGC R- GGCCCCTATATCTTGGTCCA	162	(Li et al., 2013)
<i>Fatp4</i>	F- GATTCTCCCTGTTGCTCCTGT R- CCATTGAAGCAAACAGCAGG	174	(Li et al., 2013)
<i>Fatp6</i>	F- AACCAAGTGGTGACATCTCGC R-TCCATAAAGTAAAGCGGGTCAG	158	(Li et al., 2013)
<i>Fabp3</i>	F- CATGAAGTCACTCGGTGTGG R- TGCCATGAGTGAGAGTCAGG	305	(Islam et al., 2014)
<i>Junctional zone markers</i>			
<i>Gjb3</i>	F- GGGGCTCTCC TCAGACATA R- ACCTGCTAGCCACACTTGCT	167	-
<i>Hand1</i>	F- GGAGACGCACAGAGAGCATT R- CACGTCCATCAAGTAGGCGA	137	-
<i>Prl8a8</i>	F- TCAGAGCTGCA TCTCACTGC R- GGGACA TCTTTCA TGGCACT	172	-
<i>Steroidogenesis and corticosterone handling</i>			
<i>Stard1</i>	F- TCCTCGCTACGTTCAAGCTG R- CGTCGAACTTGACCCATCCA	154	-
<i>3bhsd</i>	F- GTCATTCCCAGGCAGACCAT R- CTGTTCCCTCGTGGCCATTCA	165	-
<i>Cyp17a1</i>	F- TGGAGGCCACTATCCGAGAA R- CACATGTGTGTCCTTCGGGA	119	-
<i>Hsd11b1</i>	F- GAGGAAGGTCTCCAGAAGGTA R- ATGTCCAGTCCGCCAT	143	(Chin et al., 2017)
<i>Hsd11b2</i>	F- GGCTGGATCGCGTTGTC R- CGTGAAGCCCATGGCAT	132	(Chin et al., 2017)

3bhsd, 3 β -hydroxysteroid dehydrogenase/ Δ 5- Δ 4 isomerase; *Cd36*, fatty acid translocase; *Cyp17a1*, cytochrome P450 family 17 subfamily A member 1; *Fabp3*, fatty acid-binding protein 3 gene; *Fatp1*, fatty acid transport protein 1; *Fatp3*, fatty acid transport protein 3; *Fatp4*, fatty acid transport protein 4; *Fatp6*, fatty acid transport protein 6; *Gapdh*, glyceraldehyde 3-phosphate dehydrogenase; *Gjb3*, gap junction protein beta 3; *H19*, H19 imprinted maternally expressed transcript; *Hand1*, heart and neural crest derivatives expressed 1; *Hprt*, hypoxanthine-guanine phosphoribosyltransferase; *Hsd11b1*, 11 β -hydroxysteroid dehydrogenase type 1; *Hsd11b2*, 11 β -hydroxysteroid dehydrogenase type

2; *Igf2*, insulin-like growth factor 2; *Polr2a*, RNA polymerase II Subunit A; *Prl8a8*, prolactin-8a8; *Slc2a1*, solute carrier family 2 member 1; *Slc2a3*, solute carrier family 2 member 3; *Slc38a1*, solute carrier family 38 member 1; *Slc38a2*, solute carrier family 38 member 2; *Slc38a4*, solute carrier family 38 member 4; *Stard1*, steroidogenic acute regulatory protein; *Ubc*, Ubiquitin C; *YWhaz*, tyrosine 3-monooxygenase/tryptophan 5-monooxygenase

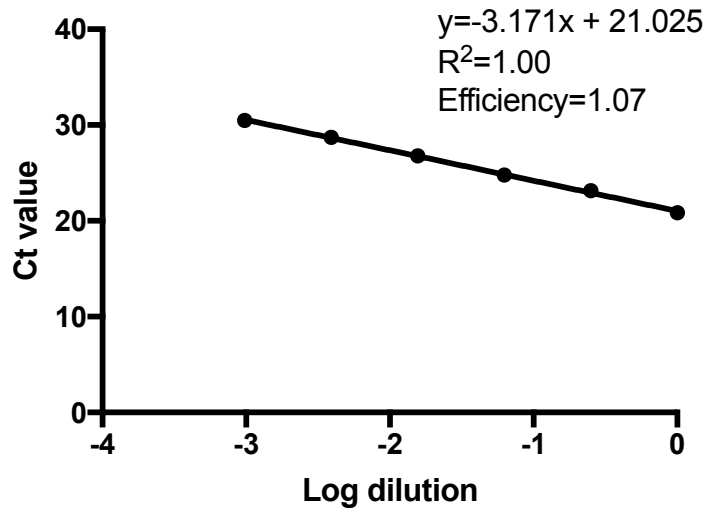


Figure 2.4. Linear standard curve for *Slc2a3* primer optimisation

2.3 Experimental procedures II: The effect of Jz-ICR1Δ on adult offspring metabolic health outcomes

2.3.1 Study design

Another cohort of Jz-ICR1Δ and control dams were left to deliver naturally for a series of experiments on the offspring (Chapter 4). Matings for offspring studies were completed by Dr Jorge Lopez-Tello. All dams were fed a standard chow diet (RM3, Table 2.3). The experimental design for the studies on the offspring is shown in Figure 2.5. Pups were weighed and sexed at postnatal day 3 (P3), by identification of a black spot above the groin region present in males only. Litters were reduced to three females and three males where possible, whereby the lightest excess pups on P3 were decapitated, biometry performed, and tissue weights recorded (pancreas, kidney, liver, heart, lung and brain). Remaining pups were weighed on P7 and weekly thereafter. At weaning (week 3), male and female offspring were fed either a standard chow diet or high sugar high fat diet (HSHF; Diet A, Table 2.3) consisting of a pelleted highly palatable high fat diet (D12451,

Research diets, USA) supplemented with sweetened condensed milk (Nestle) made into gelatinous cubes. Gelatinous sweetened condensed milk cubes were made by mixing heated water and 12g gelatine (Dr Oetker Gelatine Sachets) until dissolved. This mixture was then added to one can of sweetened condensed milk and cooled in a fridge overnight. At 16 weeks of age, one pup per sex per litter selected at random received either a glucose tolerance test (GTT) or an insulin tolerance test (ITT) after a 6 hour fast. Offspring at 16 weeks of age that did not receive a GTT or ITT were also fasted for 6 hours. At 17 weeks of age, all offspring were sacrificed by cervical dislocation and biometry was performed.

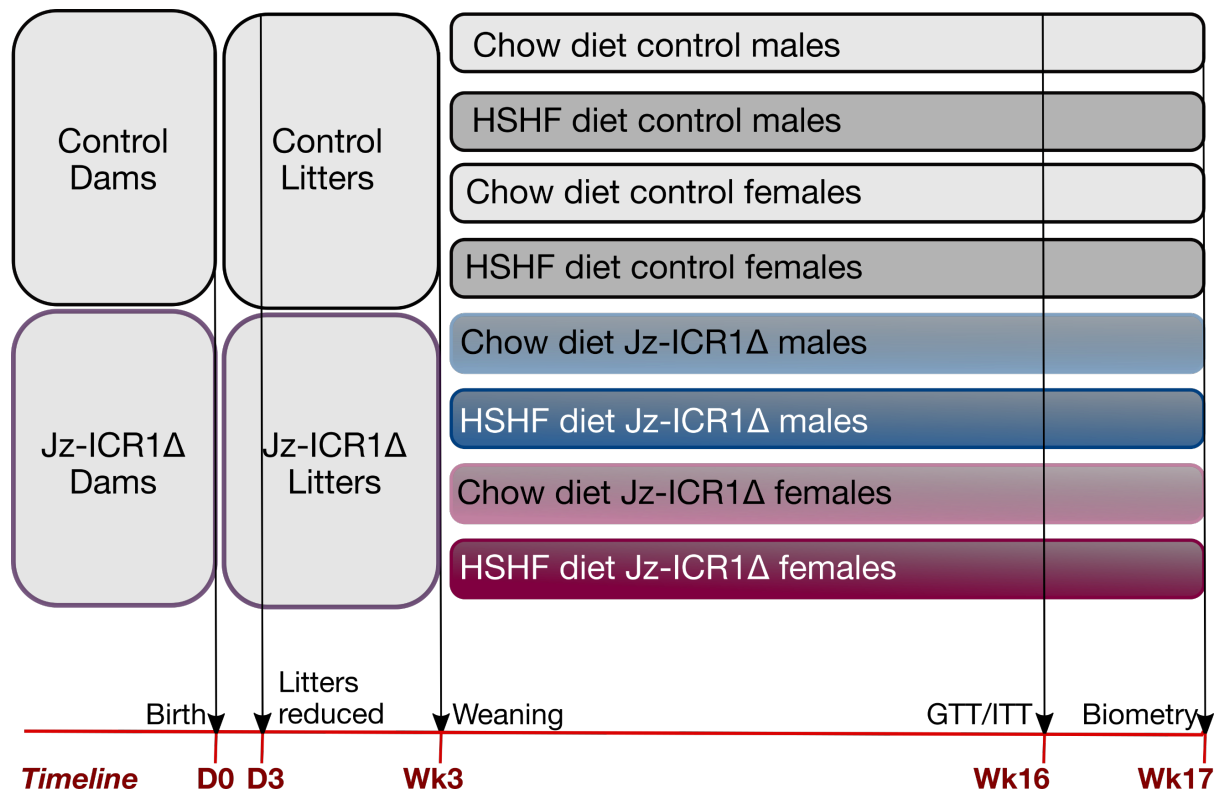


Figure 2.5. Experimental design diagram for study on offspring. D, day; Wk, week; GTT, glucose tolerance test; ITT, insulin tolerance test; HSHF, high sugar high fat.

2.3.2 Diet optimisation

The calorie dense diet utilised in the offspring study was optimised (as described in Appendix 1.1). Diet B comprised of high fat diet and condensed milk gelatine was utilised as a high sugar high fat (HSHF) diet in this study (compositions are shown in Table 2.3) and is shown alongside a chow diet (RM3 diet; Table 2.3). Mice were fed *ad libitum* and were free to choose from each diet component (i.e., high fat diet or condensed

milk gelatine). Food intake was not measured due to technical difficulties in measuring the amount of condensed milk gelatine consumed causing inconsistencies. Therefore, the dietary intake of total sugar and fat consumed by offspring remains unknown.

Table 2.3. Nutrient composition of chow diet (RM3, SDS diets), high fat diet (D12451, Research diets), condensed milk gelatine (Nestle Carnation condensed milk) and 20% sucrose water

Nutrient	RM3 diet	45% High fat diet (Diets A and B)	20% Sucrose water (Diet A)	Condensed milk gelatine (Diet B)
Energy content (%)				
Fat	11	45	-	21.7
Protein	26	20	-	12.1
Starch	22	17	-	-
Sugar	7	18	100	66.2
Energy (MJ/kg)	15.3	19.7	3.3	13.5

2.3.3 Glucose and insulin tolerance tests

Mice were fasted for six hours prior to both GTT and ITT commencing at 8 a.m. Basal glucose levels were measured in mice prior to glucose or insulin administration by making a small cut in the tail with a scalpel blade and measuring blood glucose levels with a handheld glucometer (OneTouch). For the GTT, 10% glucose solution (Dechra) was administered to mice intraperitoneally (1g/kg body weight). For the ITT, insulin solution (Actrapid) was administered to mice intraperitoneally (0.75 U/kg body weight). Thereafter, glucose measurements were taken from the same cut on the tail at 15, 45, 60, and 120 minutes. Glucose levels were plotted against time, and the area under the curve (AUC) and area above the curve (AAC) were determined for the GTT and ITT, respectively, using the Trapezium rule (GraphPad Prism, 7.0).

2.3.4 Biometry

Adult offspring were sacrificed by cervical dislocation and a sample of blood was taken from the cardiac chamber and collected in a pre-chilled EDTA tube and gently shaken. Blood glucose concentrations were measured immediately after sacrifice using a hand-held glucometer (OneTouch). The liver, pancreas, skeletal muscle (*Biceps femoris*), retroperitoneal fat, gonadal fat, peri-renal fat, heart, kidney and spleen were dissected and weighed. Mice that received an ITT had their tissues collected in PFA for stereological analysis. Mice that received a GTT or no procedure had their tissues immediately snap-frozen in liquid nitrogen and stored at -80 °C for molecular and biochemical analyses at a later date.

2.3.5 Biochemical composition

2.3.5.1 Fat content assay

Total fat content was measured in the liver using the Folch method (Folch et al., 1957). Briefly, ~100 mg liver was homogenised with 1 mL of Folch mixture (chloroform:methanol 2:1) using ribolyser tubes containing lysing matrix D ceramic beads (MPBio). Samples were disrupted on a Magna ribolyser machine (LifeScience, Roche) at 4,500 x g twice for 30s increments. Water (200 µL) was added to each sample and shaken for 10 minutes on a rocker. To precipitate lipids, the samples were centrifuged for 10 minutes at 16,800 x g and thereafter 500 µL of the lipid phase removed, added to a pre-weighed Eppendorf tube and dried overnight on a heating block at 37 °C. The Eppendorf tubes were then weighed, and fat content calculated as a percentage of the wet mass of the tissue.

2.3.5.2 Protein assay

Frozen offspring livers were crushed to create a homogeneous powdered sample. All frozen tissue (50-100 mg) was weighed in ribolyser tubes. Lysis buffer (500 µL; Appendix 3.3, Table A3.3.1) was added to liver or muscle samples. Radioimmunoprecipitation assay (RIPA) buffer (250 µL, Appendix 3.3) was added to samples of frozen adipose tissue. Liver and adipose tissue were homogenised using ribolyser tubes containing lysing matrix D ceramic beads (MPBio) whilst muscle was

homogenised with these beads in addition to one lysing matrix M bead (MPBio). Samples were disrupted on a Magna ribolyser machine at 4,500 x g three times for 20s increments, placing samples on ice for 10 minutes between each disruption. Thereafter, the homogenised tissue was incubated on ice for 20 minutes to allow for protein dissociation. Samples were centrifuged twice at 9,600 x g for 10 minutes at 4 °C with the supernatant transferred into new Eppendorf tubes after each centrifugation step. A bicinchoninic acid (BCA) protein assay (Thermoscientific) was used, following the manufacturer's instructions, to determine the protein concentration of each sample by generating a standard curve (0 to 20 µg/µL) with BSA (1 µg/µL) and adding each sample to a 96 well plate. BCA and copper sulphate mixture (1:50; 200 µL) was added to each well. Upon mixture of protein with copper ions in an alkaline environment, a purple coloured complex is formed between the peptide bonds of the protein and copper atoms, with the colour produced in this "biuret" reaction increasing proportionally with protein concentration (Smith et al., 1985). The plate was read at 540 nm on a spectrophotometer (Elx800, Microplate Reader, BioTek) to determine protein concentration using a standard curve.

2.3.5.3 Hormone and metabolite assays

Plasma concentrations of insulin, leptin, cholesterol, triglycerides and free fatty acids were measured at the Core Biochemical Assay Laboratory (Cambridge University Hospitals NHS Foundation Cambridge, UK). Leptin and insulin concentrations were measured together in a duplex electrochemiluminescence assay (MesoScale Discovery, Rockville, MD, USA, K15124C-3). The intraassay co-efficient of variation (CV) was 9.9% for leptin and 4.4% for insulin and the lower limits were 43 pg/mL and 0.07 µg/L, respectively. Cholesterol, triglycerides and free fatty acids were measured using enzymatic assays (Siemens Healthcare, DF27; Siemens Healthcare, DF69A; and Sigma Aldridge, 11383175001, respectively). The intraassay CVs for these assays were 4.9%, 3.4% and 5.0% respectively. Moreover, the lower limits for these assays were 1.3 mmol/L, 0.17 mmol/L and 50 µmol/L respectively.

Total corticosterone levels were measured in mouse plasma using a Corticosterone Competitive ELISA kit (Invitrogen, EIACORT), following the manufacturer's instructions. Briefly, the plasma samples were diluted 1:100 in 1x assay buffer prior to assay preparation. Standards were prepared (0 pg/mL to 10,000 pg/mL) and added to the

plate along with the samples. Thereafter, 75 μL assay buffer was added to each well, followed by 25 μL corticosterone conjugate. Corticosterone antibody (25 μL) was added to each well and the plate was incubated for one hour at room temperature. The wells were washed four times with wash buffer. Tetramethylbenzidine substrate (TMB; 100 μL) was added to each well and incubated for 30 minutes at room temperature. The enzyme reaction was stopped by the addition of 50 μL stop solution to each well and the absorbances of the standards and samples were read at 450 nm on a plate reader (Elx800, Microplate Reader, BioTek). Plasma corticosterone concentration was determined using the standard curve and expressed as ng/mL. The lower limit and intraassay CV for this assay were 18.6 pg/mL and 6.5% respectively.

2.3.5.4 Pancreatic insulin assay

Frozen pancreas samples were crushed to create a homogenous sample and tissue was thereafter added to 5 mL acid ethanol (Appendix 3.2, Table A3.2.2) and left at $-20\text{ }^{\circ}\text{C}$ overnight. The tissue was homogenised manually with a pestle and left at $4\text{ }^{\circ}\text{C}$ overnight. Samples were centrifuged at $2,000 \times g$ for 15 minutes at $4\text{ }^{\circ}\text{C}$ and diluted 1:1000 prior to measuring insulin levels. Pancreatic insulin levels were measured in whole homogenised pancreas using a Mouse Insulin ELISA (Merckodia, 10-1247-01) according to the manufacturer's instructions. Briefly, standards and samples were added to a 96 well plate followed by the addition of 100 μL enzyme conjugate solution. The plate was incubated for two hours at room temperature and then washed six times with wash buffer. Thereafter, 200 μL of TMB was added and the plate was incubated for 15 minutes at room temperature. The enzyme reaction was stopped by the addition of 50 μL stop solution to each well and the absorbances of the standards and samples were read at 450 nm on a plate reader (Elx800, Microplate Reader, BioTek). Pancreatic insulin content was determined using the standard curve and expressed as a concentration (ng) per mg of pancreas. The lower limit and intraassay CV for this assay was 0.2 ng/mL and 5.3% respectively. As the concentration of insulin for several samples was above the upper assay threshold (6.5 ng/mL), a MesoScale Discovery (MSD) ELISA (Rockville, MD, USA, K152BZC-3) was used to measure these (alongside a proportion of pancreatic samples measured previously to ensure equivalent values were obtained) at the Core Biochemical Assay Laboratory (Cambridge University Hospitals NHS Foundation

Cambridge, UK). The intraassay CV, lower and upper limits for this assay were 4.5%, 0.7 ng/mL and 50.0 ng/mL respectively.

2.3.6 Tissue morphology

2.3.6.1 Pancreatic islet immunohistochemistry and area analysis

Offspring pancreas were fixed in 4% PFA overnight at 4 °C and dehydrated using standard protocol (as described in section 2.2.4). Pancreas were cut longitudinally into six pieces, to ensure sampling throughout the pancreas and embedded in paraffin wax. A manual rotary Leica RM2235 microtome was used to section three 5 µm sections of pancreas at 250 µm intervals. Pancreatic sections were deparaffinised in xylene and progressively rehydrated through an ethanol series. Endogenous peroxidases were blocked by incubation with 3% hydrogen peroxide (Fisher Chemical) in methanol for 20 minutes at room temperature. Antigen retrieval was performed by heating in sodium citrate buffer (Appendix 3.2, Table A3.2.1) at 80 °C for 30 minutes. Sections were blocked for thirty minutes in 10% goat serum (Abcam) in buffer containing 2% milk (Marvel), 1% BSA (Sigma Life Science) and 0.1% Tween 80 (Acros Organics) and incubated overnight with a rabbit polyclonal antibody against insulin (Cell Signalling, 4590S) diluted 1:100 in TBST (Appendix 3.3, Table A3.3.6) with 5% goat serum in a humid chamber. Slides were washed in TBST (3 times for 5 minutes) and incubated with a goat anti-rabbit secondary antibody (Abcam, Ab6720) diluted 1:1,000 in TBST for one hour at room temperature. Thereafter, the sections were washed in TBST and incubated with streptavidin-horse radish peroxidase complex (Rockland) diluted 1:500 in TBST for one hour. Sections were washed in TBST again prior to incubation with DAB peroxidase substrate solution for ten minutes. The reaction was quenched by rinsing in distilled water and the sections were stained with fast red (Vector Laboratories, INC, H-3403). Thereafter, the sections were dehydrated through an ethanol series, placed in xylene and coverslip-mounted using DPX.

Stained pancreatic sections were scanned with the high-throughput slide scanner Nanozoomer 2.0-RS (Hamamatsu Photonics, Japan). Fields of view containing insulin-positive areas (at 20x magnification) in addition to the whole pancreatic area were saved as *.jpg* files. The area of each islet in a whole pancreatic section was manually determined, as well as the area of the whole pancreatic section itself using ImageJ

software (version 1.52a with Java 1.8.0_51 (64-bit), National Institutes of Health, USA). The ratio of insulin-positive cell area to total pancreatic area was calculated and multiplied by pancreas weight to obtain islet mass. Three sections per pancreas were analysed. Stereological analysis was performed by Mr Panayiotis Laouris without knowledge of the genotype, sex or diet group from which the sample was obtained.

2.3.6.2 Adipocyte stereology

A portion of offspring gonadal adipose was fixed in 4% PFA overnight at 4 °C prior to dehydration and embedding in paraffin wax, using standard procedures (as described in section 2.2.4.). Gonadal adipose tissue was sectioned at 12 µm using a manual rotary Leica RM2235 microtome and stained with H&E using standard protocol. H&E-stained adipose sections were scanned with the high-throughput slide scanner Nanozoomer 2.0-RS (Hamamatsu Photonics, Japan). Five random fields of view per section were saved as a *.jpg* file at 10x magnification and analysed with the Adiposoft V1.13 plugin on Fiji imaging software (Version 2.0.0 with Java 1.8.0_202 (64-bit), National Institutes of Health, USA) to determine the cross-sectional area of each adipocyte in a field of view. Stereological analysis was performed by Mr Panayiotis Laouris without knowledge of the genotype, sex or diet group from which the sample was obtained.

2.3.7 Western blotting

The abundance of several proteins involved in insulin signalling, gluconeogenesis and lipid metabolism (Table 2.4) was determined in liver, skeletal muscle and adipose tissue from 17-week-old adult offspring.

2.3.7.1 Protein extraction

Protein extraction and quantification was performed as described previously (section 2.3.4.2). Lysate was stored at -80 °C after assessment of protein concentration and prior to sample preparation and standardisation of protein concentration. Samples were prepared at 2.5 µg/µL in lysate buffer containing 1 x sodium dodecyl sulphate (1xSDS; Appendix 3.3, Table A3.3.2). Protein lysate was heated for 10 minutes at 70 °C and stored at -20 °C until further use.

2.3.7.2 SDS PAGE gel preparation and electrophoresis

A 10% acrylamide gel was prepared by combining the components listed in Table A3.3.3 (Appendix 3.3). The Mini-PROTEAN Tetra Electrophoresis System (Bio-Rad) was used in gel preparation. After the gel solution was thoroughly mixed, it was pipetted between two glass plates, with an in-built 1 mm spacer, held in place by a casting stand and clamps. A layer of 100% isobutanol was pipetted above the acrylamide gel, which was left to polymerise. The top layer of isobutanol was then removed, rinsed with milliQ water and the gel blotted dry. Thereafter, the stacking gel was prepared (Appendix 3.3, Table A3.3.3), pipetted on top of the separating gel and after the insertion of a 15-well comb, left to polymerise.

Samples were boiled for 10 minutes at 70 °C prior to loading. Gels were assembled inside a running cassette (BioRad) and placed in a gel tank, with 1x electrophoresis buffer (Appendix 3.3, Table A3.3.4). Sample (20 µL) containing 50 µg of protein was loaded into the stacking gel, with one lane reserved for the ladder (BioRad Precision Plus Protein Dual Colour Standards, 161-0374). Denatured negatively charged proteins were separated on the gel matrix according to size by electrophoresis at 60 V for 30 minutes and at 110 V for approximately 2-2.5 hours until the blue dye had reached the bottom of the gel.

2.3.7.3 SDS PAGE gel transfer

A semi-dry transfer system (TE77 ECL, Amersham Biosciences) was used to transfer proteins from the gel onto a nitrocellulose membrane (BioRad). Nitrocellulose membrane was soaked in transfer buffer (Appendix 3.3, Table A3.3.5) and placed on three pre-soaked pieces of filter paper. The stacking gel was removed from the PAGE gel and the PAGE gel was soaked in transfer buffer and placed on top of the nitrocellulose membrane. Three pieces of pre-soaked filter paper were placed on top, trapped bubbles removed by gentle rolling over the stack and proteins were transferred at 34 mA (per membrane), 5 V for 1.5 hours.

Thereafter, the membrane was washed in distilled water and stained in Ponceau-S (Sigma Life Science, diluted 1:10) to quantify total protein levels. Ponceau-S staining was removed by washing the membrane twice in TBST for 10 minutes and a blocking step was used to prevent non-specific binding of antibodies to the membrane. The membrane

was blocked in either 5% w/v milk powder (Marvel) or 5% w/v BSA (Sigma Life Sciences) in TBST (Appendix 3.3, Table 3.3.6) for the detection of unphosphorylated or phosphorylated proteins, respectively, for one hour at room temperature with gentle agitation.

2.3.7.4 Antibody detection

The membrane was incubated with the appropriate primary antibody diluted in TBST with 0.002% sodium azide (Sigma Aldrich) Table 2.4 contains information about the primary antibodies, dilutions and detection protocol utilised in the experiments. To remove unbound primary antibody, the membrane was washed in TBST three times for 10 minutes with agitation. The appropriate species-specific secondary antibody was added to the membrane, diluted 1: 10,000 in TBST containing either 2.5% milk powder or 2.5% BSA for antibodies for unphosphorylated and phosphorylated proteins, respectively, for one hour at room temperature. The secondary antibodies utilised were either an anti-mouse IgG horseradish peroxidase linked antibody (ECL, NA931V), or an anti-rabbit IgG horseradish peroxidase linked antibody (ECL, NA934V). Thereafter, the membrane was washed in TBST three times for 10 minutes with agitation. Excess fluid was removed, and protein bands were detected with an enhanced chemiluminescence (ECL) solution (Thermo Scientific) according to the manufacturer's instructions. Excess ECL was removed and immunoreactive proteins were visualised using an iBright 1500 Imaging System (ThermoFisher).

Table 2.4. Antibody details for protein abundance detection by Western blotting

Target protein	Molecular weight (kDa)	Species	Manufacturer and catalogue no.	Dilution	Incubation time
InsR	90	Rabbit	Santa Cruz (sc-711)	1/400	O/N at 4 °C
IGF1R	90	Rabbit	Santa Cruz (sc-713)	1/400	O/N at 4 °C
p110 α	110	Rabbit	Cell Signalling (4249)	1/1000	O/N at 4 °C, 2hr at RT
p85 α	85	Rabbit	Millipore (06-195)	1/5000 in 1% milk	1hr at RT
AKT	60	Rabbit	Cell Signalling (9272)	1/1000	O/N at 4 °C, 2hr at RT
pAKT T308	60	Rabbit	Cell Signalling (9275)	1/1000	3 O/N at 4 °C, 2hr at RT
pAKT S473	60	Rabbit	Cell Signalling (9271)	1/1000	3 O/N at 4 °C
GSK3	45	Rabbit	Cell Signalling (9315)	1/1000	O/N at 4 °C
pGSK3 S21/9	50	Rabbit	Cell Signalling (9331)	1/1000	O/N at 4 °C
S6K	70	Rabbit	Cell Signalling (2708)	1/1000	O/N at 4 °C
pS6K T389	70	Rabbit	Cell Signalling (9234)	1/1000	O/N at 4 °C, 1hr at RT
PEPCK	70	Mouse	Santa Cruz (sc-271029)	1/200	O/N at 4 °C
G6Pase	50	Mouse	Santa Cruz (sc-398155)	1/200	O/N at 4 °C
LPL	53	Mouse	Abcam (21356)	1/1000	O/N at 4 °C
PPAR α	52	Rabbit	Abcam (8934)	1/1500	O/N at 4 °C
PPAR γ	51-55	Mouse	Santa Cruz (sc-7273)	1/200	O/N at 4 °C

(Abbreviations for table on preceding page) AKT, protein kinase AKT (kinase B); G6Pase, glucose-6-phosphatase, GSK3, glycogen synthase kinase 3; IGF1R, insulin-like growth receptor 1; InsR, insulin receptor; LPL, lipoprotein lipase; O/N, overnight; p85 α , PDK, phosphoinositol -dependent kinase -1; PI3K regulatory subunit; p110 α , PI3K catalytic subunit alpha; p110 β , PI3K catalytic subunit beta; pAKT T308, phospho-AKT (threonine residue 308); pAKT S473, phospho-AKT (serine residue 473); pGSK3 S21/9, phospho-GSK3 (serine residue 21/9); PPAR α , peroxisome proliferator activated receptor alpha; PPAR γ , peroxisome proliferator activated receptor gamma; pS6K T389, phospho-S6K (threonine residue 389); RT, room temperature; S6K, ribosomal S6 kinase;

2.3.7.5 Antibody stripping

Membranes were stripped of previous antibodies only once, allowing for protein detection with another antibody. To strip membranes, 10 mL of stripping buffer (Thermo Fisher) was added to the membrane and incubated for 15 minutes at room temperature with gentle rocking. The membranes were washed twice for 10 minutes in TBST, and the blocking, antibody incubation and detection protocols were performed as described previously.

2.3.7.6 Western blot analysis

Images were exported from the iBright 1500 Imaging System (Invitrogen, ThermoFisher) as *.tif* files and semi-quantitative densitometric analysis was performed on each Western blot band using ImageJ software (version 1.52a with Java 1.8.0_51 (64-bit), National Institutes of Health, USA). The mean densitometry value of each Western blot and its respective Ponceau S band was measured using a rectangle of uniform size. Three measurements of background densitometry data were taken across the blot and the average value was subtracted from that of each band to standardise data. Each band value was expressed relative to its concordant Ponceau S band to give the protein content as an arbitrary value.

2.4 Experimental procedures III: The effect of Jz-ICR1A on the hepatic transcriptome in male and female fetuses

2.4.1 RNA sequencing

2.4.1.1 Sample preparation

Fetal livers were collected at E19 of pregnancy. Fetal livers used for RNA sequencing experiments were collected during the PTA procedure (section 2.2.2). At E19 fetuses were sexed visually (by identification of a black spot above the groin region present in males only), prior to confirmation with SRY sexing (section 2.2.3). The heaviest male and female liver were chosen per litter, snap frozen in liquid nitrogen and stored at -80 °C prior to RNA extraction. RNA was extracted from E19 livers as described previously (section 2.2.8). After extraction, RNA concentration was determined using a Nanodrop and all samples were normalised to 400 ng/μL prior to determining RNA quality.

2.4.1.2 RNA quality control

RNA quality was determined using an Agilent RNA ScreenTape System (Agilent Technologies) and following the manufacturer's instruction. Briefly, samples and the ladder were prepared with 1 μL RNA (400 ng/μL) or 1 μL RNA ladder (Agilent Technologies) and 5 μL RNA sample buffer (Agilent Technologies). Thereafter, both were denatured by heating at 72 °C for 3 minutes and placed on ice for 2 minutes. Samples were spun down and loaded into a 2200 TapeStation Instrument (Agilent Technologies) to obtain the RNA integrity number (RIN; Table 2.5). All samples had a RIN value > 7.0.

Table 2.5. RNA integrity numbers (RIN) for fetal liver RNA samples

Sample ID	Genotype	Sex	RIN value
A002	Control	Female	7.1
A005	Control	Female	8.0
A006	Control	Female	7.3
A007	Control	Male	8.3
A012	Control	Male	9.4
A013	Control	Male	7.9
A015	Jz-ICR1 Δ	Female	8.2
A016	Jz-ICR1 Δ	Female	7.3
A018	Jz-ICR1 Δ	Female	8.7
A019	Jz-ICR1 Δ	Female	9.5
A001	Jz-ICR1 Δ	Male	7.9
A003	Jz-ICR1 Δ	Male	9.6
A008	Jz-ICR1 Δ	Male	7.7
A009	Jz-ICR1 Δ	Male	9.7

2.4.1.3 Illumina TruSeq Stranded mRNA library preparation

mRNA was converted into total RNA using the Illumina TruSeq Stranded mRNA library preparation kit (Illumina) following the manufacturer's instructions. Briefly, 1 μ g RNA per sample was aliquoted into strip tubes and 50 μ L RNA purification beads were added into each well and mixed by pipetting. mRNA was denatured by placing samples in a thermal cycler at 65 °C for 5 minutes. Samples were incubated at room temperature for 5 minutes and centrifuged at 280 x g for 1 minute. Thereafter, strip tubes were placed on a magnetic stand and the supernatant discarded from each tube. Bead washing buffer (200 μ L) was added to each well and mixed by pipetting. Strip tubes were placed on a magnetic stand and the supernatant was discarded from each tube. Elution buffer (50 μ L) was added, mixed by pipetting and centrifuged at 280 x g for 1 minute. Thereafter, samples were placed on a thermal cycler at 80 °C for 2 minutes.

To fragment the RNA, 50 μ L bead binding buffer was added and incubated at room temperature for 5 minutes. Thereafter, strip tubes were placed on a magnetic stand and

the supernatant discarded from each tube. Bead washing buffer (200 μ L) was added to each well and the supernatant discarded after placing on a magnetic stand. Fragment, Prime, Finish Mix (19.5 μ L) was added to each tube, mixed by pipetting and centrifuging at 280 x g for 1 minute. Thereafter, samples were placed on a thermal cycler at 94 $^{\circ}$ C for 8 minutes.

First strand cDNA was synthesized by reverse transcribing the RNA fragments with random hexamers. Briefly, the strip tubes were placed on a magnetic stand and supernatant transferred to a new set of strip tubes. SuperScript II (50 μ L) was added to one tube of First Strand Synthesis Act D Mix and the mixture (8 μ L) added to each strip tube and mixed by pipetting. Thereafter, samples were placed on a thermal cycler and subjected to the following conditions: 25 $^{\circ}$ C for 10 minutes, 42 $^{\circ}$ C for 15 minutes and 70 $^{\circ}$ C for 15 minutes. Second strand cDNA was synthesised by adding 5 μ L End Repair Control diluted 1:50 in resuspension buffer and 20 μ L Second Strand Marking Master Mix to each well. Samples were placed on a thermal cycler and incubated at 16 $^{\circ}$ C for one hour and then brought to room temperature.

cDNA was purified by adding 90 μ L AMPure XP beads to each well and incubated at room temperature for 15 minutes. Samples were placed on a magnetic stand and 135 μ L was discarded from each well. Samples were washed twice by the addition of 200 μ L 80% ethanol, incubated on a magnetic stand and the supernatant removed. Samples were air-dried and 17.5 μ L of resuspension buffer was added to each sample. Thereafter samples were incubated at room temperature for 2 minutes. The samples were centrifuged at 280 x g for 1 minute, placed on a magnetic stand for 5 minutes and 15 μ L supernatant removed and placed into new strip tubes. The 3' ends were then adenylated. Briefly, 2.5 μ L A-Tailing Control (diluted 1:100 in resuspension buffer) and 12.5 μ L A-Tailing Mix were added to each well. Thereafter, samples were placed on a thermal cycler and subjected to 37 $^{\circ}$ C for 30 minutes and 70 $^{\circ}$ C for 5 minutes.

Multiple indexing adapters were ligated to the ends of the double stranded cDNA fragments. The following reagents were added to each sample: 2.5 μ L ligation control (diluted 1:100 in resuspension buffer), 2.5 μ L ligation mix and 2.5 μ L RNA adaptors. The samples were placed on a thermal cycler at 30 $^{\circ}$ C for 10 minutes. Thereafter, 5 μ L stop ligation buffer was added to each sample.

The following steps were performed to clean up ligated fragments. Briefly, 42 μL AMPure beads were added and samples were incubated at room temperature for 15 minutes. The samples were placed on a magnetic stand and the supernatant was removed from each well. Thereafter, samples were washed twice by the addition of 200 μL 80% ethanol, incubated on a magnetic stand and the supernatant removed. After air drying, resuspension buffer (52.5 μL) was added to each sample and samples were incubated at room temperature for 2 minutes. Samples were centrifuged, placed on a magnetic stand and 50 μL supernatant was transferred to new tubes. This process was repeated once more, however with 50 μL and 22.5 μL of AMPure XP beads and resuspension buffer, respectively. Thereafter, 20 μL supernatant was transferred to a new tube.

DNA fragments with adapter molecules were selectively enriched to amplify the amount of DNA. Briefly, 25 μL PCR master mix was added to each sample, centrifuged and subjected to the following conditions in a thermal cycler: 98 $^{\circ}\text{C}$ for 10 seconds, 60 $^{\circ}\text{C}$ for 30 seconds, 72 $^{\circ}\text{C}$ for 30 seconds and 72 $^{\circ}\text{C}$ for 5 minutes. To clean up amplified DNA, 50 μL AMPure XP beads were added to each well, mixed by pipetting and incubated at room temperature for 15 minutes. Thereafter, samples were centrifuged and placed on a magnetic stand and the supernatant discarded. Samples were washed twice by adding 200 μL 80% ethanol and air-dried on a magnetic stand. Resuspension buffer (32.5 μL) was added to each well and samples incubated at room temperature for 2 minutes. Samples were centrifuged, placed on a magnetic stand and 30 μL supernatant transferred to fresh strip tubes.

2.4.1.4 Validation of library quality and library normalisation

Library quality was checked using an Agilent RNA ScreenTape System (G2964AA, Agilent Technologies) and an Agilent Technologies 2100 Bioanalyser, as described above (Section 2.4.1.2), running 1 μL undiluted DNA library. The expected sample size was \sim 260 base pairs (bp). Samples were pooled together at a 10 nM concentration in preparation for sequencing. Pooled libraries were again run on an Agilent Technologies 2100 Bioanalyser. The pooled library had an average library length of 340 bp and estimated concentration of 6.6 nM.

2.4.1.5 Sequencing

Pooled libraries were sequenced by the CRUK Cambridge Institute, Genomics Core (50 bp single ended on a HiSeq 4000 workflow). The number of raw reads obtained per library was over 300 million.

2.4.1.6 Data processing

Data processing was performed by Dr Russell Hamilton (Centre of Trophoblast Research, University of Cambridge). Briefly, raw sequencing files were run through quality control using FastQC (v011.5) and fastq_screen (v0.9.3). Trim Galore! (v0.6.4) was used to trim low quality and adapter sequencing and trimmed reads were aligned to the mouse reference genome (GRCm38, ensEMBL) using hisat2 (2.1.0). Alignments were assessed using qualimap (v2.2) and featureCounts (v 1.5.0-p2). Gene quantification was performed using featureCounts (v1.5.0-p2). Principal component analysis (PCA) was used to assess sample clustering and multiple testing correction was used to produce false discovery rates using DESeq2 package (v1.22.2, R v3.5.3). The DESeq2 package was also used to perform differential gene expression analysis. An adjusted p value threshold of 0.05 and a log₂ fold change of 0.5 (fold change > 1.4) were used. All metrics from the RNA-Seq pipelines were summarised and reports and graphs produced using MultiQC (0.9.dev0).

2.4.1.7 RNA sequencing validation

A portion of the DEGs identified by RNA sequencing were validated via qPCR in fetal livers, and the expression of these was also determined in adult livers. RNA was extracted from fetal (E19) and adult livers (17 weeks) using the protocol described in section 2.2.8.1. Fetal livers were cut, and adult offspring livers crushed to create a homogenous powdered sample. Approximately 100 mg of either fetal or adult liver sample was pre-weighed prior to RNA extraction. Fetal liver samples at E19 used for qPCR were obtained both during PTA procedures and simple dam biometry. Adult liver samples utilised for qPCR were obtained from the same powdered samples used for western blotting. RNA was reverse transcribed as described previously (section 2.2.8.2). qPCR primers were optimised as described in section 2.2.8.3., the sequences of which are presented in Table 2.6. All qPCR reactions were performed as described in section 2.2.8.3.

Table 2.6. Nucleotide sequences for forward and reverse primers for target genes in fetal and adult offspring livers

Gene	Primers	Product size	Reference
<i>Npy</i>	F-CAGAAAACGCCCCCAGAA R-AAAAGTCGGGAGAACAAGTTTCATT	77	(Mayer and Belsham, 2009)
<i>Zfp36</i>	F-GCCTCCGTACCTTCTCAGAC R-CAGTGTGCCAGCTTTTCGTC	117	-
<i>Ccn1</i>	F-CCATGGCCAGAAATGCATCG R-CACGGTCAAGCCCTGAAAGA	199	-
<i>G6pc</i>	F-ATCAATCTCCTCTGGGTGGC R-GCTGTAGTAGTCGGTGTCCA	111	(Sowton et al., 2020)
<i>Rgs16</i>	F-CCTGGTACTTGCTACTCGCTTTT R-AGCACGTCGTGGAGAGGAT	68	(Huang et al., 2006)
<i>Serpina7</i>	F-GGTATGAGGGATGCCTTTGCT R-CCTCAATGCCCTTCCTAGATCC	126	-

Ccn1, cellular communication network factor 1; *G6pc*, glucose-6-phosphatase, catalytic; *Npy*, neuropeptide Y; *Rgs16*, regulator of G-protein signalling 16; *Serpina7*, serine (or cysteine) peptidase inhibitor, clade A (alpha-1 antiproteinase, antitrypsin), member 7; *Zfp36*, zinc finger protein 36

2.4.1.8 Data analysis

A Venn diagram was produced to determine shared DEGs between groups using Venny (<https://bioinfogp.cnb.csic.es/tools/venny/index.html>). DEG fold changes and heat maps of p values were graphed using R by Marta Ibanez Lligona. DEGs were subject to functional association network analysis with STRING (<https://string-db.org>; (Szklarczyk et al., 2015) to form a protein-protein interaction (PPI) network. A required interaction score of >0.4 and a false discovery rate (FDR) of 5% were used in network analyses. STRING computes a combined score between gene interactions by combining different evidence channels probabilities and correcting this by the probability of a randomly observed interaction (von Mering et al., 2005). GO terms associated with DEGs were searched using UniProt (<https://www.uniprot.org>). DEGs were subjected to enrichment analysis using EnrichR (Chen et al., 2013, Kuleshov et al., 2016), in particular using the Molecular Signatures Database (2020). For enrichment analysis an adjusted p value < 0.05 was considered significant. Enrichment analysis in separate male and female DEG lists in response to Jz-ICR1 Δ did not reach significance due to the small number of DEGs per list. Therefore, the effect of Jz-ICR1 Δ irrespective of sex was considered in enrichment analysis (shown in Appendix 1.4.1).

2.5 Statistical analysis

All data are presented as means \pm standard error of the mean (SEM) with individual values per sample shown, where possible. Overall, data were largely normally distributed as validated by a D'Agostino-Pearson (omnibus K2) normality test (GraphPad Prism, 7.0). All data was subject to a Grubb's test (Prism Grubb's test, GraphPad Software Inc.) and where an outlier was removed, details are specified in individual results chapters. Analyses of fetal and placental weights, and placental transfer assay measurements, were performed by linear mixed models repeated measures with litter as a random effect, litter size as a covariate, and genotype and sex as parameters. If significant differences were observed, a Bonferroni post hoc test was performed (Statistical Analysis System, SAS). When considering two variables, data were analysed by two-way analysis of variance (ANOVA) with either genotype and sex or genotype and diet as parameters. If significant differences were observed, a Sidak post hoc test was performed (GraphPad Prism, 7.0). The effect of genotype alone was assessed by Student's t-test using Microsoft Excel. A Student's t-test was used to determine the effect of genotype in western blots (where both

diets could not fit onto one gel) and gene expression in adult livers (where changes in gene expression were sex-specific). Offspring growth trajectories and GTT and ITT curves were measured by two-way repeated measures (RM) ANOVA. For GTT and ITT curves, the trapezoid rule was used to calculate the area under or above the curve. p values of < 0.05 were considered statistically significant, except for RNA sequencing data, where an adjusted p value of < 0.05 was considered significant.

Chapter 3: The effect of Jz-ICR1Δ on placental morphology and nutrient transport capacity

3.1 Introduction

The metabolic status of the mother influences fetal nutrient provision. In normal pregnancy a reduction in maternal insulin sensitivity elevates maternal glucose and fatty acid availability towards term, to increase nutrient provision to the fetus via the placenta. Complications such as GDM or maternal obesity, frequently accompanied by hyperglycaemia and chronic insulin resistance, may lead to adversely high glucose levels *in utero* (Herring et al., 2009, Plows et al., 2018). In the placentas of GDM patients, increases in the abundance of glucose and amino acid transporters and fat binding proteins (Gaither et al., 1999, Jansson et al., 2002, Magnusson et al., 2004, Radaelli et al., 2009) are indicative of increased fetal nutrient delivery and are likely to contribute to the increased risk of macrosomia in the infants born to women with GDM (Esakoff et al., 2009, He et al., 2015). Maternal obesity is associated with greater rates of both low and high birthweights, a disparity also seen in obese rodent dams (Roberts et al., 2011, Higgins et al., 2013, Radulescu et al., 2013, Sferruzzi-Perri et al., 2013b, Song et al., 2018, Appel et al., 2019, Gohir et al., 2019). In rodents, a maternal high fat diet increases glucose and system A amino acid transporter abundance in the placenta (Jones et al., 2009, Lin et al., 2011, Aye et al., 2015, Rosario et al., 2015). Moreover, in streptozotocin treated diabetic rats, placental glucose uptake and glycogen levels are increased, whilst placental glucose clearance is reduced (Thomas et al., 1990, Boileau et al., 1995). Overall, these studies show that a hyperglycaemic and hyperinsulinaemic maternal environment, observed in rodent models of maternal obesity and diabetes and human pregnancies complicated by these conditions, have the capacity to alter placental nutrient transport and fetal growth outcomes.

Maternal metabolic status is influenced by the endocrine milieu. Indeed, hormones such as prolactin, growth hormone, placental lactogen, resistin, leptin and progesterone induce maternal insulin resistance during pregnancy (summarised in Chapter 1, section 1.3.3; Sutter-Dub et al., 1981, Handwerger and Freemark, 2000, Zavalza-Gomez et al., 2008). Comparatively, hormones like oestrogen may serve to attenuate or exacerbate the pregnancy associated insulin resistance, depending on the maternal endocrine milieu (Ahmed-Sorour and Bailey, 1981, González et al., 2002). Hormones in the mother also

act upon the placenta via hormone receptors to alter its transport capacity (Lager and Powell, 2012, Fowden et al., 2015). For instance, administering IGF1 and IGF2 *in vivo* in mice and other small animal species increases placental glucose and amino acid transfer (Sferruzzi-Perri et al., 2007, Sferruzzi-Perri et al., 2008). Moreover, studies performed *in vitro*, by culturing human placental explants with different hormones have indicated their ability to alter glucose and amino acid transporter abundance, with adiponectin treatment decreasing glucose and system A amino acid transporter expression (Duval et al., 2016). Treatment of primary human trophoblast with increasing concentrations of apelin and resistin concomitantly increases glucose and system A amino acid transport and treatment, with insulin, leptin and the synthetic corticosterone dexamethasone also increasing system A amino acid uptake (Karl et al., 1992, Jansson et al., 2003, Di Simone et al., 2009, Vaughan et al., 2019). Moreover, treating primary human trophoblast with leptin also increases *Cd36* expression, which may be indicative of changes in fatty acid transport (Mousiolis et al., 2012). In addition to altering amino acid transporter abundance, dexamethasone treatment in mice increases *Hsd11b2* expression, which may indicate placental adaptation to limit fetal corticosterone exposure (Vaughan et al., 2012). Interestingly, maternal and placental hormones have also been shown to alter placental morphology, with likely implications for placental nutrient transport. For instance, maternal dexamethasone administration in rats reduces Lz volume, and fetal capillary length density, surface density and area (Guo et al., 2020). Moreover, abnormal Lz vasculature is also observed in conceptuses of rat dams treated with insulin and 5 α -dihydrotestosterone (Zhang et al., 2019). Overall, the hormonal milieu during pregnancy alters maternal metabolic status and fetal nutrient acquisition via actions on placental morphology and nutrient transport.

Placental morphology is also governed by several placentally expressed growth factors, such as *Igf2*, which may act in an autocrine and paracrine manner. Several studies in rodents using global and Lz-specific knockout and global over-expression of the *Igf2* gene have demonstrated the importance of IGF2 in placental formation and fetal growth (as summarised in Figure 1.3). For instance, global over-expression of *Igf2* (via a single deletion of both the *H19* gene and the ICR1) increases the placental surface area for nutrient exchange but reduces placental glucose and amino acid transport. Despite this, fetal overgrowth is observed in this model (Angiolini et al., 2011). Conversely, both global and Lz-specific *Igf2* deletion lead to reduced fetal weight, albeit at differing

degrees and stages in gestation, due to a reduction in placental nutrient transport (Constancia et al., 2005, Dilworth et al., 2010). The Lz-specific knockout of *Igf2* also results in a reduction in glycogen cell number in the Jz, which is indicative of both paracrine signalling between the two placental zones and the importance of *Igf2* in endocrine cell formation (Sferruzzi-Perri et al., 2011). However, the effect of endocrine zone manipulation via Jz-specific *Igf2* alteration on the placental morphology and nutrient transport capacity in relation to fetal growth remains to be elucidated.

The Sferruzzi-Perri laboratory has recently developed a mouse model in which there is mis-expression of *Igf2* and *H19* expression specifically in placental endocrine zone (Jz-ICR1 Δ). This is associated with Jz expansion on E16 and alterations in maternal endocrine and metabolic status (summarised in Table 1.13.1), including maternal hyperglycaemia and hyperinsulinemia. However, despite an expanded endocrine zone and maternal hyperglycaemia and hyperinsulinemia on E16 of pregnancy, fetal weight is unaltered at this gestational age, which may indicate alterations in placental nutrient transport capacity with implications for fetal nutrient acquisition and growth just prior to term (term ~E20). Moreover, little is known about the impact of Jz-ICR1 Δ on Jz production of hormones, namely sex steroids which modulate maternal glycaemia, nor the handling of corticosterone, a hormone buffered by the placenta that regulates fetal growth. Thus, it was hypothesised that Jz-ICR1 Δ alters placental morphology, endocrine capacity, nutrient transport and corticosterone handling capacity in relation to fetal growth in late gestation.

The aims of this study were to determine the impact of Jz-ICR1 Δ on:

- Placental Jz morphology and capacity for sex steroid production,
- Placental nutrient transport *in vivo*, Lz morphology and nutrient transporter expression and
- Placental Lz corticosterone handling in relation to fetal growth on E16 and E19.

3.2 Materials and methods

Animals

Experiments were performed under the UK Home Office Animals (Scientific Procedures) Act 1986, approved by the University of Cambridge. Mice were housed under 12:12 h dark/light photocycle conditions with *ad libitum* access to water and standard chow diet. Female mice in which the ICR1 of the *H19-Igf2* locus is flanked by *LoxP* sites were mated with males expressing *Cre* recombinase under the promoter of the Jz-specific gene, *Tpbpa* (*Tpbpa-Cre*; Figure 2.1). All mice were bred on a C57BL/6N (Charles River) background. The reverse parental cross was utilised as a control in all experiments. Only the placental Jz (and not the mother or fetus) has been genetically manipulated, but for ease placentas and dams will be referred to as Jz-ICR1 Δ in this study. A total of 60 and 59 female mice were mated for pregnancy experiments terminated at either E16 or E19, respectively and the number of dams used in experimental procedures and biometry are shown in Table 2.1. The presence of a copulatory plug was defined as E1 of pregnancy. Dams at E16 or E19 of pregnancy underwent a placental transport assay (PTA; Chapter 2, section 2.2.2) and/or were killed by cervical dislocation and tissues were taken for stereological or molecular analysis.

Tissue collection

Placentas were collected on E16 or E19 for analysis of structure, gene expression and glycogen content. Placentas for stereological assessment were collected in 4% PFA. For molecular analysis, placentas were either kept intact (for glycogen assays) or separated into Jz and Lz (for qPCR), and immediately flash frozen in liquid nitrogen, prior to storing at -80 °C for processing at a later date. Fetal tails were collected for SRY sexing (Chapter 2, section 2.2.3) to allow all analyses to be split by sex. Fetuses and maternal plasma from dams which underwent a PTA were processed for radioactivity determination to calculate materno-fetal clearance of MeG and MeAIB (as described in section 2.2.2).

Stereology

Placentas were collected and prepared for stereology analysis, including embedding and sectioning (Chapter 2, section 2.2.4). Placentas were H&E stained for component volume analysis (Chapter 2, section 2.2.4 and 2.2.6.1). A cohort of placentas were also stained using an immunohistochemistry protocol, to identify the fetal capillaries and trophoblast

(Chapter 2, section 2.2.5). The labyrinth structure was analysed in placentas stained with the lectin/cytokeratin immunohistochemistry protocol (Chapter 2, section 2.2.6.3).

Glycogen assay

A sub-set of E16 and E19 placentas were analysed for their glycogen content. The glycogen assay protocol is described in Chapter 2 (section 2.2.7).

RNA extraction, reverse transcription and quantitative polymerase chain reaction (qPCR)

The RNA from Jz and LZ was extracted and reverse transcribed using the protocol as described in detail in Chapter 2, sections 2.2.8.1 and 2.2.8.2. The qPCR protocol and primer sequences are described in Chapter 2, section 2.2.8.3 and Table 2.2. All housekeeping genes utilised for qPCR analysis were constant per sex and genotype.

Statistics

All data are presented as means \pm standard error of the mean (SEM) with individual values per sample shown, where possible. Overall, data were largely normally distributed as validated by a D'Agostino-Pearson (omnibus K2) normality test (GraphPad Prism, 7.0). Statistical analyses of data containing several pups from a litter (i.e., fetal and placental weights and placental transfer assay measurements) were performed by linear mixed models repeated measures with litter as a random effect, litter size as a covariate, and genotype and sex as parameters using Statistical Analysis Software (SAS). If significant differences were observed, a Bonferroni post hoc test was performed. A Student's t-test was used to analyse the effect of genotype on litter size and number of reabsorptions using Microsoft Excel. All other data were analysed by two-way ANOVA (genotype and sex) and a Sidak post hoc test (for genotype only) was performed if significance was observed (GraphPad Prism, 7.0). For qPCR data, the use of a Grubb's test (Prism Grubb's test, GraphPad Software Inc.) resulted in the removal of one outlier in two qPCR data sets prior to statistical analysis. p values of < 0.05 were considered statistically significant.

3.3 Results

3.3.1 Litter size and resorptions

Jz-ICR1 Δ did not alter litter size (including viable fetuses only) at E16 (Figure 3.1A; $p=0.08$), but increased litter size on E19 (Figure 3.1B; $p<0.05$). Therefore, litter size was used as a covariate for all analyses involving multiple pups from a single litter herein. Jz-ICR1 Δ did not affect the number of resorptions per litter or the percentage of male pups per litter at either E16 or E19 (Figure 3.1C, D, E, F).

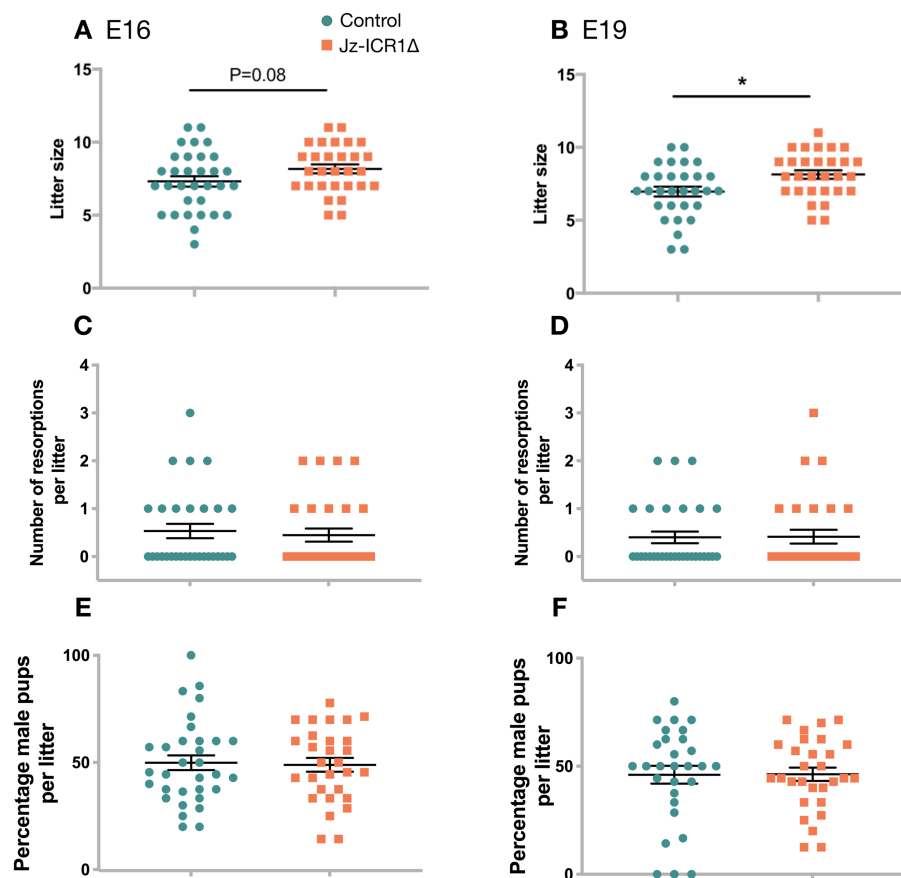


Figure 3.1. The effect of Jz-ICR1 Δ on litter size (A, B), resorptions (C, D) and the percentage of male pups (E, F) on E16 and E19 of pregnancy. Individual points represent individual litters, and the mean is denoted as a horizontal line \pm SEM. Data from 29-31 litters per group are shown and were analysed by a Student's t-test. An asterisk (*) indicates a significant difference ($p<0.05$) between genotypes.

3.3.2 Fetal and placental weights

Fetal and placental and weights in response to Jz-ICR1 Δ are shown in Table 3.1. On E16 and E19 of pregnancy, placental weight was increased by Jz-ICR1 Δ ($p<0.0001$) and

altered according to sex ($p < 0.0001$). Post hoc analysis showed that males had heavier placentas than females ($p < 0.0001$) and Jz-ICR1 Δ placentas were heavier than control placentas in both males and females ($p < 0.01$). On E16, fetal weight was unaltered by Jz-ICR1 Δ , but was affected by the sex of the fetus ($p < 0.0001$), whereby male fetal weights were heavier than in females ($p < 0.05$).

On E19 of pregnancy, fetal weight was reduced by Jz-ICR1 Δ ($p < 0.01$), with post hoc analysis showing that Jz-ICR1 Δ female fetuses were lighter than their control counterparts ($p < 0.01$). On E19 and E16 of pregnancy, the fetal/placental (F/P) ratio was decreased by genotype ($p < 0.0001$) and altered by sex ($p < 0.01$). The F/P ratios of male and female Jz-ICR1 Δ were less than their control counterparts ($p < 0.01$). Moreover, male F/P ratios were less than females ($p < 0.05$).

Table 3.1. Fetal, placental and conceptus weights on E16 and E19 of pregnancy in control and Jz-ICR1Δ mice.

Gestational age	Parameters	Control		Jz-ICR1Δ		Effect of Genotype	Effect of Sex	Interaction
		Male	Female	Male	Female			
E16	Fetal weight (mg)	401.6 ± 4.04	389.0 ± 4.10†	416.0 ± 4.005	386.7 ± 3.9†	0.14	< 0.0001	0.058
	Placental weight (mg)	109.2 ± 1.6	99.5 ± 1.6†	121.6 ± 1.6*	106.6 ± 1.5†*	< 0.0001	< 0.0001	0.13
	F/P ratio (mg/mg)	3.8 ± 0.05	4.0 ± 0.05†	3.5 ± 0.05*	3.7 ± 0.05†*	< 0.0001	0.0034	0.92
E19	Fetal weight (mg)	1202.6 ± 9.0	1201.4 ± 8.3	1197.9 ± 8.2	1165.0 ± 7.8*	0.0028	0.12	0.14
	Placental weight (mg)	102.1 ± 1.4	94.2 ± 1.3†	110.5 ± 1.3*	99.4 ± 1.2†*	< 0.0001	< 0.0001	0.25
	F/P ratio (mg/mg)	12.1 ± 0.2	13.0 ± 0.2†	11.0 ± 0.2*	11.9 ± 0.2*†	< 0.0001	< 0.0001	0.97

Data are expressed as mean ± SEM from 29-31 litters per genotype and gestational age and were analysed by were analysed by linear mixed models repeated measures with litter as a random effect, litter size as a covariate, and genotype and sex as parameters. Means comparisons were made by a Bonferroni post hoc test. p values representing a significant effect (p<0.05) are shown in bold. An asterisk (*) indicates a significant difference between control and Jz-ICR1Δ within the same sex (p<0.05). A cross (†) indicates a significant difference between males and females within the same genotype (p<0.05). E, embryonic day; F/P, fetal/placental.

3.3.3 *Igf2* and *H19* expression

Gene expression of *Igf2* and *H19* was determined in the separated zones of placentas to validate whether mis-expression of *Igf2* and *H19* is observed in the Jz of the placenta at E16 and E19 of pregnancy (Figure 3.2). A reduction in *H19* expression was observed in the Jz, and not Lz of Jz-ICR1Δ placentas at both E16 and E19 ($p < 0.001$) by 78% and 59% respectively. Post hoc analyses showed that male Jz-ICR1Δ placentas had significantly reduced *H19* mRNA levels compared to their control counterparts ($p < 0.001$). Overall, *Igf2* expression was increased in the Jz, and not Lz of Jz-ICR1Δ placentas at E16 ($p < 0.05$) by 31% but was unaltered at E19 of pregnancy. There was no effect of fetal sex on Jz or Lz *H19* or *Igf2* expression on either E16 or E19.

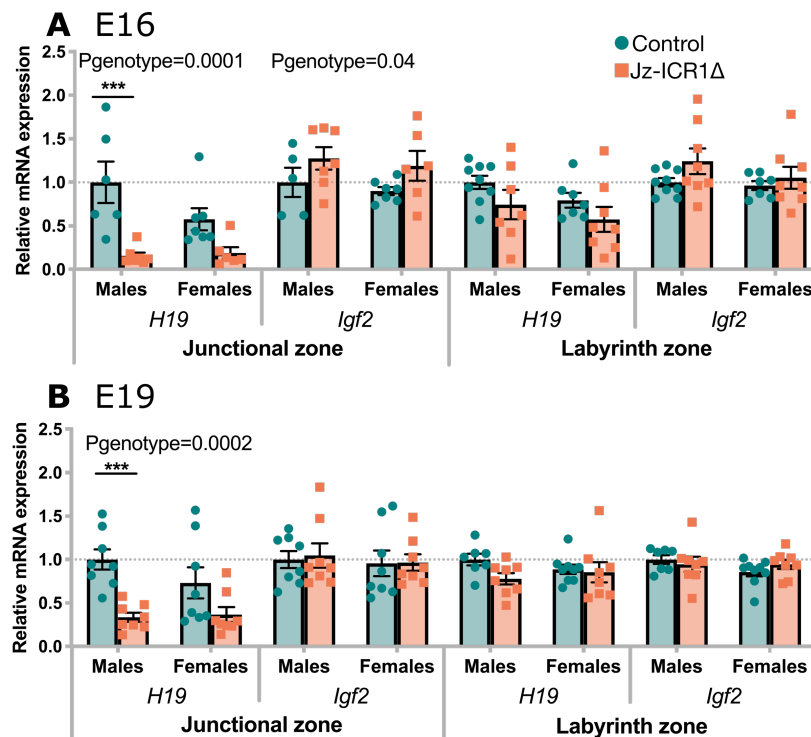


Figure 3.2. *H19* and *Igf2* gene expression in the junctional and labyrinth zones at E16 (A) and E19 (B) in control and Jz-ICR1Δ mice. Gene expression data are presented as individual points from a single sample with mean \pm SEM relative to the control male group of each separate placental zone. Gene expression in E16 Jz samples are shown relative to the geometric mean of the housekeeping genes *Gapdh*, *Ywhaz* and *Polr2a*, whilst gene expression in E19 Jz samples are shown relative to the geometric mean of the housekeeping genes *Ywhaz*, *Ubc* and *Polr2a*. The expression of genes in E16 and E19 Lz samples are shown relative to the geometric mean of the housekeeping genes *Ywhaz* and *Ubc*. Data were analysed by two-way ANOVA (genotype and sex) with a Sidak post hoc test (for genotype only). $n=6-9$ samples per sex and genotype (across 3-8 litters per sex and genotype). An asterisk (*) is used to denote significant difference between genotypes (* $p < 0.05$, ** $p < 0.01$, *** $p < 0.001$).

3.3.4 *Igf2* receptor expression

To determine *Igf2* sensitivity in the Jz of control and Jz-ICR1 Δ placentas the expression of IGF2 receptors (*Igf1r*, *Insr* and *Igf2r*) were determined on E16 and E19 of pregnancy (Figure 3.3). On E16 of pregnancy, *Igf1r*, *Insr* and *Igf2r* expression were not altered by genotype or sex (Figure 3.3A). On E19 of pregnancy, *Igf1r* and *Insr* expression was reduced in response to Jz-ICR1 Δ ($p < 0.01$). Female Jz-ICR1 Δ placentas had reduced *Igf1r* expression compared to their control counterparts ($p < 0.05$), whilst in males the effect of genotype did not reach significance post hoc ($p = 0.051$). *Insr* expression was also altered by an interaction between genotype and sex ($p < 0.05$); whereby the effect of genotype was only seen in placentas of male fetuses ($p < 0.01$). *Igf2r* expression also tended to be reduced in response to Jz-ICR1 Δ , however this was not significant ($p < 0.07$; Figure 3.3B).

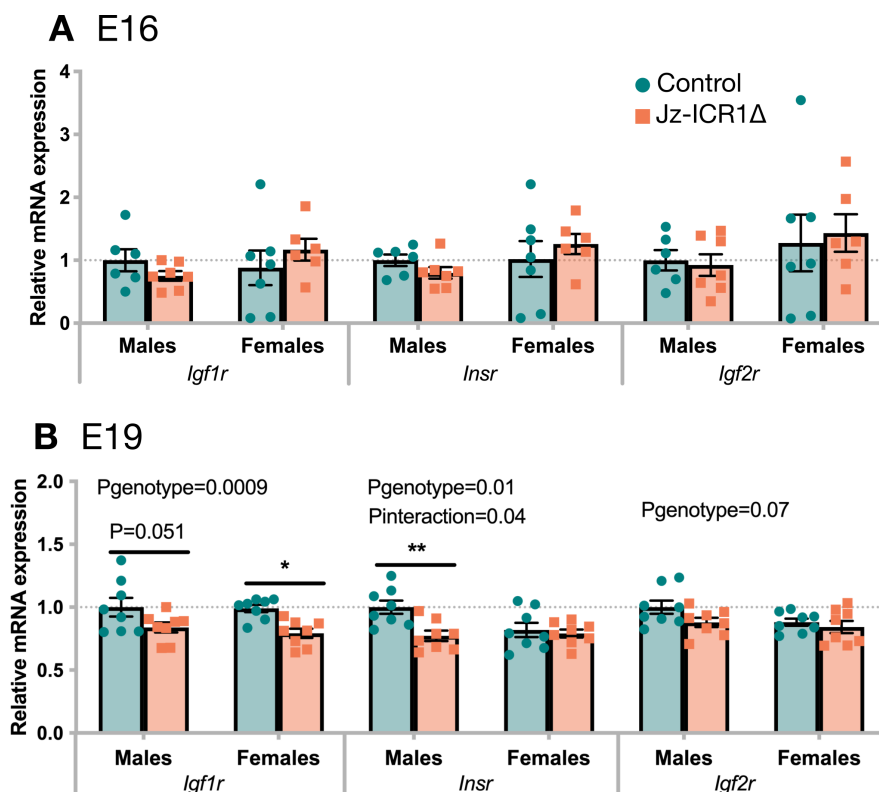


Figure 3.3. IGF2 receptor gene expression in the junctional zone at E16 (A) and E19 (B) in control and Jz-ICR1 Δ mice. Gene expression data are presented as individual points from a single sample with mean \pm SEM relative to the control male group. Gene expression in E16 Jz samples are shown relative to the geometric mean of the housekeeping genes *Gapdh*, *Ywhaz* and *Polr2a*, whilst gene expression in E19 Jz samples are shown relative to the geometric mean of the housekeeping genes *Ywhaz*, *Ubc* and *Polr2a*. Data were analysed by two-way ANOVA (genotype and sex) with a Sidak post hoc test (for genotype only). $n=6-8$ samples per sex and genotype (across 3-8 litters per sex and genotype). An asterisk (*) is used to denote significant difference between genotypes (* $p < 0.05$, ** $p < 0.01$).

3.3.5 Placental zone volume and glycogen content

To determine whether changes in *H19* and *Igf2* expression altered placental morphology, placental compartment volumes were determined in control and Jz-ICR1 Δ placentas. Representative haematoxylin and eosin-stained control and Jz-ICR1 Δ placentas are shown on E16 and E19 of pregnancy (Figure 3.4A, B). On E16 of pregnancy, Jz volume was increased in Jz-ICR1 Δ placentas (Figure 3.4C; p=0.004) although other placental compartment volumes (Lz, Db and total volume) remained unaltered. At E19 of pregnancy, Jz volume was no longer increased and other placental compartment volumes remained unchanged by Jz-ICR1 Δ compared to control (Figure 3.4D). Glycogen content was not altered by Jz-ICR1 Δ at either E16 or E19 (Figure 3.4E, F).

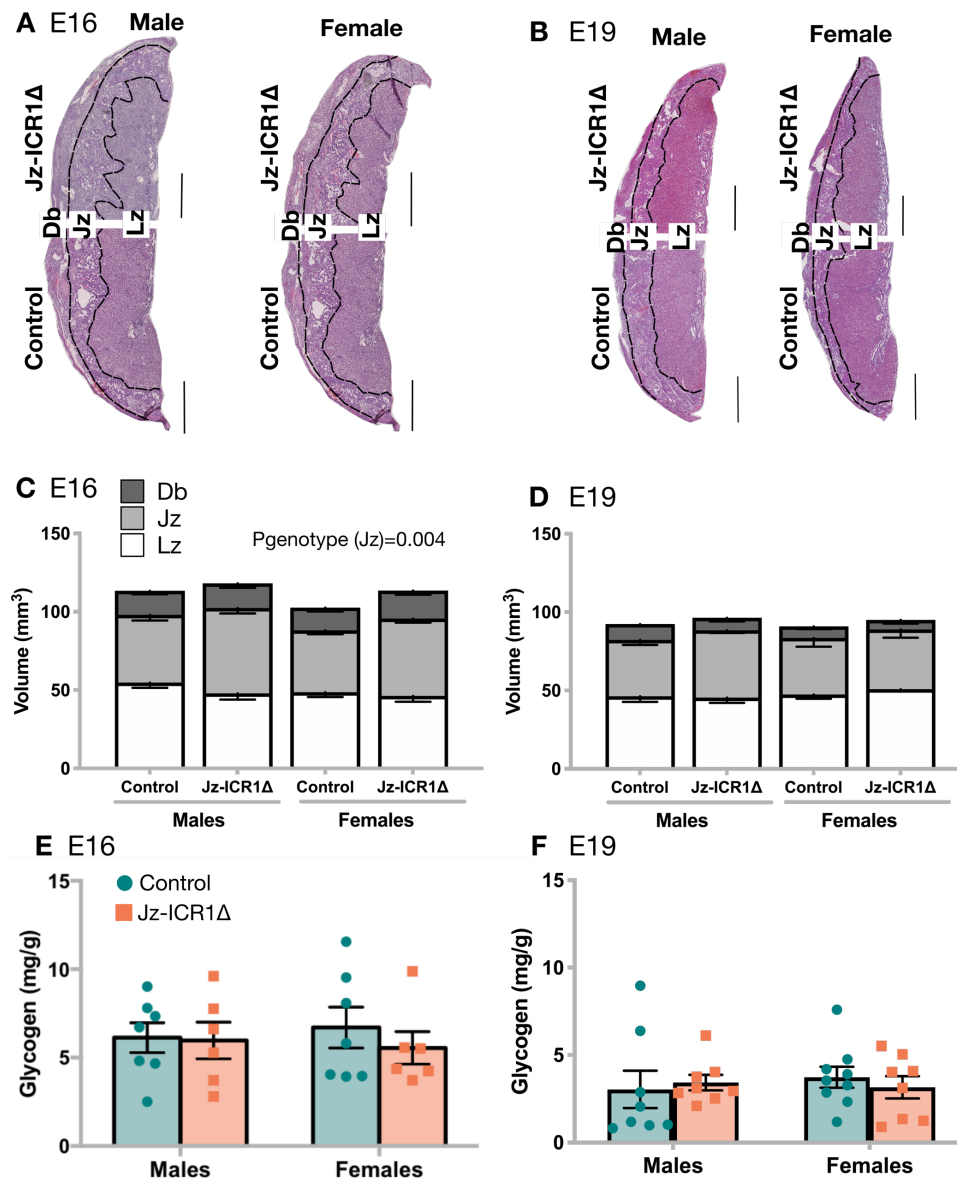


Figure 3.4. Representative H&E stained placentas (A, B), placental volumes (C,D) and placental glycogen content (E,F) on E16 and E19 of pregnancy in control and Jz-ICR1Δ mice. All data are presented as mean \pm SEM with glycogen content data also showing individual sample points. Data were analysed by two-way ANOVA (genotype and sex) with a Sidak post hoc test (for genotype only). n=4-8 samples per genotype and sex (across 3-7 litters per genotype and sex) are shown for placental compartment volumes. n=6-9 samples per genotype and sex (across 3-4 litters per genotype and sex) are shown for glycogen content. Db, decidua basalis; H&E, haematoxylin and eosin; Jz, junctional zone; Lz, labyrinth zone. Scale bars are 500 μ M.

3.3.6 Junctional zone cell volume and marker expression

To determine whether an expansion in Jz volume in Jz-ICR1 Δ placentas was associated with changes in the volume or expression of specific Jz cell types, Jz cell volumes (glycogen cells, spongiotrophoblast cells and giant cells) and mRNA levels of their cell markers (*Gjb3*, *Prl8a8* and *Hand1*, respectively) were determined in control and Jz-ICR1 Δ placentas at E16 and E19 (Figure 3.5). Gene expression was assessed in dissected Jz (including the decidua). Glycogen cell and spongiotrophoblast cell volumes tended to be increased by Jz-ICR1 Δ at E16 ($p=0.07$; Figure 3.5A), but not at E19, and there was no effect on *Gjb3* or *Prl8a8* mRNA expression at either gestational age. While there was no effect of Jz-ICR1 Δ on giant cell volume or *Hand1* expression, *Hand1* was lower in females compared to males on both E16 and E19 of pregnancy ($p<0.05$). The area and number of Jz-like clusters present in the LZ were determined but were not altered in response to Jz-ICR1 Δ at E16 or E19 (Figure 3.5E, F).

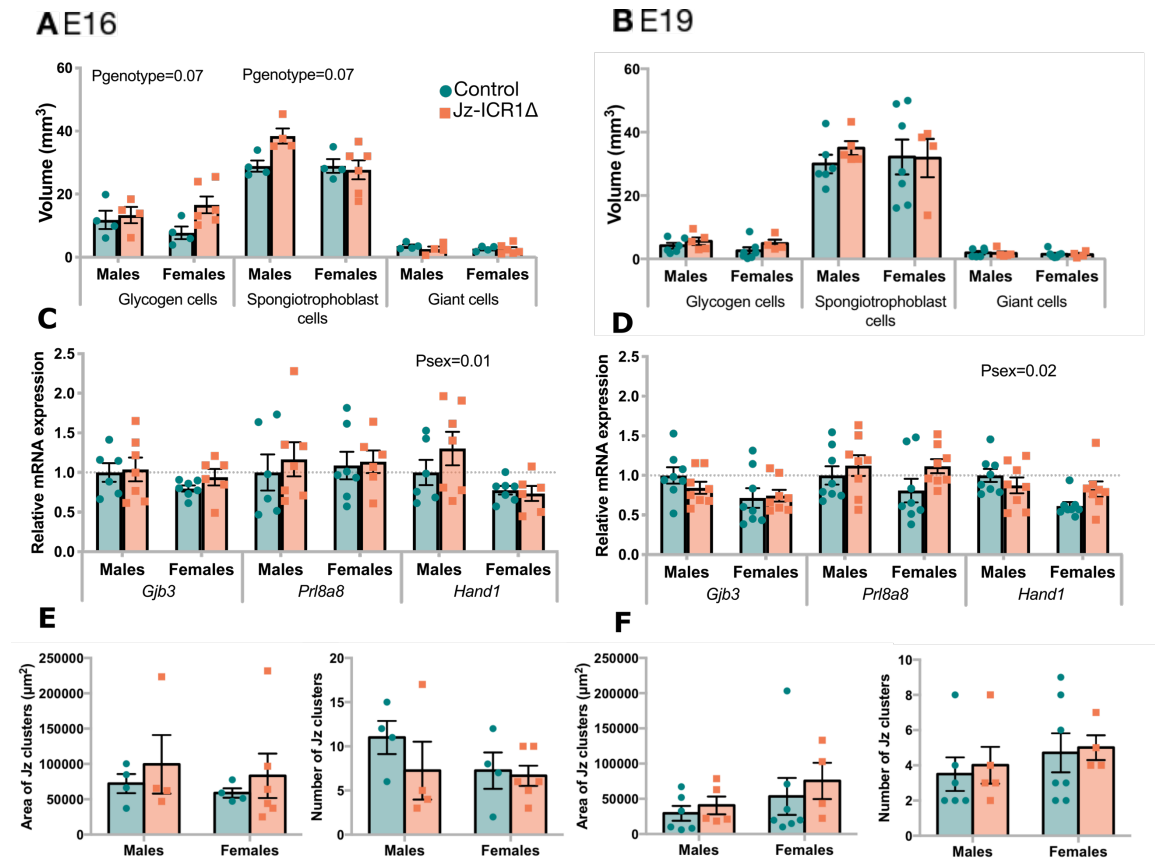


Figure 3.5. Junctional zone cell volumes (A, B), cell marker gene expression (C, D) and area and number of Jz clusters in the Lz (E, F) at E16 and E19 in control and Jz-ICR1 Δ mice. Data are presented as individual points from a single sample with mean \pm SEM. Gene expression data are shown relative to the control male group. E16 Jz samples are shown relative to the geometric mean of the housekeeping genes *Gapdh*, *Ywhaz* and *Polr2a*, whilst gene expression in E19 Jz samples are shown relative to the geometric mean of the housekeeping genes *Ywhaz*, *Ubc* and *Polr2a*. All data were analysed by two-way ANOVA (genotype and sex) with a Sidak post hoc test (for genotype only). $n=4-7$ samples per sex and genotype (across 3-7 litter per sex and genotype) for stereology data. $n=6-8$ samples per sex and genotype (across 3-8 litters per sex and genotype) for gene expression data.

3.3.7 Junctional zone steroidogenic gene expression

To determine the steroidogenic capacity of Jz-ICR1 Δ placentas, mRNA levels of genes involved in steroidogenesis (*Stard1*, *3bhsd* and *Cyp17a1*) were measured in the Jz at E16 and E19 of pregnancy (Figure 3.6). On E16 of pregnancy, the mRNA levels of steroidogenesis genes were not altered in response to Jz-ICR1 Δ or by sex (Figure 3.6A). On E19 of pregnancy, *3bhsd* expression was altered by an interaction between genotype and sex ($p < 0.05$), whereby *3bhsd* expression tended to be lower specifically in Jz-ICR1 Δ males compared to control males ($p = 0.059$). Regardless of genotype, placentas from female fetuses had lower *Cyp17a1* expression compared to males at E19 ($p < 0.05$; Figure 3.6B).

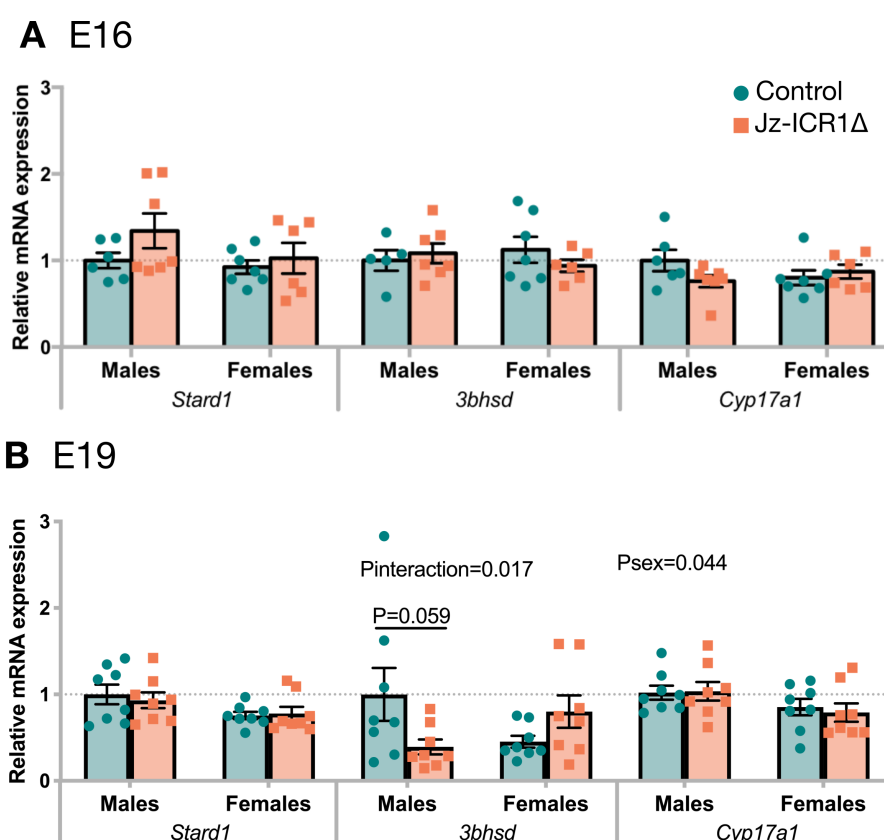


Figure 3.6. Junctional zone steroidogenic gene expression at E16 (A, C) and E19 (B, D) of pregnancy in control and Jz-ICR1 Δ mice. Gene expression data are expressed as individual points from a single sample with mean \pm SEM relative to the control male group. Gene expression in E16 Jz samples are shown relative to the geometric mean of the housekeeping genes *Gapdh*, *Ywhaz* and *Polr2a*, whilst gene expression in E19 Jz samples are shown relative to the geometric mean of the housekeeping genes *Ywhaz*, *Ubc* and *Polr2a*. Data were analysed by two-way ANOVA (genotype and sex) with a Sidak post hoc test (for genotype only). $n=6-8$ samples per sex and genotype (across 3-8 litters per sex and genotype).

3.3.8 Labyrinth zone morphology

Stereology was utilised to determine changes in labyrinth zone morphology in response to Jz-ICR1 Δ at E16 and E19 of pregnancy (Table 3.2 and Table 3.3, respectively). On E16, the average surface area of the fetal and maternal facing sides of the trophoblast interhaemal membrane in the Lz was reduced by Jz-ICR1 Δ ($p < 0.05$; Table 3.2).

Moreover, Jz-ICR1 Δ also decreased the theoretical diffusion capacity of the placenta at E16 ($p < 0.05$; Table 3.2). There was a tendency for Jz-ICR1 Δ to decrease the volume of trophoblast in the placental Lz (not significant; $p = 0.07$), whilst remaining Lz parameters (MBS and FC volumes, mean FC length and diameter, harmonic mean interhaemal membrane thickness and specific diffusion capacity) were unaltered by either genotype or sex at this gestational time point.

On E19, Lz surface area and diffusion capacity of the placenta no longer differed between Jz-ICR1 Δ and controls (Table 3.3). However, MBS volume was increased in the placenta Lz by Jz-ICR1 Δ ($p < 0.05$) and post hoc analysis showed this effect was most pronounced in Jz-ICR1 Δ females compared to their control counterparts ($p < 0.05$). The remaining Lz parameters (FC and T volumes, FC capillary length and diameter, harmonic mean membrane thickness and specific diffusion capacity) were unaltered by either genotype or sex at E19.

Table 3.2. Labyrinth zone morphology in control and Jz-ICR1Δ placentas on E16 of gestation.

	Control		Jz-ICR1Δ		Effect of Genotype	Effect of Sex	Interaction
	Male	Female	Male	Female			
Volume (mm³)							
MBS	18.88 ± 3.17	15.77 ± 2.02	14.56 ± 2.03	16.66 ± 1.57	0.39	0.95	0.22
FC	4.36 ± 1.18	6.12 ± 1.25	5.20 ± 2.16	4.58 ± 0.47	0.75	0.62	0.41
T	27.96 ± 2.06	29.59 ± 4.47	28.23 ± 3.73	22.12 ± 1.30	0.070	0.73	0.33
Surface area of the trophoblast membrane (cm²)							
	16.13 ± 1.51	14.83 ± 1.98	11.30 ± 1.22	11.99 ± 0.90	0.014	0.10	0.39
Mean capillary length (m)							
	51.76 ± 4.51	66.02 ± 8.64	56.96 ± 7.19	53.24 ± 3.05	0.37	0.26	0.27
Mean capillary diameter (μm)							
	10.10 ± 1.13	10.87 ± 1.07	10.73 ± 2.96	10.44 ± 0.50	0.95	0.88	0.73
Harmonic mean membrane thickness (μm)							
	1.60 ± 0.089	1.60 ± 0.042	1.41 ± 0.16	1.60 ± 0.12	0.45	0.46	0.42
Theoretical diffusion capacity (mm² min⁻¹ kPa⁻¹)							
	0.015 ± 0.0015	0.014 ± 0.0018	0.012 ± 0.00078	0.0011 ± 0.00031	0.017	0.60	0.64
Specific diffusion capacity (mm² min⁻¹ kPa⁻¹)							
	3.42 ± 0.36	3.06 ± 0.48	2.69 ± 0.25	2.80 ± 0.094	0.096	0.88	0.34

Data are expressed as mean ± SEM. Effects of genotype, sex and interaction determined by two-way ANOVA and a Sidak post hoc test (for genotype only). p values representing a significant effect (p<0.05) are shown in bold. n=4-7 samples per sex and genotype (across 3 to 5 litters per sex and genotype).

Table 3.3. Labyrinth zone morphology in control and Jz-ICR1Δ placentas on E19 of gestation.

	Control		Jz-ICR1Δ		Effect of Genotype	Effect of Sex	Interaction
	Male	Female	Male	Female			
Volume (mm³)							
MBS	11.72 ± 1.56	10.10 ± 0.73	14.03 ± 2.01	15.89 ± 2.56*	0.024	0.94	0.30
FC	7.97 ± 1.87	7.61 ± 1.23	6.83 ± 1.049	7.73 ± 0.76	0.72	0.85	0.67
T	26.63 ± 1.50	29.69 ± 2.54	27.30 ± 3.95	27.22 ± 1.84	0.74	0.59	0.57
Surface area of the trophoblast membrane (cm²)							
	15.36 ± 2.46	15.61 ± 0.89	13.59 ± 0.90	15.10 ± 1.52	0.70	0.82	0.50
Mean capillary length (m)							
	65.57 ± 6.14	65.58 ± 6.91	75.13 ± 10.18	76.94 ± 7.87	0.20	0.91	0.91
Mean capillary diameter (μm)							
	12.21 ± 1.07	12.15 ± 1.05	10.93 ± 1.14	11.47 ± 1.06	0.40	0.84	0.80
Harmonic mean membrane thickness (μm)							
	1.13 ± 0.05	1.19 ± 0.05	1.17 ± 0.07	1.22 ± 0.10	0.64	0.40	0.96
Theoretical diffusion capacity (mm² min⁻¹ kPa⁻¹)							
	0.020 ± 0.0033	0.018 ± 0.0016	0.017 ± 0.0014	0.018 ± 0.0017	0.58	0.89	0.57
Specific diffusion capacity (mm² min⁻¹ kPa⁻¹)							
	1.72 ± 0.31	1.57 ± 0.10	1.52 ± 0.15	1.61 ± 0.15	0.68	0.89	0.56

Data are expressed as mean ± SEM. Effects of genotype, sex and interaction determined by two-way ANOVA and a Sidak post hoc test (for genotype only). p values representing a significant effect (p<0.05) are shown in bold. An asterisk (*) indicates a significant difference between control and Jz-ICR1Δ within the same sex (p<0.05). n=4-7 samples per sex and genotype (across 4-7 litters per sex and genotype).

3.3.9 Placental MeG and MeAIB clearance

MeG (glucose) and MeAIB (system A amino acid) clearance was determined in response to Jz-ICR1 Δ as a means to evaluate *in vivo* changes in nutrient transport to the fetus. At E16 of pregnancy, placental glucose clearance, corrected for placental weight, was reduced in response to Jz-ICR1 Δ ($p < 0.01$; Figure 3.7A). This effect was significant for female Jz-ICR1 Δ placentas compared to their control counterparts ($p < 0.05$). Conversely, placental MeAIB clearance was not altered at E16 by Jz-ICR1 Δ regardless of fetal sex (Figure 3.7C). When corrected for the surface area of the Lz interhaemal trophoblast membrane, there was no longer a change in placental glucose clearance, however MeAIB clearance was increased by Jz-ICR1 Δ ($p < 0.01$; Figure 3.7B, D).

At E19 of pregnancy, placental MeG and MeAIB clearance were both reduced in response to Jz-ICR1 Δ ($p < 0.05$), regardless of whether placental clearance was corrected for placental weight (Figure 3.7E, G) or Lz surface area (3.7F, H). Placental MeG clearance (corrected for placental weight and Lz surface area) was significantly reduced for both male and female Jz-ICR1 Δ placentas compared to their control counterparts ($p < 0.05$). MeAIB clearance relative to Lz surface area was significantly reduced for female Jz-ICR1 Δ placentas compared to female controls ($p < 0.05$). Regardless of genotype, MeAIB clearance adjusted for placental weight or Lz surface area was greater in females than in males at E19 ($p < 0.05$). There was no effect of fetal sex on placental MeG clearance at E19.

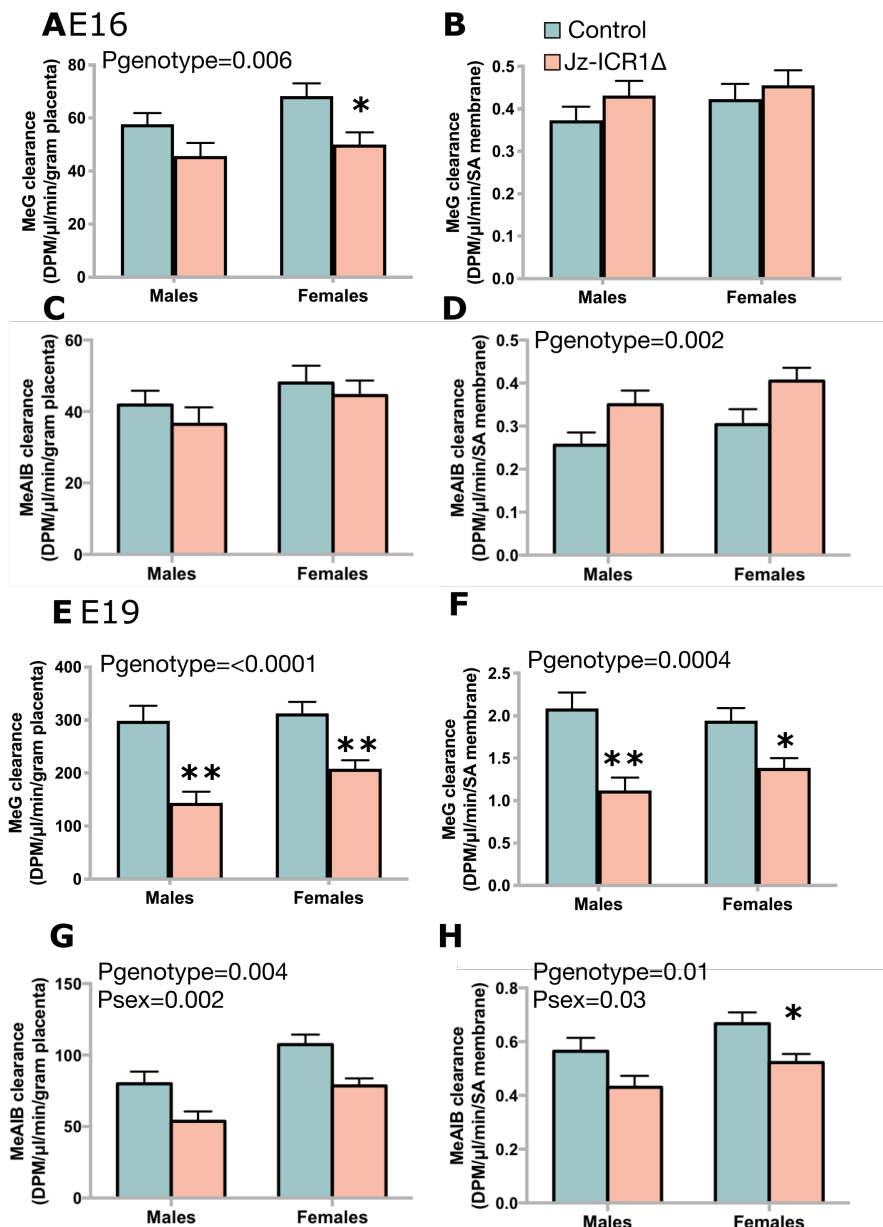


Figure 3.7. Placental MeG and MeAIB clearance, corrected either to placental weight (A, C, E, G) or surface area of the trophoblast membrane (B, D, F, H), at E16 (A, B, C, D) and E19 (E, F, G, H) of pregnancy in control and Jz-ICR1 Δ mice. Data are expressed as mean \pm SEM and were analysed by linear mixed models repeated measures with litter as a random effect, litter size as a covariate, and genotype and sex as parameters. Means comparisons were made by a Bonferroni post hoc test. N=6-8 litters per genotype and gestational time point. An asterisk (*) is used to denote significant difference between genotypes (* p <0.05, ** p <0.01, *** p <0.001). DPM, disintegrations per minute; SA, surface area.

3.3.10 Nutrient transporter expression in the labyrinth zone

Glucose (*Slc2a1*, *Slc2a3*) and amino acid (*Slc38a1*, *Slc38a2*, *Slc28a4*) transporter mRNA levels in the placental Lz were not affected by either *Jz-ICR1Δ* or fetal sex at E16 and E19 of pregnancy (Figure 3.8). At E16 of pregnancy, *Fatp4* expression was affected by sex and an interaction between genotype and sex ($p < 0.05$), whereby *Jz-ICR1Δ* tended to reduce *Fatp4* expression in males and increase *Fatp4* expression in females. At E19, *Fatp4* expression was no longer affected by an interaction of genotype with fetal sex, however there was an overall effect of *Jz-ICR1Δ* to decrease *Cd36* and *Fabp3* expression in the placental Lz ($p < 0.05$). Other fatty acid transporter and binding protein genes measured were not altered by genotype or sex at E16 or E19 (Figure 3.8A, B).

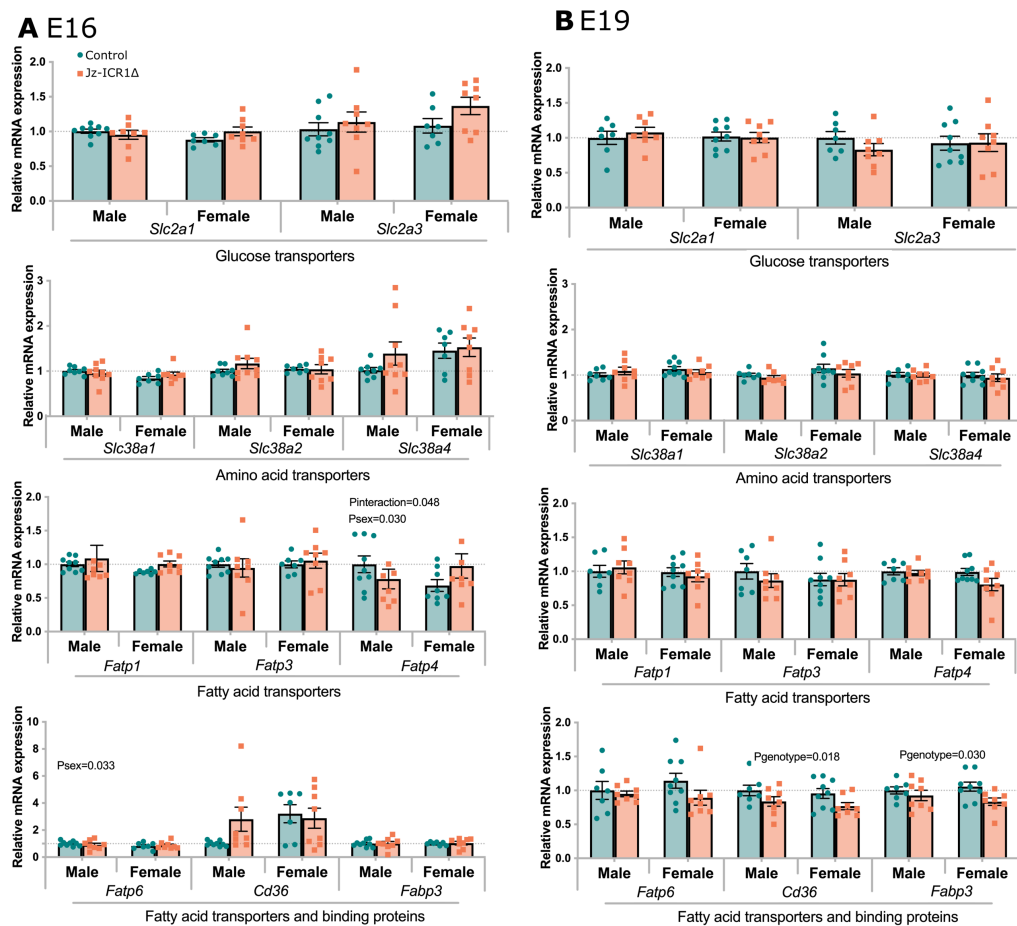


Figure 3.8. Labyrinth zone glucose, system A amino acid and fatty acid transporter gene expression at E16 (A) and E19 (B) of pregnancy in control and *Jz-ICR1Δ* mice. Gene expression data are expressed as individual points from a single sample with mean \pm SEM relative to the control male group. The expression of genes in E16 and E19 Lz samples are shown relative to the geometric mean of the housekeeping genes *Ywhaz* and *Ubc*. Data were analysed by two-way ANOVA (genotype and sex) and a Sidak post hoc test (for genotype only). $n=7-9$ samples per genotype and sex (across 6-8 litters per genotype and sex).

3.3.11 Corticosterone handling in the labyrinth zone

The impact of Jz-ICR1Δ on placental corticosterone handling was determined by assessing the expression of the glucocorticoid receptor (*Gr*) and genes involved in converting corticosterone to its active (*Hsd11b1*) and inactive (*Hsd11b2*) form in the Lz at E16 and E19 (Figure 3.9A, B). At E16 of pregnancy, *Hsd11b1* mRNA levels were increased in the Lz in response to Jz-ICR1Δ ($p < 0.05$), with post hoc analysis showing this effect was significant for female fetuses (Figure 3.9A). There was no effect of Jz-ICR1Δ or fetal sex on *Hsd11b2* and *Gr* mRNA levels in the placental Lz at E16. At E19, *Hsd11b1* was no longer affected by Jz-ICR1Δ, and *Hsd11b2* and *Gr* mRNA levels remained unchanged by genotype, as well as fetal sex (Figure 3.9B).

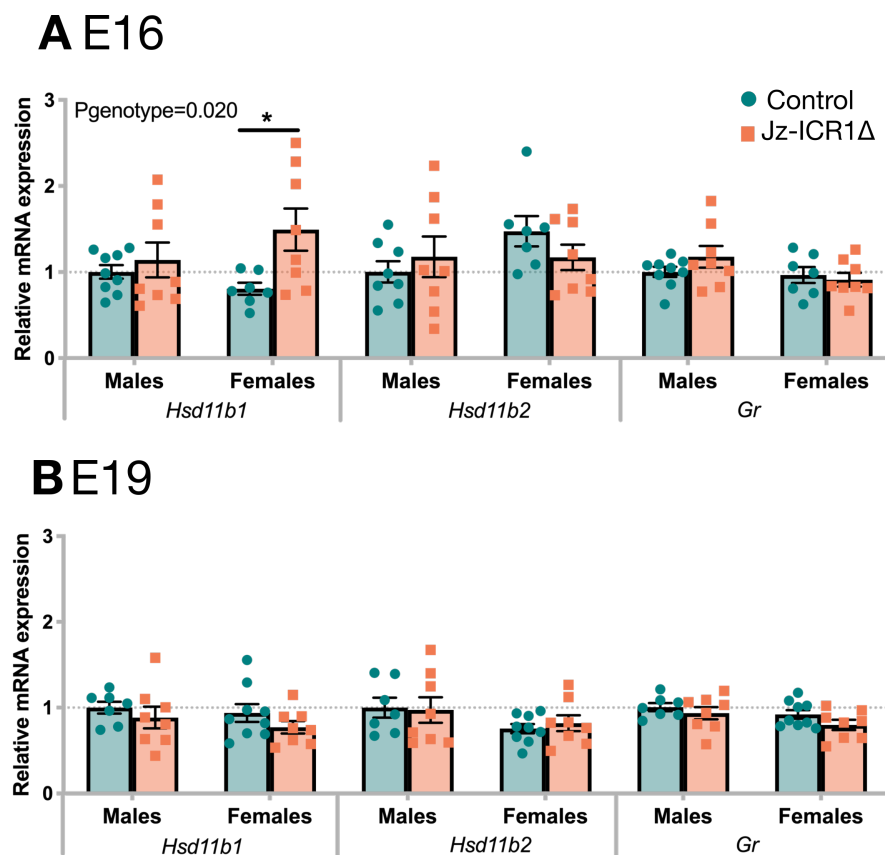


Figure 3.9. Labyrinth zone expression of glucocorticoid metabolising enzymes and receptor on E16 and E19 of pregnancy in control and Jz-ICR1Δ mice. Gene expression data are expressed as individual points from a single sample with mean \pm SEM relative to the control male group. The expression of genes in E16 and E19 Lz samples are shown relative to the geometric mean of the housekeeping genes *Ywhaz* and *Ubc*. Data were analysed by two-way ANOVA (genotype and sex) and a Sidak post hoc test (for genotype only). $n=7-9$ samples per genotype and sex (across 6-8 litters per genotype and sex). An asterisk (*) is used to denote significant difference between genotypes ($*p < 0.05$).

3.4 Discussion

During pregnancy, the balance between the fetal genetic drive for growth and the capacity for maternal nutrient provision is crucial in maintaining maternal and offspring health. In part, fetal nutrient acquisition is determined by placental endocrine function, which influences maternal metabolism (Lager and Powell, 2012). Moreover, the paternally expressed gene *Igf2* is critical in both the formation of placental endocrine cells and in determining materno-fetal resource allocation during mouse pregnancy (Constancia et al., 2002, Angiolini et al., 2011). In response to a Jz-specific deletion of *H19* ICR1, several placental morphological changes and alterations in placental nutrient transport were observed (as summarised in Figure 3.4.1). In particular, a reduction in placental surface area and glucose and amino acid transport were observed, leading to a reduction in fetal weight towards term.

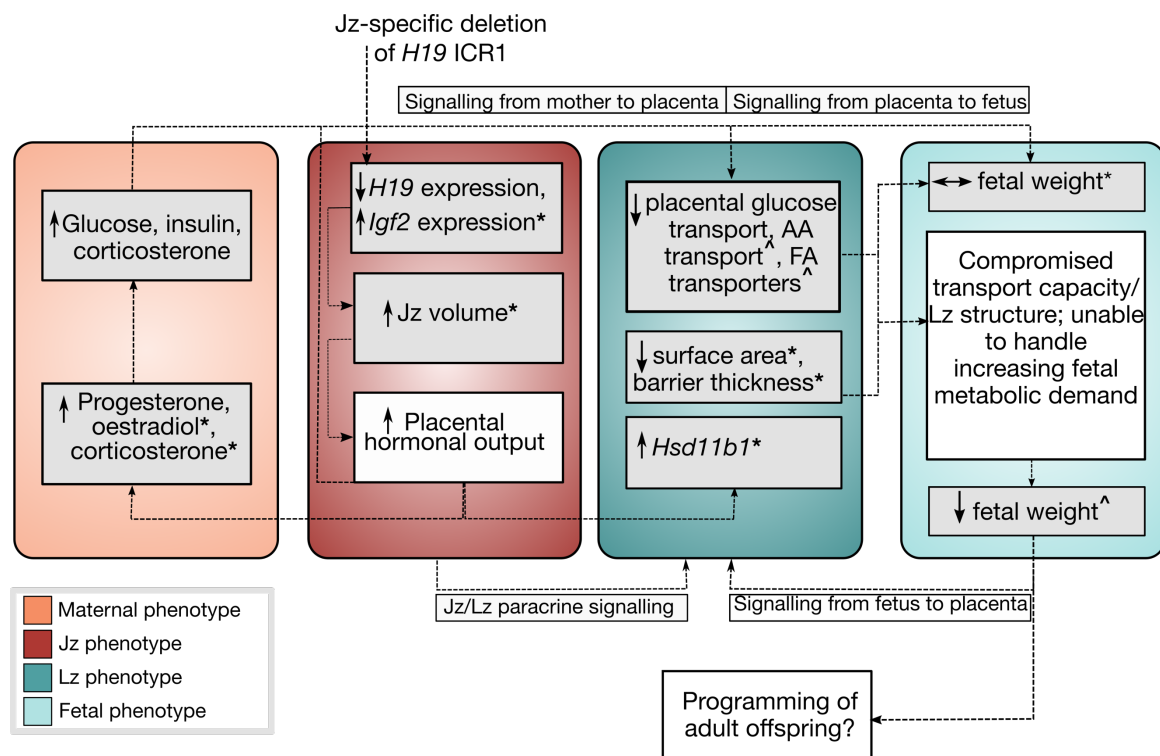


Figure 3.4.1. Summary diagram for maternal, placental and fetal phenotypes in response to Jz-ICR1A. Grey boxes represent experimental findings; white boxes represent extrapolations from findings. An asterisk (*) indicates a phenotype present only on E16; an arrow (^) indicates a phenotype present only on E19. Data for the maternal phenotype were collected by Dr Jorge Lopez-Tello and Dr Amanda Sferruzzi-Perri. AA, amino acid; FA, fatty acid; ICR1, imprinting control region 1; *Igf2*, insulin-like growth factor 2; Jz, junctional zone; Lz, labyrinth zone

3.4.1 The effect of *Igf2* and *H19* expression on Jz-ICR1Δ placental morphology

In the current model, a Jz-specific disruption in the *H19* ICR1 reduced *H19* expression, and increased *Igf2* expression and Jz volume at E16 of pregnancy. An expanded Jz was partly explained by a greater volume of glycogen cells and spongiotrophoblast cells with Jz-ICR1Δ, although neither reached statistical significance when compared to control (p=0.07). Indeed, *Igf2* expression is highest in spongiotrophoblast cells in early gestation and then highly abundant in the glycogen cells upon their differentiation (Redline et al., 1993). As expansion of the Jz coincides with an increase in *Igf2* expression on E16, *Igf2* may induce differentiation or proliferation of these trophoblast populations in the Jz at this time point. The ontology of *Tpbpa* expression, beginning at E7.5 and E8.5 is also consistent with the early expression of *Igf2* at E5.5 and during subsequent stages of placental development (Redline et al., 1993, Hasan et al., 2015, Cindrova-Davies et al., 2017). Moreover, *Igf2* expression is indeed observed in glycogen, spongiotrophoblast and giant cells within the junctional zone which arise from *Tpbpa* precursors (Redline et al., 1993, Simmons et al., 2007). *Igf2* inducing the proliferation of the Jz in the current model is also consistent with previous work (Lopez et al., 1996, Esquiliano et al., 2009), albeit glycogen content in response to Jz-ICR1Δ was not altered in comparison to these previous global *H19* null models, indicating that Lz *Igf2* may be important in stimulating glycogen synthesis. Whilst *Igf2* has proliferative actions on trophoblast cells as shown *in vitro* (Kanai-Azuma et al., 1993, Forbes et al., 2008) and *in vivo* with an increase in placental size upon global *Igf2* over-expression (Angiolini et al., 2011), *Igf2* also has anti-apoptotic effects on trophoblast (Forbes et al., 2008). These anti-apoptotic effects may also contribute to an expansion in Jz volume in this model and may be assessed in future by determining markers of apoptosis, such as BCL-2-associated X protein (*Bax*) in the Jz.

On E16, *Igf2* was over-expressed by only 31% in the Jz in response to Jz-ICR1Δ. In part, the level of *Igf2* over-expression with Jz-ICR1Δ may have been diluted by contamination of dissected Jz samples with LZ, as the LZ is known to have much greater *Igf2* expression compared to the Jz (Redline et al., 1993, Sandovici et al., 2019, Aykroyd et al., 2020). Using fluorescence activated cell sorting to isolate the endocrine cells from the control and Jz-ICR1Δ mouse placenta would be one way to avoid this in future work (Napso et al., 2020). Future work may also quantify the amount of LZ contamination in each Jz sample by determining the expression of Lz-specific markers (such as *P0*) in the Jz. Moreover, Jz contamination in the LZ may be determined by assessing the expression of

Tpbpa in each Lz sample. Nonetheless, previous data shows a similar degree of *Igf2* overexpression upon *H19* ICR1 deletion in mouse skeletal muscle (Srivastava et al., 2000). These data indicate the existence of other mechanisms controlling *Igf2* expression in addition to the *H19* ICR1. For instance, a large cluster of tissue-specific enhancers and nuclear factor binding elements may also contribute to the imprinting mechanism of *Igf2* in the placenta (Ishihara et al., 2000). Moreover, both CTCF and the *H19* differentially methylated region (DMR) participate in regulating the imprinting of *Igf2* (Thorvaldsen et al., 2006, Li et al., 2008, Qiu et al., 2008, Zhang et al., 2011a). Furthermore, miR483, an *IGF2* intronic microRNA, reduces the binding of CTCF to the *IGF2* promoter leading to biallelic expression of *IGF2* (Zhang et al., 2017) and interestingly, an overexpression of *IGF2*-derived intronic miR483 is also observed in macrosomia placentas (Li et al., 2018). Overall, these studies indicate a multifaceted mechanism of *Igf2* imprinting that only in part involves the ICR1, which was deleted in the current model.

On E19 of pregnancy, *Igf2* expression was no longer altered by Jz-ICR1 Δ , despite a continued reduction in *H19* expression in the Jz, albeit this reduction was of a lesser magnitude than that observed at E16 (78% at E16 and 59% at E19). When the *H19* structural gene is replaced with a protein-coding gene, *Igf2* expression is not altered, indicating that *H19* RNA *per se* is not essential for the imprinting of *Igf2* (Jones et al., 1998). Moreover, global *H19* deletion results in strongest *Igf2* expression in glycogen cells, and overall *Igf2* expression is highest in Jz glycogen cells during the second half of pregnancy (Redline et al., 1993, Esquiliano et al., 2009). However, these cells undergo lysis to provide an energy source of glucose for the fetus towards term (Bouillot et al., 2006, Coan et al., 2006, Tunster et al., 2020). Thus, a reduction in glycogen cell number as part of normal gestation may contribute to the lack of change in *Igf2* expression, as well as a normalisation of Jz volume in our Jz-ICR1 Δ model at E19. Indeed, regardless of fetal sex, *Igf2* expression by the Jz is reduced in both control and Jz-ICR1 Δ placentas between E16 and E19 (see Appendix 1.2, Table 1.2.1). Moreover, both glycogen cell volume and placental glycogen content are reduced at E19 compared to E16 (see Appendix 1.2, Tables 1.2.2 and 1.2.3), which has also been indicated previously (Lopez et al., 1996). When analysed regardless of fetal sex, glycogen cell volume is significantly increased in response to Jz-ICR1 Δ (Table 1.2.2, Appendix 1.2). Jz-ICR1 Δ did not alter the expression of glycogen, spongiotrophoblast or giant cell markers (*Gjb3*, *Pr18a8*, and *Hand1* respectively). Whilst the expression of these markers were determined in dissected

Jz, it is important to note that these dissections also included the decidua, therefore *Gjb3* expression is representative of GlyT populations in both the Jz and decidua. Moreover, *Hand1* regulates the formation of all TGC subtypes (Simmons et al., 2007), indicating that overall, Jz-ICR1 Δ did not affect the abundance of all giant cell subtypes, as also indicated in stereology analysis whereby TGC volume remained unaltered in response to Jz-ICR1 Δ . Nonetheless, in future to determine the abundance of P-TGC specifically, the expression of *Prl3d1/Pll* may be determined (Simmons et al., 2008, Hu and Cross, 2011). However, this should be done at an earlier point in gestation, as *Prl3d1/Pll* expression is highest at E9.5 and reduced thereafter (Simmons et al., 2008).

Upon Jz-specific *H19* ICR1 deletion in this model, *miR-675*, a micro-RNA located in exon 1 of *H19* (Cai and Cullen, 2007), is also deleted. Previous studies have shown that *miR-675* suppresses trophoblast proliferation, as ablation of *H19* and *miR-675* (with no alteration in placental *Igf2* expression) results in placental overgrowth (Keniry et al., 2012). Although *miR-675* levels were not measured in Jz-ICR1 Δ placentas, the expression of *Igf1r*, which is negatively regulated by this miRNA, was unaltered and decreased at E16 and E19, respectively. These data indicate that *miR-675* is unlikely to contribute to the expansion in Jz volume in our model. At E19 of pregnancy, *Igf1r* and *Insr* mRNA levels in the Jz were reduced in response to Jz-ICR1 Δ , which may have decreased sensitivity and signalling capacity for IGF2 in the Jz. A downregulation of IGF2 sensitivity and signalling via its main receptors in the placental Jz may reflect a negative feedback mechanism due to excess *Igf2* earlier in gestation. Indeed, consistent with this notion, recent work has demonstrated *Insr* mRNA levels are instead upregulated upon *Igf2* under-expression in the Jz (Aykroyd et al., 2020). Decreased *Igf1r* and *Insr* expression and hence, reduced IGF2 signalling capacity at E19 may explain the normalisation or lack of effect on Jz volume in response to Jz-ICR1 Δ . Indeed, in a normal mouse pregnancy, Jz expansion is maximal at E16.5 and declines thereafter (Coan et al., 2004). *Igf2r* expression tended to decrease in the Jz of Jz-ICR1 Δ placentas ($p < 0.07$) compared to genotype controls. This receptor is involved in both IGF2 lysosomal degradation and signalling (Harris et al., 2011), however the mechanism governing each outcome is not known. It is also not known whether a tendency for a change in *Igf2r* mRNA expression with Jz-ICR1 Δ would have implications for the endocrine phenotype of the placenta. In future, the protein abundance of IGF2 receptors, alongside downstream

signalling mediators may be measured in the Jz and Lz to determine changes in IGF2 signalling sensitivity.

3.4.2 Placental endocrine capacity in response to Jz-ICR1Δ

Increased Jz volume at E16 may be indicative of enhanced placental hormone output in Jz-ICR1Δ dams. Interestingly, the expression of steroidogenic enzymes (*Cyp17a1*, *Stard1*, *3bhsd*) was unaltered in response to Jz-ICR1Δ at E16 of pregnancy. Conversely *3bhsd*, which is involved in the conversion of pregnenolone to progesterone (Payne and Hales, 2004) was altered at E19 by an interaction between genotype and sex. To accurately deduce whether Jz-ICR1Δ increases the steroidogenic capacity of the Jz, an earlier time in gestation should be studied in the future, as the abundance of steroidogenic proteins (including 3β-HSD and StAR) decreases towards the end of gestation in rodents (Arensburg et al., 1999). During the latter half of pregnancy, the rodent placenta has an increased capacity to produce androstenedione (Jackson and Albrecht, 1985). Moreover, ovarian formation of oestradiol, preferentially utilising androstenedione, increases throughout gestation in rodents (Jackson and Albrecht, 1985) and indeed, in the mouse, ovarian steroidogenesis maintains the pregnancy throughout gestation (Murr et al., 1974). Therefore, an increase in ovarian steroidogenesis in Jz-ICR1Δ dams via placental-ovarian crosstalk cannot be discounted. Thus, in the future, steroidogenic enzyme activity should also be determined alongside mRNA and protein levels, in both the placenta and ovaries.

Moreover, it remains unknown whether Jz-ICR1Δ placentas display altered expression of non-steroid hormones, for instance mouse placental lactogen-II, which is critical in placental development and shows colocalization in the placenta with IGF2 (Ishida et al., 2007) and prolactin family members. Indeed, Jz-specific *Igf2* deletion reduces *Prl3b1* expression in the Jz (Aykroyd et al., 2020). Moreover, previous work in the Jz-ICR1Δ model indicates placental endocrine malfunction in these placentas, as shown by changes in the placental secretome. For instance, alterations in the secretion of prolactins (PR6A1, PR8A6), and pregnancy specific glycoproteins (B2RSG7, Q497W1) were shown in Jz-ICR1Δ placentas (data not shown). Furthermore, the involvement of non-coding RNAs (ncRNA) and placental exosomes in the Jz-ICR1Δ phenotype may be studied prospectively, as previous work has indicated alterations in placental expression of ncRNA and cross talk between placental exosomes and maternal tissues in GDM (Jayabalan et al., 2017, Tang et al., 2020). Upregulation of endocrine function in Jz-

ICR1 Δ placentas via Jz expansion at E16 would be expected to increase hormone levels in dams. Indeed, previous work has shown that Jz-ICR1 Δ mice also have increased concentrations of plasma progesterone and oestradiol at E16, but not at E19 when the Jz is no longer expanded (Table 1.13.1, Lopez-Tello et al, unpublished). These findings collectively indicate an important role of the placental Jz in determining maternal sex steroid levels during pregnancy. Previous studies have demonstrated that progesterone treatment in ovariectomised rats increases insulin concentrations in the portal vein, whilst progesterone receptor antagonism causes hypoglycaemia in mice (Mandour et al., 1977, Picard et al., 2002). Conversely, the knockout of oestrogen receptor induces hyperglycaemia and hyperinsulinemia in mice (Bryzgalova et al., 2006). These data are partly in accordance with the hyperinsulinemia and hyperglycaemia observed in Jz-ICR1 Δ dams (Table 1.13.1, Lopez-Tello et al, unpublished), and indicate that increased progesterone and oestradiol concentrations have metabolic consequences in these dams. However, much more work is required to understand changes in placental endocrine capacity in relation to maternal metabolic profile through the whole index of pregnancy in response to Jz-ICR1 Δ .

3.4.3 Placental Lz morphology and nutrient transport capacity in response to Jz-ICR1 Δ

Changes in placental Lz morphology and transport capacity in response to Jz-ICR1 Δ may reflect alterations in the paracrine communication of the Jz with the Lz due to Jz *Igf2* and/or *H19* misexpression. The potential for paracrine signalling between placental zones has been indicated previously in the *P0* (Lz-specific) *Igf2* knockout, whereby glycogen cell volume is decreased in the Jz (Sferruzzi-Perri et al., 2011). Moreover, knockout of p110 α signalling in the trophoblast alters fetal capillary volume, which is indicative of paracrine signalling between the cellular compartments of the Lz (López-Tello et al., 2019). In response to Jz-ICR1 Δ , there was a reduction in trophoblast membrane surface area and theoretical diffusing capacity at E16 and an increase in MBS volume at E19. Alterations in the morphology of the Jz-ICR1 Δ placenta may act in concert with functional changes to affect fetal growth during gestation. Lz morphological characteristics (i.e. trophoblast surface area and barrier thickness) influence fetal oxygen transfer, which occurs via simple diffusion (Burton et al., 2016). Thus, a reduced surface area and theoretical diffusion capacity for oxygen at E16 in response to Jz-ICR1 Δ may have limited fetal oxygen provision and hence, fetal growth. Interestingly, despite the

reduction in theoretical diffusion capacity, the specific diffusion capacity of the placenta, which is adjusted for fetal weight, was not changed and may indicate that, at E16, the fetus is receiving appropriate oxygen levels to maintain normal growth. However, it is also possible that the morphological defects seen in the Lz at E16 with Jz-ICR1 Δ contributed to the fetal weight reduction at E19. Changes in Lz morphology on E16 with Jz-ICR1 Δ were the opposite to those seen in the global (fetoplacental) *Igf2* overexpression via *H19* and ICR1 deletion (Angiolini et al., 2011). The discrepancy between studies may reflect complexities of paracrine signalling between placental zones as well as suggest a role for fetal IGF2 in driving Lz formation (Sandovici et al., 2019), as fetal IGF2 was genetically increased in the global mutant, but is not known to be increased in the Jz-ICR1 Δ mutant. The increase in MBS volume seen at E19 in our Jz-ICR1 Δ model was however, observed in the global *Igf2* overexpression mutant (Angiolini et al., 2011). As *Igf2* was not over-expressed at E19 in our model, there may be changes brought about by the enhanced Jz *Igf2* expression on E16, which only manifest in the Lz at E19. Indeed, IGF2 has been shown to affect the expression of several angiogenic factor genes, such as *Vegf*, and FMS related receptor tyrosine kinase 1 (*Flt1*); (Kawahara et al., 2010), and upregulates inducible nitric-oxide synthase (iNOS) expression (Kaliman et al., 1999, Krause et al., 2011); all of which may regulate maternal blood flow to the placenta. Increased MBS volume in response to Jz-ICR1 Δ may also be indicative of spiral artery remodelling and changes in blood perfusion in the Lz. Alternatively, increased MBS volume may be attributed to reduced branching in the Lz, which would disrupt the shaping of MBS (Adamson et al., 2002). Disruptions in the extensive villous branching that creates the labyrinth is observed in *C/EBP α / β* knockout mice, resulting in embryonic lethality at E10 (Bégay et al., 2004). Moreover, the knockout of *Ppar γ* induces vascular defects in the placenta, with fetal vessels rarely traversing the chorionic plate into the Lz and MBS are dilated and adjoined (Barak et al., 1999). Thus, given the morphological defects observed in the Lz of Jz-ICR1 Δ placentas, the Lz expression of *Ppar γ* and *Cebp/ α* may be determined in future.

Glucose transport via the placenta is another determinant of fetal growth. Indeed, in a healthy pregnancy, glucose transport to the fetus is maximal towards term (Catalano et al., 1992). Despite the hyperglycaemic environment in Jz-ICR1 Δ dams (Table 1.13.1, Lopez-Tello et al, unpublished), which is usually associated with increased fetal weight (Wahab et al., 2020), fetal weight was unaltered at E16 and reduced at E19. This is

indicative of the placenta being unable to support the increasing metabolic requirements of the fetus towards term and is likely due to the reduction in placental glucose clearance seen at both E16 and E19 of pregnancy and reduced placental MeAIB clearance at E19 with Jz-ICR1 Δ . Indeed, on both E16 and E19 the fetal/placental ratios are decreased, which further suggests placental inefficiency. Changes in glucose transporter (*Slc2a1*, *Slc2a3*) and system A amino acid transporter (*Slc28a1*, *Slc38a2*, *Slc38a4*) mRNA levels, however, were not observed in the Lz in response to Jz-ICR1 Δ . This discrepancy between nutrient transport *in vivo* and mRNA levels of transporters has been observed previously in models of maternal high fat diet or dexamethasone treatment (Jones et al., 2009, Vaughan et al., 2013), and may show that transporter protein abundance at the surface of the syncytiotrophoblast is more indicative of placental glucose and amino acid transport, rather than transporter mRNA levels. As glucose transport occurs via facilitated diffusion, levels of placental glucose transport are also determined by Lz morphology and indeed, in Jz-ICR1 Δ mice, a reduction in placental glucose clearance was associated with the decrease in trophoblast membrane surface area on E16, but not E19 of pregnancy. Moreover, when placental glucose clearance was corrected for the surface area of the trophoblast membrane, it was no longer decreased at E16 in Jz-ICR1 Δ mice. These findings indicate that reduced glucose transport is due to decreased surface area at E16, although the cause of the reduction at E19 requires study.

Despite the decreased Lz surface area at E16, placental MeAIB transfer was not decreased per gram of placenta and adaptively increased relative to the available surface area in response to Jz-ICR1 Δ . This adaptive increase in placental MeAIB may have compensated for the diminished MeG transport and maintained fetal weight at E16 with Jz-ICR1 Δ . This may also be a consequence of Jz-IGF2 signalling to the Lz, as upon global *Igf2* knockout, MeAIB transport is reduced (Constancia et al., 2005). Conversely, at E19, MeAIB clearance was reduced in Jz-ICR1 Δ mice, an effect that remained even after accounting for the area available for exchange. Previous work has shown reduced total amino acid levels in the maternal circulation at E19 in Jz-ICR1 Δ mice (Table 1.13.1, Lopez-Tello et al, unpublished). It is important to note however, that whilst maternal amino acid levels are indicative of all amino acids in the circulation, MeAIB clearance is a proxy for system A amino acid transport only and so the relevance of earlier work in the model is unclear. Together, the diminished placental MeG and MeAIB transport at E19 with Jz-ICR1 Δ was in line with the reduction in fetal weight at this gestational age. It was

also in line with the reduced *in vivo* placental transport of MeG and MeAIB in the global *Igf2* overexpression mutant (Angiolini et al., 2011). In spite of the variability in Lz morphology between Jz-ICR1Δ and global *H19-Igf2* mutation, a reduction in nutrient transport in both models may be adaptive, to mitigate from the teratogenic effects of excess glucose and avoid an excessive drain of maternal resources, given that litter size is increased at E19 in response to Jz-ICR1Δ.

There were also alterations in placental capacity for lipid transfer with Jz-ICR1Δ. On E16 of pregnancy an interaction between genotype and sex influenced *Fatp4* expression, whilst on E19 of pregnancy, fatty acid translocase and binding protein (*Cd36*, *Fabp3*) mRNA levels were decreased by Jz-ICR1Δ. Interestingly, at E19 of pregnancy, triglycerides and non-esterified fatty acids (NEFA) are increased in the maternal circulation (Table 1.13.1, Lopez-Tello et al, unpublished) and, therefore, reductions in *Cd36* and *Fabp3* mRNA levels may compensate for changes in the maternal environment with Jz-ICR1Δ. Placental lipid transport has an important impact on fetal growth and lipid accumulation (Friedman et al., 1978, Chambaz et al., 1985), however, as the mechanisms of fatty acid transport across the trophoblast membrane have been less well characterised, it is difficult to delineate the specific significance of decreased *Cd36* and *Fabp3* expression may be in our Jz-ICR1Δ model, which shows reduced fetal weight near term. Several studies in both rodent models of obesity, and human obese and GDM patients, show changes in placental fatty acid translocase/binding protein expression (Radaelli et al., 2009, Dubé et al., 2012, Brass et al., 2013, Sasson et al., 2015, Louwagie et al., 2018). However, the direction of change varies between studies and may in part be dependent on the time in gestation, species studied and/or maternal plasma fatty acid levels. Given the alterations in lipid metabolism gene expression in the placenta in this model, it would be of interest to determine fetal lipid content in response to Jz-ICR1Δ in future.

3.4.4 Maternal physiology and Jz-ICR1Δ placental morphology and nutrient transport capacity

Alterations in plasma hormones and metabolites in Jz-ICR1Δ dams may have contributed to the increased placental weight, changes in Lz morphology and placental nutrient transport capacity. Indeed, Jz-ICR1Δ dams had increased concentrations of circulating glucose, insulin and leptin on E16 and E19, whilst oestradiol, progesterone and corticosterone concentrations were increased on E16 only. Alterations in the lipid profile

(LDL-C, triglycerides and NEFA) of Jz-ICR1Δ dams was also evident and dependent on gestational age (summarised in Table 1.13.1). For instance, full oestradiol and partial progesterone replacement in ovariectomised pregnant rats is linked to reduced Lz, Jz, whole placental, and fetal weights (Mark et al., 2006). Both insulin and glucose alter placental size, as indicated in studies that report placentomegaly in hyperglycaemic streptozotocin treated rats and reduced placental weight in hyperinsulinemic dams (Skarzinski et al., 2009, Nteeba et al., 2020). Moreover, oestrogen treatment in rats causes underdevelopment of the Lz (Kagawa et al., 2014). In rats, prenatal dexamethasone exposure reduced the surface area of the fetal capillaries and theoretical oxygen diffusion capacity (Guo et al., 2020). The latter alterations in Lz morphology also observed in our Jz-ICR1Δ model, whereby dams have increased corticosterone levels on E16 of pregnancy (Table 1.13.1, Lopez-Tello et al, unpublished). Moreover, despite Jz volume being unaltered in response to Jz-ICR1Δ at E19, the observed increase in placental weight during this time may in part be due to changes in dam hormone/metabolite concentrations.

Corticosterone treatment in dams also reduces placental glucose and amino acid transport, the effects of which are dependent on gestational age and maternal feeding (Vaughan et al., 2012, Vaughan et al., 2015). Thus, elevated corticosterone concentrations in Jz-ICR1Δ dam circulation may in part influence the changes in placental glucose and amino acid transport observed. A hyperglycaemic maternal environment, as occurs in streptozotocin treated rats, results in an increase in placental glucose uptake and reduced clearance, a phenomenon also observed upon insulin injection in dams (Leturque et al., 1986, Thomas et al., 1990, Boileau et al., 1995). Interestingly, streptozotocin treatment also reduces fetal weight and placental efficiency (Nteeba et al., 2020), as is observed in the current Jz-ICR1Δ model. Moreover, LPL protein abundance is reduced in the placentas of GDM patients given insulin (Ruiz-Palacios et al., 2017). Therefore, the reduction in placental glucose clearance and reduced expression of lipid metabolism markers observed in response to Jz-ICR1Δ may in part be mediated by increased glucose and insulin concentrations in Jz-ICR1Δ dam circulation. A reduction in placental *Slc2a1* or GLUT1 protein abundance is observed upon treatment of rodent dams with leptin or synthetic oestrogens respectively (Kagawa et al., 2014, Denisova et al., 2020), with Jz-ICR1Δ dams having increased circulating leptin and oestradiol concentrations. Interestingly, the effect of leptin administration on *Slc2a1* expression is sex-specific,

being observed only in female placentas (Denisova et al., 2020). This is in accordance with the magnitude of reduction in glucose transport in response to Jz-ICR1Δ on E16 being greater in females (27%) compared to males (21%) and post hoc analysis only reaching significance in females. Overall, whether specific hormones in the endocrine milieu of Jz-ICR1Δ dams are influencing changes in placental glucose and amino acid transport should be further explored. To discriminate whether changes in placental weight, Lz morphology and nutrient transport are due to alterations in Jz/Lz paracrine signalling and/or alterations in maternal metabolism in our Jz-ICR1Δ model, mixed litters may be used in future studies, whereby maternal metabolism remains unaltered due to wild type and mutant placentas being present in the same pregnancy. This could be complemented by studies determining the activation of the IGF2 signalling pathway in the placental Lz in mixed litters, as well as those where the whole litter is Jz-ICR1Δ.

3.4.5 Placental corticosterone handling in response to Jz-ICR1Δ

There were also alterations in the placental Lz handling of corticosterone in response to Jz-ICR1Δ. Despite increased maternal corticosterone concentrations on E16 of pregnancy, *Hsd11b1* expression was increased in the Lz at E16, specifically in females, but not males in response to Jz-ICR1Δ. These findings suggest that female fetuses may receive more corticosterone than males in response to Jz-ICR1Δ, as *Hsd11b1* converts inactive 11-dehydrocorticosterone to active corticosterone (Blasco et al., 1986, Burton et al., 1996). A previous study has indicated that, in response to maternal psychological stress with high corticosterone levels in gestation, there are differences in the timing and level of induction of *Hsd11b2* expression in the placenta of male compared to female fetuses (Wieczorek et al., 2019). This corroborates our findings in Jz-ICR1Δ dams with high corticosterone levels by highlighting overall, a sexual disparity in placental response to a suboptimal uterine environment. As corticosterone treatment in dams reduces placental glucose clearance (Vaughan et al., 2015) it may be that enhanced active corticosterone in the placental Lz of female but not male fetuses causes a more pronounced reduction in MeG transfer in females on E16 and causes an interaction of sex and genotype on *Fatp4* expression. Indeed, in future plasma corticosterone, glucose, amino acid and fatty acid concentrations should be determined in Jz-ICR1Δ male and female fetus'. This would be key in determining how changes in placental nutrient transport and corticosterone handling influence fetal phenotypes.

The current Jz-ICR1 Δ model studies the effect of endocrine zone expansion, assuming increased endocrine output on changes in placental nutrient transport and fetal outcomes. Overall, Jz-specific *H19* ICR1 deletion led to Jz expansion at E16 with concomitant increased Jz-*Igf2* expression. Endocrine zone expansion likely increases placental endocrine capacity, as evidenced by increased maternal concentrations of progesterone and oestradiol with consequent maternal metabolic consequences (as summarised in Figure 3.4.1). A limitation in this model is that despite a placental-specific manipulation being utilised, an increase in Jz-*Igf2* expression was not maintained throughout pregnancy and changes in maternal metabolism also likely influence the placental and fetal phenotypes observed. Despite this, Jz-ICR1 Δ induced molecular, structural and functional changes in the placenta and interestingly, only a portion of these changes were dependent on fetal sex. Although Jz-specific manipulation was utilised, reductions in placental nutrient capacity and changes in Lz morphology were observed. Alterations in Lz phenotype may be in response to changes in maternal metabolism, paracrine signalling between the Jz and Lz, or signalling directly from the fetus, as well as a combination of these paradigms. Moreover, endocrine mediators from the Jz may also signal directly to the fetus. It remains unknown how the placenta is able to sense a hyperglycaemic environment and adapt morphologically and functionally to meet fetal needs. Endocrine signalling to the fetus and placenta via IGF2 in the maternal circulation appears to be unlikely as IGF2 concentration in the maternal plasma is unaltered in Jz-ICR1 Δ mice (Table 1.13.1, Lopez-Tello et al, unpublished). However, other metabolites and hormones in the maternal circulation may signal via the fetus or directly to the placenta. Indeed, the placenta contains several nutrient sensing signalling pathways (AMP-activated protein kinase (AMPK), GSK3, amino acid response signal transduction pathway and mTORC1) which respond to changes in nutrient levels (Jansson and Powell, 2013). Placental structural and nutrient transport changes are dependent on whether *Igf2* is deleted from the fetus, fetoplacental unit or placenta alone, indicating that fetal IGF2 levels are a critical signal of fetal nutrient demand (Constancia et al., 2005, Coan et al., 2008b) and could potentially signal back to the placenta and contribute to the changes seen in our Jz-ICR1 Δ mice. In turn, it is possible that the placenta secretes endocrine mediators, namely IGF2 into the fetus to exert direct impacts on fetal growth and nutrient handling. Therefore, IGF2 levels in fetal plasma should be determined in the future in the Jz-ICR1 Δ model to identify if an increase in *Igf2* expression in the Jz may impact fetal IGF2 circulating levels. Whatever the mechanisms governing this, placental adaptation in

response to Jz-ICR1 Δ overall compromises Lz structure and nutrient transport capacity leading to reduced fetal weight at E19. Reduced fetal weight is commonly used as a proxy for reduced fetal nutrient acquisition, which is also likely occurring in response to Jz-ICR1 Δ . Overall, a reduction in fetal nutrient acquisition and weight induced by placental morphological and functional changes in response to Jz-ICR1 Δ may have impacts for perinatal health and consequent adverse offspring metabolic programming.

Chapter 4: The effect of Jz-ICR1Δ on adult offspring metabolic health outcomes

4.1 Introduction

The diagnostic criteria for metabolic syndrome, as set out by the World Health Organisation (WHO), include insulin resistance or elevated fasting glucose or impaired glucose tolerance in addition to at least two other symptoms, namely central obesity, increased blood pressure, dyslipidaemia or microalbuminuria (Alberti and Zimmet, 1998). The prevalence of metabolic syndrome has been rising in Western countries, with a concomitant increase in unhealthy diet habits such as calorie dense diets and sedentary lifestyles likely being contributing factors. Indeed, recent estimates suggest one in four people have metabolic syndrome world-wide (O'Neill and O'Driscoll, 2015, Saklayen, 2018). In addition to contributing lifestyle factors, a suboptimal environment during gestation is also known to increase the risk of offspring developing metabolic syndrome in adulthood. The Developmental Origins of Health and Disease hypothesis is now a commonly accepted paradigm which makes associations between the quality of the environment *in utero* and the risk of developing metabolic syndrome during adulthood (Barker and Osmond, 1986). For instance, in human GDM or obese pregnancies, frequently characterised by a hyperglycaemic gestational environment, the propensity for offspring to develop obesity and glucose intolerance during adulthood is increased (Petitt et al., 1985, Dabelea, 2007). An unhealthy diet, such as consumption of a calorie dense diet has been shown to exacerbate the ill effects of adverse gestational environments in offspring (Li et al., 2015b, Li et al., 2015c). Moreover, altered fetal weight (either decreased or increased) is often used as an indicator of an adverse gestational environment, with both birth outcomes associated with an increased propensity for poor offspring metabolic health in adulthood (Dabelea, 2007).

Fetal growth outcomes are influenced by the maternal environment during pregnancy. Alterations in the maternal environment including hyperglycaemia or increased glucocorticoid levels are mediators of developmental programming via changes in fetal growth (Fowden and Forhead, 2004, Catalano et al., 2012). Glucocorticoids are critical in promoting organ maturation of the fetus in the lead-up to term. Animal models have indicated that the maternal administration of the synthetic glucocorticoid dexamethasone, or inhibition of placental 11βHSD2, is associated with the development of glucose

intolerance and hyperglycaemia in offspring (Lindsay et al., 1996, Saegusa et al., 1999, Franko et al., 2010, Somm et al., 2012). In rodent models of maternal diabetes (streptozotocin treatment) and obesity (high fat diet), there are also programmed alterations in adult offspring metabolism, with glucose intolerance, insulin resistance, hyperglycaemia and hyperinsulinaemia observed (as summarised in Table 1.1). Morphological alterations in adipocyte and pancreatic islet masses are also observed and may, in part, influence whole body physiology (Theys et al., 2011, Oliveira et al., 2015, Bringhenti et al., 2016). These changes in rodent offspring metabolism are governed by the misexpression and altered abundance of candidate genes and proteins involved in the insulin signalling pathway, gluconeogenesis, lipid metabolism, inflammation, growth and development, mitochondrial metabolism and ion transport (as summarised in Table 1.1, (Christoforou and Sferruzzi-Perri, 2020).

During pregnancy, the placenta, via its endocrine function, alters maternal metabolism to ensure nutrients are supplied to the fetus for growth (Napso et al., 2018). For instance, via its production of steroid and peptide hormones the placenta induces a state of physiological insulin resistance in the mother to partition glucose and lipids to the fetus (Sferruzzi-Perri et al., 2020). However, abnormalities in placental endocrine function may lead to inappropriate maternal metabolic changes with consequences for fetal nutrient supply and growth. Thus, it has been proposed that placental endocrine dysfunction may contribute to adverse pregnancy and fetal and offspring outcomes. Indeed, placental endocrine dysfunction has been indirectly implicated in pregnancy pathologies associated with abnormal maternal metabolic adaptations and/or a high glucose intrauterine environment. For instance, dysregulated expression of several hormones such as leptin, placental growth hormone variant and human placental lactogen has been observed in the placenta of women who developed GDM (Hu et al., 1999, Lea et al., 2000), whilst circulating concentrations of progesterone, oestradiol, leptin and IGF1 are also increased in GDM (Liao et al., 2017, Ngala et al., 2017). Moreover, in a mouse model of maternal obesity, reduced placental prolactin expression indirectly implicates placental endocrine capacity in the maternal metabolic consequences of obesity (Musial et al., 2017). However, the role of the endocrine placenta in the programming of offspring metabolic health has never been directly demonstrated, whilst placental-specific manipulation would offer a means to do so.

The mouse placenta serves as an excellent model to study the effect of placental endocrine function on offspring metabolism, as the endocrine Jz is morphologically and functionally distinct from the transport Lz. Moreover, our Jz-ICR1 Δ model allows for selective Jz manipulation to study offspring metabolic outcomes. Indeed, as previously shown, Jz-ICR1 Δ results in altered placental endocrine volume (see Chapter 3), maternal metabolic and endocrine state (including elevated circulating glucose, insulin and corticosterone; see Table 1.13.1) and abnormalities in fetal nutrient supply and growth (see Chapter 3) during pregnancy. Thus, it was hypothesised that Jz-ICR1 Δ would also programme adult offspring metabolic ill-health.

The aims of this study were to evaluate the effect of Jz-ICR1 Δ on offspring:

- Growth trajectory and the morphology of key metabolic organs,
- Glucose and insulin handling and
- Molecular pathways governing glucose, insulin and lipid handling in key metabolic organs in response to a standard chow and a high sugar high fat diet from weaning.

4.2 Materials and methods

Animals

Experiments were performed under the UK Home Office Animals (Scientific Procedures) Act 1986, approved by the University of Cambridge. Mice were housed under 12:12 h dark/light photocycle conditions with *ad libitum* access to liquids and standard chow diet. Female mice in which the ICR1 of the *H19-Igf2* locus is flanked by *LoxP* sites were mated with males expressing *Cre* recombinase under the promoter of the Jz-specific gene, *Tpbpa* (*Tpbpa-Cre*; Figure 2.1). All mice were bred on a C57BL/6N (Charles River) background. The reverse parental cross was utilised as a control in all experiments. Only the placental Jz (and not the mother or fetus) has been genetically manipulated, but for ease placentas, dams and offspring will be referred to as Jz-ICR1 Δ in this study. n = 30 mice were mated for all offspring experiments. Female mice were placed in a cage with a stud in the afternoon and the presence of a copulatory plug in the following morning was defined as E1 of pregnancy. Dams were fed a standard chow diet throughout gestation (RM3, Table 2.3) and allowed to deliver naturally. Pups were weighed and sexed at postnatal day 3 (P3) and litters standardised to 3 female and 3 male pups per litter as far as possible. Pups culled on P3 for litter standardisation provided organ weight (biometrical) data. After weaning litters of female or male pups were randomly allocated to be provided with standard chow or high sugar and high fat diet (HSHF; Table 2.3). The offspring experimental programme is described in detail in section 2.3.1 (and Figure 2.5). The number of offspring used in experimental procedures and biometry are shown in Table 2.1.

GTT, ITT and biometry

A glucose or insulin tolerance test was performed on offspring at week 16 (adulthood). The GTT and ITT protocol is described in detail in section 2.3.3. Offspring were then left to recover for one week and at week 17, offspring were sacrificed, biometry performed, and bloods collected as described in section 2.3.4.

Fat and protein assays

The fat content in liver, and protein content in liver, adipose and skeletal muscle, were measured using a Folch and BCA assay, respectively. The protocols for these assays are described in sections 2.3.5.1 and 2.3.5.2.

Metabolite assays

Corticosterone, insulin, leptin, cholesterol, triglycerides and free fatty acids were measured in offspring mouse plasma. The protocols for these assays are described in detail in section 2.3.5.3.

Adipocyte stereology

Gonadal white adipose tissue was embedded, sectioned, H&E stained, and adipocyte area analysed using the Adiposoft V1.13 plugin on Fiji imaging software (Version 2.0.0 with Java 1.8.0_202 (64-bit), National Institutes of Health, USA) as described in detail in section 2.3.6.2.

Pancreatic insulin content and islet area

Offspring pancreatic insulin content was measured using an ELISA kit as described in section 2.3.5.4. Offspring pancreas islet area, mass and the number of islets per mm² of total pancreas area were determined by immunohistochemistry for insulin (as described in section 2.3.6.1) and stereological analysis using ImageJ software (version 1.52a with Java 1.8.0_51 (64-bit), National Institutes of Health (NIH), USA), as described in section 2.3.6.1.

Western blotting

The abundance of proteins involved in insulin, glucose and lipid handling was analysed in offspring liver, skeletal muscle and adipose tissue as described in section 2.3.7.

Statistics

All data are presented as means \pm standard error of the mean (SEM). Overall, data were largely normally distributed as validated by a D'Agostino-Pearson (omnibus K2) normality test (GraphPad Prism, 7.0). Where one variable (i.e., genotype) was assessed, Student's t-tests were performed using Microsoft Excel. Offspring growth trajectories and

GTT and ITT curves were measured by two-way repeated measures (RM) ANOVA. For GTT and ITT curves, the trapezoid rule was used to calculate the area under or above the curve, and these were analysed by two-way ANOVA with genotype and diet as parameters and a Sidak post hoc test. For data sets involving several pups from a litter, litter means were used, and a two-way ANOVA (genotype and diet) was performed with a Sidak post hoc test. Male and female offspring were analysed separately throughout this study to control for sex differences. Analyses were performed using GraphPad Prism 7.0 and p values of < 0.05 were considered statistically significant.

4.3 Results

4.3.1 Gestation and delivery

Jz-ICR1 Δ did not alter gestational length, litter size (live births only), number of stillbirths, the percentage of male pups per litter or the percentage of pups to survive to postnatal day 3 (P3; Figure 4.1). Litter size was determined at birth.

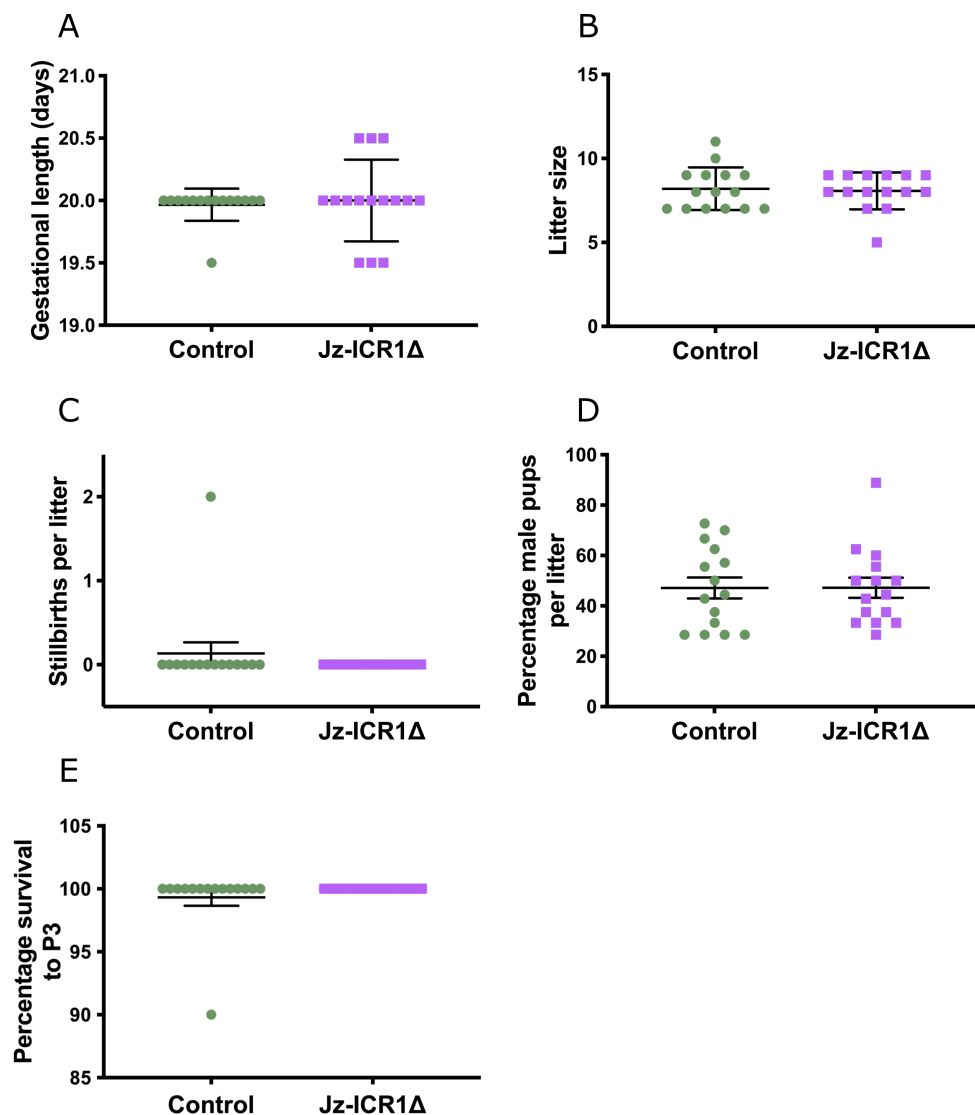


Figure 4.1. The effect of Jz-ICR1 Δ on gestational length (A), litter size (B), stillbirths (C) the percentage of male pups (D) and the percentage to survive to postnatal day 3 (P3). Individual points represent individual litters, and the mean is denoted as a horizontal line \pm SEM. Data from 15 litters per genotype are shown and were analysed by Student's t-test.

4.3.2 Postnatal day 3 biometry

Biometry for male and female offspring on P3 in response to Jz-ICR1 Δ are shown in Figures 4.2 and 4.3, respectively. At P3, Jz-ICR1 Δ was not associated with altered body, brain, liver, pancreas, heart, kidney, spleen or lung weights (either as an absolute weight or percentage of body weight) in male offspring. Moreover, Jz-ICR1 Δ exposure did not alter the brain/liver ratio in male offspring at P3.

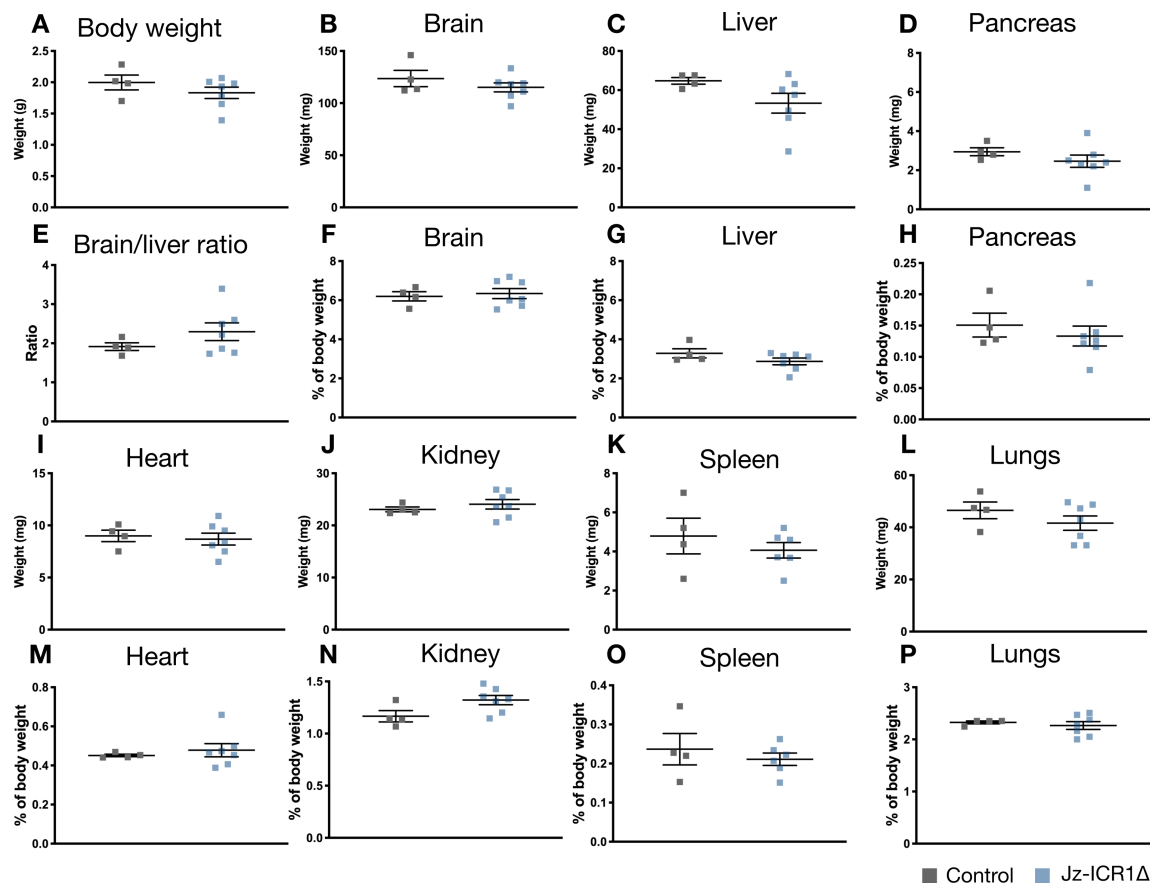


Figure 4.2. The effect of Jz-ICR1 Δ on male offspring biometry on postnatal day 3 (P3). Biometry data are presented either as total weight or as a percentage of body weight. Individual points represent litter means and the mean is denoted as a horizontal line \pm SEM. Data from 4-7 litters per genotype are shown and were analysed by Student's t-test.

Female offspring at P3 that had been exposed to Jz-ICR1Δ had unaltered body, brain, liver, pancreas, heart, kidney, spleen or lung weights (either as an absolute weight or percentage of body weight), and unaltered brain/liver ratio compared to controls. There was a tendency for pancreas weight to be reduced in female Jz-ICR1Δ offspring, although not significantly so (p=0.06; Figure 4.3D).

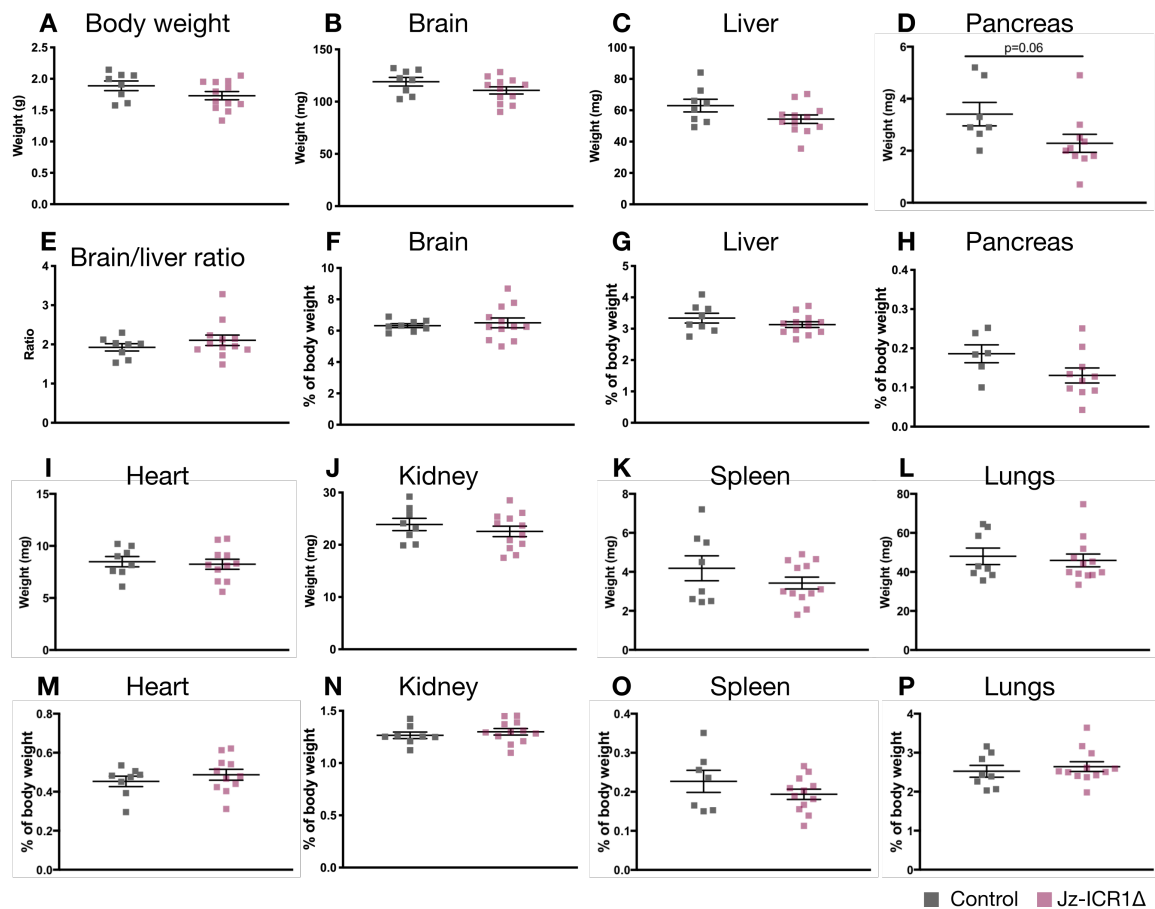


Figure 4.3. The effect of Jz-ICR1Δ on female offspring biometry on postnatal day 3 (P3). Biometry data are presented either as total weight or as a percentage of body weight. Individual points represent litter means and the mean is denoted as a horizontal line ± SEM. Data from 8-12 litters per genotype are shown and were analysed by Student's t-test.

4.3.3 Offspring growth trajectory

Male and female offspring growth trajectories in response to Jz-ICR1 Δ are shown from P3 to P21 in Figure 4.4A, F, and from week 4 to week 17 (on either a standard chow or HSHF diet) in Figure 4.4C, D, H, I. From P3 to P21, in both male and female offspring time increased body weight, whilst Jz-ICR1 Δ reduced the rate of this increase in body weight relative to controls and an interaction between time and genotype was observed ($p < 0.001$; Figure 4.4A, F). In response to Jz-ICR1 Δ , both male and female offspring had a reduced body weight at P14 and P21 compared to controls ($p < 0.01$; Figure 4.4A, F). Male Jz-ICR1 Δ offspring continued to be lighter than their control counterparts from week 4-16 ($p < 0.05$; Figure 4.4C). Conversely, Jz-ICR1 Δ male offspring weight was not different to control males on a HSHF diet from weeks 4-16 (Figure 4.4D). There was no difference in Jz-ICR1 Δ female offspring weight versus control, regardless of diet from weeks 4-16 (Figure 4.4H, I). However, time increased body weight in all offspring, regardless of sex or diet from weeks 4-16 ($p < 0.0001$; Figure 4.4C, D, H, I).

The specific growth rates of male and female offspring from P3 to P21 were not altered by Jz-ICR1 Δ (Figure 4.4B, G). Moreover, genotype did not alter the specific growth rates of male or female offspring on a chow or a HSHF diet from weeks 4-16 (Figure 4.4E, J). However, the growth rates of both male and female offspring from weeks 4-16 were increased by a HSHF diet compared to a chow diet regardless of genotype ($p < 0.01$; Figure 4.4E, J).

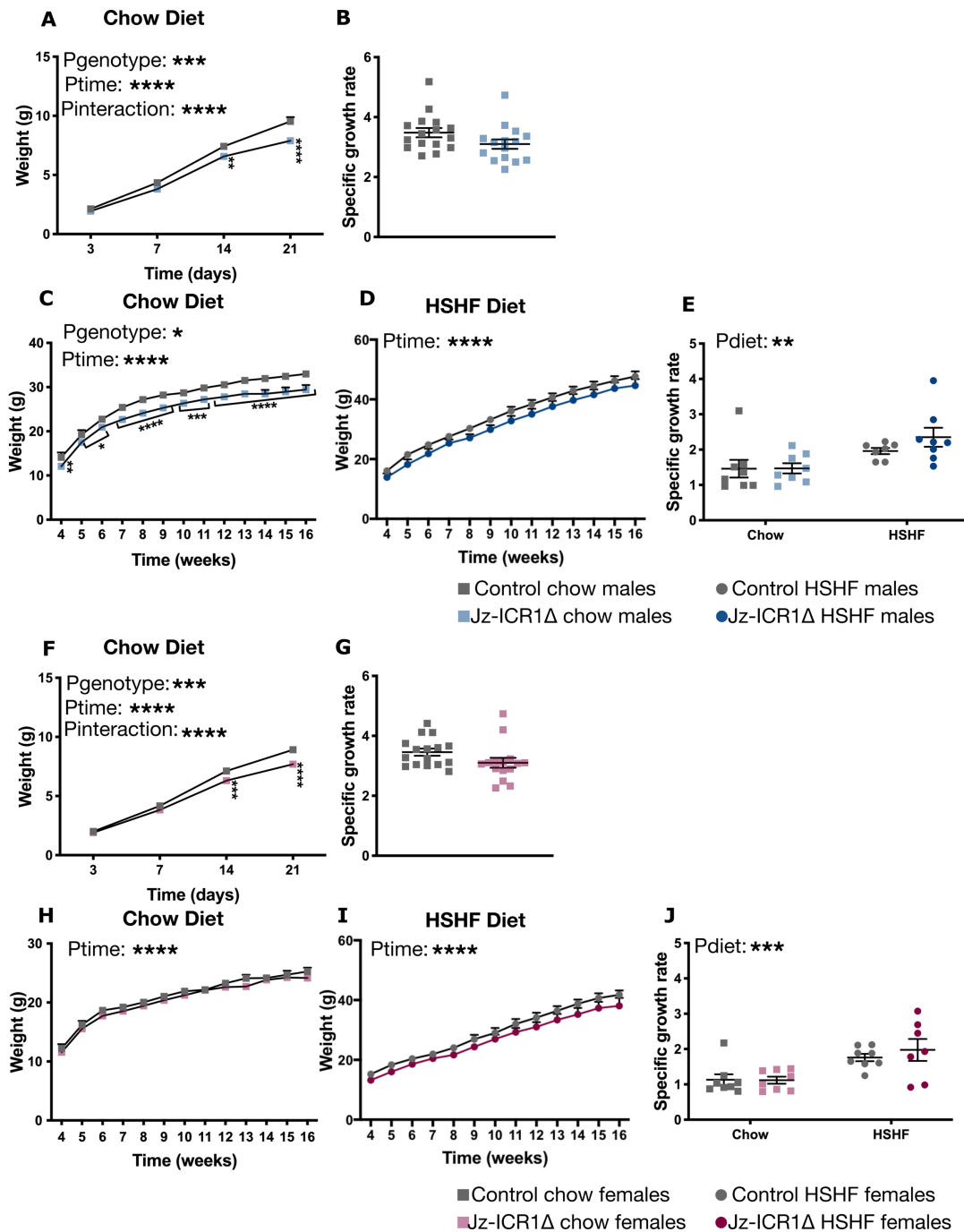


Figure 4.4. The effects of Jz-ICR1Δ and postnatal diet on offspring growth trajectory. The growth of male (A-E) and female (F-J) offspring consuming a chow (A, C, F, H) or HSHF (D, I) diet is shown from postnatal day 3 (P3) to weaning (P21; A, F) and from week 4 to week 17 (C, D, H, I). Individual points represent the mean weight or growth rate of litter means \pm SEM and the group mean is denoted as a horizontal line. 15-16 litters per genotype are shown from P3-21 and 7-8 litters per genotype and diet are shown from week 4-16. Growth trajectory data were analysed by two-way repeated measures ANOVA (genotype, time) with a Sidak post hoc test. Growth rates were analysed by Student's t-test or two-way ANOVA (genotype, diet). Specific growth rates were calculated using the equation: $(\text{weight at T2} - \text{weight at T1}) / \text{weight at T1}$ where T2 represents either P21 (B, G) or week 16 (E, J) and T1 represents either P3 (B, G) or week 3 (E, J). An asterisk (*) is used to denote significant difference for genotype in a post hoc test (* $p < 0.05$, ** $p < 0.01$, *** $p < 0.001$, **** $p < 0.0001$). HSHF, high sugar high fat.

4.3.4 Offspring biometry

The effects of Jz-ICR1 Δ and postnatal diet on offspring biometry at 17 weeks of age are shown in Figure 4.5. Overall, in response to Jz-ICR1 Δ male offspring showed reduced liver and heart weights ($p < 0.05$; Figure 4.5A, B). In particular, male Jz-ICR1 Δ offspring on a chow or HSHF diet had a lower heart weight compared to their genotype controls of the same diet ($p < 0.05$; Figure 4.5B) and male Jz-ICR1 Δ fed a HSHF diet had a lower liver weight compared to their genotype controls ($p < 0.05$; Figure 4.5A). When liver weight was assessed as a percentage of body weight, an interaction between genotype and diet was observed, whereby Jz-ICR1 Δ male offspring had a lower liver weight than their genotype controls when they were fed a HSHF diet ($p < 0.05$; Figure 4.5E). Male offspring exposed to Jz-ICR1 Δ also displayed increased kidney weight as a percentage of body weight when both dietary groups were analysed collectively ($p < 0.05$; Figure 4.5G). Regardless of genotype, a HSHF diet increased absolute liver, heart, kidney and spleen weights in male offspring ($p < 0.01$; Figure 4.5A, B, C, D); however, when weights were presented as a percentage of body weight, a HSHF diet instead reduced heart, kidney and spleen weight ($p < 0.05$; Figure 4.5F, G, H).

In female offspring at 17 weeks of age, heart weight was altered by genotype, diet, and an interaction between both parameters ($p < 0.05$), with Jz-ICR1 Δ female offspring having a lower heart weight than their genotype controls when they were fed a HSHF diet ($p < 0.01$; Figure 4.5J). Genotype, diet and an interaction between both parameters ($p < 0.05$) also influenced liver and kidney weights when presented as a percentage of body weight in the female offspring (Figure 4.5M, O). Jz-ICR1 Δ female offspring consuming a HSHF diet had lower fractional liver weights ($p < 0.0001$; Figure 4.5M) and greater relative kidney weights compared to their genotype controls on a HSHF diet ($p < 0.01$; Figure 4.5O). However, regardless of genotype, a HSHF diet increased absolute liver, kidney and spleen weights ($p < 0.001$; Figure 4.5I, K, L), but reduced the fractional heart and spleen weight ($p < 0.01$; Figure 4.5N, P) in female offspring.

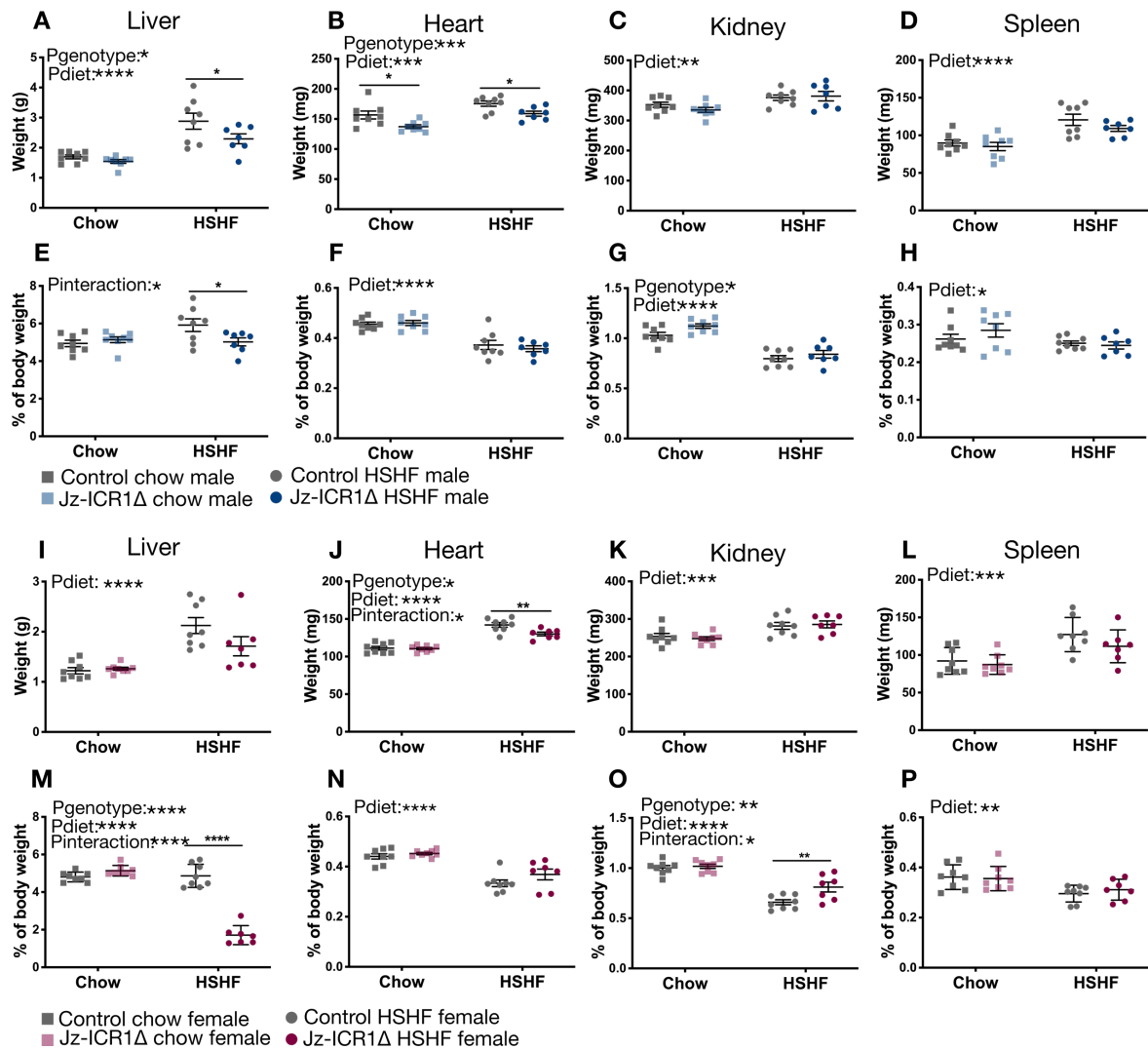


Figure 4.5. The effects of *Jz-ICR1Δ* and postnatal diet on 17-week-old adult offspring biometry. Biometry data are presented either as absolute weight or as a percentage of body weight. Individual points represent litter means and the mean is denoted as a horizontal line \pm SEM. Data from 7-8 litters per group are shown and were analysed by two-way ANOVA (genotype and diet) and a Sidak post hoc test (for genotype only). An asterisk (*) is used to denote significant difference for genotype within the one diet (* p <0.05, ** p <0.01, *** p <0.001, **** p <0.0001).

4.3.5 Offspring adiposity

Male and female offspring adiposity and adipocyte area in response to Jz-ICR1 Δ and postnatal diet are shown in Figure 4.6. In male offspring, Jz-ICR1 Δ reduced absolute gonadal fat weight regardless of diet ($p < 0.05$; Figure 4.6C). Regardless of diet, Jz-ICR1 Δ was associated with reductions in the weight of the sum of all fat pads surveyed in male offspring (both as absolute weight and a percentage of body weight; all $p < 0.05$; Figure 4.6D, H). Moreover, Jz-ICR1 Δ offspring on a chow showed a reduction in total fat pad weight when it was calculated a percentage of body weight and compared to their control counterparts ($p < 0.05$, Figure 4.6H).

An interaction between genotype and diet influenced both the absolute and fractional weight of the retroperitoneal fat in male offspring ($p < 0.05$), whereby male Jz-ICR1 Δ had reduced retroperitoneal fat weight compared to control males when they were fed a chow diet ($p < 0.05$; Figure 4.6A, E). Irrespective of postnatal diet, there was a tendency for adipocyte area to be reduced in male offspring exposed to Jz-ICR1 Δ , although this did not reach significance ($p = 0.056$; Figure 4.6I). While Jz-ICR1 Δ was not associated with a change in the adipocyte area distribution in male offspring fed a chow diet (Figure 4.6J), those consuming a HSHF diet had a greater proportion of small ($0-3000\mu\text{m}^2$) adipocytes ($p < 0.05$) than control HSHF fed offspring (Figure 4.6K).

Overall, Jz-ICR1 Δ was associated with reduced absolute weight of the renal fat depot in female offspring ($p < 0.05$; Figure 4.6M). Moreover, genotype, diet and an interaction between both parameters influenced the weight of the gonadal fat and the sum of all fat pads surveyed (both as absolute weight and a percentage of body weight) in female offspring ($p < 0.05$). In particular, Jz-ICR1 Δ female offspring consuming a HSHF diet showed reduced gonadal fat weight and the sum of the fat pads assessed compared to control offspring fed a HSHF diet ($p < 0.001$; Figure 4.6N, O, R, S). Jz-ICR1 Δ was not associated with a change in the adipocyte area or area distribution in female offspring regardless of the diet consumed (Figure 4.6T-V). Irrespective of genotype, a HSHF diet increased fat pad (retroperitoneal, renal, gonadal) weight, as well as the sum of all fat pads, when expressed as an absolute weight and a percentage of body weight, in female and male offspring ($p < 0.0001$). Moreover, a HSHF diet increased adipocyte area in both male and female offspring ($p < 0.0001$; Figure 4.6I, T).

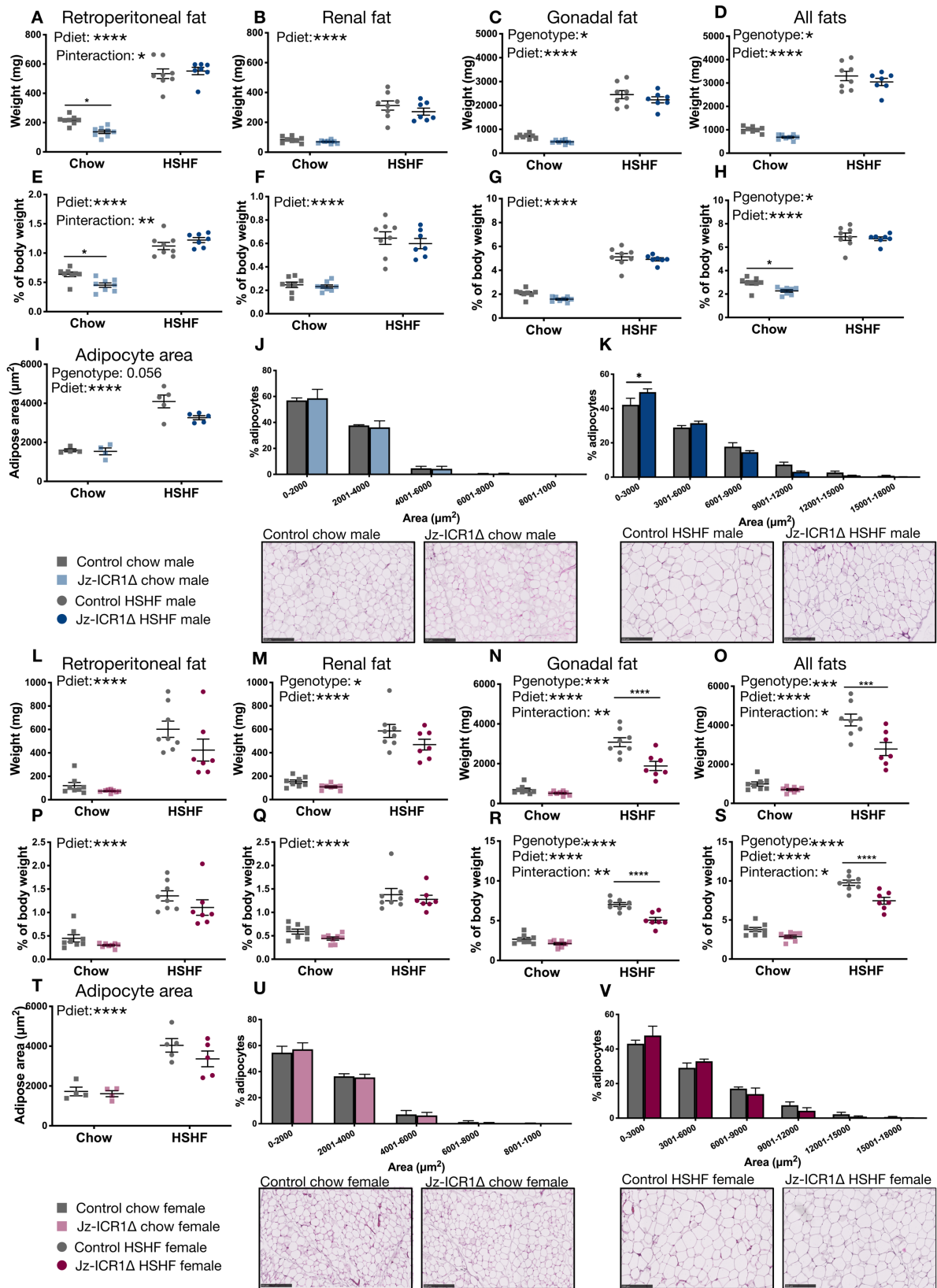


Figure 4.6. (preceding page). The effects of Jz-ICR1Δ and postnatal diet on adipose organ weights and adipocyte area in 17-week-old male and female adult offspring. Biometry data are presented either as absolute weight or as a percentage of body weight. Individual points for biometry data and adipocyte areas represent litter means and individual mice, respectively. The average per group is denoted as a horizontal line \pm SEM. Scale bars are 250 μ m. Data from 4-5 litters (stereology) or 7-8 litters (biometry) per group are shown and were analysed by two-way ANOVA (genotype and diet) and a Sidak post hoc test (for genotype only). Adipocyte area distribution curves were analysed by two-way ANOVA (genotype, adipocyte area) and a Sidak post hoc test. An asterisk (*) is used to denote significant difference for genotype within the one diet (* p <0.05, ** p <0.01, *** p <0.001, **** p <0.0001).

4.3.6 Offspring glucose and insulin handling *in vivo*

Offspring glucose and insulin handling were monitored during glucose and insulin tolerance tests, respectively, in response to Jz-ICR1Δ and postnatal diet and are shown in Figure 4.7. Male offspring exposed to Jz-ICR1Δ and fed a chow or HSHF diet did not display changes in glucose clearance upon glucose tolerance testing when compared to their respective control offspring (Figure 4.7A, B). Moreover, genotype did not alter the area under the curve (AUC) during a glucose tolerance test, however a HSHF diet significantly increased the AUC compared to a chow diet regardless of genotype (p <0.0001; Figure 4.7C). During the insulin tolerance tests, Jz-ICR1Δ male offspring on a chow diet showed reduced insulin sensitivity at 60 minutes post-insulin injection compared to control offspring (p <0.05; Figure 4.7D). Jz-ICR1Δ male offspring on a HSHF diet also showed reduced insulin sensitivity at 60- and 120-minutes post-insulin injection compared to their control offspring (p <0.01; Figure 4.7E). Overall, Jz-ICR1Δ decreased the area above the curve (AAC) during an insulin tolerance test in male offspring (p <0.01), with male Jz-ICR1Δ offspring consuming a HSHF diet having a reduced AAC compared to their genotype controls (p <0.01; Figure 4.7F).

Jz-ICR1Δ did not alter glucose tolerance in chow female offspring compared to genotype controls (Figure 4.7G). However, female Jz-ICR1Δ offspring fed a HSHF diet were more tolerant to glucose during the glucose tolerance test at 30- and 45-minutes post injection compared to control HSHF female offspring (p <0.05; Figure 4.7H). In female offspring,

the AUC of the glucose tolerance test was affected by genotype and diet, and an interaction between both parameters ($p < 0.05$). Moreover, the AUC of Jz-ICR1 Δ female offspring on a HSHF diet was lower compared to control HSHF female offspring ($p < 0.01$; Figure 4.7I). The insulin sensitivity and calculated AAC during an insulin tolerance test were not altered by either genotype or diet in female offspring (Figure 4.7J-L).

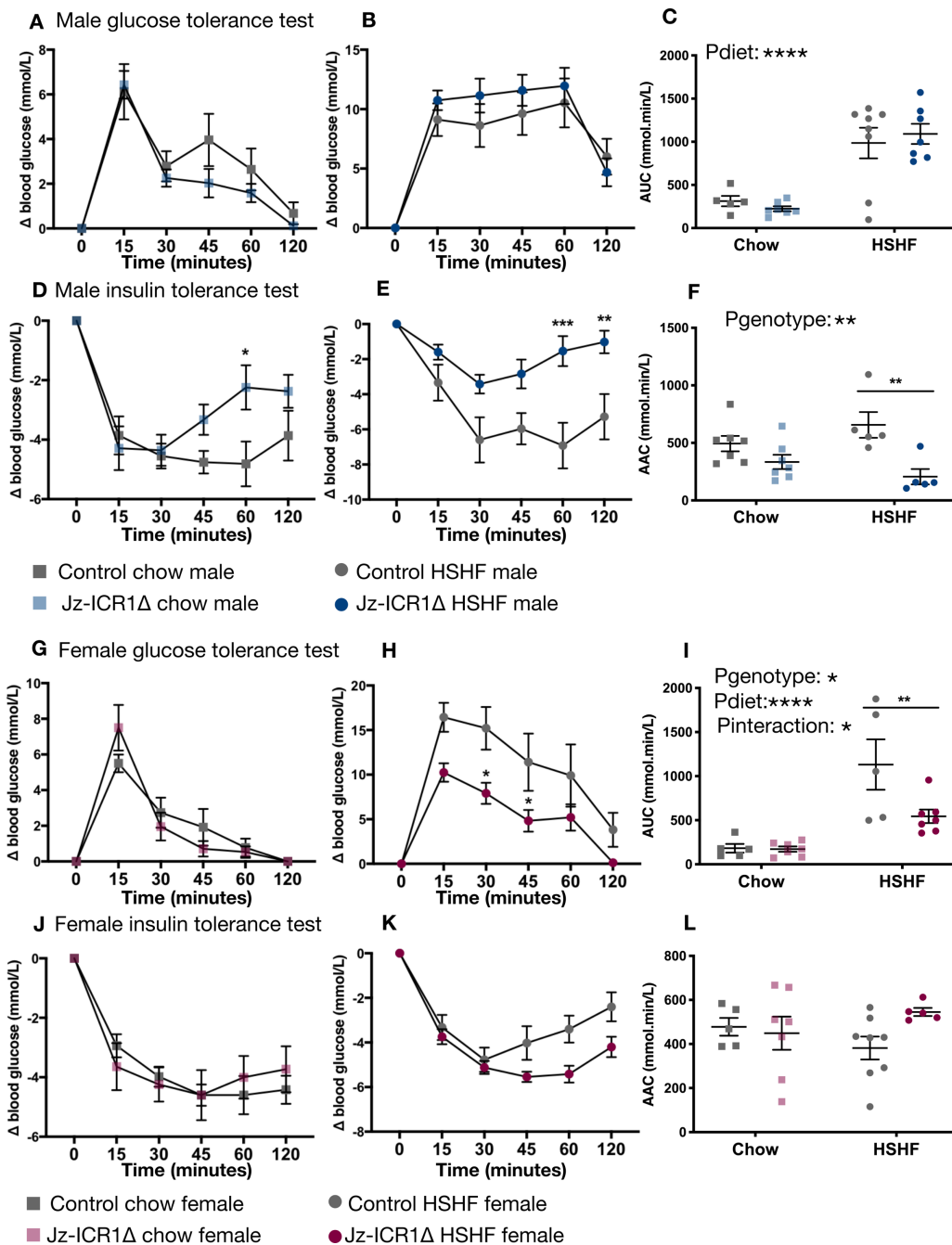


Figure 4.7. The effects of Jz-ICR1Δ and postnatal diet on glucose tolerance and insulin tolerance in 16-week-old adult offspring. Absolute glucose change during a glucose tolerance test in males or females (A, B, G, H) and absolute glucose change during an insulin tolerance test in males or females (D, E, J, K) are shown. Area under the curve (AUC) in males and females (C, I) and area above the curve (AAC) in males and females (F, L) are shown for glucose and insulin tolerance tests, respectively. Data are expressed as mean \pm SEM from 5-7 litters per group. Individual points shown in insulin and glucose tolerance test curves represent the group mean at a given time point, whilst individual points in AUC and AAC graphs represent individual animals with the mean denoted as a horizontal line. Statistical analysis on the absolute glucose change was performed by two-way repeated measures ANOVA with a Sidak post hoc test. AUC and AAC were analysed by two-way ANOVA (genotype, diet) with a Sidak post hoc test (for genotype only). An asterisk (*) is used to denote significant difference for genotype within the one diet (* p <0.05, ** p <0.01, *** p <0.001, **** p <0.0001).

4.3.7 Offspring pancreas biometry and morphology

Male and female offspring pancreas weight, insulin content and islet area in response to Jz-ICR1 Δ and diet are shown in Figures 4.8. Pancreas weight was not altered by genotype or diet in either female or male offspring (Figure 4.8A, I). However, when pancreas weight was expressed as a percentage of body weight, Jz-ICR1 Δ was associated with increased pancreas weight in male but not female offspring compared to respective genotype controls ($p < 0.05$; Figure 4.8B, J). In male, though not female offspring, pancreatic insulin content was altered by an interaction between genotype and diet ($p < 0.05$), with pancreatic insulin content tending to be reduced in chow fed Jz-ICR1 Δ male offspring compared to their genotype controls ($p = 0.05$; Figure 4.8C, K). Regardless of diet, male offspring exposed to Jz-ICR1 Δ showed unaltered islet mass but reduced pancreatic islet area ($p < 0.05$; Figure 4.8D, E). Specifically, in chow fed male Jz-ICR1 Δ offspring, a reduction in pancreatic islet area was associated with a greater proportion of small ($< 500 \mu\text{m}^2$) islets ($p < 0.0001$) and a reduced proportion of islets $500\text{-}1500 \mu\text{m}^2$ ($p < 0.05$; Figure 4.8F). However, overall, Jz-ICR1 Δ was associated with increased islet density (number of islets per area of pancreas) in male offspring ($p < 0.01$; Figure 4.8H). In female offspring, Jz-ICR1 Δ did not alter pancreatic islet mass or area, although overall, it increased islet density ($p < 0.05$; Figure 4.8L, M, P).

A HSHF diet reduced relative pancreas weight ($p < 0.0001$; Figure 4.8B, J) and increased pancreatic insulin content ($p < 0.001$; Figure 4.8C, K) in both male and female offspring regardless of the genotype. In males specifically, a HSHF diet also increased pancreatic islet area regardless of genotype ($p < 0.01$; Figure 4.8E); whilst in females there was only a tendency for this parameter to be increased ($p = 0.053$; Figure 4.8M). In females and not males, overall, a HSHF diet increased islet mass and the islet density (number of islets per area of pancreas; $p < 0.01$; Figure 4.8D, H, L, P).

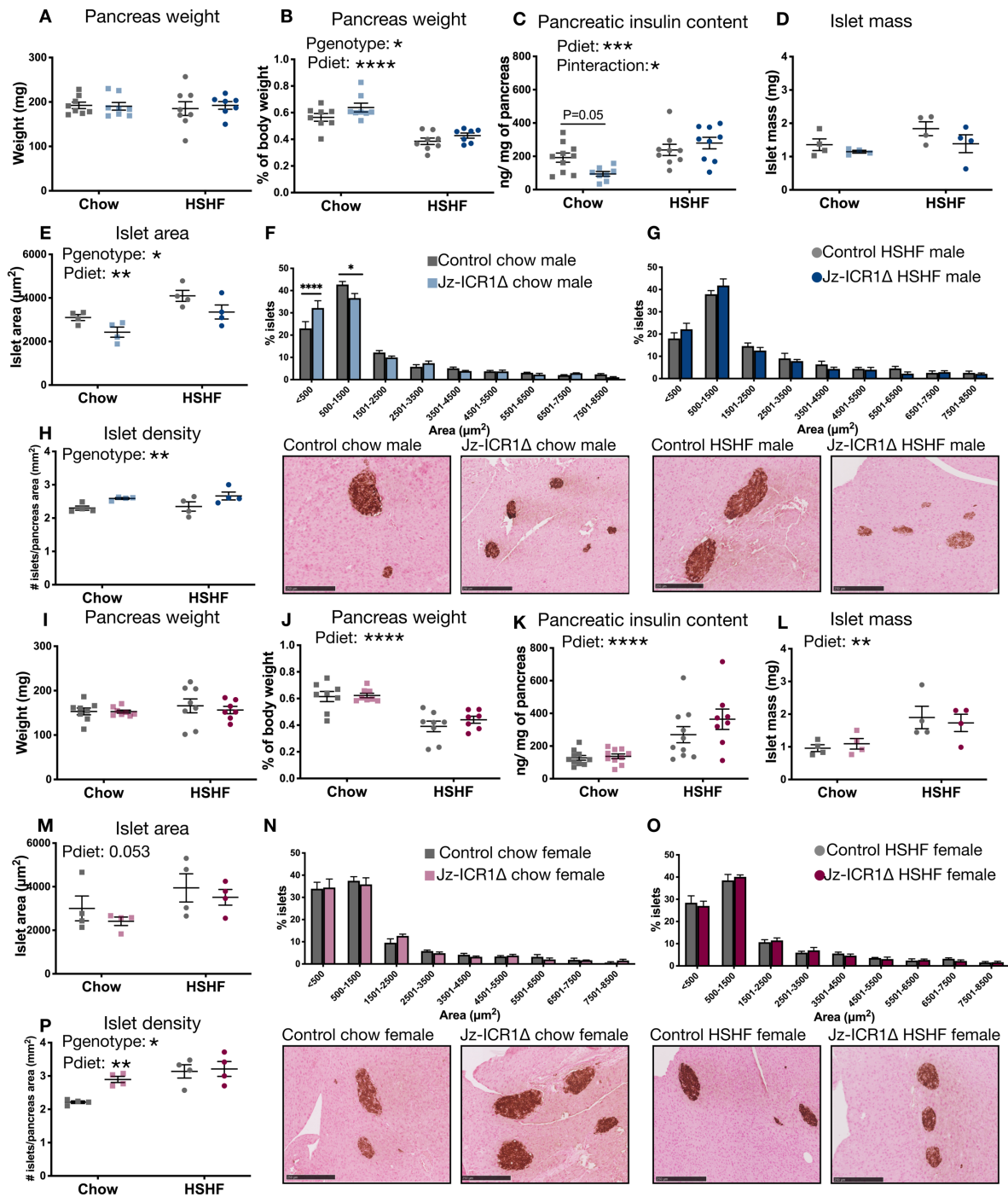


Figure 4.8. The effects of Jz-ICR1Δ and postnatal diet on pancreatic weight, insulin content and islet area in 17-week-old male and female adult offspring. Biometry data are presented either as total weight or as a percentage of body weight. Individual points for biometry data and pancreas stereology represent litter means and individual mice, respectively. The mean is denoted as a horizontal line \pm SEM. Scale bars are 250 μ m. Data from 4 litters (stereology) or 7-8 litters (biometry) per group are shown and were analysed by two-way ANOVA (genotype and diet) and a Sidak post hoc test (for genotype only). Islet area distribution curves were analysed by two-way ANOVA (genotype, islet area) and a Sidak post hoc test. An asterisk (*) is used to denote significant difference (* p <0.05, ** p <0.01, *** p <0.001, **** p <0.0001).

4.3.8 Offspring tissue biochemical composition

The effects of Jz-ICR1 Δ , postnatal diet and the interaction between the two parameters, on the liver, skeletal muscle and adipose tissue biochemical composition in male and female offspring are shown in Table 4.1. Overall, Jz-ICR1 Δ was associated with a reduction in hepatic protein content and the percentage of fat in the liver of male offspring ($p < 0.05$). The reduction in hepatic fat content was most pronounced in Jz-ICR1 Δ males that had been fed with a HSHF diet compared to genotype controls of the same diet ($p < 0.05$) and was also reflected by an interaction between genotype and diet ($p < 0.05$). There was no effect of genotype on biochemical composition of the liver in female offspring. However, there was a tendency for an overall increase in protein content of the white adipose tissue in females but not males, in response to Jz-ICR1 Δ ($p = 0.051$).

Regardless of genotype, liver fat content percentage was increased by HSHF diet consumption in both male and female offspring ($p < 0.001$). Consumption of a HSHF diet also increased total fat content in the liver of male offspring and total glycogen in the liver of male and female offspring ($p < 0.05$). In both male and female offspring, a HSHF diet reduced the protein content of the liver, skeletal muscle and white adipose tissue ($p < 0.001$).

Table 4.1. The effects of Jz-ICR1Δ and postnatal diet on tissue biochemical composition in 17-week-old adult offspring.

	Chow diet		HSHF diet		Effect of genotype	Effect of diet	Interaction
	Control	Jz-ICR1Δ	Control	Jz-ICR1Δ			
<i>Males</i>							
Liver							
Protein content (mg/g)	119.65 ± 4.47	95.84 ± 5.18	217.17 ± 31.87	165.52 ± 13.66	0.027	<0.0001	0.39
Glycogen (mg/g)	61.77 ± 4.95	80.07 ± 5.76	73.86 ± 9.21	80.73 ± 9.27	0.11	0.42	0.47
Total glycogen (mg)	106.43 ± 10.38	124.27 ± 9.73	203.92 ± 32.50	182.83 ± 28.52	0.95	0.0023	0.41
Fat content (%)	5.41 ± 0.74	4.58 ± 0.46	15.05 ± 1.93	9.28 ± 0.76*	0.0097	<0.0001	0.047
Total fat content (mg)	3.12 ± 0.44	2.93 ± 0.32	5.48 ± 0.61	4.71 ± 0.41	0.14	<0.0001	0.29
Skeletal muscle							
Protein content (mg/g)	97.20 ± 7.17	97.13 ± 8.24	48.07 ± 5.27	43.00 ± 3.67	0.68	<0.0001	0.69
WAT							
Protein content (mg/g)	32.04 ± 2.43	34.59 ± 2.32	23.33 ± 1.74	21.34 ± 1.74	0.89	<0.0001	0.27
<i>Females</i>							
Liver							
Protein content (mg/g)	86.48 ± 5.81	76.63 ± 1.66	150.33 ± 17.75	118.29 ± 15.96	0.13	0.0005	0.41
Glycogen (mg/g)	53.25 ± 6.33	55.65 ± 6.10	50.19 ± 5.07	57.06 ± 10.88	0.51	0.91	0.75
Total glycogen (mg)	69.34 ± 10.82	69.89 ± 8.28	104.75 ± 8.66	87.20 ± 11.26	0.39	0.011	0.36
Fat content (%)	7.71 ± 0.46	6.49 ± 0.55	11.97 ± 1.42	11.47 ± 1.95	0.98	0.0002	0.34
Total fat content (mg)	6.25 ± 0.53	5.24 ± 0.47	5.42 ± 0.32	5.43 ± 0.51	0.88	0.81	0.051
Skeletal muscle							
Protein content (mg/g)	107 ± 12.23	113.94 ± 27.96	56.61 ± 6.98	58.02 ± 5.11	0.77	0.0004	0.85
WAT							
Protein content (mg/g)	40.27 ± 3.20	46.80 ± 5.17	14.85 ± 2.46	22.33 ± 1.79	0.051	<0.0001	0.89

Data are expressed as mean ± SEM. Effects of genotype, diet and interaction were determined by two-way ANOVA and a Sidak post hoc test (for genotype only). p values representing a significant effect are shown in bold. An asterisk (*) indicates a significant difference between control and Jz-ICR1Δ within the same diet (p <0.05). n=5-9 offspring per genotype and diet (across 3-8 litters per genotype and diet). WAT, white adipose tissue (gonadal fat depot).

4.3.9 Offspring plasma hormone and metabolite concentrations

The effects of Jz-ICR1 Δ , postnatal diet, and the interaction between the two parameters, on plasma hormone and metabolite concentrations in male and female offspring are shown in Table 4.2. Overall, male Jz-ICR1 Δ offspring showed reduced corticosterone concentration compared to their genotype controls ($p < 0.05$). The effect was most pronounced in Jz-ICR1 Δ male offspring on a HSHF diet where an interaction between genotype and diet ($p < 0.05$) identified that plasma corticosterone was reduced when compared to HSHF control counterparts ($p < 0.01$). In male offspring, an interaction between genotype and diet also affected plasma cholesterol concentrations ($p < 0.05$), whereby cholesterol concentration tended to be decreased in Jz-ICR1 Δ male offspring consuming a chow diet but increased in Jz-ICR1 Δ male offspring fed a HSHF diet compared to their genotype controls of the respective diet, although post hoc analysis did not reach significance.

Jz-ICR1 Δ was not associated with an alteration in either corticosterone or cholesterol concentrations in female offspring, regardless of diet. However, Jz-ICR1 Δ was associated with reduced leptin concentrations in female offspring ($p < 0.01$) and in particular, Jz-ICR1 Δ female offspring on a HSHF diet had reduced leptin levels compared to their control HSHF counterparts ($p < 0.001$; also reflected by a significant interaction between genotype and diet for plasma leptin in females). In female offspring, an interaction between genotype and diet influenced plasma insulin and *ad libitum* fed glucose concentrations ($p < 0.01$). In particular, insulin concentration tended to be increased in Jz-ICR1 Δ female offspring consuming a chow diet and significantly decreased in those consuming a HSHF diet ($p < 0.05$) compared to genotype controls of the same diet. In addition, *ad libitum* fed glucose concentration in female offspring was influenced by an interaction between genotype and diet, whereby there was a significantly reduced concentration in Jz-ICR1 Δ female offspring consuming a chow diet ($p < 0.05$) and a significantly increased concentration in Jz-ICR1 Δ female offspring consuming a HSHF diet ($p < 0.05$) compared to their genotype controls of the respective diet.

In both male and female offspring regardless of genotype, a HSHF diet increased circulating glucose (fasted, not *ad libitum* fed), insulin, leptin and cholesterol concentrations ($p < 0.05$). In male offspring only, a HSHF diet increased free fatty acid

levels ($p < 0.05$). Whereas, in female offspring only, a HSHF diet increased corticosterone and triglyceride levels ($p < 0.05$).

Table 4.2. The effects of Jz-ICR1Δ and postnatal diet on circulating hormone and metabolite concentrations in adult offspring at 17 weeks of age.

	Chow diet		HSHF diet				
<i>Males</i>	Control	Jz-ICR1Δ	Control	Jz-ICR1Δ	Effect of genotype	Effect of diet	Interaction
Glucose Fed state (mM)	10.56 ± 0.65	10.54 ± 0.70	11.2 ± 0.71	10.82 ± 1.56	0.82	0.59	0.83
Glucose Fasted 6hr (mM)	10.00 ± 0.51	9.98 ± 0.98	15.17 ± 1.24	12.24 ± 0.51	0.084	0.0001	0.088
Insulin (μg/L)	0.88 ± 0.25	1.07 ± 0.33	6.71 ± 1.29	4.89 ± 1.39	0.40	0.0005	0.49
Corticosterone (ng/mL)	31.69 ± 3.94	30.69 ± 4.34	76.94 ± 18.69	25.48 ± 1.33*	0.028	0.082	0.031
Leptin (ng/mL)	3.84 ± 0.66	3.12 ± 0.52	49.74 ± 9.95	48.99 ± 9.69	0.79	<0.0001	0.73
Cholesterol (mM)	2.66 ± 0.23	2.02 ± 0.32	4.40 ± 0.20	5.18 ± 0.42	0.82	<0.0001	0.034
Triglycerides (mM)	2.18 ± 0.32	1.68 ± 0.24	2.59 ± 0.23	2.06 ± 0.25	0.97	0.14	0.085
Free fatty acids (mM)	1.04 ± 0.079	0.81 ± 0.064	0.64 ± 0.14	0.74 ± 0.12	0.12	0.030	0.52
<i>Females</i>	Control	Jz-ICR1Δ	Control	Jz-ICR1Δ	Effect of genotype	Effect of diet	Interaction
Glucose Fed state (mM)	9.65 ± 0.61	7.44 ± 0.47*	9.21 ± 1.24	10.37 ± 0.62*	0.96	0.25	0.0009
Glucose Fasted 6hr (mM)	8.77 ± 0.33	9.21 ± 0.31	10.56 ± 0.29	9.97 ± 0.41	0.84	0.0013	0.15
Insulin (μg/L)	1.06 ± 0.67	2.56 ± 1.58	2.45 ± 0.71	0.94 ± 0.13*	0.59	0.035	0.021
Corticosterone (ng/mL)	43.18 ± 7.59	72.10 ± 9.84	110.35 ± 21.15	111.48 ± 36.55	0.48	0.017	0.52
Leptin (ng/mL)	3.56 ± 0.96	1.90 ± 0.44	58.20 ± 10.70	23.17 ± 9.13*	0.0057	0.0002	0.0096
Cholesterol (mM)	1.90 ± 0.11	1.66 ± 0.20	4.84 ± 0.50	3.70 ± 0.55	0.096	<0.0001	0.27
Triglycerides (mM)	1.41 ± 0.09	1.24 ± 0.15	1.66 ± 0.17	1.91 ± 0.17	0.84	0.0047	0.20
Free fatty acids (mM)	0.85 ± 0.14	0.94 ± 0.26	0.61 ± 0.15	0.80 ± 0.099	0.44	0.30	0.77

Data are expressed as mean ± SEM. Effects of genotype, diet and interaction were determined by two-way ANOVA and a Sidak post hoc test (for genotype only). p values representing a significant effect (p<0.05) are shown in bold. An asterisk (*) indicates a significant difference between control and Jz-ICR1Δ within the same diet (p< 0.05). n=4-10 offspring per genotype and diet (across 4-8 litters per genotype and diet). All concentrations shown are from plasma samples apart from glucose concentration which is from blood samples. Concentrations are from *ad libitum* fed animals unless stated otherwise.

4.3.10 Hepatic gluconeogenesis

Due to limitations in the number of samples able to fit onto one gel, the effect of genotype only was considered in western blot analyses. The hepatic abundance of the rate-limiting enzymes in gluconeogenesis, G6Pase and PEPCCK in 17-week-old Jz-ICR1Δ chow male offspring was increased relative to control chow offspring ($p < 0.01$; Figure 4.9A, C). Jz-ICR1Δ female offspring on a chow diet showed decreased hepatic G6Pase abundance ($p < 0.05$; Figure 4.9E, G), compared to dietary controls, whilst PEPCCK protein levels remained unaltered. Hepatic G6Pase and PEPCCK protein levels were unaffected by genotype in male and female offspring who had been fed a HSHF diet (Figure 4.9B, D, F, H).

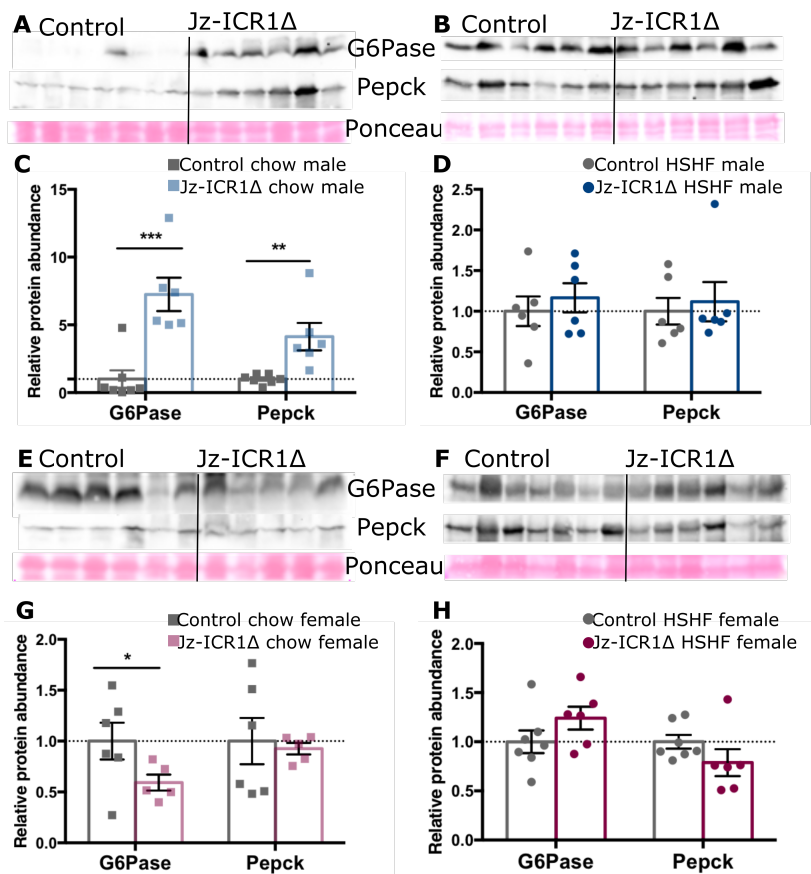


Figure 4.9. The effect of Jz-ICR1Δ on the abundance of proteins involved in gluconeogenesis in the liver of 17-week-old male (A, B, C, D) and female (E, F, G, H) offspring fed a chow (A, C, E, G) or HSHF (B, D, F, H) diet. Protein abundance data are expressed as individual points from a single sample with mean \pm SEM relative to the respective diet and sex control group. Protein abundance was normalised to the respective Ponceau band and a representative Ponceau stained membrane is shown to indicate protein loading for each sample. The effect of genotype was analysed by Student's t-test with the asterisk (*) denoting significant difference from the control genotype (* $p < 0.05$, ** $p < 0.01$, *** $p < 0.001$). $n = 5-7$ samples per genotype (across 5-6 litters per genotype).

4.3.11 Insulin signalling

4.3.11.1 Liver insulin signalling

The abundance of insulin signalling pathway proteins were assessed in the liver of 17-week-old male and female offspring that had been exposed to Jz-ICR1 Δ and either fed a chow or HSHF diet after weaning (Figure 4.10) with respective representative blots shown in Figure 4.11. The protein abundance of the receptors (IGF1R and InsR) was reduced in Jz-ICR1 Δ offspring consuming a chow diet, relative to control offspring ($p < 0.01$). In contrast, downstream mediators of the insulin signalling pathway (p110 α , total AKT, pAKT T308, ratio of phosphorylated (T308) to total AKT, pGSK3 S21/9, ratio of phosphorylated (S21/9) to total GSK3, pS6K T389 and ratio of phosphorylated (T389) to total S6K) were increased in Jz-ICR1 Δ offspring consuming a chow diet relative to control offspring ($p < 0.05$; Figure 4.10A). When consuming a HSHF diet, male Jz-ICR1 Δ offspring had lower hepatic protein abundance of p110 α and total GSK3 but an increased ratio of phosphorylated (S21/9) to total GSK3 relative to control offspring ($p < 0.01$; Figure 4.10B).

Protein levels of the downstream mediators (p110 α , total AKT, pAKT S473) were reduced in Jz-ICR1 Δ female offspring consuming a chow diet relative to control offspring ($p < 0.05$). Conversely, female Jz-ICR1 Δ chow offspring had increased ratios of phosphorylated AKT (T308) and S6K (T389) to total protein compared to their dietary controls ($p < 0.01$; Figure 4.10C). When consuming a HSHF diet, Jz-ICR1 Δ female offspring had higher hepatic protein abundance of InsR, p110 α , pGSK3 S21/9 and ratio of phosphorylated (S21/9) to total GSK3 ($p < 0.05$) but lower total S6K ($p < 0.05$) compared to their control counterparts (Figure 4.10D).

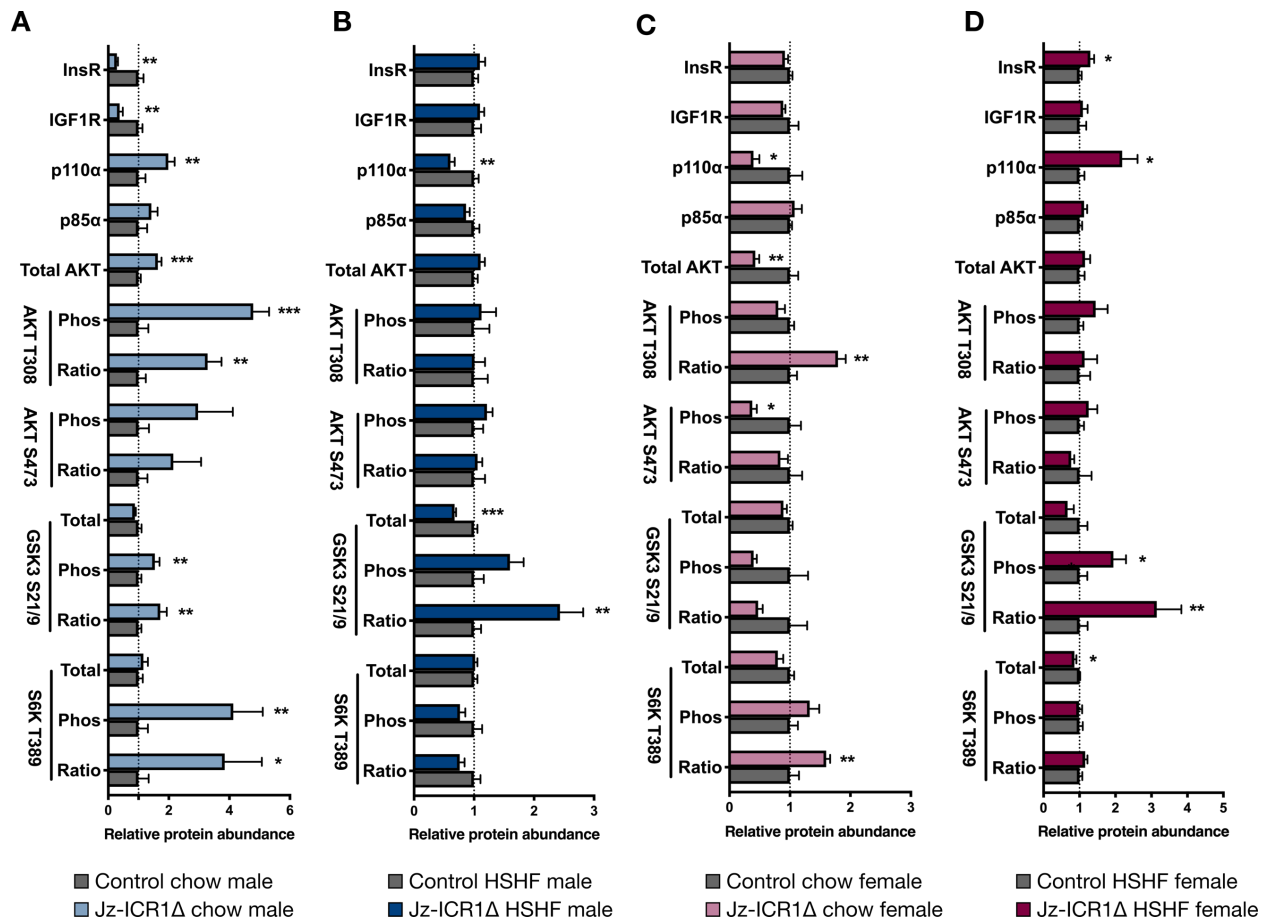


Figure 4.10. The effect of Jz-ICR1Δ on the abundance of proteins involved in insulin signalling in the liver of 17-week-old male (A, B) or female (C, D) offspring fed a chow (A, C) or HSHF (B, D) diet. Data are expressed as mean \pm SEM relative to the respective diet and sex control group. Protein abundance was normalised to the respective Ponceau band. The effect of genotype was analysed by Student's t-test with the asterisk (*) denoting significant difference from the control genotype (* p <0.05, ** p <0.01, *** p <0.001). n =5-7 samples per genotype (across 5-6 litters per genotype).

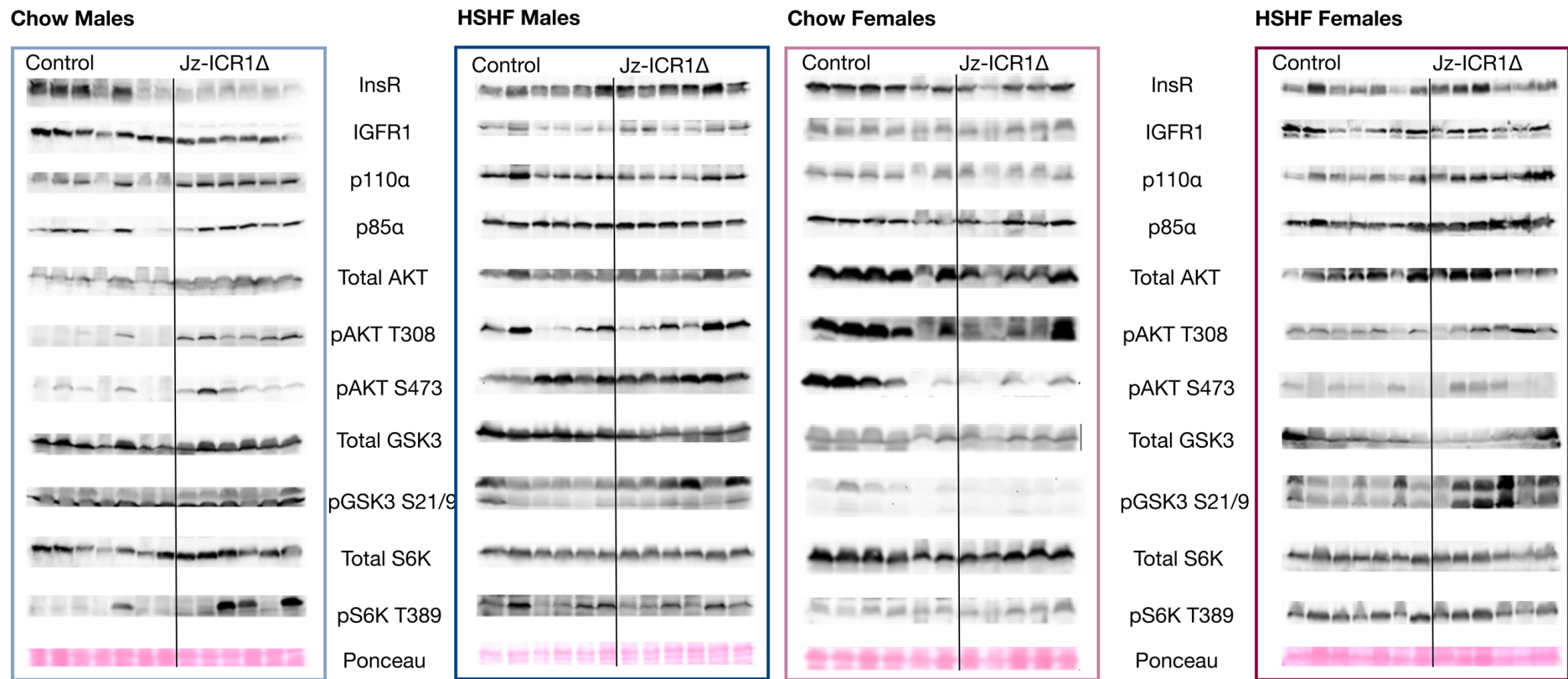


Figure 4.11. Representative scans of Western blots performed on liver homogenates showing the abundance of proteins involved in the insulin signalling pathway in 17-week-old male and female offspring fed a chow or high sugar high fat (HSHF) diet. Each band represents a single animal and multiple litters are within each group. Representative Ponceau stained membranes are shown to indicate protein loading for each sample.

4.3.11.2 Skeletal muscle insulin signalling

The abundance of insulin signalling pathway proteins were assessed in skeletal muscle of 17-week-old male and female offspring that had been exposed to Jz-ICR1 Δ and either fed a chow or HSHF diet after weaning (Figure 4.12), with respective representative blots shown in Figure 4.13. There was no effect of Jz-ICR1 Δ on the skeletal muscle protein abundance of the insulin signalling pathway in male offspring consuming a chow diet (Figure 4.12A). When consuming a HSHF diet, Jz-ICR1 Δ male offspring had higher skeletal muscle protein abundance of IGF1R, total AKT, pAKT T308 and pAKT S473 compared to their control counterparts ($p < 0.05$; Figure 4.12B).

Protein levels of InsR, total AKT, pAKT T308, total GSK3, pGSK3 S21/9 and pS6K T389 were higher in Jz-ICR1 Δ female offspring consuming a chow diet compared to their control counterparts ($p < 0.05$). Conversely, the ratio of phosphorylated (T308) to total AKT protein levels were reduced in Jz-ICR1 Δ female chow offspring compared to their genotype controls ($p < 0.05$; Figure 4.12C). When consuming a HSHF diet, Jz-ICR1 Δ female offspring had higher skeletal muscle protein abundance of p110 α , pGSK3 S21/9 and ratio of phosphorylated (S21/9) to total GSK3 ($p < 0.05$) and a tendency for increased pS6K T389 ($p = 0.052$) compared to their control counterparts (Figure 4.12D).

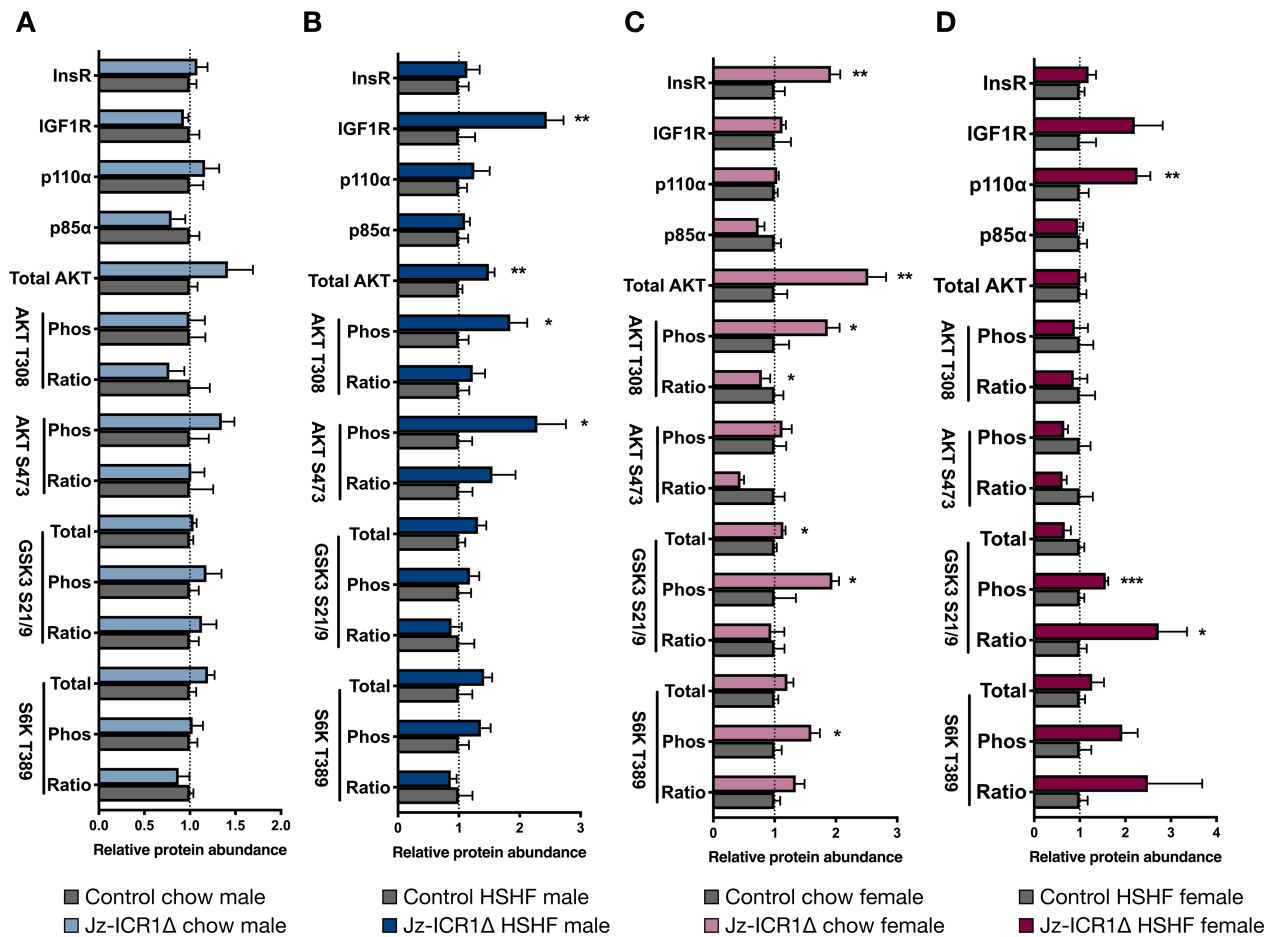


Figure 4.12. The effect of Jz-ICR1Δ on the abundance of proteins involved in insulin signalling in the skeletal muscle of 17-week-old male (A, B) or female (C, D) offspring fed a chow (A, C) or HSHF (B, D) diet. Data are expressed as mean ± SEM relative to the respective diet and sex control group. Protein abundance was normalised to the respective Ponceau band. The effect of genotype was analysed by Student's t-test with the asterisk (*) denoting significant difference from the control genotype (*p<0.05, **p<0.01, ***p<0.001). n=5-6 samples per genotype (across 5-6 litters per genotype).

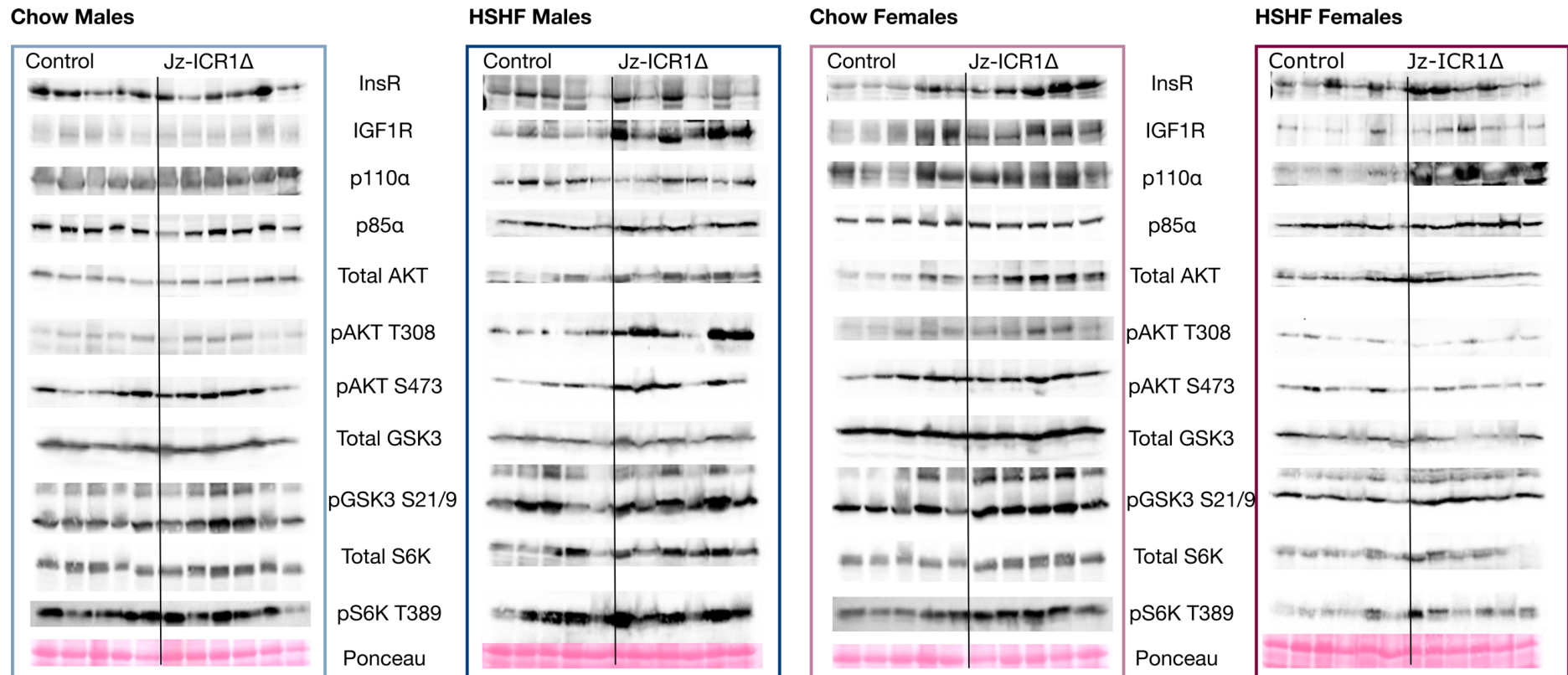


Figure 4.13. Representative scans of Western blots performed on skeletal muscle homogenates showing the abundance of proteins involved in the insulin signalling pathway in 17-week-old male and female offspring fed a chow or high sugar high fat (HSHF) diet. Each band represents a single animal and multiple litters are within each group. Representative Ponceau stained membranes are shown to indicate protein loading for each sample.

4.3.11.3 White adipose tissue insulin signalling

The abundance of insulin signalling pathway proteins were assessed in white adipose tissue of 17-week-old male and female offspring that had been exposed to Jz-ICR1 Δ and either fed a chow or HSHF diet after weaning (Figure 4.14), with respective representative blots shown in Figure 4.15. Protein levels of p110 α and total AKT were increased in the white adipose tissue of Jz-ICR1 Δ male offspring consuming a chow diet compared to their respective controls ($p < 0.05$; Figure 4.14A). There was no effect of Jz-ICR1 Δ on the white adipose tissue protein abundance of the insulin signalling pathway in male offspring consuming a HSHF diet (Figure 4.14B). White adipose tissue protein levels of InsR, pAKT T308, pGSK3 S21/9 and ratio of phosphorylated (S21/9) to total GSK3 were higher in Jz-ICR1 Δ female offspring consuming a chow diet compared to their control counterparts ($p < 0.05$; Figure 4.14C). Protein levels of p85 α and the ratio of phosphorylated (S21/9) to total GSK3 were increased in the white adipose tissue of Jz-ICR1 Δ female offspring consuming a HSHF diet compared to their genotype controls of the same diet ($p < 0.05$; Figure 4.14D). pS6K T389 and total S6K could not be detected in white adipose tissue.

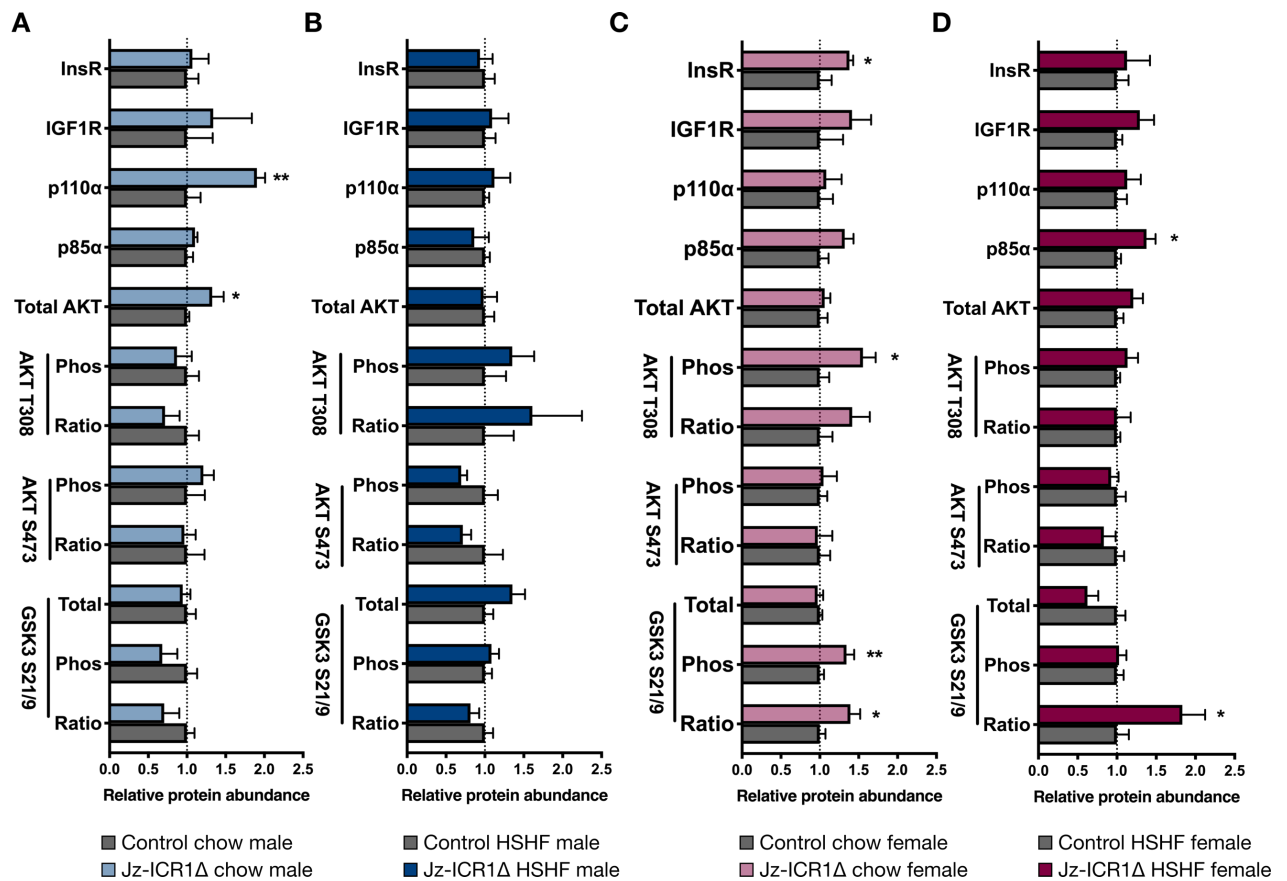


Figure 4.14. The effect of Jz-ICR1Δ on the abundance of proteins involved in insulin signalling in the white adipose (gonadal) tissue of 17-week-old male (A, B) or female (C, D) offspring fed a chow (A, C) or HSHF (B, D) diet. Data are expressed as mean \pm SEM relative to the respective diet and sex control group. Protein abundance was normalised to the respective Ponceau band. The effect of genotype was analysed by Student's t-test with the asterisk (*) denoting significant difference from the control genotype (* p <0.05, ** p <0.01, *** p <0.001). n =5-7 samples per genotype (across 3-6 litters per genotype)

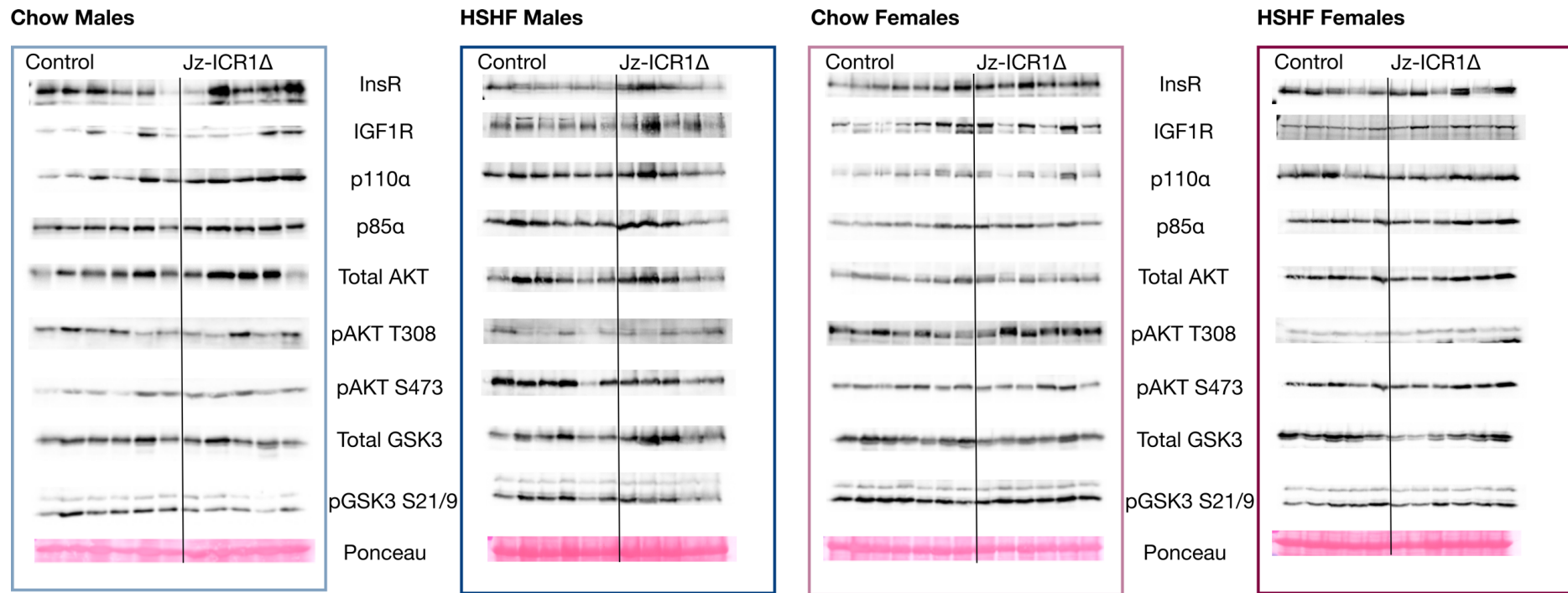


Figure 4.15. Representative scans of Western blots performed on white adipose (gonadal) tissue homogenates showing the abundance of proteins involved in the insulin signalling pathway in 17-week-old male and female offspring fed a chow or high sugar high fat (HSHF) diet. Each band represents a single animal and multiple litters are within each group. Representative Ponceau stained membranes are shown to indicate protein loading for each sample.

4.3.12 Lipid metabolism

4.3.12.1 Liver lipid metabolism

The abundance of hepatic LPL, PPAR α and PPAR γ were higher in Jz-ICR1 Δ male chow offspring relative to their control counterparts ($p < 0.05$; Figure 4.16A, C). In contrast, PPAR α was decreased ($p < 0.01$) and LPL and PPAR γ levels unaltered in the liver of Jz-ICR1 Δ female chow offspring relative to their controls (Figure 4.16E, G). LPL, PPAR α and PPAR γ were unaltered in male Jz-ICR1 Δ fed a HSHF diet, compared to control offspring (Figure 4.16B, D). Hepatic LPL, PPAR α and PPAR γ protein abundance was greater in female Jz-ICR1 Δ compared to control offspring when they consumed a HSHF diet ($p < 0.05$; Figure 4.16F, H).

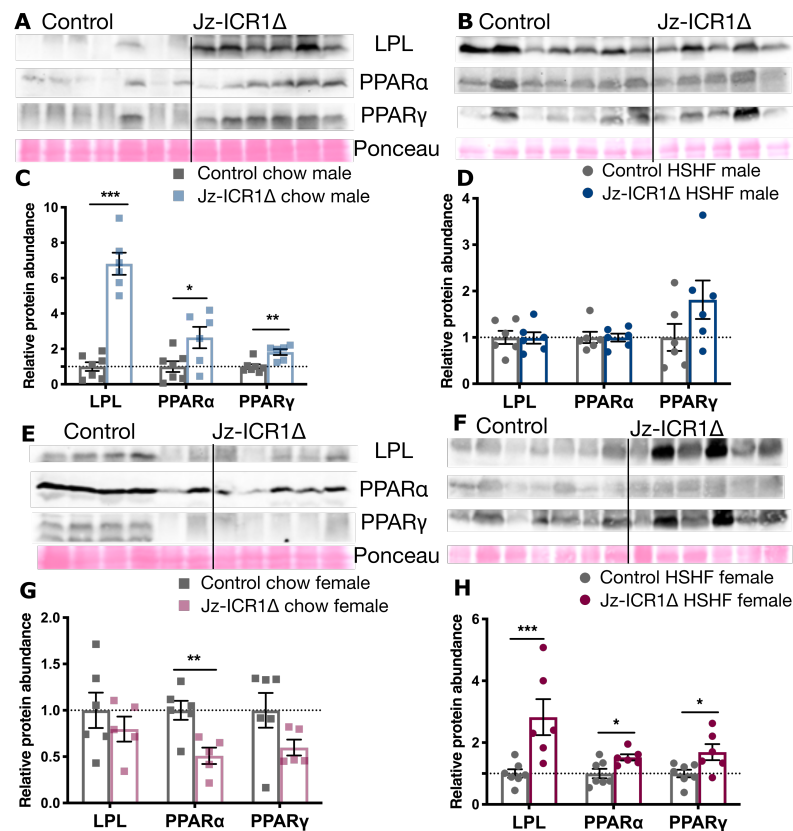


Figure 4.16. The effect of Jz-ICR1 Δ on the abundance of proteins involved in lipid metabolism in the liver of 17-week-old male (A, B, C, D) and female (E, F, G, H) offspring fed a chow (A, C, E, G) or HSHF (B, D, F, H) diet. Protein abundance data are expressed as individual points from a single sample with mean \pm SEM relative to the respective diet and sex control group. Protein abundance was normalised to the respective Ponceau band and a representative Ponceau stained membrane is shown to indicate protein loading for each sample. The effect of genotype was analysed by Student's t-test with the asterisk (*) denoting significant difference from the control genotype (* $p < 0.05$, ** $p < 0.01$, *** $p < 0.001$). $n = 5-7$ samples per genotype (across 5-6 litters per genotype).

4.3.12.2 Skeletal muscle lipid metabolism

In chow-fed female, but not male Jz-ICR1 Δ offspring, the abundance of PPAR α was increased in the skeletal muscle ($p < 0.001$; Figure 4.17A, C, E, G), whilst LPL and PPAR γ remained unaltered in both sexes. On a HSHF diet, LPL abundance was increased in the skeletal muscle of male though not female Jz-ICR1 Δ offspring compared to control ($p < 0.05$) and PPAR α and PPAR γ abundance remained unaltered in either sex (Figure 4.17B, D, F, H).

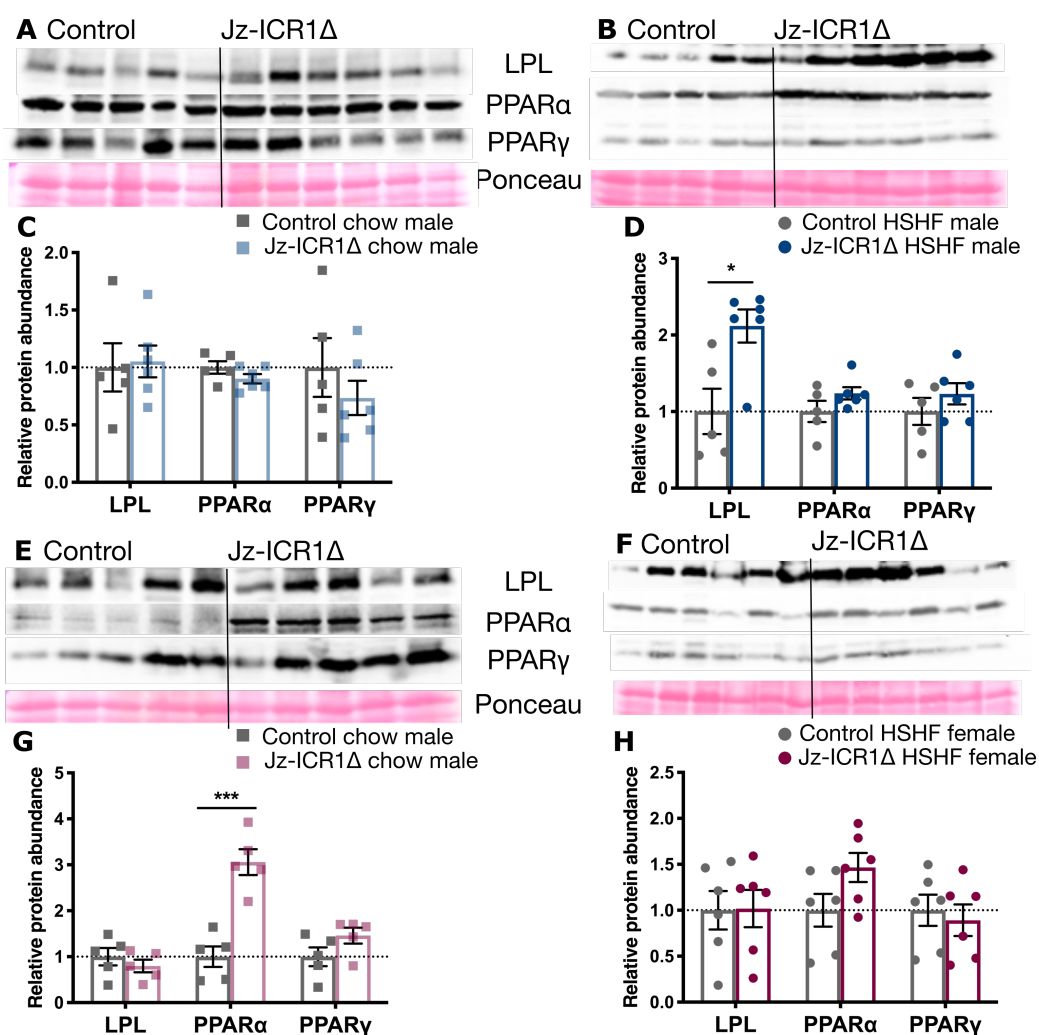


Figure 4.17. The effect of Jz-ICR1 Δ on the abundance of proteins involved in lipid metabolism in the skeletal muscle of 17-week-old male (A, B, C, D) and female (E, F, G, H) offspring fed a chow (A, C, E, G) or HSHF (B, D, F, H) diet. Protein abundance data are expressed as individual points from a single sample with mean \pm SEM relative to the respective diet and sex control group. Protein abundance was normalised to the respective Ponceau band and a representative Ponceau stained membrane is shown to indicate protein loading for each sample. The effect of genotype was analysed by Student's t-test with the asterisk (*) denoting significant difference from the control genotype (* $p < 0.05$, ** $p < 0.01$, *** $p < 0.001$). $n = 5-6$ samples per genotype (across 5-6 litters per genotype).

4.3.12.3 White adipose tissue lipid metabolism

Jz-ICR1 Δ increased PPAR α protein abundance in the white adipose tissue of chow fed male and female offspring ($p < 0.05$), whilst LPL and PPAR γ protein abundance remained unaltered in either sex (Figure 4.18A, C, E, G). In contrast, Jz-ICR1 Δ did not alter LPL, PPAR α and PPAR γ protein abundance in the white adipose tissue of male or female offspring when they were fed a HSHF diet (Figure 4.18B, D, F, H).

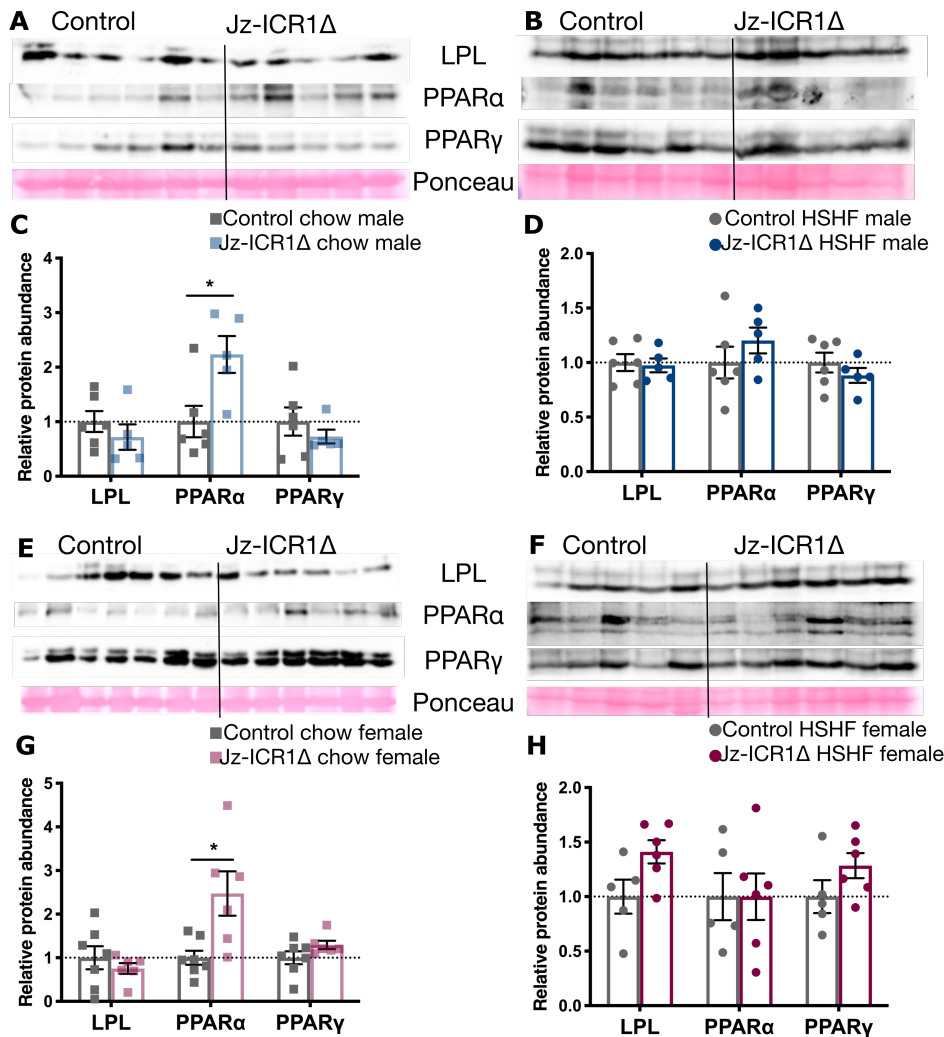


Figure 4.18. The effect of Jz-ICR1 Δ on the abundance of proteins involved in lipid metabolism in the white adipose (gonadal) tissue of 17-week-old male (A, B, C, D) and female (E, F, G, H) offspring fed a chow (A, C, E, G) or HSHF (B, D, F, H) diet. Protein abundance data are expressed as individual points from a single sample with mean \pm SEM relative to the respective diet and sex control group. Protein abundance was normalised to the respective Ponceau band and a representative Ponceau stained membrane is shown to indicate protein loading for each sample. The effect of genotype was analysed by Student's t-test with the asterisk (*) denoting significant difference from the control genotype (* $p < 0.05$, ** $p < 0.01$, *** $p < 0.001$). $n = 5-7$ samples per genotype (across 3-6 litters per genotype).

Summaries of protein abundance changes in response to Jz-ICR1 Δ in the liver, skeletal muscle and white adipose tissue of male or female offspring fed a chow or HSHF diet are presented below in Tables 4.3 and 4.4 respectively. In response to Jz-ICR1 Δ , chow male offspring had increased hepatic abundance of proteins involved in the downstream insulin signalling pathway, gluconeogenesis and lipid metabolism, but these were unaltered in skeletal muscle. Jz-ICR1 Δ HSHF male offspring had reduced hepatic insulin signalling protein abundance and increased skeletal muscle insulin signalling and lipid metabolism protein abundance compared to genotype controls. In these offspring adipose protein abundance of insulin signalling pathway, gluconeogenesis and lipid metabolism mediators was unaltered in response to Jz-ICR1 Δ . Both male and female chow offspring had increased protein abundance of mediators of the insulin signalling pathway and lipid metabolism in adipose tissue in response to Jz-ICR1 Δ . In response to Jz-ICR1 Δ chow female offspring had reduced hepatic abundance of proteins involved in the insulin signalling pathway, gluconeogenesis and lipid metabolism, but these were increased in the skeletal muscle. HSHF female offspring had increased hepatic, skeletal muscle and adipose protein abundance of proteins involved in insulin signalling and lipid metabolism in response to Jz-ICR1 Δ .

Table 4.3. Summary of the effect of Jz-ICR1Δ on the relative expression of proteins involved in insulin signalling, gluconeogenesis and lipid metabolism in key metabolic tissues (liver, muscle, adipose) from 17-week-old male offspring fed a chow or HSHF diet. ↑, increase; ↓, decrease; =, no change (compared to offspring of the control genotype on the same diet). HSHF, high sugar high fat; ND, not determined.

	Liver		Muscle		Adipose		
	Chow	HSHF	Chow	HSHF	Chow	HSHF	
Insulin signalling	InsR	↓	=	=	=	=	
	IGF1R	↓	=	=	↑	=	
	p110α	↑	↓	=	=	↑	=
	p85α	=	=	=	=	=	=
	Total AKT	↑	=	=	↑	↑	=
	pAKT T308	↑	=	=	↑	=	=
	pAKT S473	=	=	=	↑	=	=
	Total GSK3	=	↓	=	=	=	=
	pGSK3 S21/9	↑	=	=	=	=	=
	Total S6K	=	=	=	=	ND	ND
	pS6K T389	↑	=	=	=	ND	ND
	Gluconeogenesis	G6Pase	↑	=	ND	ND	ND
PEPCK		↑	=	ND	ND	ND	
Lipid metabolism markers	LPL	↑	=	=	↑	=	
	PPARα	↑	=	=	=	↑	
	PPARγ	↑	=	=	=	=	

Table 4.4. Summary of the effect of Jz-ICR1Δ on the relative expression of proteins involved in the insulin signalling pathway, gluconeogenesis and lipid metabolism in key metabolic tissues (liver, muscle, adipose) from 17-week-old female offspring on a chow or HSHF diet. ↑, increase; ↓, decrease; =, no change (compared to offspring of the control genotype on the same diet). HSHF, high sugar high fat; ND, not determined.

	Liver		Muscle		Adipose		
	Chow	HSHF	Chow	HSHF	Chow	HSHF	
Insulin signalling	InsR	=	↑	↑	=	↑	=
	IGF1R	=	=	=	=	=	=
	p110α	↓	↑	=	↑	=	=
	p85α	=	=	=	=	=	↑
	Total AKT	↓	=	↑	=	=	=
	pAKT T308	=	=	↑	=	↑	=
	pAKT S473	↓	=	=	=	=	=
	Total GSK3	=	=	↑	=	=	=
	pGSK3 S21/9	=	↑	↑	↑	↑	=
	Total S6K	=	↓	=	=	ND	ND
	pS6K T389	=	=	↑	=	ND	ND
	Gluconeogenesis	G6Pase	↓	=	ND	ND	ND
PEPCK		=	=	ND	ND	ND	
Lipid metabolism markers	LPL	=	↑	=	=	=	
	PPARα	↓	↑	↑	=	↑	
	PPARγ	=	↑	=	=	=	

4.4 Discussion

The results show that placental endocrine zone malfunction (Jz-ICR1 Δ) leads to the programming of offspring growth trajectory, adiposity, and metabolic health. Alterations in metabolism in Jz-ICR1 Δ offspring related in part to changes in insulin production and signalling in peripheral tissues, both on a chow and HSHF postnatal diet. Critically, metabolic outcomes were largely dependent on sex, the metabolic organ studied and on the postnatal diet consumed by offspring (as summarised in Figures 4.4.1 and 4.4.2). As gestational length, litter size, stillbirths and the percentage of male fetuses were not altered by Jz-ICR1 Δ , these parameters likely do not affect offspring programming. Jz-ICR1 Δ did however alter offspring growth trajectory, with offspring growth restricted from day 14 to 21 of postnatal life, regardless of sex. Thereafter, whilst females (on a chow and HSHF diet) and males (on a HSHF diet) displayed catchup growth, male offspring on a chow diet continued to be growth restricted compared to their respective control groups in response to Jz-ICR1 Δ . Sexual disparity in postnatal growth has been previously observed during prenatal testosterone excess, whereby female but not male sheep display catchup growth postnatally (Manikkam et al., 2004), and overall differing growth trajectories may contribute to sexually dimorphic metabolic outcomes in Jz-ICR1 Δ offspring. In future, the concentration of circulating growth hormone and IGF1, which are main mediators of postnatal growth and adiposity and moreover signal through the insulin signalling pathway (Holt, 2002, Kadakia et al., 2016), should be assessed to determine the mechanism by which disparities in offspring growth relate to altered metabolism.

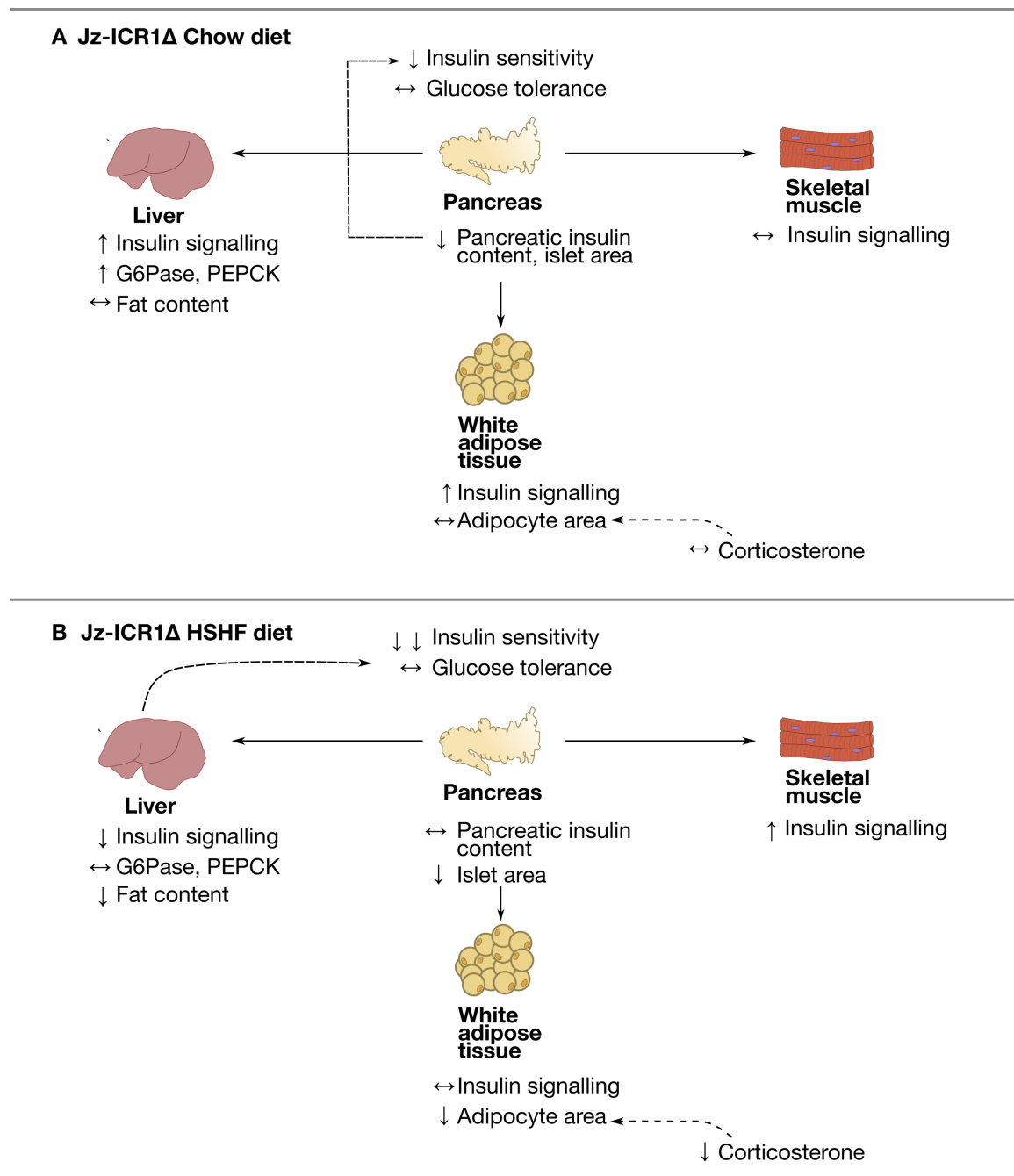


Figure 4.4.1. Summary of the effect of Jz-ICR1Δ and postnatal diet on male offspring metabolic phenotypes consuming a chow (A) or HSHF (B) diet. ↑, increase; ↓, decrease; ↔, no change (compared to genotype control of the same diet). Dashed arrows indicate potential connections between observed phenotypes. HSHF, high sugar high fat.

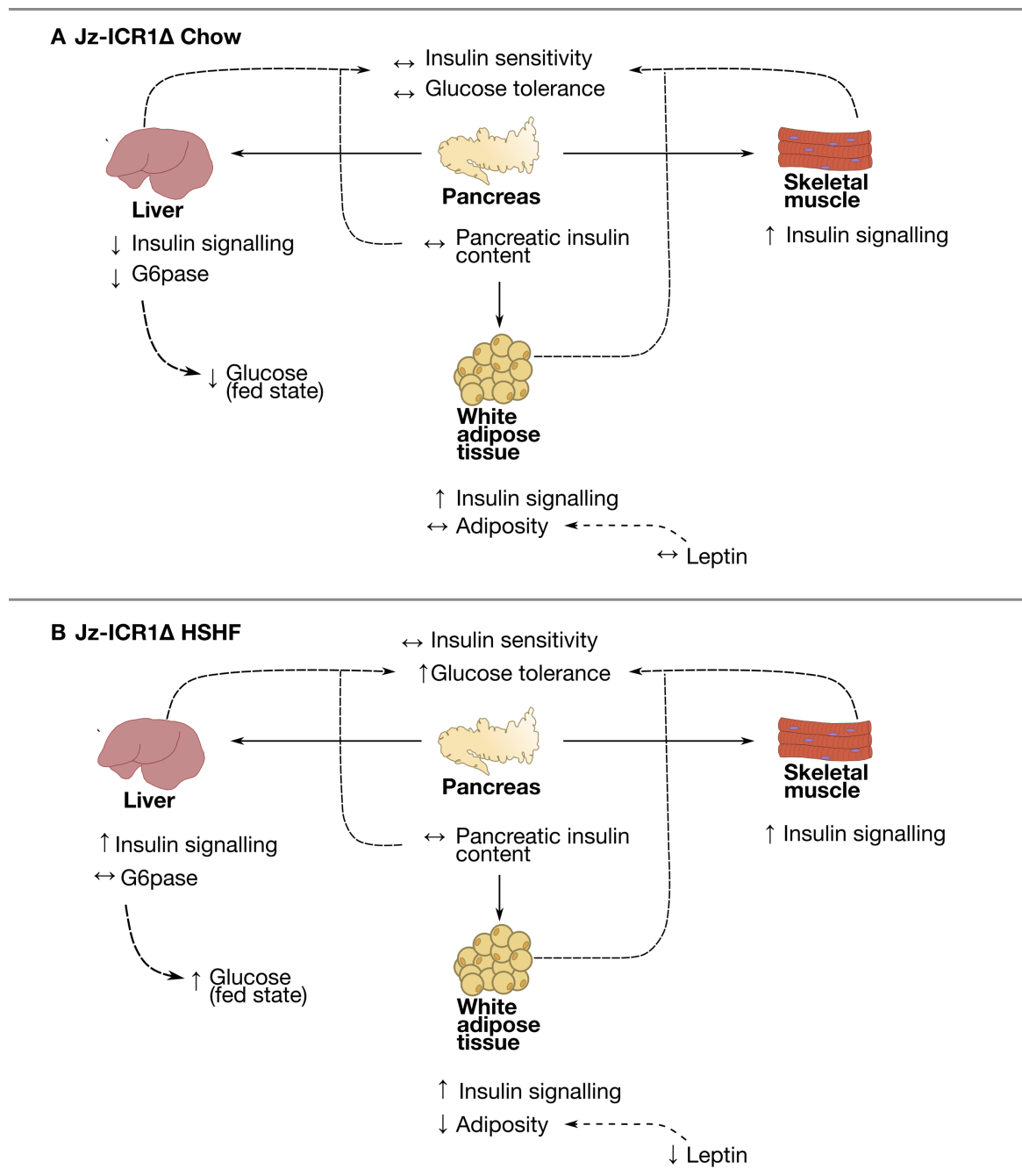


Figure 4.4.2. Summary of the effect of Jz-ICR1Δ and postnatal diet on female offspring metabolic phenotypes consuming a chow (A) or HSHF (B) diet. ↑, increase; ↓, decrease; ↔, no change (compared to genotype control of the same diet). Dashed arrows indicate potential connections between observed phenotypes. HSHF, high sugar high fat.

4.4.1 Adult offspring adiposity and adipose morphology in response to Jz-ICR1Δ

Jz-ICR1Δ offspring displayed either unaltered or reduced adiposity, in a sex and fat depot dependent manner. Similarly, changes in offspring adiposity in response to maternal obesity is also specific to the fat depot and sex studied (Lecoutre et al., 2016). Total fat mass was reduced in Jz-ICR1Δ female but not male offspring when consuming a HSHF diet compared to their genotype controls of the same diet. Similarly, in response to maternal obesity, male and female offspring display increased and reduced fat mass respectively, with an interaction between maternal diet and sex influencing offspring leptin and insulin concentrations (Dahlhoff et al., 2014). Indeed, in the current study, a concomitant reduction in circulating leptin and insulin was observed only in HSHF fed Jz-ICR1Δ female versus female HSHF control offspring and may relate to the reduced adiposity observed. Moreover, human studies also show that in response to GDM, male but not female offspring are at greater risk of childhood obesity (Li et al., 2017, Le Moullec et al., 2018), further indicating sexual disparities in offspring adiposity in response to a suboptimal gestational environment. Interestingly, despite Jz-ICR1Δ chow male offspring displaying reduced total adiposity, compared to control chow offspring, these animals were insulin resistant, as has been observed in transgenic mouse models with reduced or absent white adipose tissue (Moitra et al., 1998, Shimomura et al., 1998). These findings collectively highlight that white adipose tissue is required to maintain whole body insulin sensitivity. Conversely, female Jz-ICR1Δ offspring on a HSHF diet displayed reduced adiposity and increased glucose tolerance compared to control offspring suggesting they were protected against the effect of a HSHF diet to induce obesity and metabolic impairment. Previous studies indicate that increased white adipose tissue browning occurs in adult offspring after suboptimal nutrition *in utero* (Delahaye et al., 2010, Dumortier et al., 2017). In addition, high fat diet induced glucose intolerance is prevented by adipose tissue browning (Armani et al., 2014). Thus, in future, white adipose tissue (WAT) expression of mitochondrial uncoupling protein 1 (*Ucp1*) and neuropeptide Y (*Npy*) expression may be evaluated and high-resolution respirometry utilised to determine mitochondrial function in adipose tissue. In combination these techniques would determine whether Jz-ICR1Δ programmes sexual discrepancies in WAT browning in relation to metabolic outcomes as indeed, in mice, female gonadal WAT has an inherently higher browning capacity compared to male (Wang et al., 2019b). Additionally, Jz-ICR1Δ may also be programming the amount and/or activity of brown

adipose tissue (BAT) during fetal development, with consequences on adult metabolism, however, to date BAT from Jz-ICR1Δ offspring has not been collected. Future experiments may also involve isolating mesenchymal stem cells (MSC) from Jz-ICR1Δ and control offspring bone marrow to deduce changes in BAT and WAT differentiation beginning *in utero*.

Jz-ICR1Δ also altered adipocyte area in a sex and diet dependent fashion, with male Jz-ICR1Δ offspring on a HSHF diet having a greater proportion of small adipocytes than control HSHF offspring. Despite this, adipose PPAR γ , which is involved in adipogenesis (Rosen et al., 1999), remained unaltered in these offspring. It also remains unknown whether the observed phenotype is due to increased adipocyte differentiation. A reduced adipocyte area in male Jz-ICR1Δ offspring on a HSHF diet may in part be due to lower circulating corticosterone in these offspring, as it has been shown in rats that corticosterone administration increases adipocyte size (Rebuffé-Scrive et al., 1992) and Cushing's syndrome patients have increased adipocyte size (Rebuffé-Scrive et al., 1988). Interestingly, despite male Jz-ICR1Δ on a HSHF diet having lower plasma corticosterone concentrations, they also have pronounced insulin resistance. As corticosterone treatment in mice induces insulin resistance (Kaikaew et al., 2019), whilst male Jz-ICR1Δ on a HSHF diet have reduced insulin sensitivity and reduced plasma corticosterone concentrations, this may indicate that the hypothalamic-pituitary-adrenal (HPA) axis is not driving metabolic outcomes in these mice. The activity or protein abundance of 11 β HSD1 and 11 β HSD2 in adipose tissue of Jz-ICR1Δ offspring may be determined in future to determine whether there may be local changes in glucocorticoid bioavailability, as these enzymes convert glucocorticoids into the active and inactive forms, respectively (Chapman et al., 2013).

4.4.2 Adult offspring insulin production and pancreas morphology in response to Jz-ICR1Δ

Overall, Jz-ICR1Δ altered pancreas weight, morphology and capacity to secrete insulin in a sexually dimorphic manner. At P3, female but not male Jz-ICR1Δ offspring showed a tendency for reduced pancreas weight ($p=0.06$), albeit the significance of this is unknown as the lightest pups are culled for litter standardisation. Nonetheless, this may be the residual effects of compromised pancreas development during gestation to prioritise nutrients to the brain during gestation (Hales and Barker, 1992), as fetal weight was also

reduced at E19 in response to Jz-ICR1 Δ . Conversely, during adulthood, male but not female Jz-ICR1 Δ offspring overall showed an increased proportional pancreas weight. Despite this increase in weight, pancreatic insulin content tended to be reduced in chow fed adult males in response to Jz-ICR1 Δ ($p=0.05$), however circulating insulin and glucose concentration remained unaltered. Nonetheless, a reduction in pancreatic insulin content may contribute to the insulin resistance observed in these offspring and in future, determining glucose stimulated insulin secretion in offspring by measuring insulin in fasted animals in response to glucose *in vivo* or determining islet insulin secretion and cytosolic calcium concentration *ex vivo*, may provide further information on pancreatic function. A reduction in pancreatic insulin content in chow Jz-ICR1 Δ male offspring may be attributed to a decrease in pancreatic islet area and an increase in the proportion of small ($< 500 \mu\text{m}^2$) islets, as has also been observed in patients with type 2 diabetes (Deng et al., 2004). Moreover, clinical studies indicate that β -cell dysfunction precedes the development of hyperglycaemia (Holman, 1998), as is likely to occur in Jz-ICR1 Δ male offspring and may indicate that these offspring are at an early stage of metabolic disease. In both male and female offspring, an increase in islet number in response to Jz-ICR1 Δ may be a compensatory response to maintain appropriate insulin concentrations. However, whilst in males an increase in islet number was associated with an increase in the percentage of very small islets, in Jz-ICR1 Δ females this is likely due to an increase in islets of all sizes. Indeed, female offspring showed unaltered pancreatic insulin content and islet area in response to Jz-ICR1 Δ alongside increased islet density, which may be indicative of reduced β -cell function. Similar sexual discrepancies have been observed in offspring from dams consuming high fat diet during pregnancy, whereby male and female offspring also displayed reduced and unaltered pancreatic islet area respectively, which was related to a reduction in the expression of a transcription factor critical in islet neogenesis, pancreatic and duodenal homeobox 1 (*Pdx-1*) in males only (Yokomizo et al., 2014). Thus, in the future, islet *Pdx-1* expression may be determined to delineate the mechanism underlying the sexual discrepancies observed, as currently it is not known whether in male offspring a reduced islet area is due to changes in islet hypertrophy or hyperplasia in association with altered islet proliferation and/or apoptosis. Islet proliferation and apoptosis may be determined in future by immunostaining of Ki67 and Caspase-3 respectively. Moreover, whilst immunohistochemistry was employed to stain for insulin, in future, staining β -cell nuclei using immunofluorescent techniques would allow us to determine the number of β -cells within each islet. Interestingly, previous

studies indicate that oestrogen enhances β -cell mass, increases pancreatic insulin content and protects against islet apoptosis (Fraenkel-Conrat et al., 1941, Choi et al., 2005, Zhou et al., 2018). Thus, inherently higher oestrogen levels in female offspring may in part protect against changes in pancreas morphology and function as indeed, islet area remained unaltered in response to both Jz-ICR1 Δ and HSHF feeding, and pancreatic insulin content remained unaltered in response to Jz-ICR1 Δ in female offspring. Furthermore, sexual dimorphism in pancreatic function may in part relate to the sexual disparities observed in offspring glucose handling.

4.4.3 Adult offspring insulin and glucose handling in response to Jz-ICR1 Δ

Jz-ICR1 Δ altered the capacity of offspring to handle glucose and insulin in tolerance tests, and the outcomes of which were largely dependent on both sex and postnatal diet. Male Jz-ICR1 Δ offspring on a chow diet displayed minor insulin resistance and were increasingly insulin resistant on a HSHF diet compared to their dietary male control groups. Several studies have indicated a deterioration in insulin sensitivity in mice upon the consumption of a postnatal HSHF diet after an insult *in utero* (Reynolds et al., 2013, Pereira et al., 2015). Lower hepatic InsR and IGF1R protein abundance in male chow mice and reduced downstream PI3K pathway protein levels (p110 α , total GSK3) in male HSHF mice in response to Jz-ICR1 Δ is concomitant with the observed insulin resistance in male Jz-ICR1 Δ offspring compared to their genotype controls of the same respective diet. Interestingly, downstream mediators of the PI3K pathway were increased in the liver of chow fed Jz-ICR1 Δ male mice and may be indicative of increased receptor phosphorylation to propagate increased signalling in a compensatory manner. However, phosphorylation levels at the receptors have not been assessed to date in any tissue obtained from Jz-ICR1 Δ offspring and requires study in the future. Protein levels of the PI3K pathway were elevated in the skeletal muscle and unaltered in the adipose tissue of male HSHF offspring in response to Jz-ICR1 Δ . Moreover, chow fed male Jz-ICR1 Δ offspring displayed unaltered and increased PI3K signalling protein levels in skeletal muscle and adipose tissue respectively compared to their genotype controls of the same diet. Thus, in Jz-ICR1 Δ HSHF offspring defective hepatic insulin signalling may relate to whole body insulin resistance, which is in accordance with a previous study showing that high fat diet feeding in mice induces insulin resistance in the liver prior to development in skeletal muscle (Kraegen et al., 1991). In future, abundance of the insulin sensitive glucose transporter, GLUT4 at the plasma membrane of the skeletal muscle and white

adipose tissue may be determined to provide greater information on tissue-specific changes in glucose uptake in Jz-ICR1 Δ offspring. Previous studies have shown that adipose-specific downregulation or overexpression of the GLUT4 encoding gene (*Slc2a4*) impacts insulin sensitivity of the liver and skeletal muscle (Abel et al., 2001, Carvalho et al., 2005), which is indicative of peripheral tissue cross-communication that serves to maintain appropriate whole-body glucose metabolism. Whether such a phenomenon involving peripheral tissue cross-communication indeed occurs in male and female Jz-ICR1 Δ offspring remains to be defined. Moreover, whilst gonadal adipose tissue was used for Western blot and stereology studies, offspring white adipose morphology and insulin resistance in response to adverse gestational environments has been shown to be depot-specific in a manner also determined by sex (Lecoutre et al., 2016); therefore, other fat tissue depots may be studied in future.

Conversely, chow fed Jz-ICR1 Δ female mice had unaltered insulin sensitivity and glucose tolerance compared to control. Interestingly, increased PI3K signalling protein abundance (InsR, total AKT, pAKT T308, total GSK3, pGSK3 S21/9 and pS6K T389) in skeletal muscle and adipose tissue and reduced PI3K signalling protein abundance (p110 α , total AKT and pAKT S473) in the liver was observed in these offspring. Thus, tissue-dependent increases and reductions in PI3K signalling may overall be maintaining insulin sensitivity and glucose tolerance in female chow offspring in response to Jz-ICR1 Δ . Interestingly, HSHF fed female Jz-ICR1 Δ offspring were more tolerant to glucose when compared to their HSHF control group, which may be due to increased PI3K signalling protein abundance in peripheral organs (liver, skeletal muscle and white adipose tissue) despite reductions in circulating insulin. Increased glucose tolerance in the HSHF fed female Jz-ICR1 Δ offspring may also be due to increased insulin secretion in response to glucose during the challenge, however this has not been assessed to date. Furthermore, hepatic PPAR γ was increased in HSHF fed Jz-ICR1 Δ female offspring and chow fed Jz-ICR1 Δ males compared to their genotype controls of the same respective diet. As PPAR γ antagonism has been shown to alleviate insulin resistance (Yamauchi et al., 2001), the increased hepatic PPAR γ likely explains the elevated abundance of downstream insulin signalling proteins in chow fed males (p110 α , total AKT, pAKT T308, pGSK3 S21/9 and pS6K T389) and HSHF fed female offspring (InsR, p110 α and total GSK3) in response to Jz-ICR1 Δ .

White adipose PPAR α protein abundance was increased in both chow fed male and female Jz-ICR1 Δ offspring compared to their respective genotype controls. As PPAR α agonism improves insulin sensitivity and reduces adiposity (Sandoval-Rodriguez et al., 2020), enhanced white adipose PPAR α abundance is in accordance with a reduction in adiposity and increased adipose insulin signalling proteins in the chow fed male and female Jz-ICR1 Δ offspring. Moreover, increased hepatic PPAR α abundance in chow fed male offspring and reduced hepatic PPAR α abundance in chow fed females in response to Jz-ICR1 Δ is also in accordance with increased and reduced hepatic insulin signalling protein abundance in these male and female offspring respectively. Further to this, both PPAR α and insulin signalling protein abundance were increased in the skeletal muscle of chow fed female offspring in response to Jz-ICR1 Δ . However, in chow female offspring, despite a reduction in hepatic PI3K signalling (p110 α , total AKT, pAKT S473) proteins being observed in response to Jz-ICR1 Δ , the ratio of phosphorylated (T308)/total AKT and phosphorylated (T389)/total S6K was increased and may be indicative of an increased magnitude of phosphorylation compared to substrate abundance to increase hepatic insulin signalling and overall maintain whole body insulin sensitivity in these offspring.

The anomaly of increased glucose tolerance in Jz-ICR1 Δ female offspring consuming a HSHF diet may be representative of a “prediabetic state,” as has been shown previously in response to maternal low protein diet, where rat offspring were more tolerant to glucose at 3 months of age prior to developing glucose intolerance at 15 months of age (Hales et al., 1996). Moreover, ventromedial hypothalamic-lesioned rats are more responsive and then less responsive to insulin at 1 and 6 weeks after applying the lesion, respectively (Pénicaud et al., 1986). Collectively, these data indicate that during the timeline of diabetes pathophysiology, increased insulin response and glucose tolerance may be observed prior to insulin resistance and glucose intolerance in later life. Thus, increased glucose tolerance in female Jz-ICR1 Δ offspring fed a HSHF diet compared to their genotype controls of the same diet may be indicative of these offspring having the propensity to develop deteriorations in metabolic health as they age. In comparison, at the same age, male offspring already display reductions in insulin sensitivity in response to Jz-ICR1 Δ . Previous studies show female rodents have a longer life-span than males (Hales et al., 1996) and that maternal obesity accelerates metabolic aging in rat offspring in a manner that depends on sex (Rodríguez-González et al., 2019). Therefore, in future,

it would be of interest to perform telomere length analysis (Tarry-Adkins and Ozanne, 2018) and measure the expression of cellular senescence markers (cyclin dependent kinase inhibitor 1A, cyclin dependent kinase inhibitor 2A) in metabolic tissues at a young and older age to evaluate the effect of Jz-ICR1 Δ on the timing of metabolic dysfunction onset in both sexes with both a chow and HSHF postnatal diet. Moreover, the PI3K pathway mediates the activation of genes/pathways involved in inflammation (JNK, p38), proliferation (MAPK) and apoptosis (BCL-2, BAX) and it cannot be discounted that Jz-ICR1 Δ is programming sex-specific changes in these pathways in offspring leading to sexually dimorphic metabolic outcomes.

4.4.4 Adult offspring hepatic biochemical composition and gluconeogenesis in response to Jz-ICR1 Δ

Jz-ICR1 Δ was associated with altered hepatic weight and biochemical composition in adult offspring. On a HSHF diet, Jz-ICR1 Δ offspring had reduced proportional liver weight, regardless of sex, compared to their dietary controls. Interestingly, lower liver weight in HSHF diet fed male but not female Jz-ICR1 Δ offspring was associated with reduced hepatic fat and protein content. This was despite the fact that S6K, which regulates protein synthesis was unchanged in male but reduced in female Jz-ICR1 Δ offspring that had been fed the HSHF diet. Altered hepatic tissue composition may contribute to poor metabolic outcomes in HSHF fed Jz-ICR1 Δ males and moreover, aberrant lipid deposition in other tissues may occur in these offspring due to reduced hepatic fat content. Together with the increased LPL abundance observed in the skeletal muscle of HSHF fed Jz-ICR1 Δ males, these may lead to storage of lipids like triglycerides in muscle, contributing to insulin resistance (Kim et al., 2001). However, to date, lipid levels have not been investigated in offspring skeletal muscle tissue.

Jz-ICR1 Δ was also associated with altered abundance of proteins involved in gluconeogenesis in the liver of the offspring. In particular, G6Pase and PEPCK protein levels were elevated in the liver of chow fed Jz-ICR1 Δ male offspring, whilst G6Pase was decreased in chow fed Jz-ICR1 Δ female offspring. As insulin inhibits gluconeogenesis, these data are somewhat in alignment with the reduced insulin sensitivity seen in chow fed Jz-ICR1 Δ males, as well as the *ad libitum* fed hypoglycaemia in chow fed Jz-ICR1 Δ females. Gluconeogenesis may also be regulated by the actions of free fatty acids in the liver (Ferre et al., 1979, Gross et al., 2008) and whether reduced

hepatic fat content is related to the augmented G6Pase and PEPCK protein levels in chow fed Jz-ICR1 Δ male offspring is unknown. HSHF fed Jz-ICR1 Δ female offspring had increased *ad libitum* fed glucose levels compared to their respective HSHF control group, however, hepatic G6Pase and PEPCK protein levels remained unaltered between these two groups. These findings may suggest that in some instances, activity of these enzymes rather than protein abundance, is more indicative of gluconeogenic capacity. Overall, hepatic glycogen content in the offspring was unaltered in response to Jz-ICR1 Δ . This is despite an increase in hepatic phosphorylated GSK3 and ratio of phosphorylated/total GSK3 in chow fed males, and HSHF fed females in response to Jz-ICR1 Δ . Moreover, an increased ratio of phosphorylated/total GSK3 was observed in HSHF fed Jz-ICR1 Δ males and overall is supportive of other work showing that GSK3 phosphorylation is dispensable for functional hepatic glucose metabolism (Wan et al., 2013). Whilst a HSHF diet increased total hepatic glycogen levels in offspring regardless of genotype, when corrected for liver weight, glycogen levels were not impacted by offspring diet. This is in contrast to other studies indicating reduced hepatic glycogen levels in response to high fat diet feeding (Eisenstein et al., 1974, Simi et al., 1991), and disparities may be attributed to differing lengths of time rodents were fed HSHF diet, and differing compositions of these calorically dense diets. Parameters such as insulin sensitivity, glucose tolerance, adiposity, as well as fasted glucose concentration were overall altered by HSHF feeding, as has been reported previously (Huang et al., 2004). However, in some instances, parameters altered by a HSHF diet were sex-specific, for example corticosterone and triglycerides were elevated in females and free fatty acid concentrations were increased in males.

4.4.5 Adult offspring biometry in response to Jz-ICR1 Δ

Jz-ICR1 Δ also altered parameters not directly related to metabolic health, such as heart and kidney weights. Heart weight was reduced in chow and HSHF fed males and HSHF fed females by Jz-ICR1 Δ , with a similar reduction in offspring heart weight previously described in response to maternal undernutrition (Desai et al., 2005a). Moreover, Jz-ICR1 Δ was associated with an increase in the fractional weight of the kidneys in males regardless of diet and in HSHF diet fed females. Increased kidney weight has been previously observed in rat offspring that were exposed to intrauterine growth restriction and in humans with early juvenile diabetes (Mogensen and Andersen, 1973, Lim et al., 2011). Whilst male Jz-ICR1 Δ offspring displayed an increase in kidney size and reduced

heart size, regardless of diet, female Jz-ICR1 Δ offspring only displayed these phenotypes upon consumption of a HSHF diet. These data may indicate that female renal and cardiac functions are more protected against a poor intrauterine environment due to Jz-ICR1 Δ . Indeed, it has been shown that in female rats, oestradiol may mitigate the detrimental programming effects of a maternal low protein diet on offspring cardiac function postnatally (Braz et al., 2017). It needs to be explored in future whether changes in organ weights as a result of Jz-ICR1 Δ are accompanied by alterations in cardiac and renal morphology and function and may be linked to offspring hypertension and cardiometabolic disorders.

3.4.6 Limitations in study design and mechanisms of offspring programming

The study design utilised raises several limitations; gestational length may impact offspring metabolic programming, as placental-derived hormones which may be modified by Jz-ICR1 Δ may determine gestational length. Although gestational length was not significantly different in this model, to assess this more accurately, dams would have to be filmed to determine the exact time of birth, which would also offer a means to accurately deduce birth weight. Litters were standardised at P3 as litter size impacts neonatal growth, and as such is a major determinant of offspring metabolic outcomes (Parra-Vargas et al., 2020). However, reducing rodent litters in studies of developmental programming, as in this study, is known to programme offspring metabolic phenotypes when compared to unrestricted/unstandardized litters (O'Dowd et al., 2008, Wadley et al., 2008, Briffa et al., 2019). Granted both control and Jz-ICR1 Δ litters were standardised, however, to determine whether litter reduction influences the metabolic programming of offspring overall, studies would have to be repeated without litter standardisation. Furthermore, at P3, the lightest excess pups were sacrificed, and biometry performed, however a limitation in biometry data at this time point is that it is not representative of the whole litter. Moreover, despite the ratio of males/females born being unaltered in response to Jz-ICR1 Δ , there appear to be more females culled at P3, which may be due to larger litters (which are standardised) having more females, compared to smaller litters (which are not standardised) having more males. Nonetheless, reducing the smallest pups from the litter maintains consistency across litters and moreover smaller pups are more likely to be unviable later in life. Jz-ICR1 Δ may cause changes in offspring food intake and energy expenditure, both of which have been shown to influence metabolism (Kohjima et al., 2010, Tang et al., 2010). To accurately deduce these parameters,

offspring may be placed in metabolic cages to determine energy expenditure. Moreover, mice were culled at 17 weeks of age, and therefore young adults with their metabolic perturbances being relatively mild in severity. The appearance of metabolic perturbances at a young age in mice in response to Jz-ICR1 Δ has clinical relevance as type 2 diabetes is becoming increasingly diagnosed in younger adults and adolescents (Alberti et al., 2004). Nonetheless, offspring may be studied at several ages in future to determine whether Jz-ICR1 Δ accelerates the timing of metabolic disease onset and aging, perhaps in a manner also determined by sex.

In this study where the endocrine placenta was manipulated solely, it remains unknown to what extent the environment *in utero* is programming offspring metabolic outcomes compared to the weaning period, which has also been shown to impact offspring programming (George et al., 2019). Previous work in the lab indicates that Jz-ICR1 Δ dams continue to have metabolic perturbances 12 weeks postpartum and are glucose intolerant with elevated concentrations of insulin and corticosterone but diminished concentrations of leptin (data not shown). These continued metabolic perturbances in dams may influence offspring metabolism during weaning and indeed, during the weaning period, Jz-ICR1 Δ offspring were growth restricted, with alterations in growth trajectory likely impacting metabolic physiology (Hales and Ozanne, 2003). Changes in growth and programming during weaning may be due to altered composition of dam milk or changes in offspring feeding behaviour, which could be assessed using mass spectrometry and infra-red video recordings, respectively. To further delineate the relative consequences of intrauterine and postnatal effects for offspring metabolic programming, in future, cross-fostering studies may be conducted. Moreover, the postnatal diet consumed heavily influences the metabolic outcomes observed in Jz-ICR1 Δ offspring. Indeed, in this study two HSHF diets were optimised to determine which was appropriate to exacerbate metabolic outcomes in Jz-ICR1 Δ offspring and showed varied results in offspring insulin sensitivity (Figure A1.1, Appendix 1.1). Furthermore, it has been shown that in isogenic mice fed a HSHF diet, a subset is more resistant to these effects with metabolic differentiation occurring via increased activation of mitochondrial oxidative pathways in resistant mice, and lead to variability in outcome measures (Boulangé et al., 2013). An increase in sample size would enable the separation of responders and non-responders to a HSHF diet and allow a more accurate evaluation of the effect of Jz-ICR1 Δ on metabolic phenotypes. Moreover, in future it may be of interest to superimpose

another postnatal stressor, such as a low protein diet, or calorie restriction to determine changes in offspring metabolism.

Striking sex differences were observed in the metabolic outcomes and molecular alterations in organs of Jz-ICR1 Δ offspring when consuming both a chow and a HSHF diet, however, the mechanisms driving this sexual disparity remain unknown. Innate differences in sex steroids between female and male offspring may influence insulin and glucose handling as it is known that whilst oestrogen increases insulin sensitivity, androgens such as testosterone potentiate insulin resistance (Takeda et al., 2003, Gasparini et al., 2019), and as described in detail in Chapter 1, section 1.11.1). It would be valuable to determine whether circulating oestrogen in female (offspring would need to be monitored to control for the stage of the oestrous cycle) and testosterone concentrations in male offspring are altered by Jz-ICR1 Δ and may explain in part the varying metabolic outcomes. Several factors in the environment *in utero* may also influence offspring programming in a sexually dimorphic manner, namely sex differences in hormonal and temporal fetal development and corticosterone concentrations as well as incomplete inactivation of X-linked genes (Tsunoda et al., 1985, Montano et al., 1993, Howerton et al., 2013, Chin et al., 2017) and as described in detail in Chapter 1, section 1.11.2). In future, the use of embryo transfer experiments by using pseudo pregnant zygote recipients may aid in identifying whether programming of Jz-ICR1 Δ offspring begins *in utero* and which specific periods during gestation induce offspring metabolic programming. Moreover, it may be determined whether Jz-ICR1 Δ alters fetal phenotypes by causing molecular changes in fetal metabolic organs.

Chapter 5: The effect of Jz-ICR1Δ on the hepatic transcriptome in male and female fetuses

5.1 Introduction

The “thrifty phenotype” hypothesis states that in response to an inadequate nutritional environment during gestation, the fetus prioritises nutrition to key organs such as the brain for survival, at the expense of metabolic organs served by peripheral vascular beds (e.g., the liver or pancreas). Permanent structural and functional alterations in fetal metabolic organs may negatively impact adult metabolic health (Hales and Barker, 1992). For instance, in *Igf2* knockout mice, brain weight is preserved despite a reduction in body weight, indicating a brain sparing effect concordant with nutritional deficiency, as in this model placental amino acid transport capacity is reduced (Constancia et al., 2005, Lopez et al., 2018). In response to maternal undernutrition or protein restriction, the rodent fetus displays a reduction in pancreatic β -cell mass, vascularisation and insulin content (Dahri et al., 1991, Valtat et al., 2011). Whereas, in response to maternal obesity, adipogenic differentiation is increased in fetal mice (Yang et al., 2013). Exposure to maternal psychological stress, alcohol consumption, or hypercholesterolemia *in utero* also alters the morphology and function of the rodent fetal liver, reducing the number of mitochondria in parenchyma cells and glycogen content and increasing triglyceride abundance (Shen et al., 2014, Franko et al., 2017, Dumolt et al., 2019). Such alterations are accompanied by changes in hepatic gene expression in the fetus, with *G6pase* and *Foxo1* expression increased and *Igf1* expression reduced in the case of maternal psychological stress, alcohol consumption and uterine ligation (Fu et al., 2009, Shen et al., 2014, Franko et al., 2017). Markers of inflammation, namely TNF α and phosphorylated JNK are also increased in the liver of rat fetuses exposed to maternal protein restriction (Liu et al., 2014). In the aforementioned poor intrauterine environments, alongside changes in fetal phenotypes, offspring subsequently show alterations in metabolic health in postnatal life (Dahri et al., 1991, Liu et al., 2014, Christoforou and Sferruzzi-Perri, 2020). Thus, these results highlight that the study of fetal metabolic organs is key in determining the molecular mechanisms *in utero* that underpin the DOHaD hypothesis.

Sexual dimorphism is evident in the prevalence and pathophysiology of type 2 diabetes mellitus and metabolic syndrome and this has been corroborated by both human

epidemiological studies and rodent models of developmental programming (Logue et al., 2011, Lecoutre et al., 2016, Li et al., 2017, Inoguchi et al., 2019). In our model of endocrine zone malfunction (Jz-ICR1Δ), major sexual disparities were also observed with regard to whole body glucose and insulin handling and molecular pathways governing metabolism in key metabolic tissues in adult offspring (Chapter 4). Previous work has reported inherent sex differences in gene expression in the adult mouse liver, with 70% of active genes varying between males and females (Yang et al., 2006). Differences in the hepatic transcriptome between the sexes may in part contribute to disparity in metabolic programming of male and female offspring. Sex differences in gene expression in the fetal liver have also been documented in mice (Lowe et al., 2015), with maternal stressors during pregnancy such as diabetes or low protein diet further altering fetal gene expression in a sexually dimorphic manner (Kwong et al., 2007, Fornes et al., 2018). Differences in gene expression between males and females may be influenced by endocrine factors including sex steroids and glucocorticoids, which are critical in fetal and postnatal developmental outcomes, both during healthy pregnancies and in response to a suboptimal gestational environment. For instance, females and males have higher levels of oestradiol and testosterone, respectively when compared to the opposite sex, and this is evident from fetal life, including detectable changes in the amniotic fluid of mouse fetuses (vom Saal et al., 1983, vom Saal, 1989). In addition, oestrogen exerts protective effects against the development of insulin resistance in adulthood (Guillaume et al., 2017, Guillaume et al., 2019) and whilst less is known about the effects of oestrogen *in utero* on fetal development and programming, intrauterine exposure to a xenoestrogen (bisphenol A) in rodents alters offspring hepatic gene expression in a sexually dimorphic manner (Ilagan et al., 2017). Testosterone may also contribute to sexually dimorphic metabolic outcomes, with prenatal testosterone treatment in sheep associated with intrauterine growth restriction in both sexes but only postnatal catchup growth in female progeny (Manikkam et al., 2004). Differences in the hypothalamic-pituitary-adrenal (HPA) axis between the sexes are also governed by androgens and oestrogens during adulthood, which inhibit and enhance HPA function, respectively (Handa et al., 1994). In the adrenals, corticosterone is the major steroid secreted in rodents, and its levels are influenced by sex steroids (Handa et al., 1994).

Glucocorticoids are widely recognised as mediators of programming *in utero*, through their influence on fetal organ development. For example, genetic manipulation in mice

has revealed that glucocorticoid signalling is required in the programming of fetal β -cell dysfunction in response to maternal undernutrition (Valtat et al., 2011). In the mouse, serum corticosteroid levels are higher in female compared to male fetuses (Montano et al., 1993). Conversely in human cord blood, cortisol concentrations are similar between males and females (Clifton et al., 2007), whilst total testosterone is higher in the cord blood of males compared to females (Keelan et al., 2012). However, in both humans and mice, sex dependent alterations in placental 11 β HSD2 activity and expression are observed in response to maternal psychological stress and betamethasone exposure (Stark et al., 2009, Wiczorek et al., 2019), indicating that glucocorticoid exposure may be influenced by the placenta in a sexually dimorphic manner in both species. Indeed, the placenta develops from extraembryonic tissues and therefore has the same sex as the fetus. Moreover, the placenta may differentially influence fetal adaptations to suboptimal gestational environments in a manner dependent on sex. For instance, in response to a maternal high fat diet, there are sex dependent epigenetic alterations evident in the placenta (Gallou-Kabani et al., 2010). Mounting evidence suggests that several factors *in utero* dictate the sexual dimorphism observed in the programming of metabolic disease. As disparities in metabolism and molecular alterations were observed in female and male offspring in response to Jz-ICR1 Δ (Chapter 4), we sought to identify whether this may relate to sex-dependent changes in the transcriptome of a key metabolic organ, the liver, *in utero*. It was hypothesised that Jz-ICR1 Δ changes the expression of genes involved in metabolism in the fetal liver in a sexually dimorphic manner with potential long-lasting effects on adult health.

Thus, the aims of this study were:

- To determine the effects of Jz-ICR1 Δ on hepatic gene expression in male and female fetuses via RNA sequencing.
- To bioinformatically identify pathways/networks in the Jz-ICR1 Δ fetal hepatic transcriptome, such as those linked to sex steroid or glucocorticoid action which may mediate metabolic changes in Jz-ICR1 Δ male and female adult offspring.
- To assess whether changes in fetal hepatic gene expression in response to Jz-ICR1 Δ persist in the adult liver.

5.2 Materials and methods

Animals

Experiments were performed under the UK Home Office Animals (Scientific Procedures) Act 1986, approved by the University of Cambridge. Mice were housed under 12:12h dark/light photocycle conditions with *ad libitum* access to water and standard chow diet. Female mice in which the ICR1 of the *H19-Igf2* locus is flanked by *LoxP* sites were mated with males expressing *Cre* recombinase under the promoter of the Jz-specific gene, *Tpbpa* (*Tpbpa-Cre*; Figure 2.1). All mice were bred on a C57BL/6N (Charles River) background. The reverse parental cross was utilised as a control in all experiments. Only the placental Jz (and not the mother or fetus) has been genetically manipulated, but for ease placentas, dams and offspring will be referred to as Jz-ICR1 Δ in this study. In total, n=59 female mice were mated for pregnancy experiments terminated at E19, and of these n=7 female mice were used for fetal liver RNA sequencing and another n=14 female mice were used for qPCR validation experiments. The presence of a copulatory plug was defined as E1 of pregnancy. Dams at E19 of pregnancy underwent a placental transport assay (described in Chapter 2, section 2.2.2) and during this procedure, the livers from one female and one male fetus per litter were weighed and snap frozen for gene expression analyses. The brain of these fetuses was also weighed.

Tissue collection

Fetal livers were collected on E19 for RNA extraction. The heaviest male and female fetuses per litter were selected, and initially sexed visually (by the presence of a black mark above the groin region in males). Fetuses were sacrificed by decapitation and blood glucose levels immediately measured using a hand-held glucometer (OneTouch). Fetal livers were immediately flash frozen in liquid nitrogen, prior to storing at -80 °C for processing at a later date. Fetal tails were collected from all experiments for SRY sexing (Chapter 2, section 2.2.3) to validate the visual identification of fetal sex and allow analyses to be split by sex.

RNA extraction and quality control

The RNA from fetal and adult livers (the same cohort used in Chapter 4) was extracted using the protocol described in detail in Chapter 2, section 2.2.8.1. RNA was also extracted from separate fetal liver biological replicates for validation of RNA sequencing by qPCR. The liver of only one male or female fetus/adult per litter was utilised for RNA analyses, as far as possible. RNA quality for sequencing was determined using an Agilent RNA ScreenTape System (G2964AA, Agilent Technologies; Chapter 2, 2.4.1.2). A RIN number of >7.0 was a requirement to indicate RNA quality suitable for RNA sequencing.

Illumina TruSeq Stranded mRNA library preparation, sequencing and data processing

Hepatic mRNA was converted into RNA using the Illumina TruSeq Stranded mRNA library preparation kit (Illumina, 20020594; Chapter 2, section 2.4.1.3). Library quality was checked by an Agilent RNA ScreenTape System (G2964AA, Agilent Technologies) and libraries were pooled as described in detail in Chapter 2, section 2.4.1.4. Pooled libraries were sequenced (50 bp single ended on a HiSeq 4000 workflow; Chapter 2, 2.4.1.5). Data were processed by Dr Russell Hamilton (Centre of Trophoblast Research, University of Cambridge) as described in detail in Chapter 2, 2.4.1.6 to identify differentially expressed genes (DEGs) between control and Jz-ICR1 Δ male and female fetal livers. Due to the sex differences observed in adult Jz-ICR1 Δ phenotypes, all analyses in the fetal hepatic transcriptome were split by sex.

Quantitative polymerase chain reaction (qPCR)

A subset of DEGs identified by RNA sequencing were validated using qPCR. Moreover, the expression of these DEGs was assessed in adult livers. A combination of upregulated and downregulated genes present either in both male and females or exclusively in one sex were chosen, the names and primers of which are shown in Table 2.6. Genes were chosen according to both the magnitude of their fold change and their biological relevance to adult Jz-ICR1 Δ phenotypes. Fetal hepatic RNA (from both technical and separate biological replicates) and adult hepatic RNA was reverse transcribed into cDNA (Chapter 2, section 2.2.8.2). qPCR reactions were performed as described in Chapter 2, section 2.2.8.3.

Data analysis

Shared DEGs between groups were shown in a Venn diagram, and fold changes and heat maps of p values were presented using Venny

(<https://bioinfogp.cnb.csic.es/tools/venny/index.html>) and R, respectively. DEGs were subject to functional association network analysis with STRING (<https://string-db.org>; (Szkłarczyk et al., 2015) and gene ontology (GO) terms associated with DEGs were determined using UniProt (<https://www.uniprot.org>) as described in Chapter 2, section 2.4.1.8 DEGs in response to Jz-ICR1Δ (irrespective of sex) were subjected to enrichment analysis using EnrichR (Chen et al., 2013, Kuleshov et al., 2016) as described in Chapter 2, section 2.4.1.8 and shown in Appendix 1.4.1 (Figure A1.4.1).

Statistics

The effects of genotype and sex on fetal liver and brain weights, and blood glucose levels, were determined by two-way ANOVA with a Sidak post hoc test. DESeq2 was used to calculate DEGs and their adjusted p values (analysis performed by Dr Russell Hamilton, Centre for Trophoblast Research, University of Cambridge). An adjusted p value threshold of 0.05 and a log₂ fold change of 0.5 (fold change > 1.4) were used. Overall, qPCR data were largely normally distributed as validated by a D'Agostino-Pearson (omnibus K2) normality test (GraphPad Prism, 7.0). The effect of genotype on gene expression in adult offspring livers was assessed by a Student's t-test using Microsoft Excel.

5.3 Results

5.3.1 Biometry of E19 fetuses

Fetal organ weights and blood glucose levels on E19 of pregnancy are shown in Figure 5.1. On E19, brain weight was increased in Jz-ICR1 Δ fetuses, expressed both as absolute weight and as a percentage of body weight, compared to their control counterparts ($p < 0.05$; Figure 5.1B, E). Brain weight expressed as a percentage of body weight was increased in female Jz-ICR1 Δ fetuses compared to female control fetuses ($p < 0.05$; Figure 5.1E). However, liver weight, the brain/liver ratio and blood glucose levels remained unaltered in fetuses in response to Jz-ICR1 Δ . Moreover, there were no effects of fetal sex on any of these parameters (Figure 5.1).

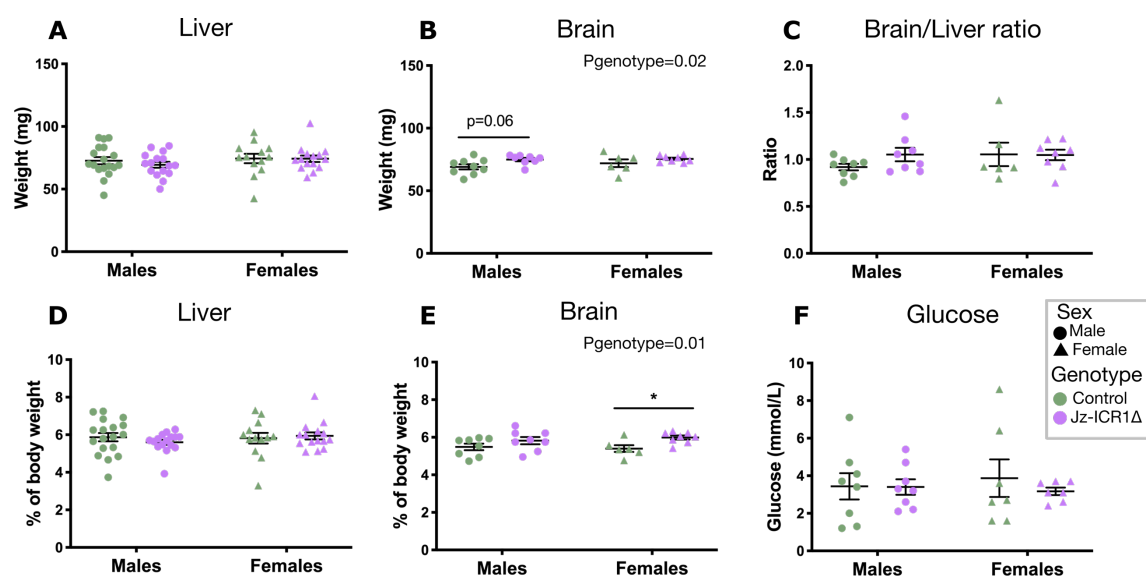


Figure 5.1. The effect of Jz-ICR1 Δ on female and male fetal liver (A, D) and brain (B, E) weights, and blood glucose levels (F) at E19. Data from individual fetuses (one male and female per litter) are shown with bars representing mean \pm SEM. Data were analysed by two-way ANOVA (genotype and sex), followed by a Sidak post hoc test. $n = 7-18$ (per genotype and sex).

5.3.2 Differentially expressed genes (DEGs) in response to Jz-ICR1Δ and fetal sex

The number of upregulated and downregulated genes in the fetal liver in response to genotype and sex are shown in Table 5.1. An adjusted p value < 0.05 and a log₂ fold change > 0.5 (fold change > 1.4) were considered significant. A total of 4 genes were upregulated and 27 genes were downregulated in response to Jz-ICR1Δ (irrespective of sex). When comparing control and Jz-ICR1Δ males, 2 genes were upregulated and 9 genes were downregulated. Moreover, when comparing control and Jz-ICR1Δ females, 3 genes were upregulated and 16 genes were downregulated.

A total of 7 genes were affected by fetal sex (irrespective of genotype), with 3 being upregulated and 4 downregulated. Moreover, 8 and 4 genes were upregulated and downregulated, respectively, in control males compared to control females. When comparing Jz-ICR1Δ males to Jz-ICR1Δ females, 2 genes were upregulated and 4 genes were downregulated. The differentially expressed genes (DEGs) influenced by fetal sex are shown in Appendix 1.4.2. As sexual dimorphism was observed in adult Jz-ICR1Δ phenotypes, and discrepancies in the DEGs in response to Jz-ICR1Δ were observed according to fetal sex, comparisons in DEGs between control and Jz-ICR1Δ males and control and Jz-ICR1Δ females were undertaken herein.

Table 5.1. The effect of Jz-ICR1Δ and sex on the number of upregulated and downregulated genes in the fetal liver at E19.

	Upregulated genes	Downregulated genes
Jz-ICR1Δ vs control *	4	27
Jz-ICR1Δ males vs control males	2	9
Jz-ICR1Δ females vs control females	3	16
Males vs females†	3	4
Control males vs control females	8	4
Jz-ICR1Δ males vs Jz-ICR1Δ females	2	4

* Irrespective of sex; † Irrespective of genotype

5.3.3 Differentially expressed gene (DEG) analysis in male and fetal fetuses in response to Jz-ICR1Δ

Figure 5.2A shows principal component analysis (PCA) of global gene expression profiles in the liver at E19 for male and female, and control and Jz-ICR1Δ fetuses. Complete separation of the four groups is indicative of a unique phenotype, which is dependent on both sex and genotype. The variation in gene expression between groups was caused to a greater degree by sex (PC1=29.4%) compared to genotype (PC2=16.5%). A Venn diagram indicates the distribution of DEGs in response to Jz-ICR1Δ in male and female fetuses separately (Figure 5.2B). In male fetal livers only, 3 DEGs were downregulated and 2 were upregulated by placental Jz-ICR1Δ mutation. Comparatively, 10 DEGs were downregulated and 3 upregulated in female fetal livers only by Jz-ICR1Δ. In response to Jz-ICR1Δ, a total of 6 DEGs were downregulated in both female and male fetuses. A portion of DEGs was validated by qPCR. These were *Npy*, *Zfp36* and *Ccn1* in male fetal livers and *Npy*, *G6pc*, *Rsg16* and *Serpina7* in female fetal livers. A strong correlation between the fold changes by RNA sequencing and qPCR was indicated ($R^2=0.98$; Figure 5.2C).

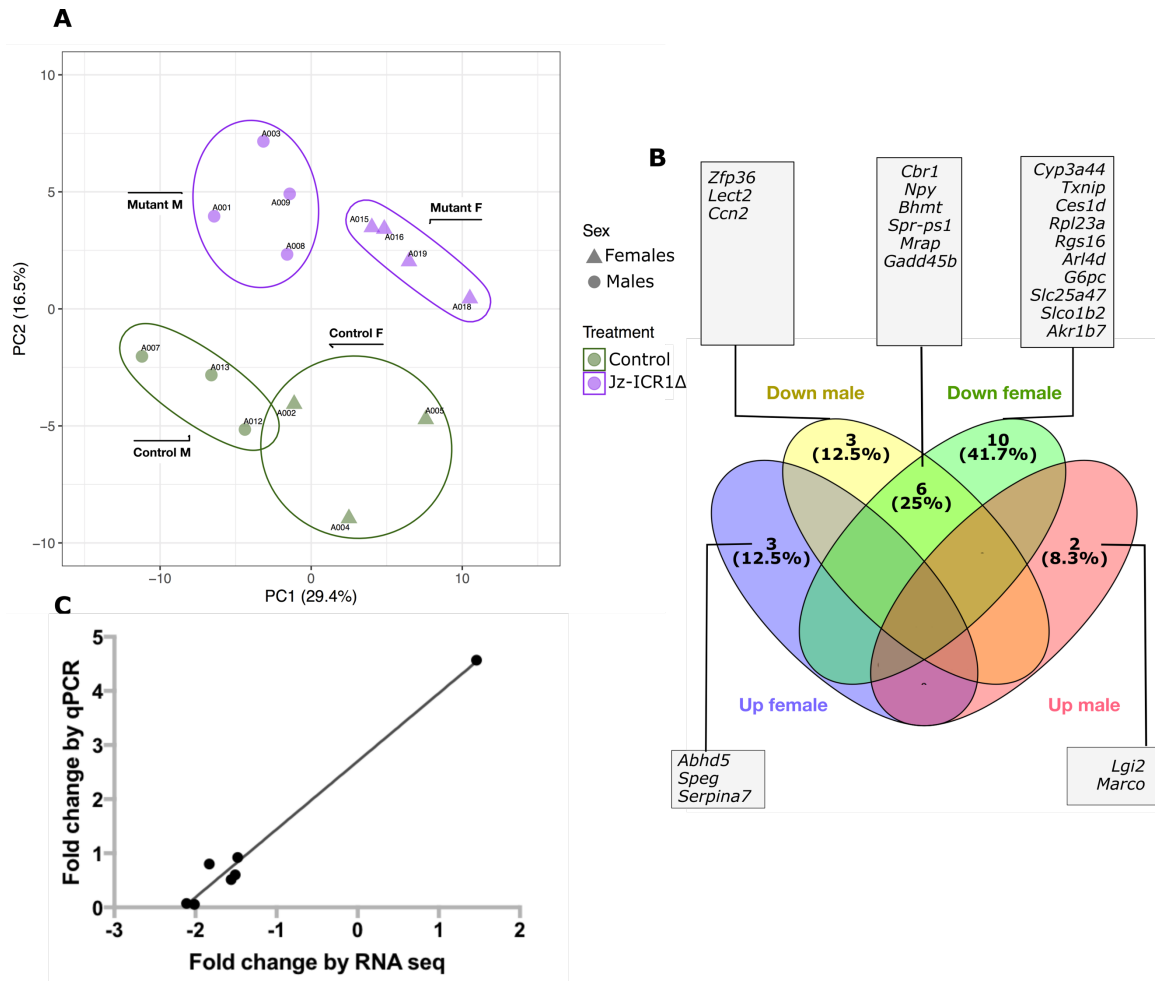


Figure 5.2. Principal component analysis (PCA) plot (A), Venn diagram showing upregulated and downregulated genes in fetal liver in response to Jz-ICR1Δ according to fetal sex (B) and qPCR validation of RNA sequencing data (C). PCA was performed to assess sample clustering with the DESeq2 package (v1.22.2, R v3.5.3) using the top 500 differentially expressed genes. n=3-4 per genotype and sex (from different litters). Differentially expressed genes (DEGs) presented in the Venn diagram were calculated using a log₂ fold change (FC) of 0.5 (FC > 1.4) and an adjusted p value threshold of 0.05. Validation was performed for 7 genes by plotting qPCR and RNA sequencing fold changes of both technical and independent biological replicates for control (n=3 and n=5, respectively) and Jz-ICR1Δ (n=4 and n=6, respectively) fetal liver samples at E19 (from different litters). qPCR gene expression was calculated relative to the geometric mean of *Polr2a* and *Hprt* and relative to the control group.

Volcano plots showing significant DEGs in control compared to Jz-ICR1Δ in male and female fetal livers are shown in Figure 5.3A and Figure 5.3B respectively. DEGs with the largest fold change difference in response to Jz-ICR1Δ are labelled. Of the labelled DEGs, only *Npy* is common between males and females in response to Jz-ICR1Δ, whilst all other labelled DEGs are sex-specific in response to Jz-ICR1Δ.

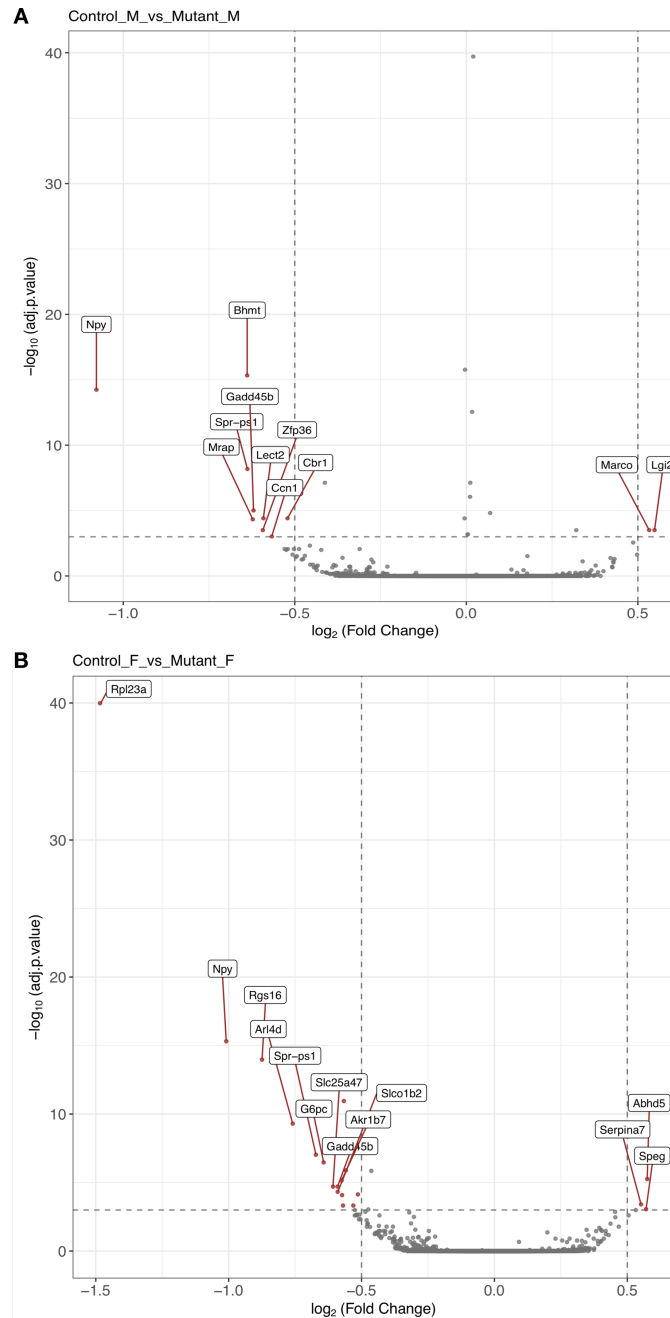


Figure 5.3. Volcano plot analyses comparing gene expression in male (A) and female (B) fetal livers from control and Jz-ICR1Δ groups at E19. Grey dots indicate the genes that are not significant for the group comparison. Red dots indicate the genes that are significant in Jz-ICR1Δ compared to control in either male (A) or female (B) fetal livers (\log_2 fold change > 0.5 , adjusted p value < 0.05). The x axis depicts logarithm to base 2 of the fold change and the y axis depicts logarithm to base 10 of the adjusted p value.

The fold change and p value of DEGs in male and female fetal livers in response to Jz-ICR1Δ are shown in Figures 5.4A, B. Network analysis identifying known and predicted physical and/or functional gene interactions in male and female fetal livers in response to Jz-ICR1Δ was performed (Figure 5.4C), to better elucidate the function of each individual gene in association with the whole DEG list. Scores for gene interactions are computationally predicted (Chapter 2, section 2.4.1.8). In females, an interaction between betaine-homocysteine methyltransferase (*Bhmt*) and solute carrier organic anion transporter family, member 1b2 (*Slco1b2*; co-expression, combined score=0.41; Figure 5.4C) was identified. Interactions between cytochrome P450, family 3, subfamily a, polypeptide 44 (*Cyp3a44*) and *Slco1b2*, as well as between *Slco1b2* and glucose-6-phosphatase (*G6pc*) were identified (co-expression and co-mentioned in abstracts, combined score=0.49 and 0.45, respectively). An interaction between *G6pc* and aldo-keto reductase family 1, member B7 (*Akr1b7*) was also identified (co-expression, association in curated databases and co-mentioned in abstracts, combined score=0.65). Moreover, in females, an interaction between *G6pc* and thioredoxin interacting protein (*Txnip*) and between abhydrolase domain containing 5 (*Abhd5*) and carboxylesterase 1D (*Ces1d*) was also identified (co-mentioned in abstracts, combined score=0.48 and 0.58 respectively). In contrast, no interactions between DEGs in response to Jz-ICR1Δ were identified in male fetal livers (data not shown).

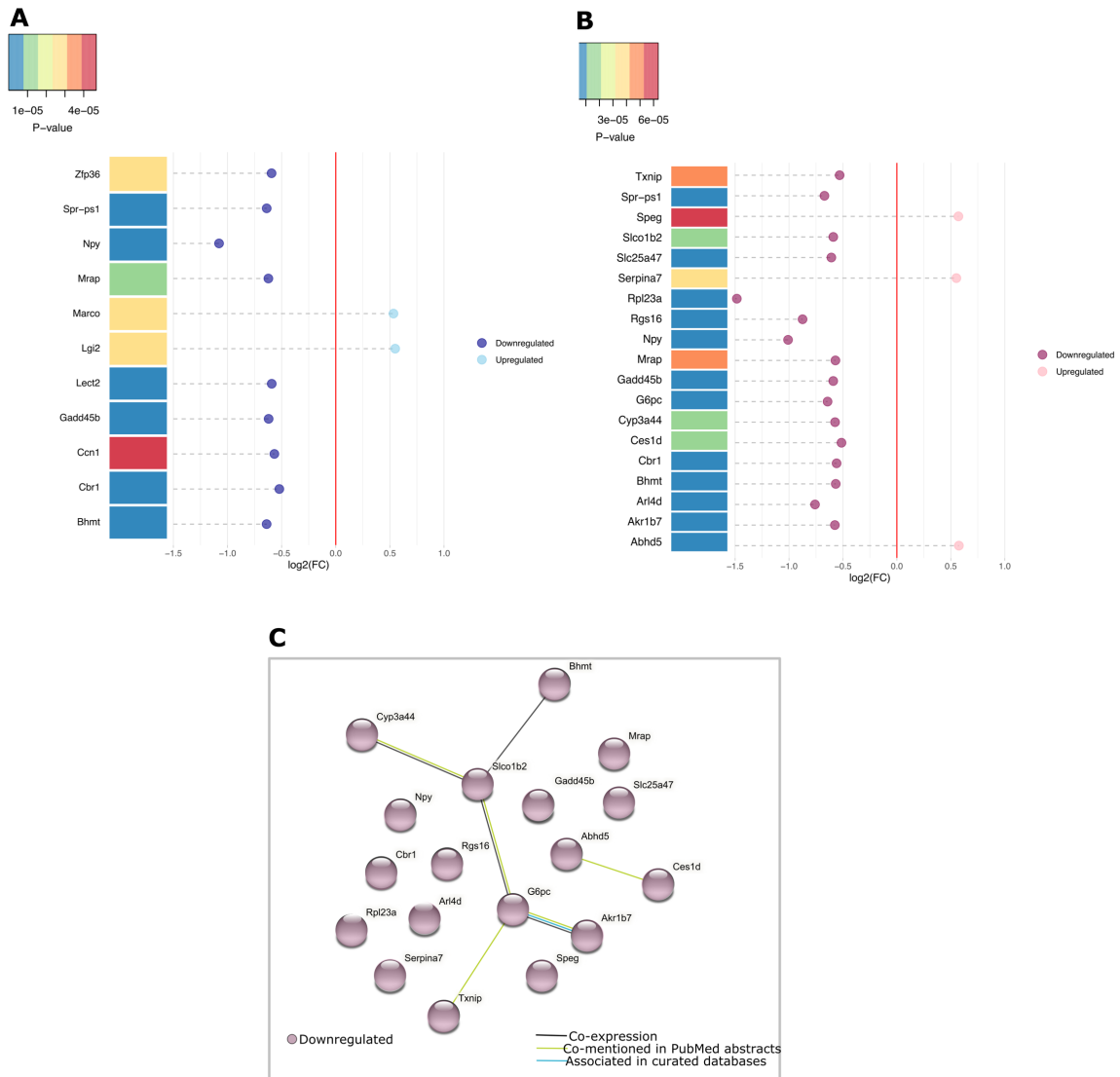


Figure 5.4. Differentially expressed genes in male (A) and female (B) fetal livers at E19 in response to Jz-ICR1 Δ and molecular network analysis in female fetal livers (C). The dot plot graph represents $\log_2(\text{fold change})$ of DEGs in male (A) or female (B) fetuses in response to Jz-ICR1 Δ ; the heat map represents each DEG p value from blue (lowest) to red (highest). Graphs 5.3A, B were drawn using R by Marta Ibanez-Lligona. Molecular network analysis was performed with String (<https://string-db.org/>) to identify physical and/or functional gene interactions. Lines in the molecular network represent associations between genes (co-expression, co-mentioned in abstracts or associated in curated databases). The positions of genes in Figure 5.4C are arbitrary.

5.3.4 DEG knockout phenotypes

Gene ontology (GO) terms and adult mouse knockout phenotypes associated with a subset of DEGs present in the fetal liver of both males and females, or only males or only females in response to Jz-ICR1 Δ are shown in Tables 5.2, 5.3 and 5.4, respectively. The GO terms associated with DEGs in response to Jz-ICR1 Δ present in both male and female livers included neuropeptide hormone and methyltransferase activity (GO:0005184, GO:0008168), corticotropin hormone receptor binding (GO:0031780), apoptotic processes (GO:0006915) and drug metabolic processes (GO:0017144). The knockouts of *Bhmt* and melanocortin 2 receptor accessory protein (*Mrap*) are linked to changes in adiposity (Teng et al., 2012, Asai et al., 2013), whilst neuropeptide Y (*Npy*) knockout is associated with reduced food intake in mice (Bannon et al., 2000). Moreover, the knockout of growth arrest and DNA-damage-inducible 45 beta (*Gadd45b*) and carbonyl reductase 1 (*Cbr1*) are associated with increased hepatic apoptosis sensitivity and inhibition of fibrosis in models of chronic liver injury, respectively (Olson et al., 2003, Gupta et al., 2005).

DEGs in response to Jz-ICR1 Δ in male fetuses had GO terms associated with inflammatory processes including cellular response to lipopolysaccharide (GO:0071222) and innate immune response (GO:0045087). Other GO terms included chemotaxis (GO:0006935) and insulin-like growth factor binding (GO:0005520). The knockout of zinc finger protein 36 (*Zfp36*) in adult mice leads to the development of inflammatory arthritis (Phillips et al., 2004). Moreover, leukocyte cell-derived chemotaxin 2 (*Lect2*) and macrophage receptor with collagenous structure (*Marco*) knockouts increase hepatic natural killer T (NKT) cell number and enhance dendritic cell migratory capacity in response to C-C Motif Chemokine Ligand 21 (CCL-21), respectively (Saito et al., 2004, Komine et al., 2013). The knockout of cellular communication network factor 1 (*Ccn1*) induces ostium primum atrial septal defects (Mo and Lau, 2006).

DEGs in response to Jz-ICR1 Δ in female fetuses had GO terms associated with response to insulin, glucocorticoids, oestradiol and progesterone (GO:0032869, GO:0051384, GO:0032355, GO:0032570). Other GO terms included lipid metabolic processes, cholesterol biosynthetic and steroid metabolic process (GO:0006629, GO:0006695, GO:0008202). *G6pc* and *Txnip* knockouts in adult mice are linked to reduced circulating glucose concentrations (Lei et al., 1996, Chutkow et al., 2008). Moreover, the knockouts

of *Ces1d* and *Abhd5* are protected against hepatic triacylglycerol accumulation and insulin resistance induced by a high fat diet (Brown et al., 2010, Lian et al., 2019). The knockouts of *Cyp3a44*, *Akr1b7*, regulator of G-protein signalling 16 (*Rgs16*) and *Slco1b2* are associated with enhanced bile acid synthesis, increased adiposity and elevated plasma ketone levels and conjugated hyperbilirubinemia (Lu et al., 2008, Pashkov et al., 2011, Volat et al., 2012, Hashimoto et al., 2013).

Table 5.2. Selected differentially expressed genes in response to Jz-ICR1Δ in both male and female fetal livers at E19

Gene	FC (males)	FC (females)	Gene function	GO terms	Adult mouse knockout phenotype	References
Neuropeptide Y (<i>Npy</i>)	-2.11	-2.013	Neuropeptide	G protein-coupled receptor binding (GO:0001664), G protein-coupled receptor activity (GO:0004930), Signalling receptor binding (GO:0005102), Hormone activity (GO:0005179), Neuropeptide hormone activity (GO:0005184)	Reduced food intake	(Bannon et al., 2000)
Betaine-homocysteine methyltransferase (<i>Bhmt</i>)	-1.56	-1.48	Cytosolic enzyme	Methyltransferase activity (GO:0008168), Zinc ion binding (GO:0008270), Transferase activity (GO:0016740), Metal ion binding (GO:0046872), Betaine-homocysteine S-methyltransferase activity (GO:0047150)	Altered choline and one-carbon metabolism, fatty liver, lower fat mass, smaller adipocytes, increased insulin and glucose sensitivity	(Teng et al., 2011, Teng et al., 2012)
Melanocortin 2 receptor accessory protein (<i>Mrap</i>)	-1.54	-1.48	Modulator of melanocortin receptors	Protein binding (GO:0005515), Corticotropin hormone receptor binding (GO:0031780), Type 3 melanocortin receptor binding (GO:0031781), Type 4 melanocortin receptor binding (GO:0031782), Type 5 melanocortin receptor binding (GO:0031783)	Increased weight gain, adiposity	(Asai et al., 2013)
Growth arrest and DNA-damage-inducible 45 beta (<i>Gadd45b</i>)	-1.54	-1.51	Regulation of growth and apoptosis	Protein binding (GO:0005515), Activation of MAPKK activity (GO:0000186), Apoptotic process (GO:0006915), Cell differentiation	Hematopoietic cells are more sensitive to apoptosis induced by genotoxic stress	(Gupta et al., 2005)

Carbonyl reductase 1 (<i>Cbr1</i>)	-1.44	-1.47	NADPH-dependent reductase	(GO:0030154), Positive regulation of the JNK cascade (GO:0046330) Carbonyl reductase (NADPH) activity (GO:0004090), Oxidoreductase activity (GO:0016491), Prostaglandin-E2 9-reductase activity (GO:0050221), Drug metabolic process (GO:0017144), Vitamin K metabolic process (GO:0042373)	Inhibition of liver fibrosis	(Olson et al., 2003)
--------------------------------------	-------	-------	---------------------------	--	------------------------------	----------------------

Only genes for which a knockout/antagonism phenotype was found are shown. GO terms associated with DEGs were determined using UniProt (<https://www.uniprot.org>). GO, gene ontology; JNK, c-Jun N-Terminal kinase; MAPKK, mitogen-activated protein kinase kinase; NADPH, nicotinamide adenine dinucleotide phosphate

Table 5.3. Selected differentially expressed genes in response to Jz-ICR1Δ in male fetal livers only at E19

Gene	FC	Gene function	GO terms	Adult mouse knockout phenotype	References
Zinc finger protein 36 (<i>Zfp36</i>)	-1.51	Destabilises cytoplasmic AU-rich element (ARE)-containing mRNA transcripts	mRNA binding (GO:0003729), C-C chemokine binding (GO:0019957), Cellular response to glucocorticoid stimulus (GO:0071385), Cellular response to granulocyte macrophage colony-stimulating factor stimulus (GO:0097011), Cellular response to lipopolysaccharide (GO:0071222)	Develop inflammatory arthritis	(Phillips et al., 2004)
Leukocyte cell-derived chemotaxin 2 (<i>Lect2</i>)	-1.51	Chemotactic factor to neutrophils	Protein binding (GO:0005515), Metal ion binding (GO:0046872), Chemotaxis (GO:0006935), Negative regulation of Wnt signalling pathway (GO:0030178)	Increased number of hepatic NKT cells	(Saito et al., 2004)
Cellular communication network factor 1 (<i>Ccn1</i>)	-1.48	Promotes cell proliferation, chemotaxis, angiogenesis and cell adhesion	Integrin binding (GO:0005178), Extracellular matrix structural constituent (GO:0005201), Insulin-like growth factor binding (GO:0005520), Heparin binding (GO:0008201), Chemotaxis (GO:0006935)	Ostium primum atrial septal defects	(Mo and Lau, 2006)
Macrophage receptor with collagenous structure (<i>Marco</i>)	1.45	Pattern recognition receptor	Amyloid-beta binding (GO:0001540), G protein-coupled receptor binding (GO:0001664), Scavenger receptor activity (GO:0005044), Innate immune response (GO:0045087)	Dendritic cells have enhanced migratory capacity in response to CCL-21	(Komine et al., 2013)

(Table preceding page) Only genes for which a knockout/antagonism phenotype was found are shown. GO terms associated with DEGs were determined using UniProt (<https://www.uniprot.org>). CCL-21, C-C Motif Chemokine Ligand 21, GO, gene ontology; NKT cells, natural killer T cells

Table 5.4: Selected differentially expressed genes in response to Jz-ICR1Δ in female fetal livers only at E19

Gene	FC	Gene function	GO terms	Adult mouse knockout phenotype	References
Regulator of G-protein signalling 16 (<i>Rgs16</i>)	-1.83	Regulation of G protein signalling	GTPase activity (GO:0003924), Protein binding (GO:0005515), Calmodulin binding (GO:0005516)	Higher rate of hepatic fatty acid oxidation, higher plasma β -ketone levels	(Pashkov et al., 2011)
Glucose-6-phosphatase, catalytic (<i>G6pc</i>)	-1.56	Hydrolysis of glucose-6-phosphate to glucose	Glucose-6-phosphatase activity (GO:0004346), Hydrolase activity (GO:0016787), Phosphate ion binding (GO:0042301), Cellular response to insulin stimulus (GO:0032869), Gluconeogenesis (GO:0006094), Glycogen metabolic process (GO:0005977)	Hypoglycaemia, growth retardation, hepatomegaly, hyperlipidaemia, hyperuricaemia and kidney enlargement	(Lei et al., 1996)
Solute carrier organic anion transporter family, member 1b2 (<i>Slco1b2</i>)	-1.51	Mediates the sodium-independent uptake of organic anions	Bile acid transmembrane transporter activity (GO:0015125), Organic anion transmembrane transporter activity (GO:0008514), Liver development (GO:0001889), Response to glucocorticoid (GO:0051384), Response to lipopolysaccharide (GO:0032496)	Moderate conjugated hyperbilirubinemia, decreased hepatic uptake/toxicity of microcystin-LR and phalloidin	(Lu et al., 2008)

Aldo-keto reductase family 1, member B7 (<i>Akr1b7</i>)	-1.49	Reducing aliphatic and aromatic aldehydes to corresponding alcohols	Alcohol dehydrogenase (NADP+) activity (GO:0008106), Oxidoreductase activity (GO:0016491), Cellular lipid metabolic process (GO:0044255)	Increased adiposity, adipocyte size, liver steatosis and insulin resistance	(Volat et al., 2012)
Cytochrome P450, family 3, subfamily a, polypeptide 44 (<i>Cyp3a44</i>)	-1.49	Monooxygenase, oxidoreductase	Heme binding (GO:0020037), Oxidoreductase activity (GO:0016491), Steroid metabolic process (GO:0008202), Steroid hydroxylase activity (GO:0008395)	Decreased capacity for xenobiotic detoxification, enhanced bile acid synthesis	(van Herwaarden et al., 2007, Hashimoto et al., 2013)
Thioredoxin interacting protein (<i>Txnip</i>)	-1.44	Inhibits thioredoxin activity	Ubiquitin protein ligase binding (GO:0031625), Enzyme inhibitor activity (GO:0004857), Response to oestradiol (GO:0032355), Response to glucose (GO:0009749), Response to oxidative stress (GO:0006979), Response to progesterone (GO:0032570)	Reduced β -cell death during ER stress. Decreased glucose and insulin. On a high fat diet, display increased fat mass and insulin sensitivity	(Chutkow et al., 2008, Chutkow et al., 2010, Lerner et al., 2012)
Carboxylesterase 1D (<i>Ces1d</i>)	-1.43	Lipase	Fatty-acyl-ethyl-ester synthase activity (GO:0030339), Sterol esterase activity (GO:0004771), Triglyceride lipase activity (GO:0004806), Cholesterol biosynthetic process (GO:0006695), Very-low-density lipoprotein particle assembly (GO:0034379)	Protected against hepatic triacylglycerol accumulation induced by high sugar high fat diet	(Lian et al., 2019)

SPEG complex locus (<i>Speg</i>)	1.49	Serine/threonine-protein kinase, transferase	ATP binding (GO:0005524), Protein serine/threonine kinase activity (GO:0004674), Cardiovascular system development (GO:0072358), Muscle cell differentiation (GO:0042692)	Dilated cardiomyopathy, embryonic/perinatal mortality	(Liu et al., 2009b)
Abhydrolase domain containing 5 (<i>Abhd5</i>)	1.49	Coenzyme A-dependent lysophosphatidic acid acyltransferase	Carboxylic ester hydrolase activity (GO:0052689), 1-acylglycerol-3-phosphate O-acyltransferase activity (GO:0003841), Lipid metabolic process (GO:0006629), Cell differentiation (GO:0030154)	Hepatic steatosis, but protection against insulin resistance induced by high fat diet	(Brown et al., 2010)

Only genes for which a knockout/antagonism phenotype was found are shown. GO terms associated with DEGs were determined using UniProt (<https://www.uniprot.org>). ATP, adenosine triphosphate; ER, endoplasmic reticulum; GO, gene ontology

5.3.5 The expression of fetal DEGs in adult Jz-ICR1Δ livers

The expression of the same subset of genes validated in fetal livers via qPCR was also determined in adult livers from 17-week-old male and female control and Jz-ICR1Δ offspring fed a chow diet (Figure 5.5). *Npy* was not expressed in the adult livers (data not shown). A tendency for *Rgs16* and *G6pc* expression to be decreased in female livers in response to Jz-ICR1Δ was observed ($p < 0.06$; Figure 5.5C, D). None of the other genes assessed had statistically significant differences in expression in response to Jz-ICR1Δ in either adult male or female liver.

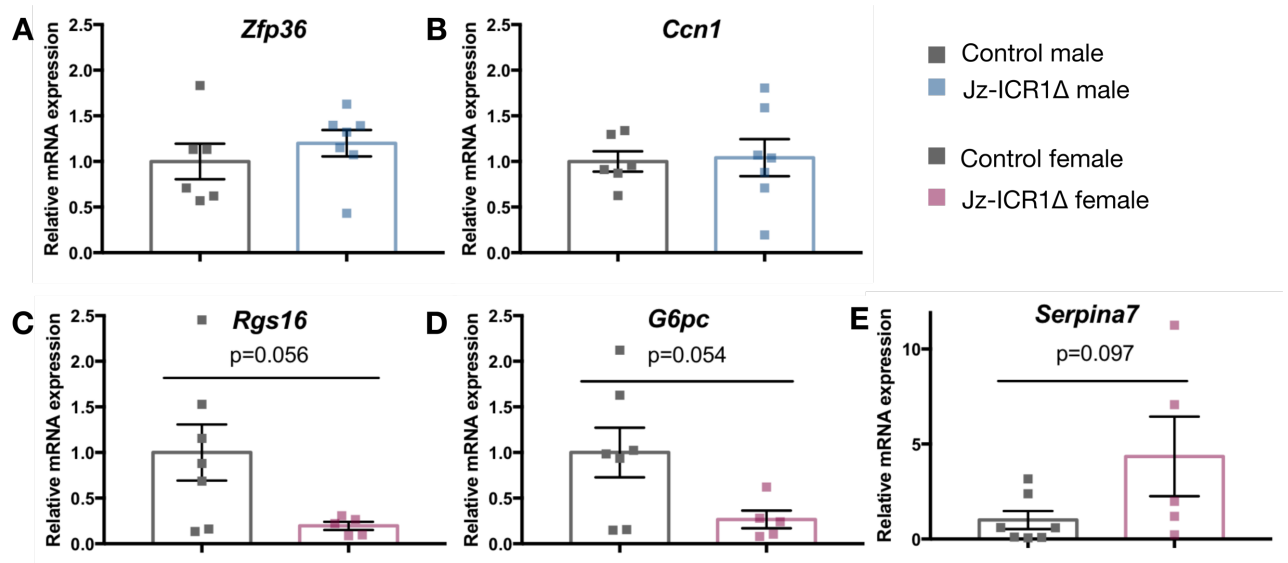
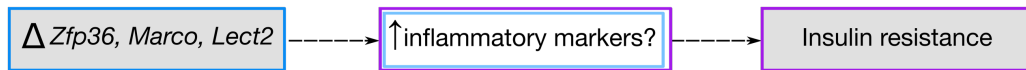


Figure 5.5. The effect of Jz-ICR1Δ on hepatic gene expression in 17-week-old male (A, B) and female (C, D, E) adult offspring fed a chow diet. Gene expression data are presented as individual points from a single sample with mean \pm SEM relative to the control male or control female group. Gene expression in samples are shown relative to *Hprt*. Data were analysed by Student's t-test. $n=5-7$ samples per genotype and sex (across 5-6 litters per genotype and sex).

5.4 Discussion

The environment *in utero* induced by Jz-ICR1 Δ causes alterations in fetal and organ weights, as fetal weight was reduced (Chapter 3, Table 3.1) and fetal brain weight increased (Figure 5.1). This brain sparing phenotype is frequently observed in models of maternal malnutrition (Hales and Barker, 1992), and in this model, may be due to reduced placental glucose and amino acid clearance and, therefore, decreased fetal nutrient provision in Jz-ICR1 Δ dams (Chapter 3, Figure 3.7). An increase in the relative weight of the brain was observed in Jz-ICR1 Δ fetuses, and this may be occurring at the expense of other organs, such as the liver. Indeed, alterations in fetal hepatic gene expression have been observed in response to maternal diabetes in rodents and interestingly, this occurs in a sex dependent manner (Fornes et al., 2018). In this study, changes in gene expression were observed both in response to genotype (Jz-ICR1 Δ) and in response to sex (Table 4.1). Interestingly, of the 12 DEGs observed in response to sex in control fetuses (Appendix 1.4.2, Table A1.4.2.2), only the expression of the housekeeping gene ribosomal protein L23A (*Rpl23a*) was also altered in response to Jz-ICR1 Δ (regardless of sex). In response to Jz-ICR1 Δ , sexual dimorphism in gene expression begins *in utero*, as evidenced by the majority of hepatic DEGs in response to Jz-ICR1 Δ being dependent on fetal sex, and only a small subset (25%) of DEGs seen in both sexes (Figure 5.2B). This is in accordance with the sexual disparity observed at the whole body metabolic and hepatic molecular changes in adult female and male offspring in response to Jz-ICR1 Δ (Chapter 4). It has been previously shown in mice that the female placenta is more adaptive in response to suboptimal maternal diet, showing more alterations in gene expression with a low protein or high fat maternal diet (Mao et al., 2010). Similarly, in this study, female fetal livers had more DEGs than males in response to Jz-ICR1 Δ , and these DEGs also displayed molecular and functional interactions between each other, which was not observed amongst DEGs in male Jz-ICR1 Δ fetal livers. Changes in fetal hepatic gene expression in response to Jz-ICR1 Δ and associations between these DEGs may relate to sexually dimorphic metabolic outcomes in adult offspring, as hypothesised in Figure 5.4.1.

A ♂



B ♀

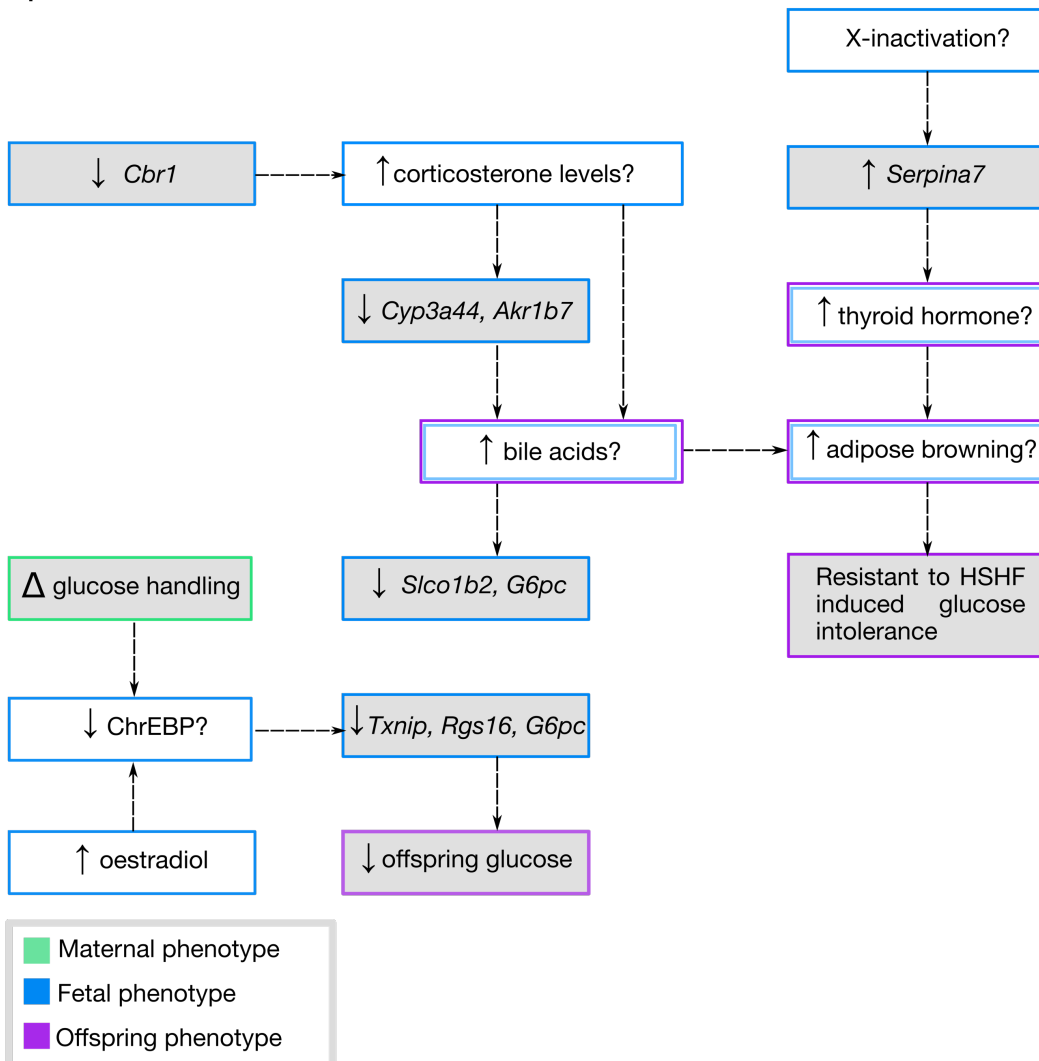


Figure 5.4.1 Summary diagram showing hypothesised mechanism of Jz-ICR1A programming in male (A) and female (B) offspring. Grey boxes represent experimental findings; white boxes represent hypotheses from findings. Data for the maternal phenotype were collected by Dr Jorge Lopez-Tello and Dr Amanda Sferruzzi-Perri. Δ, change in; *Akr1b7*, aldo-keto reductase family 1, member 7; *Cbr1*, carbonyl reductase 1; ChrEBP, carbohydrate response element binding protein; *Cyp3a44*, cytochrome P450, family 3, subfamily a, polypeptide 44; *G6pc*, glucose-6-phosphatase, catalytic; HSHF, high sugar high fat; *Lect2*, leukocyte cell-derived chemotaxin 2; *Marco*, macrophage receptor with collagenous structure; *Serpina7*, serine (or cysteine) peptidase inhibitor, clade A (alpha-1 antiproteinase); *Slco1b2*, solute carrier organic anion transporter family, member 1b2; *Txnip*, thioredoxin interacting protein; *Zfp36*, zinc finger protein 36

5.4.1 Sex differences in DEGs in response to Jz-ICR1Δ

It has been hypothesised that proteomic changes prior to X inactivation in females may persist and in part contribute to sexually dimorphic programming (Aiken and Ozanne, 2013). Indeed, of the DEGs upregulated by Jz-ICR1Δ in female livers, serine (or cysteine) peptidase inhibitor, clade A (alpha-1 antiproteinase, antitrypsin) member 7 (*Serpina7*) is an X-linked gene. The *Serpina7* gene product is a thyroid hormone binding globulin. Previously it has been shown that fetal hypothyroidism in sheep promotes growth of fetal white adipose tissue and decreases *Ucp1* expression (Harris et al., 2020). Therefore, in the future, levels of circulating thyroid hormones (free and binding globulin bound using high performance liquid chromatography or ELISAs), as well as thyroid hormone signalling proteins and markers of adipocyte browning like *Ucp1* (by Western blotting and qPCR) may be determined in Jz-ICR1Δ fetal and adult offspring. Indeed, discrepancies in thyroid hormone abundance and signalling, as well as adipose phenotype between male and female in Jz-ICR1Δ offspring may also contribute to sexually dimorphic metabolic outcomes seen postnatally. Furthermore, sexual dimorphism in corticosteroid exposure *in utero* has also been hypothesised to be a source of sexual disparity in metabolic programming (Seckl and Holmes, 2007). Reduced hepatic *Cyp3a44* and *Akr1b7* expression in female (and not male) fetuses in response to Jz-ICR1Δ may be a contributing factor to sexual dimorphism, as interestingly, during adulthood these genes are highly expressed by the liver in females but not males (Sakuma et al., 2002, Kotokorpi et al., 2004), with their expression influenced by glucocorticoid-dependent mechanisms (Kotokorpi et al., 2004, Bhadhprasit et al., 2007). In mice, it has been shown previously that in adverse environments *in utero*, glucocorticoid exposure differs depending on fetal sex (Chin et al., 2017, Wiczorek et al., 2019) and influences the expression of genes involved in several processes during gestation (Fowden and Forhead, 2004). Indeed, an increase in *Hsd11b1* expression in response to Jz-ICR1Δ was observed in female but not male placentas, which may be indicative of sex-specific changes in fetal corticosterone exposure (Chapter 3, Figure 3.9). Therefore, in future experiments, it would be of interest to investigate whether the reduced *Cyp3a44* and *Akr1b7* expression in female livers is influenced by sex differences in corticosteroid exposure in response to Jz-ICR1Δ during gestation. This may be achieved by treating dams with a placental 11βHSD inhibitor, namely carbenoxolone (Saegusa et al., 1999), to determine whether changes in placental *Hsd11b1* expression are indirectly influencing

gene expression of genes in the fetal liver via sex-specific levels of fetal corticosterone. However, it is important to note that carbenoxolone will likely also induce systemic effects in Jz-ICR1 Δ dams. Interestingly, 11 β HSD1 is also involved in bile acid metabolism (Penno et al., 2014), albeit the significance of this in the placenta remains unknown.

Cyp3a44 is involved in bile acid metabolism, whereby *Cyp3a* knockout mice show enhanced hepatic bile acid synthesis (Hashimoto et al., 2013). Moreover, *Akr1b7* is induced by Farnesoid X receptor (FXR) and metabolises bile acids (Schmidt et al., 2011). Thus, in the future, bile acid concentrations should be measured in fetal plasma via ELISA to determine potential sexual disparities in concentration. During intrauterine development, haematopoietic cells in the fetal liver are directly exposed to bile acids (Strazzabosco and Fabris, 2012), and bile acids have been shown to protect fetal liver hematopoietic stem cells from unfolded protein stress in mice (Sigurdsson et al., 2016). Interestingly, *Txnip* transcription is elevated during endoplasmic reticulum (ER) stress, leading to the unfolded protein response (Anthony and Wek, 2012), however *Txnip* expression was downregulated only in female fetal livers in response to Jz-ICR1 Δ . Thus, in future it would be of interest to measure oxidative stress levels and the unfolded protein response in male and female fetal and adult livers by performing an OxyBlot of proteins (to determine oxidation status) and determining the levels of unfolded protein response activator proteins (Inositol-requiring enzyme 1, Protein kinase R-like endoplasmic reticulum kinase and Activating transcription factor 6) respectively. Moreover, in adult mice fed a high fat diet, bile acid administration prevents insulin resistance and increases energy expenditure in brown adipose tissue, an effect mediated by thyroid hormone activation (Watanabe et al., 2006). These findings are interesting given the increased expression of the thyroid hormone globulin *Serpina7* in female Jz-ICR1 Δ livers compared to controls. *Slco1b2* and *G6pc* expression in the liver was reduced specifically in female fetuses exposed to Jz-ICR1 Δ . These genes are also decreased in the liver in lean mouse lines that represent a polygenic form of obesity resistance (Simončič et al., 2011). *Slco1b2* belongs to a family of SLCO transporters involved in bile acid uptake, and high levels of bile acids are known to downregulate *Slco* and *G6pc* expression in the liver (Fickert et al., 2001, Yamagata et al., 2004). Interestingly, *Slco1b2*, also responds to glucocorticoid stimuli (GO:0051384), with corticosterone treatment increasing circulating bile acid concentrations (Sigurdsson et al.,

2020). *G6pc*, *Rgs16* and *Txnip* are transcriptional targets of carbohydrate-responsive element-binding protein (ChreBP; Yamashita et al., 2001, Minn et al., 2005, Ma et al., 2006, Pedersen et al., 2007, Pashkov et al., 2011) and these genes were also reduced in female fetal livers in response to Jz-ICR1 Δ . *Txnip* knockout protects against obesity related insulin resistance (Chutkow et al., 2010) and interestingly, oestradiol is known to reduce *Txnip* and ChreBP expression (Tiano and Mauvais-Jarvis, 2012, Lan et al., 2017). This is of interest as female mouse fetuses inherently display higher plasma oestradiol concentrations than males (vom Saal, 1989). Thus, it may be postulated that the female fetus is better able to adapt to maternal hyperglycaemia in response to Jz-ICR1 Δ , and this may in part be mediated by inherently higher oestradiol levels in females. Note that placental glucose transport was decreased at E16 and E19, however it is unknown whether maternal hyperglycaemia precedes this with effects on the fetal hepatic transcriptome.

Inflammatory pathways are critical in the pathophysiology of diabetes and insulin resistance, with both hepatic insulin resistance and non-alcoholic fatty liver disease associated with an increase in inflammatory mediators, namely IL-6 and TNF α (Cai et al., 2005). Therefore, it is perhaps not surprising to observe changes in genes involved in inflammatory processes, namely *Zfp36*, *Lect2* and *Marco* in liver of Jz-ICR1 Δ male fetuses (as postnatally these offspring show compromised insulin sensitivity and whole-body metabolism). Indeed, knockdown of *Zfp36* leads to the development of inflammatory arthritis in mice (Phillips et al., 2004), whilst *Lect2* knockdown increases the number of hepatic NKT cells (Saito et al., 2004). Moreover, enhanced expression of *Marco*, which was upregulated in Jz-ICR1 Δ male fetal livers, is observed in the liver of mice fed a high fat diet (Yoshimatsu et al., 2004). Interestingly, *Gadd45b*, which is involved in the activation of the MAPK/JNK cascade (Takekawa and Saito, 1998), was conversely downregulated in both female and male fetal livers by Jz-ICR1 Δ . When the effect of Jz-ICR1 Δ was considered irrespective of sex, the most enriched pathways included TNF α signalling via NF-kB (adjusted p value < 0.0007) and hypoxia (adjusted p value < 0.0004; Appendix 1.4.1), indicating that these pathways may be involved in the aetiology of metabolic disease in Jz-ICR1 Δ offspring. This may in part be related to the reduction in placental theoretical diffusing capacity in response to Jz-ICR1 Δ , irrespective of fetal sex (Chapter 3, Table 3.2), which would reduce oxygen delivery to fetuses. Moreover, increased hepatic TNF α and phosphorylated JNK have been observed in

fetuses exposed to maternal protein restriction (Liu et al., 2014). Overall, when considering the data split by sex, alterations in DEGs involved in inflammatory processes seen in the Jz-ICR1 Δ male fetal livers may contribute to a pro-inflammatory hepatic environment *in utero* and thereafter, to the deterioration of metabolic health seen in adulthood. However, the concentration of inflammatory markers and mediators (for instance TNF α , CD36 and IL-6) would have to be determined in fetal and adult offspring plasma via ELISA to validate these findings.

5.4.2 Common DEGs in males and females in response to Jz-ICR1 Δ

In addition to DEGs expressed exclusively in male and females in response to Jz-ICR1 Δ , a subset of genes were shared by both sexes, including *Npy*. Previous studies in rodents have indicated that *Npy* knockout and NPY-antagonism reduces food intake and prevents white adipose growth, inducing lipolysis (Bannon et al., 2000, Margareto et al., 2000, Margareto et al., 2002). However, as *Npy* is expressed in the liver during fetal but not adult life, *Npy* likely plays a critical role in liver development (Ding et al., 1997) and thus, reduced *Npy* expression in the fetal liver in response to Jz-ICR1 Δ may be indicative of abnormal hepatic development. Reduced hepatic *Ccn1* expression in the male Jz-ICR1 Δ fetus may also be indicative of aberrant liver morphology, as *Ccn1* is required for biliary repair and resolves liver fibrosis by bile duct ligation or carbon tetrachloride intoxication in mice (Kim et al., 2013, Kim et al., 2015). *Bhmt*, which was downregulated in both the liver of male and female Jz-ICR1 Δ fetuses, is involved in one-carbon metabolism (Awad et al., 1983). Moreover, *Bhmt* knockout mice display reduced fat mass (Teng et al., 2012), as was observed in male and female Jz-ICR1 Δ adult offspring. These data suggest that programmed alterations in one-carbon metabolism may contribute to certain phenotypes in Jz-ICR1 Δ adult offspring. Whilst studies indicate that restricting folate and methionine in the maternal diet leads to increased insulin resistance in offspring (Sinclair et al., 2007), the mechanism associating insulin resistance and liver disease with one-carbon metabolism has not yet been described. Furthermore, alterations in lipid metabolic processes may be involved in the female Jz-ICR1 Δ phenotype, as the knockout of *Abhd5*, which was conversely upregulated in female livers, leads to hepatic steatosis (Brown et al., 2010). Moreover, knockout of *Ces1d* in mice, which was downregulated in female Jz-ICR1 Δ livers, is protective against high-sucrose diet induced triacylglycerol accumulation in the liver (Lian et al., 2019).

5.4.3 Association of fetal DEGs in response to Jz-ICR1Δ with adult offspring phenotypes

The function of the identified DEGs in the fetal liver may differ to that of the adult, especially as knockout studies are characterised in adult life and little is known regarding the fetal phenotype of the knockout. However, of the DEGs identified in male and female fetal livers in response to Jz-ICR1Δ, a proportion have been reported to display altered expression in the liver of fetuses from maternal or fetal genetic manipulation. Global *Igf2* knockout, which is characterised by reduced amino acid transport to the fetus (Constancia et al., 2005), impacts the expression of *Ppara* in the newborn liver, alongside other genes related to lipid metabolism (Lopez et al., 2018). Interestingly, in response to the knockout of *Ppara* in the fetal liver, *Serpina7* expression is increased (Rando et al., 2016), with increased *Serpina7* expression also observed in the female Jz-ICR1Δ liver. Moreover, *Cyp3a44* expression is increased when comparing *Ppara* *-/-* fetal livers from *Ppara* *-/-* fasted dams to *Ppara* *+/-* fetuses from *Ppara* *+/-* dams (Bowman et al., 2019), whilst conversely, *Cyp3a44* expression is reduced in the liver of female fetuses in response to a suboptimal gestational environment due to Jz-ICR1Δ. Interestingly, dysregulations in PPARα protein abundance were observed in adult offspring livers in a manner determined by sex (Chapter 4). Therefore, the contribution of the *Ppara* axis during prenatal and postnatal life in governing programmed alterations in the offspring may be further explored in the Jz-ICR1Δ model in future.

Overall, the DEGs identified by RNA sequencing in fetal livers may contribute to adult metabolic phenotypes developed in response to the altered maternal environment due to Jz-ICR1Δ. A limitation when drawing comparisons between changes in gene expression in the fetal and adult stages is that the hepatic transcriptome changes ontogenically in the mouse. For instance, as previously mentioned, *Npy* is expressed in the liver at the fetal stage, but not in adulthood (Ding et al., 1997), which was corroborated in this study. During development, the mouse liver changes from a major haematopoietic organ towards a metabolic one, to support gluconeogenesis in adulthood and moreover, liver development continues postnatally (Crawford et al., 2010). Furthermore, the fetus does not produce glucose in well fed mothers, and gluconeogenic enzymes (i.e. G6Pase, PEPCK) dramatically increase in expression and activity on postnatal day 1 (Lin et al., 2003). Despite these differences between the fetal and adult liver, there was evidence that changes in fetal gene expression in response to Jz-ICR1Δ are maintained in adulthood,

with a tendency for *G6pc* and *Rgs16* expression to be reduced ($p < 0.06$) in liver of adult Jz-ICR1 Δ females. A concomitant reduction in G6Pase protein abundance was also observed in the liver of adult females consuming a chow diet in response to Jz-ICR1 Δ (Chapter 4, Figure 4.9), indicating that these changes are maintained at the protein level also. Interestingly, in accordance with this, during adulthood, female Jz-ICR1 Δ offspring consuming a chow diet also displayed *ad libitum* fed hypoglycaemia (Chapter 4, Table 4.2). In future, the expression of all the remaining DEGs identified in Jz-ICR1 Δ fetal livers should be determined in adult livers, as a means to delineate the extent by which male and female adult offspring maintain hepatic gene expression in response to Jz-ICR1 Δ . Although Jz-ICR1 Δ induced changes in fetal hepatic gene expression, it remains unknown what mechanisms are responsible. Previous studies in maternal models of suboptimal gestational environments have indicated the importance of epigenetic factors, namely DNA methylation, histone modifications and non-coding RNAs in mitigating changes in metabolic gene expression (reviewed in Christoforou and Sferruzzi-Perri, 2020). Thus, the epigenetic modifications that may underlie the observed changes in fetal hepatic gene expression in response to Jz-ICR1 Δ may be explored in the future.

Chapter 6: General discussion

Understanding the mechanisms of gestational programming is critical in mitigating metabolic disease. The placenta, through its endocrine and nutrient transport functions, is key in maintaining optimum fetal outcomes. However, little is known about the role of the endocrine placenta in fetal nutrient acquisition, fetal growth and development, and subsequent offspring metabolic outcomes. This study determined the effect of direct manipulation of the endocrine zone of the mouse placenta (by Jz-ICR1 Δ mutation) on the consequences for placental transport capacity and resultant offspring metabolic programming. In our model of placental endocrine zone malfunction, the imprinted growth factor gene *Igf2* was increased with a concomitant increase in endocrine zone (Jz) volume at E16 of pregnancy. Jz-ICR1 Δ reduced placental glucose and amino acid transport in addition to compromising the morphology of the transport zone (Lz), with the resultant phenotype likely to reduce fetal nutrient and oxygen acquisition. Secondly, Jz-ICR1 Δ led to the programming of offspring metabolic health, however the manner by which this occurred was dependent on offspring sex, with male offspring largely showing deteriorations in metabolic health which were not evident in female offspring. Moreover, offspring metabolic health in response to Jz-ICR1 Δ was also dependent on the presence of a postnatal challenge (i.e., HSHF diet consumption), which exacerbated detrimental metabolic outcomes in male, but in part improved metabolic health in female animals. Although the mechanisms underlying this sexual disparity are likely multifaceted, alterations in fetal hepatic gene expression in response to Jz-ICR1 Δ also occurred in a sex dependent manner, which indicates that the intrauterine environment at least partly contributes to the programming of sexually dimorphic adult metabolic outcomes. Further to this, an increased number of DEGs observed in response to Jz-ICR1 Δ in the female compared to male fetal liver may be indicative of an aptitude of females to better adapt to adverse environments *in utero*, which may contribute to their healthier metabolic state in adulthood.

In response to Jz-ICR1 Δ , the programming of offspring metabolism and metabolic tissues was observed. Although a placenta-specific manipulation was utilised, this induced several changes in maternal metabolic and endocrine state, as well as altered placental nutrient transport capacity, although the order of the phenotypic outcomes observed is not known. As shown in Figure 6.1, programming of Jz-ICR1 Δ offspring may be attributed

to: (1) alterations in the endocrine capacity of the placenta due to expansion of Jz volume and altered hormone output, (2) perturbations in maternal metabolism (i.e., glucose, insulin, corticosterone and lipid levels, as summarised in Table 1.13.1) and (3) changes in placental nutrient transport capacity and Lz morphology. Therefore, it is likely that the offspring programming observed in this model may be attributed at least in part, to all three outcomes, which also likely interact with each other.

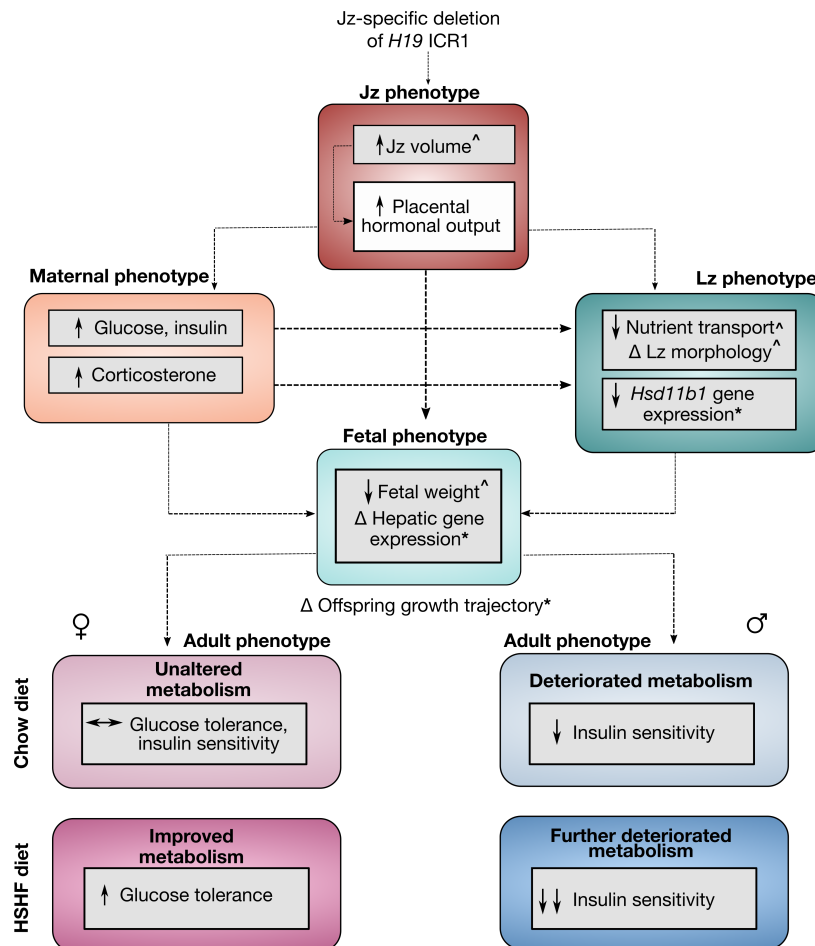


Figure 6.1. Diagram to summarise the effects of Jz-ICR1Δ on the dam, placenta, fetus and adult offspring. Grey boxes represent experimental findings; a white box represents extrapolations from findings. An asterisk (*) represents a phenotype dependent on sex which may contribute to sexual disparity in adult offspring metabolism; an arrow (^) represents a phenotype present regardless of sex. Data for the maternal phenotype were collected by Dr Jorge Lopez-Tello and Dr Amanda Sferruzzi-Perri. Δ, change in; *Hsd11b1*, 11β-Hydroxysteroid dehydrogenase type 1; HSHF, high sugar high fat.

6.1 The maternal environment in offspring programming

Jz-ICR1Δ may lead to changes in placental endocrine output in association with Jz expansion, and subsequently influence offspring programming. Although the precise alterations in endocrine output in response to Jz-ICR1Δ remain unknown, maternal levels

of circulating progesterone, oestrogen, corticosterone and leptin are increased in response to Jz-ICR1 Δ . The ability of these hormones to impact offspring metabolic programming has been shown by maternal administration of these hormones in rodent models. For instance, exposure to a xenoestrogen (bisphenol A) causes perturbations in glucose homeostasis in male, but not female offspring (Susiarjo et al., 2015, Galyon et al., 2017). As in the current Jz-ICR1 Δ model, a similar deterioration of metabolic health is observed in male offspring only, this is indicative that increased oestrogen levels *in utero* may in part negatively impact male but not female metabolic programming. Although maternal progesterone antagonism is known to induce preterm birth in rodents (Dudley et al., 1996), less is known about the effect of progesterone overexposure on offspring metabolic outcomes. Maternal leptin administration alters offspring growth and development, reducing body and adipose tissue weights in adult offspring (Nilsson et al., 2003, Pollock et al., 2015), as generally occurs in response to Jz-ICR1 Δ and thus maternal hyperleptinemia may be a causative factor. Maternal corticosterone treatment reduces fetal weight in mice (Vaughan et al., 2012), suggesting that increased maternal corticosterone concentrations in Jz-ICR1 Δ dams may partly contribute to the fetal growth restriction observed at E19, with potential consequences for metabolic health in adulthood.

6.2 The gestational period in offspring programming

The Jz-ICR1 Δ model provides an excellent example of how the placenta is able to morphologically and functionally adapt in response to a suboptimal maternal environment. Jz expansion may lead to changes in the types and/or amounts of hormones produced, with consequent maternal hyperglycaemia being observed in response to Jz-ICR1 Δ . Moreover, it is possible that changes in maternal glucose handling regulate the Jz-ICR1 Δ placenta hormonal milieu, as it has been shown that in response to HSHF feeding in mouse dams, changes in placental prolactin expression occur (Musial et al., 2017). Overall, in response to Jz expansion and maternal hyperglycaemia, placental glucose and amino acid clearance was reduced and Lz morphology altered to limit nutrient and oxygen provision to the fetus and prevent overgrowth. Thus, it may be postulated that the IUGR observed at E19 may be partly due to changes in placental morphology and transport function. Moreover, on E19 of pregnancy, fetal brain weight was increased in response to Jz-ICR1 Δ , which may indicate brain sparing and subsequent

detrimental alterations in metabolic organ development, a phenotype frequently observed in response to maternal malnutrition (Hales and Barker, 1992). Indeed, at P3, female Jz-ICR1Δ offspring had a tendency for reduced pancreas weight, which may be associated with aberrant pancreatic development due to reduced fetal nutrient acquisition, as previously shown in rodent models of maternal malnutrition (Dahri et al., 1991, Valtat et al., 2011). At P3 growth restriction is no longer evident and this may be due to the absence of the placenta post-gestationally, which *in utero* was acting to limit fetal growth. In response to Jz-ICR1Δ, a reduction in offspring weight (during lactation), reduced adiposity and adipocyte diameter were observed in a sex and postnatal diet-dependent manner. Interestingly, the aforementioned phenotypes have also been shown in some instances in rodent models of maternal undernutrition or low protein diet (Desai et al., 2005b, Ferland-McCollough et al., 2012). Conversely, growth, adiposity and adipocyte diameter are increased in offspring exposed to hyperglycaemia *in utero* in rodent models of maternal obesity and diabetes (Yang et al., 2013, Latouche et al., 2014, Desai et al., 2015, Oliveira et al., 2015, Seet et al., 2015, Fante et al., 2016). However, whilst models of maternal obesity show increased placental glucose and amino acid transport (Jones et al., 2009, Lin et al., 2011, Aye et al., 2015, Rosario et al., 2015), these parameters were reduced in response to Jz-ICR1Δ. Thus, reduced nutrient transport may programme growth and adiposity phenotypes in the offspring, despite maternal hyperglycaemia in response to Jz-ICR1Δ. However, it is difficult to delineate which offspring phenotypes occur due to changes in the maternal endocrine and metabolite milieu and which are caused by reductions in placental nutrient transport, or a combination of both. Interestingly, changes in LZ morphology did not occur in a sexually dimorphic manner and are unlikely to directly influence sexual disparities in offspring metabolic outcomes. Although reductions in placental glucose and amino acid transport were not sex-specific, the magnitude of reduction in glucose clearance was larger in females (27%) compared to males (21%) at E16 of pregnancy, so that it cannot be discounted that these discrepancies also influence adult offspring metabolic programming in a sex-specific manner.

Indeed, metabolic programming in Jz-ICR1Δ offspring was largely sexually dimorphic, and several factors *in utero* are likely to be responsible for this, as evidenced by sex-dependent changes in fetal hepatic gene expression. High maternal corticosterone levels in Jz-ICR1Δ dams may cause changes in the fetal liver transcriptome, as several genes whose expression are either controlled by corticosterone or are involved in its metabolism

were downregulated in female and male fetal livers in response to Jz-ICR1 Δ , namely *Cyp3a44*, *Akr1b7*, *Slco1b2*, *Cbr1* and *Zfp36*. This is of significance as corticosterone is a widely recognised candidate for mediating offspring programming (Seckl and Holmes, 2007). *Cyp3a44* and *Akr1b7* display sexually dimorphic expression in wild type adult mice due to glucocorticoid-dependent mechanisms (Kotokorpi et al., 2004, Sakuma et al., 2008). The bile acid transporter *Slco1b2*, also responds to glucocorticoid stimuli (GO:0051384), and moreover, *Cbr1* is involved in the metabolism of corticosterone (Morgan et al., 2017). Concordantly, placental *Hsd11b1* expression, which is involved in catalysing the regeneration of glucocorticoids (Thompson et al., 2002), is significantly increased by Jz-ICR1 Δ in female placentas only and thus may increase female corticosterone levels with subsequent alterations in fetal hepatic gene expression. Furthermore, in the male Jz-ICR1 Δ fetal liver, the expression of *Zfp36* is downregulated, and it has been previously shown that glucocorticoids upregulate *Zfp36* expression (Smoak and Cidlowski, 2006). Nonetheless, it would be necessary to measure fetal corticosterone concentrations to validate whether sex-specific changes in fetal hepatic gene expression in response to Jz-ICR1 Δ may be influenced by corticosterone. It may be further hypothesised that higher corticosterone levels would mature fetal organs more quickly, potentially offering a postnatal advantage to female offspring. Moreover, other placental genes that relate to fetal liver DEGs may be examined in the future. *Cyp3a44* knockout decreases xenobiotic detoxification capacity, whilst *Akr1b7* is a transcriptional target of xenobiotic receptors (van Herwaarden et al., 2007, Liu et al., 2009a), and both these genes are downregulated in female fetal livers by Jz-ICR1 Δ . Thus, the expression of placental ATP-binding cassette (ABC) transporters, which are involved in waste metabolite exchange, mediating drug and xenobiotic exposure and modulating glucocorticoid efflux toward the maternal circulation (Joshi et al., 2016), may be determined to further delineate placental sex differences influencing fetal programming. Indeed, sex-specific changes in *Abcg2* gene expression has been observed previously in response to maternal undernutrition in mice (Connor et al., 2020). An interaction between sex and genotype influenced Lz *Fatp4* expression; however, as all other parameters measured in the placenta to date showed no sex differences, this may indicate that the placenta only partly accounts for sexual dimorphism *in utero*.

Alterations in fetal hepatic gene expression in response to Jz-ICR1 Δ may be induced to mitigate an adverse gestational environment. For instance, reduced *G6pc* expression in

the female fetal liver may be a compensatory mechanism in the female fetus in response to a hyperglycaemic maternal environment on E19 of pregnancy (Table 1.13.1). Interestingly, placental glucose transport was reduced at E16 and E19, however it remains unknown whether Jz-ICR1Δ dams are hyperglycaemic earlier in gestation, at a time when placental glucose transport is perhaps unaltered. In adult female livers, a tendency for reduced hepatic *Rgs16* and *G6pc* was observed, with these genes also decreased in the liver of female fetuses in response to Jz-ICR1Δ. Moreover, in adult female Jz-ICR1Δ mice, hepatic G6Pase protein abundance was diminished alongside *ad libitum* fed hypoglycaemia. These data provide preliminary evidence that indeed, aspects of fetal phenotypes in response to adverse gestational environments are maintained into adulthood. As none of these phenotypes, namely hypoglycaemia and reductions in *Rgs16* and *G6pc* expression, in the fetus or adult were observed in male Jz-ICR1Δ offspring, it may be postulated that females more readily adapt to a hyperglycaemic maternal environment with consequences for adult metabolism. Although changes in gene expression were observed in the fetal liver, the limited number of DEGs identified may be indicative of post-gestational factors also influencing offspring metabolic outcomes. Moreover, the involvement of post-translational changes in Jz-ICR1Δ programming cannot yet be discounted.

6.3 The post-gestational period in offspring programming

Jz-ICR1Δ offspring were growth restricted during the lactational period, with offspring growth frequently used as a proxy to determine susceptibility to perturbations in metabolic health. Although growth restriction during lactation was not sex-specific, the growth trajectory after week four was dependent on sex and postnatal diet, with all groups apart from male chow offspring displaying catch-up growth. It has been suggested that catchup growth after IUGR is detrimental to offspring outcomes (Hales and Ozanne, 2003) and this may be due to increased accumulation of adipose tissue compared to lean muscle mass during this period of rapid growth (Law et al., 1992). Indeed, in response to Jz-ICR1Δ, whilst HSHF males and chow and HSHF females displayed catchup growth, only HSHF males had unaltered adiposity whilst females had reduced adiposity. Jz-ICR1Δ dams are also glucose intolerant 12 weeks postpartum (data not shown), and this may also contribute to postnatal offspring phenotypes during weaning. Moreover, sex steroids likely influence sex-specific metabolic outcomes and indeed, androgens and

oestrogens modify the synthesis of somatostatin and growth hormone releasing hormone respectively during the post-pubertal period (Chowen et al., 2004). As offspring biometry, pancreatic insulin content and morphology, and the abundance of proteins involved in insulin handling, lipid metabolism and gluconeogenesis were also widely dependent on offspring sex and the postnatal diet consumed, they are likely contributing factors to sexually dimorphic metabolic outcomes in the adult offspring, however the mechanisms instigating these sex-specific changes remain largely unknown.

6.4 Limitations and future directions

Several limitations arise from the use of a *CreLoxP* mouse model, including potential toxicity of *Cre* recombinase and variability in the recombination efficiency (Schmidt-Supprian and Rajewsky, 2007). Any toxic effect of the *Cre* gene is controlled for by using the reverse parental cross as a control (hence all conceptuses have the same genotype, *Tpbpa/H19-Flox* but vary in which parent provides the allele). However, the use of the reverse parental cross control presents a limitation in itself, as it is impossible to know whether the H19-Flox line, although it has been on a C57Bl6 background for >10 generations (like the *Tpbpa-Cre* line), may impact maternal, placental or offspring phenotypes without comparisons to wild type mice, which may be an avenue to explore in the future. The use of the mouse as a model is advantageous as it is possible to specifically manipulate the endocrine Jz, which, unlike in the human placenta, is physically and functionally distinct from the transport Lz. However, mice and humans differ in their pregnancies and overall metabolism. Placental hormones secreted by mice and humans differ as discussed in Chapter 1, section 1.3, and moreover unlike humans the mouse is a litter bearing species. Indeed, in a mouse litter the position of pups in the uterus during gestation, for instance if they are positioned next to pups of a similar or different sex, influences the levels of oestrogen and testosterone they are exposed to (vom Saal et al., 1983, vom Saal, 1989), which may affect placental phenotypes during pregnancy and post-gestational offspring metabolic outcomes. However, the position of fetuses during gestation were not considered in pregnancy experiments and it was not known where adult offspring were positioned when in the uterus. Placentas closest to the mean placental weight of each litter was chosen for morphological and gene expression analyses, as placental weight is known to impact Lz morphology and nutrient transporter gene expression (Coan et al., 2008a). However, despite this, significant variation in gene

expression was observed between placentas of the same genotypic group, which may in part be attributed to differences in placental steroid hormone exposure. Importantly, such differences in placental gene expression may also contribute to variations in the propensity of adult offspring to develop adverse metabolic outcomes. Species differences in metabolism are evident between humans and mice, with the deletion of *InsR* in mice leading to early neonatal death, but in humans, the mutation and absence of *InsR* causes insulin resistance (Taylor, 1992, Accili et al., 1996). The mechanisms of sexually dimorphic metabolic programming are also likely to differ in mice and humans, as corticosterone levels are different between female and male mouse fetuses but are similar between sexes in human blood cord samples (Montano et al., 1993, Clifton et al., 2007). These species differences are a major limitation in extrapolating our data from mouse models to a clinical setting. Nonetheless, the mouse offers an excellent preliminary tool for studying the effect of placental endocrine malfunction on offspring metabolic programming in a manner that allows causality of variables to be determined and offers tissue accessibility during pregnancy and follow up of offspring with tissues collected in a timely fashion in a way that is not possible in the clinic.

During an insulin tolerance test, used in this study to determine insulin sensitivity, potential hypoglycaemia upon insulin injection and subsequent counter-regulatory homeostatic mechanisms may alter insulin sensitivity estimations (Muniyappa et al., 2008). Thus, hyperinsulinaemic euglycemic clamps are considered the gold-standard when evaluating insulin sensitivity in rodents and may be employed in *Jz-ICR1Δ* offspring in the future (Musial et al., 2016). Insulin sensitivity *in vitro* was determined by measuring the protein abundance of mediators of the PI3K signalling pathway. The PI3K signalling pathway activates mediators involved in inflammation (JNK, p38), proliferation (MAPK) and apoptosis (BCL-2, BAX; Sawatzky et al., 2006, Ola et al., 2011, Zhou et al., 2015b), which may contribute to changes in offspring insulin sensitivity but have not been investigated to date. In the liver, protein levels were determined in powdered homogenates, as it is known that gene expression varies depending on the lobe sampled (Irwin et al., 2005). In future, studying specific cell types (i.e., hepatocytes, β -cell cultures, or skeletal muscle fibre types) may provide further information on insulin production and handling. Moreover, candidate hormones identified as being altered in the *Jz* in response to *Jz-ICR1Δ*, via unbiased approaches such as RNA sequencing and secretome analysis, may be used to treat hepatocytes, β -cells or

adipocytes in culture or injected into dams to potentially recapitulate results in offspring molecular and metabolic outcomes, respectively. In this way, placental endocrine biomarkers involved in offspring metabolic programming may be identified in mice, and further validated in human placental samples and correlated to health outcomes in children.

Whilst metabolic organs (i.e., the pancreas, adipose, skeletal muscle and liver) were studied in Jz-ICR1 Δ offspring to date, metabolic syndrome is intricately linked to cardiovascular disease. Indeed, the programming of offspring cardiovascular outcomes in response to suboptimal gestational environments has been shown in a range of models (Vickers et al., 2000, Wlodek et al., 2008), and in response to Jz-ICR1 Δ , changes in heart weight were observed in a sex dependent manner. Thus, electromyography and Langendorff heart preparations may be performed on offspring to determine vascular and cardiac function. Moreover, the structure and function of Jz-ICR1 Δ offspring oocytes and sperm may be studied, as it has been shown previously that a suboptimal gestational environment alters DNA methylation in gametes and subsequently leads to programming of offspring metabolic health (Ge et al., 2014a, Ge et al., 2014b). Any such alterations in offspring oocyte function would be a mechanism by which detrimental metabolic programming may be propagated to the subsequent (F2) generation which may also be determined in the future.

Limitations in the study determining changes in the fetal hepatic transcriptome in response to Jz-ICR1 Δ via RNA sequencing included the use of a sample size of 3-4, whilst a sample number > 6 in such analyses have been shown to identify a higher number of DEGs due to an increase in statistical power (Schurch et al., 2016). Moreover, due to the limited number of DEGs identified, pathway analysis did not reach statistical significance when taking the adjusted p value into account and could not be performed with separate male and female DEG lists. In future, the molecular mechanisms causing alterations in fetal liver gene expression may be determined. For instance, transcription factors influencing gene expression may be determined computationally and their genomic binding sites identified using chromatin immunoprecipitation and sequencing (ChIP-seq). Several previous studies in rodent models of developmental programming have shown alterations in non-coding RNA, histone modifications and changes in methylation influencing the expression of genes in offspring metabolic organs (reviewed

in (Christoforou and Sferruzzi-Perri, 2020), and this may also be investigated in the fetal liver of Jz-ICR1 Δ offspring to identify the epigenetic mechanisms altering gene expression.

In future, if alterations in DNA methylation were observed in the Jz-ICR1 Δ fetal livers, these dams may be given a diet high in methyl donors in an attempt to reverse such changes. For instance, restoration of methylation at specific genes and genome-wide methylation in rodent offspring tissues arising from maternal protein restriction has been achieved by the maternal intake of folate, a methyl group donor (Lillycrop et al., 2005, Altobelli et al., 2013). Insulin and metformin are routinely used to treat GDM patients and their administration in rodent dams fed a high fat diet prevents the metabolic programming of offspring (Rowan et al., 2008, Salomäki et al., 2014). However, as Jz-ICR1 Δ leads to fetal growth restriction at E19, as is observed in patients suffering with diabetes of extended duration or vasculopathy (Lucas et al., 1989), treatment with metformin or insulin may further exacerbate programmed offspring metabolic outcomes. Indeed, it has been suggested that in GDM patients with growth restricted babies, strict glycaemic control may be further detrimental (Parikh et al., 2007). Nonetheless, by identifying how best to concurrently improve maternal health and mitigate offspring programming induced by Jz-ICR1 Δ , this may be translated to a clinical setting and would be critical in preventing the propagation of metabolic disease via adverse environments *in utero*.

6.5 Concluding remarks

The incidence of metabolic disease is exponentially rising in Western societies (O'Neill and O'Driscoll, 2015, Saklayen, 2018), and as a suboptimal gestational environment increases the propensity of offspring developing metabolic disease in later life, mitigating pregnancy complications would reduce the spread of metabolic disease to subsequent generations. This is the first study to show, via direct placental manipulation (Jz-ICR1 Δ), the importance of placental endocrine function on placental nutrient transport, fetal outcomes and adult offspring metabolic programming. In response to Jz-ICR1 Δ sexually dimorphic phenotypes were observed, which were largely detrimental to male but not female offspring. Indeed, clinical studies corroborate current findings, as it has been shown that GDM is a risk factor for childhood obesity in male, but not female offspring (Li et al., 2017, Le Moullec et al., 2018). In the current study, the observation that Jz-

ICR1Δ induces sex-specific changes in the fetal transcriptome suggests that sexually dimorphic offspring programming begins *in utero*, although the precise factors governing this are unidentified to date. Nonetheless, this study provides initial evidence that placental endocrine malfunction influences adult metabolic health in a sexually dimorphic manner. It remains unknown whether certain placental endocrine factors are in part programming offspring metabolic health. However, deducing these endocrine factors would enable the use of placental biomarkers to ascertain if pregnancies are associated with placental endocrine malfunction and subsequently identify offspring at risk for developing metabolic disease. Overall, delineating the mechanisms involved in metabolic programming via placental endocrine malfunction would be instrumental not only in improving pregnancy outcomes, but also in providing the knowledge to diagnose metabolic disease at an earlier stage and improve outcomes in a clinical setting.

Appendices

Appendix 1: Supplementary data

A1.1: Offspring diet optimisation

A variety of calorie dense diets have been used in rodent models to induce obesity and insulin resistance including highly processed diets comprised of high fat laboratory diets supplemented with condensed milk or sucrose water, and cafeteria style diets (Sumiyoshi et al., 2006, Musial et al., 2017, Lang et al., 2019). Determining the optimal diet composition for experiments is critical, as high fat compared to high sucrose diets have been shown to induce different types of glucose intolerance in mice (Sumiyoshi et al., 2006). To determine which calorie dense diet was appropriate to exacerbate metabolic outcomes in Jz-ICR1 Δ offspring, but without inducing overt outcomes that would mask the effect of placental genotype, two calorie dense diets were tested. At weaning, offspring were given either a calorie dense diet comprised of high fat diet (D12451, Research diets, USA) with sucrose water (20%; Diet A) or with condensed milk gelatine (Diet B) and results were compared to those fed the control RM3 chow. The diet compositions are shown in Section 2.3.2, Table 2.3.

Insulin tolerance tests (Section 2.3.3) were performed at 16 weeks of age on offspring that had consumed either Diet A or Diet B (Figure A1.1), or a chow diet (not shown). Analysis of the area above the curve (AAC) suggested that a calorie dense diet comprised of high fat diet with sucrose water (Diet A) did not alter insulin sensitivity in Jz-ICR1 Δ compared to control mice, whilst a high fat diet and condensed milk gelatine (Diet B) was sufficient to alter insulin sensitivity in Jz-ICR1 Δ offspring, indicated by decreased AAC in males and increased AAC in females ($p < 0.05$; Figure A1.1D, H). Consequently, in all further results (Chapter 4), data from a calorie dense diet comprised of high fat diet and condensed milk gelatine will be referred to as a high sugar high fat (HSHF) diet and are shown in comparison to a chow diet.

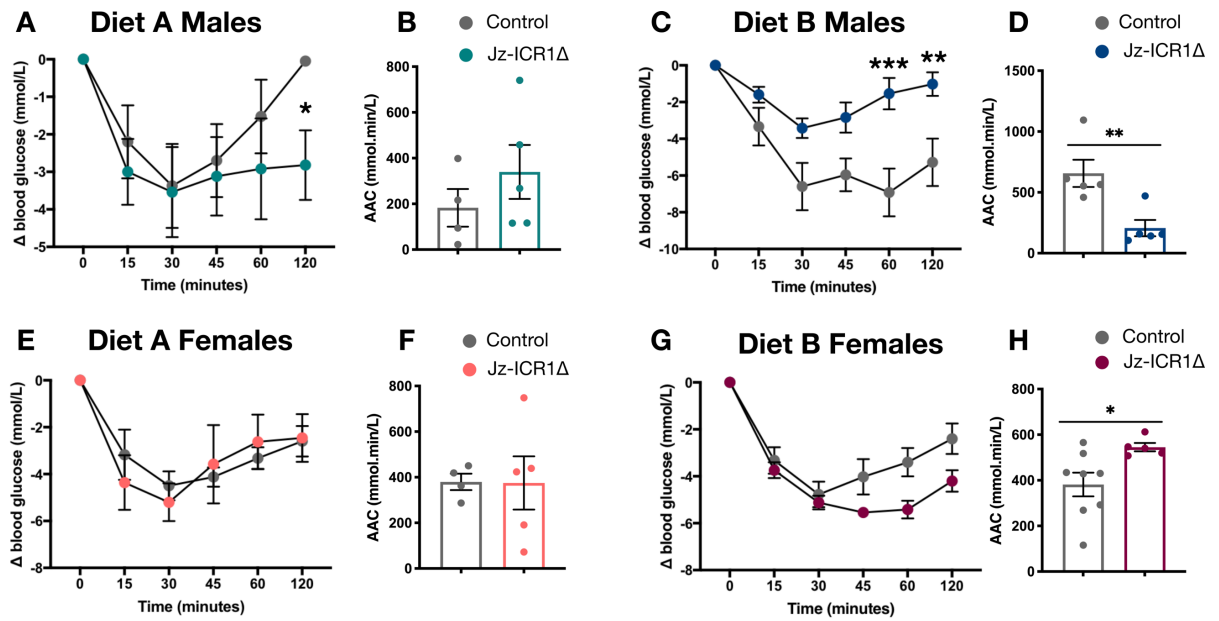


Figure A1.1. The effect of Diet A and Diet B on insulin tolerance of 16-week-old male and female offspring. Data are expressed as means \pm SEM (Diet A, $n=4$ control and $n=5$ Jz-ICR1 Δ ; Diet B, $n=5-7$ control and $n=5$ Jz-ICR1 Δ). Statistical analysis on the absolute glucose change (A, C, E, G) was performed by two-way repeated measures ANOVA with Sidak's multiple comparisons post hoc test. Area above the curve (AAC; B, D, F, H) were analysed by a Student's t-test. An asterisk (*) is used to denote significant difference from the control genotype (* $p<0.05$, ** $p<0.01$, *** $p<0.001$).

A1.2. The effect of gestational age on placental parameters

A1.2.1. Jz *Igf2* expression over time

The effects of gestational age and genotype on Jz *Igf2* expression are shown in Table A1.2.1, and referred to in Chapter 3, section 3.4. Overall, *Igf2* expression was lower at E19 compared to E16 ($p < 0.001$) but unaltered by genotype ($p = 0.394$). In particular, both control and Jz-ICR1 Δ placentas had lower *Igf2* expression at E19 compared to E16 ($p < 0.01$).

Table A1.2.1. Jz *Igf2* expression on E16 and E19 of pregnancy

Gestational age	Control	Jz-ICR1 Δ	Effect of gestational age	Effect of genotype	Interaction
E16	1.00 \pm 0.11	1.11 \pm 0.08			
E19	0.59 \pm 0.06†	0.60 \pm 0.05†	<0.001	0.394	0.516

Gene expression is expressed relative to *Polr2a* (whose expression is unaltered by genotype and over gestation) and relative to control samples on E16. Data are shown as mean \pm SEM and were analysed by two-way ANOVA (genotype, gestational age) with a Sidak post hoc test. $n = 13-16$ per genotype and gestational age (across 7-11 litters per genotype and gestational age). A cross (†) indicates a significant difference between E16 and E19 within the same genotype ($p < 0.05$).

A1.2.2. Glycogen cell volume over time

The effects of gestational age and genotype on glycogen cell volume are shown in Table A1.2.2, and referred to in Chapter 3, section 3.4. Overall, glycogen cell volume was reduced at E19 of pregnancy compared to E16 of pregnancy ($p < 0.0001$). In particular, both control and Jz-ICR1 Δ placentas had reduced glycogen cell volume at E19 compared to E16 ($p < 0.01$). Overall, Jz-ICR1 Δ placentas had increased glycogen cell volume compared to control placentas ($p < 0.01$) and at E16 Jz-ICR1 Δ placentas had increased glycogen cell volume compared to control placentas ($p < 0.05$).

Table A1.2.2. Glycogen cell volume (mm²) on E16 and E19 of pregnancy

Gestational age	Control	Jz-ICR1Δ	Effect of gestational age	Effect of genotype	Interaction
E16	9.82 \pm 1.80	15.34 \pm 1.87*	<0.0001	0.0083	0.20
E19	3.30 \pm 0.73†	5.28 \pm 0.80†			

Data are shown as mean \pm SEM and were analysed by two-way ANOVA (genotype, gestational age) with a Sidak post hoc test. n=8-13 per genotype and gestational age (across 4-12 litters per genotype and gestational age). An asterisk (*) indicates a significant difference between control and Jz-ICR1 Δ within the same gestational age ($P < 0.05$). A cross (†) indicates a significant difference between E16 and E19 within the same genotype ($p < 0.05$). An asterisk (*) indicates a significant difference between control and Jz-ICR1 Δ within the same gestational time point.

A1.2.3. Glycogen content over time

The effects of gestational age and genotype on placental glycogen content are shown in Table A1.2.3, and referred to in Chapter 3, section 3.4. Overall, placental glycogen content was reduced at E19 compared to E16 of pregnancy ($p < 0.0001$) but unaltered by genotype ($p = 0.51$). In particular, control and Jz-ICR1 Δ placentas had reduced glycogen content at E19 compared to E16 ($p < 0.05$).

Table A1.2.3. Placental glycogen content (mg/g) on E16 and E19 of pregnancy

Gestational age	Control	Jz-ICR1 Δ	Effect of gestational age	Effect of genotype	Interaction
E16	6.41 \pm 0.69	5.76 \pm 0.66	<0.0001	0.51	0.64
E19	3.41 \pm 0.58†	3.29 \pm 0.38†			

Data are shown as mean \pm SEM and were analysed by two-way ANOVA (genotype, gestational age) with a Sidak post hoc test. $n = 12-17$ per genotype and gestational age (across 5-12 litters per genotype and gestational age). An asterisk (*) indicates a significant difference between control and Jz-ICR1 Δ within the same gestational age ($P < 0.05$). A cross (†) indicates a significant difference between E16 and E19 within the same genotype ($p < 0.05$).

A1.3: Western blot images

A1.3.1. Liver western blot images

The full Western blot images of the PI3K pathway, gluconeogenesis and lipid metabolic pathways in liver from adult male control and Jz-ICR1Δ offspring fed a chow diet are shown in Figure A1.3.1.1.

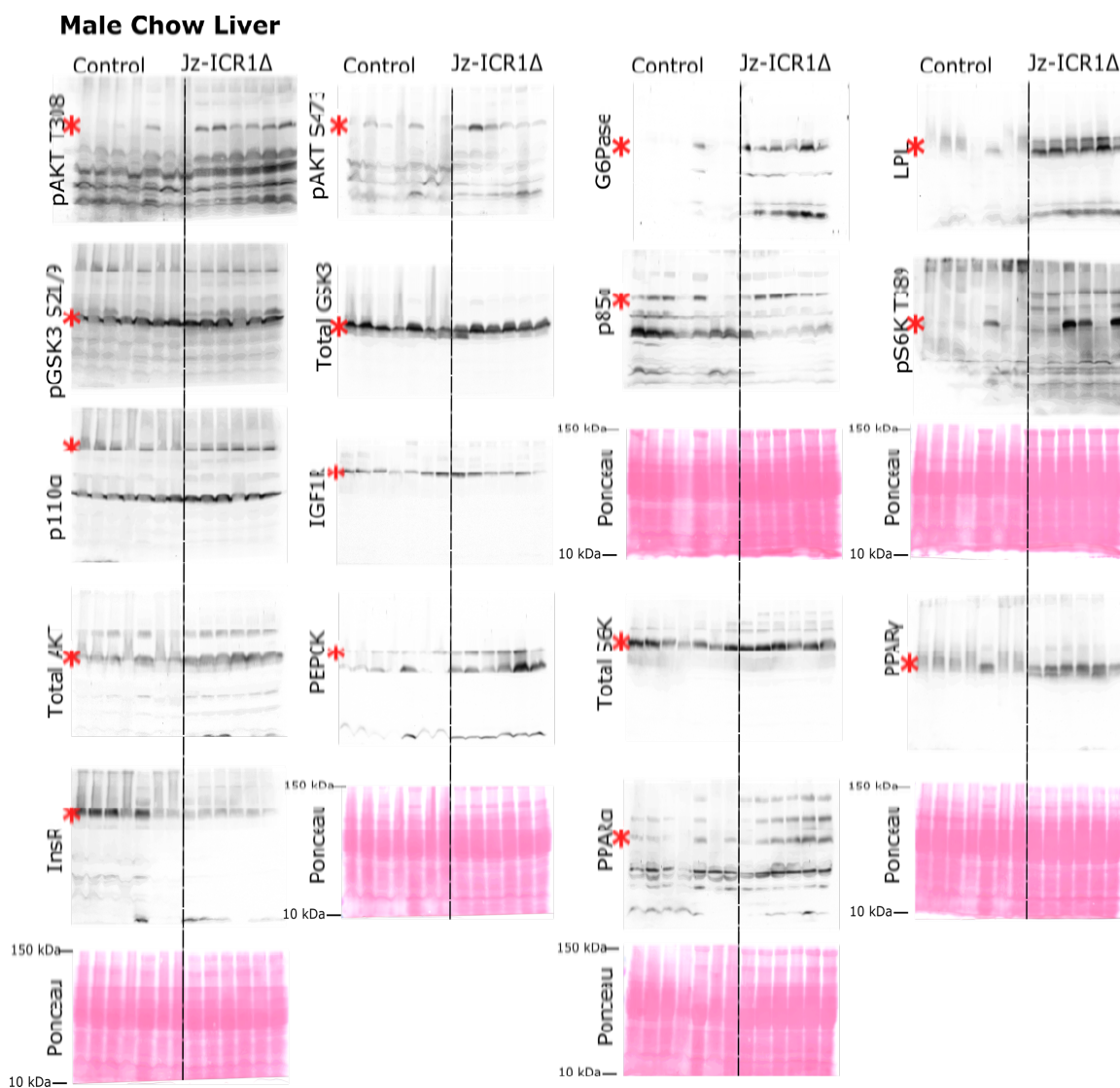


Figure A1.3.1.1. Full Western blot images and corresponding Ponceau staining in liver from adult male control and Jz-ICR1Δ offspring fed a chow diet. Western blot images are shown in the order of antibody probing. A red asterisk (*) indicates the protein of interest. The corresponding Ponceau stained membrane for each detected protein (or series of detected proteins) is shown below the Western blot images and indicates loading for each sample.

The full Western blot images of the PI3K pathway, gluconeogenesis and lipid metabolic pathways in liver from adult male control and Jz-ICR1Δ offspring fed a HSHF diet are shown in Figure A1.3.1.2.

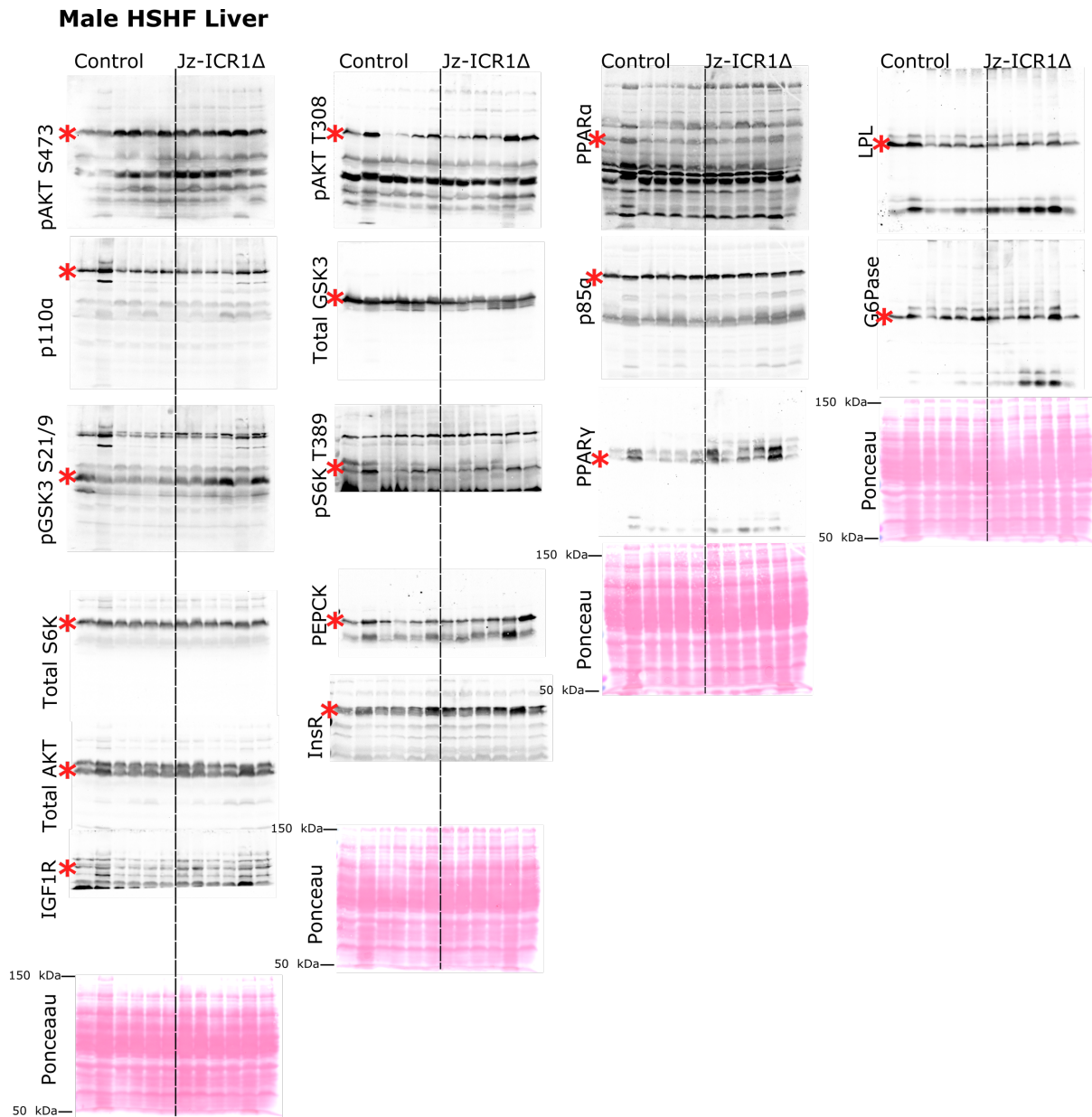


Figure A1.3.1.2. Full Western blot images and corresponding Ponceau staining in liver from adult male control and Jz-ICR1Δ offspring fed a HSHF diet. Western blot images are shown in the order of antibody probing. A red asterisk (*) indicates the protein of interest. The corresponding Ponceau stained membrane for each detected protein (or series of detected proteins) is shown below the Western blot images and indicates loading for each sample. HSHF, high sugar high fat.

The full Western blot images of the PI3K pathway, gluconeogenesis and lipid metabolic pathways in liver from adult female control and Jz-ICR1Δ offspring fed a chow diet are shown in Figure A1.3.1.3.

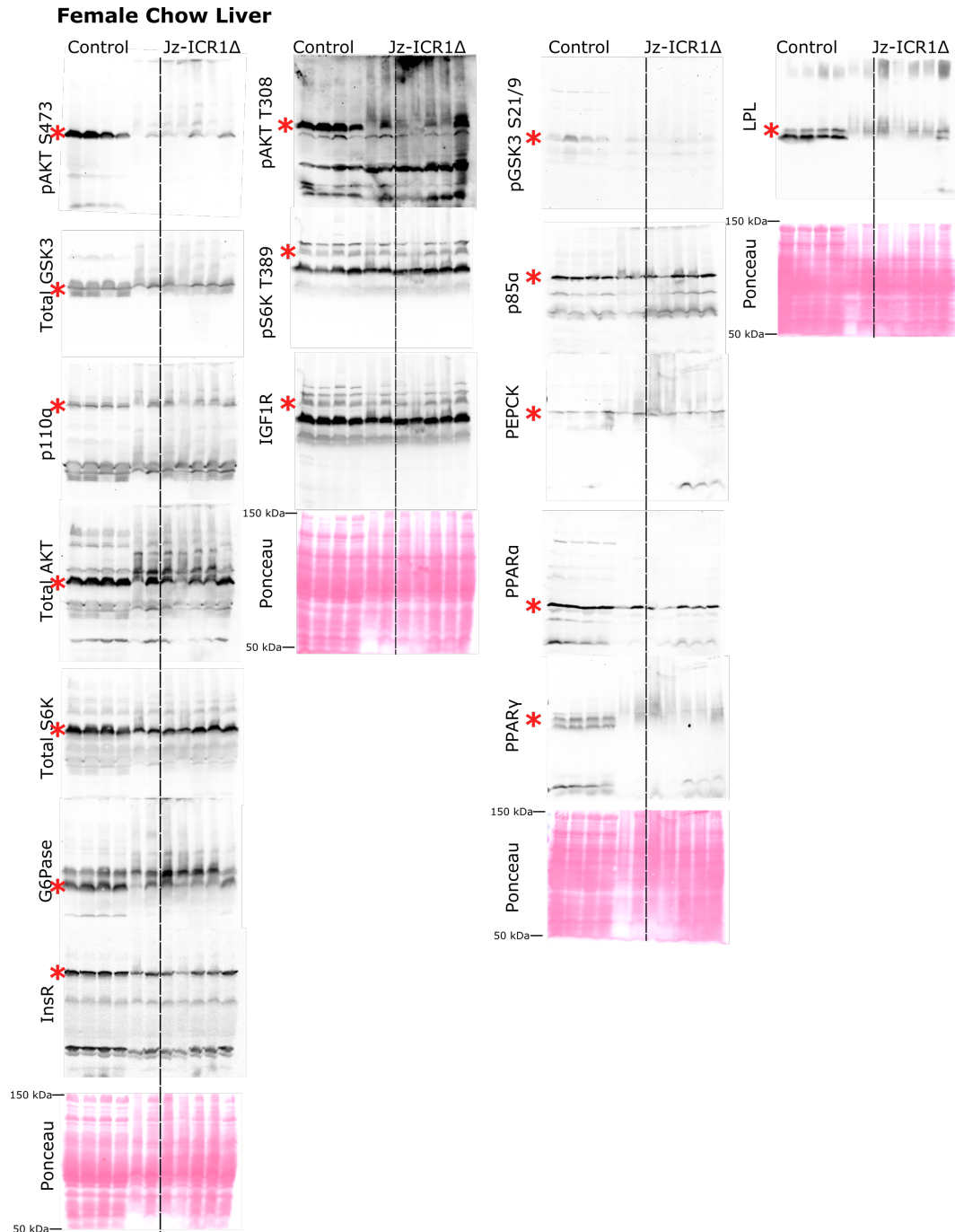


Figure A1.3.1.3. Full Western blot images and corresponding Ponceau staining in liver from adult female control and Jz-ICR1Δ offspring fed a chow diet. Western blot images are shown in the order of antibody probing. A red asterisk (*) indicates the protein of interest. The corresponding Ponceau stained membrane for each detected protein (or series of detected proteins) is shown below the Western blot images and indicates loading for each sample.

The full Western blot images of the PI3K pathway, gluconeogenesis and lipid metabolic pathways in liver from adult female control and Jz-ICR1Δ offspring fed a HSHF diet are shown in Figure A1.3.1.4.

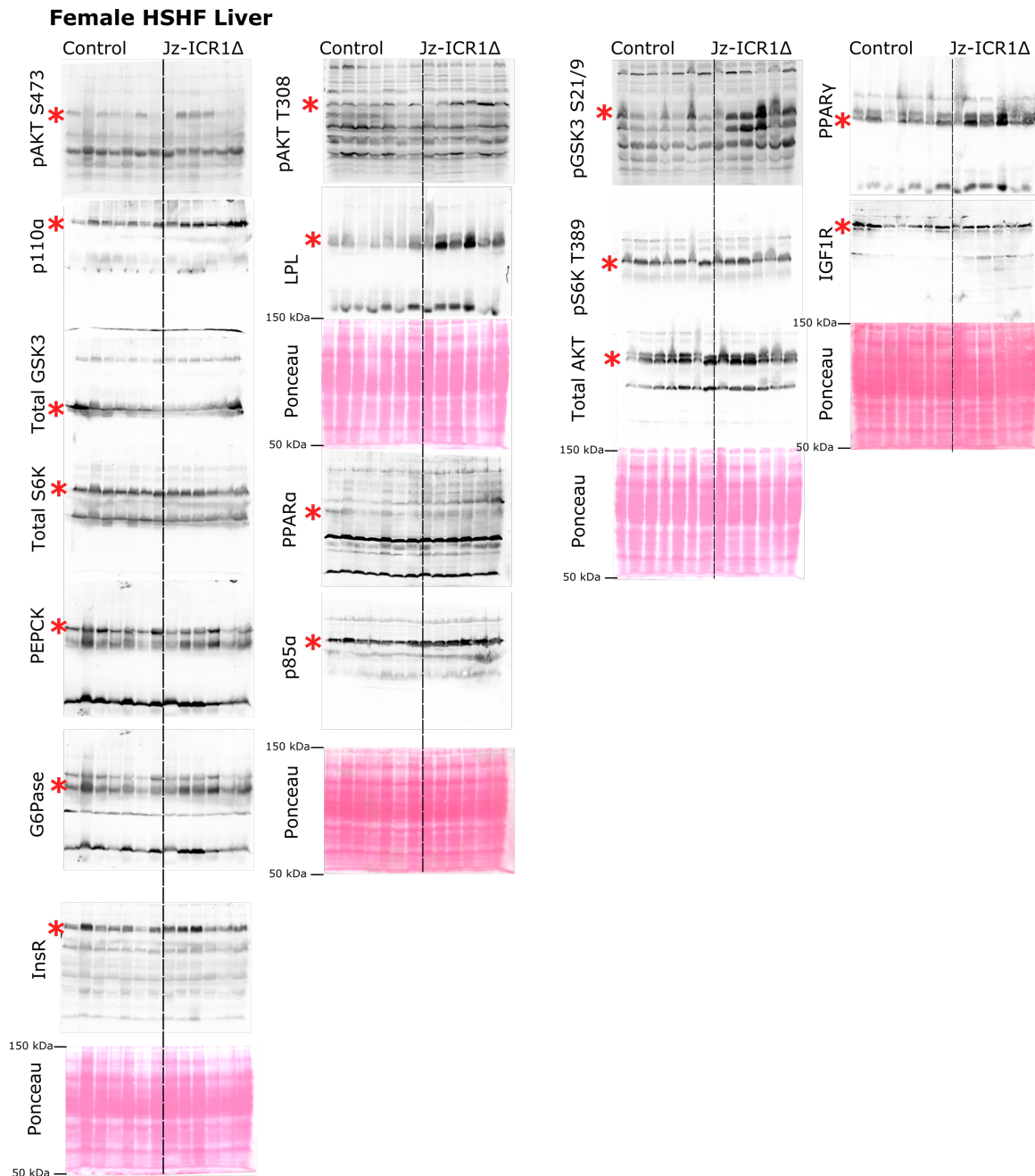


Figure A1.3.1.4. Full Western blot images and corresponding Ponceau staining in liver from adult female control and Jz-ICR1Δ offspring fed a HSHF diet. Western blot images are shown in the order of antibody probing. A red asterisk (*) indicates the protein of interest. The corresponding Ponceau stained membrane for each detected protein (or series of detected proteins) is shown below the Western blot images and indicates loading for each sample. HSHF, high sugar high fat.

A1.3.2. Skeletal muscle western blot images

The full Western blot images of the PI3K pathway and lipid metabolic pathways in skeletal muscle from adult male control and *Jz-ICR1Δ* offspring fed a chow diet are shown in Figure A1.3.2.1.

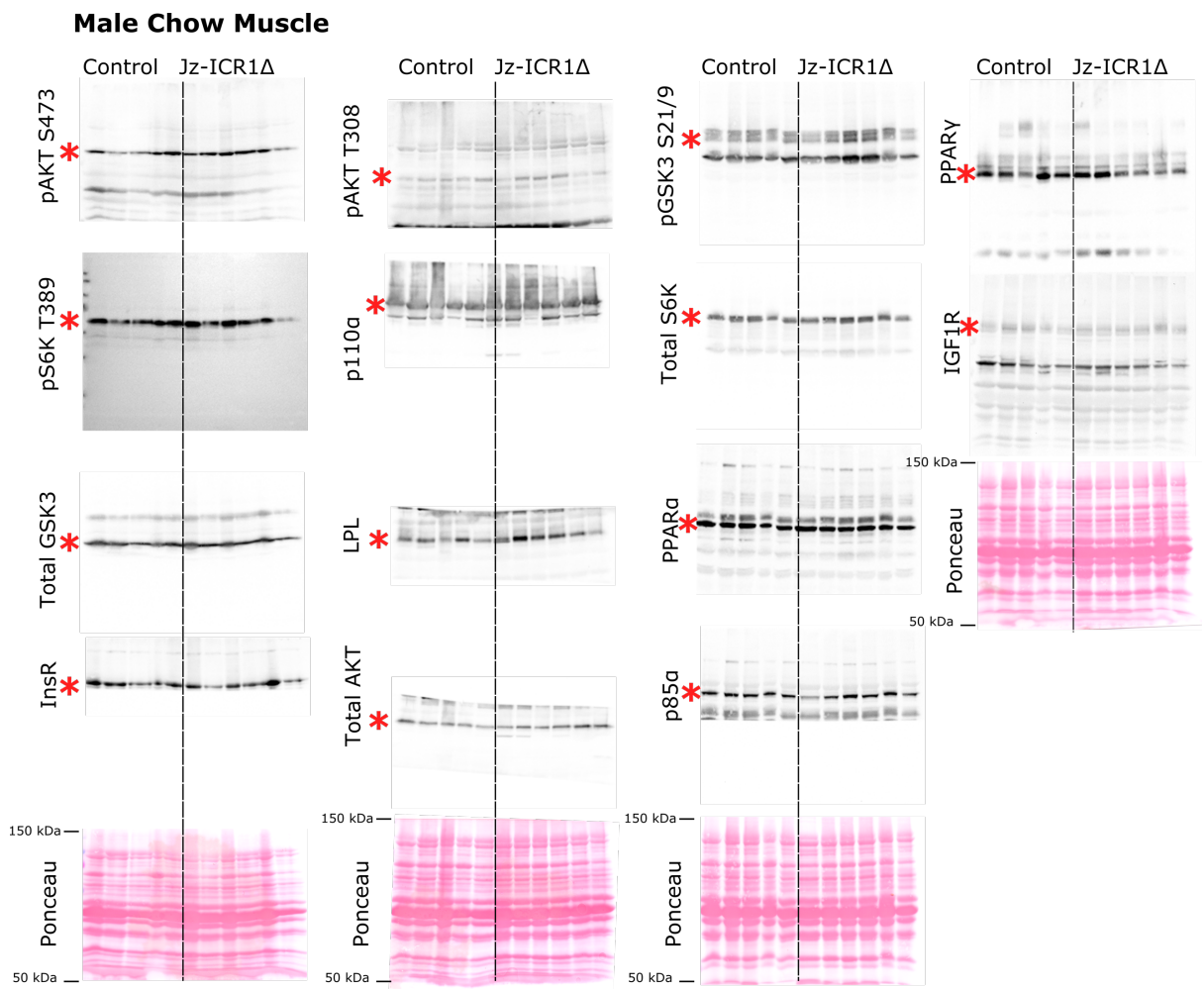


Figure A1.3.2.1. Full Western blot images and corresponding Ponceau staining in skeletal muscle from adult male control and *Jz-ICR1Δ* offspring fed a chow diet. Western blot images are shown in the order of antibody probing. A red asterisk (*) indicates the protein of interest. The corresponding Ponceau stained membrane for each detected protein (or series of detected proteins) is shown below the Western blot images and indicates loading for each sample.

The full Western blot images of the PI3K pathway and lipid metabolic pathways in skeletal muscle from adult male control and Jz-ICR1Δ offspring fed a HSHF diet are shown in Figure A1.3.2.2.

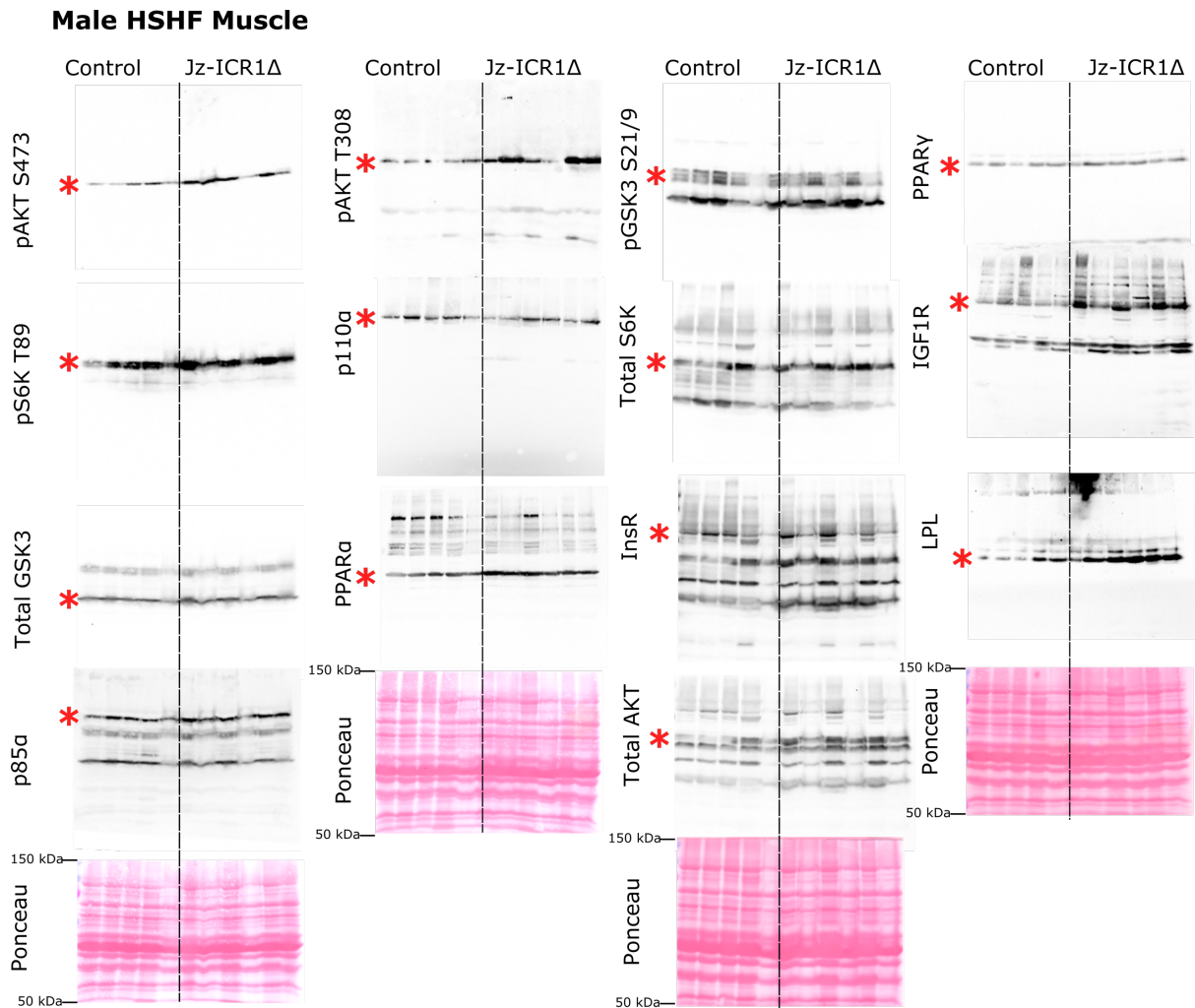


Figure A1.3.2.2. Full Western blot images and corresponding Ponceau staining in skeletal muscle from adult male control and Jz-ICR1Δ offspring fed a HSHF diet. Western blot images are shown in the order of antibody probing. A red asterisk (*) indicates the protein of interest. The corresponding Ponceau stained membrane for each detected protein (or series of detected proteins) is shown below the Western blot images and indicates loading for each sample. HSHF, high sugar high fat.

The full Western blot images of the PI3K pathway and lipid metabolic pathways in skeletal muscle from adult female control and Jz-ICR1Δ offspring fed a chow diet are shown in Figure A1.3.2.3.

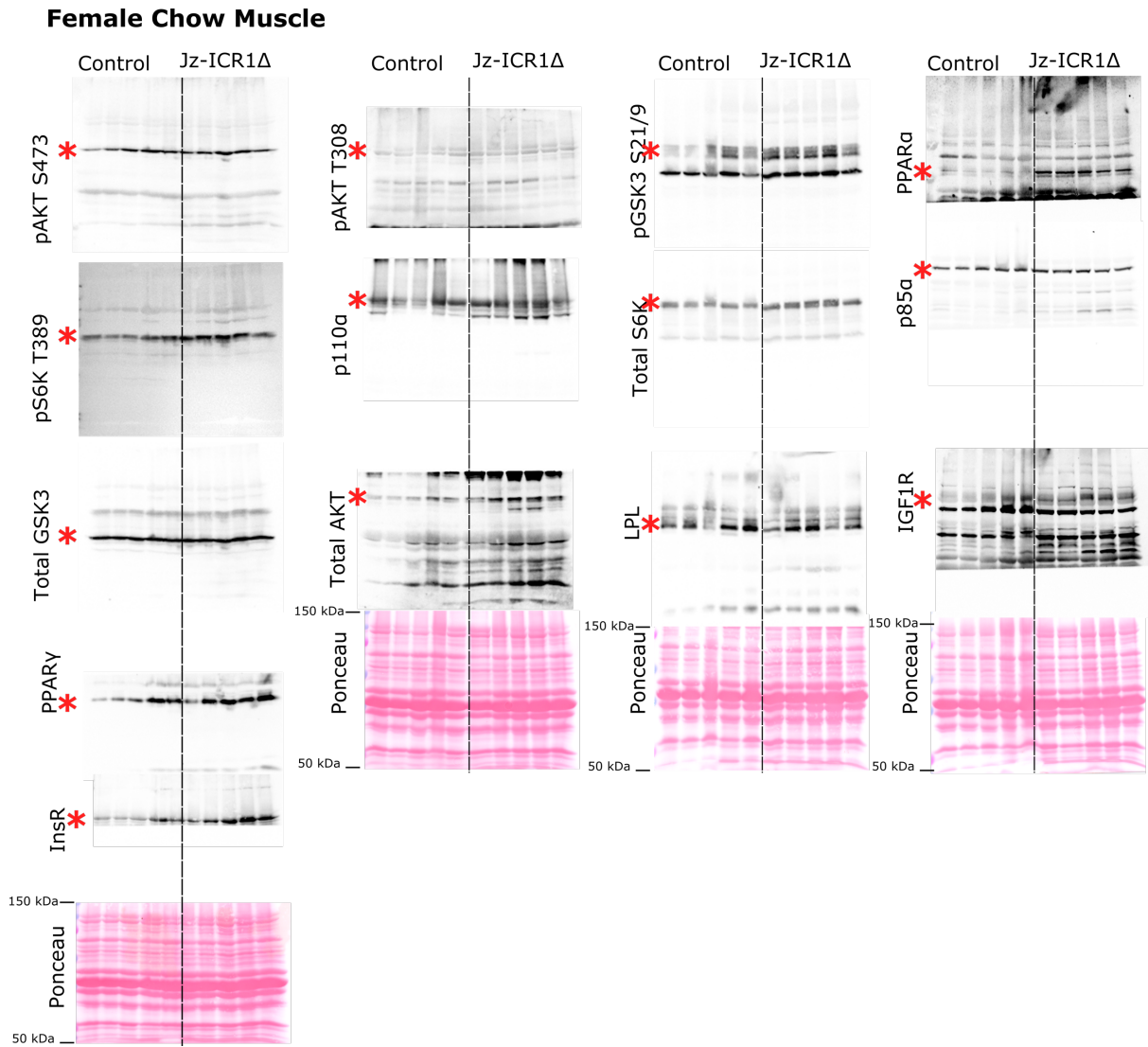


Figure A1.3.2.3. Full Western blot images and corresponding Ponceau staining in skeletal muscle from adult female control and Jz-ICR1Δ offspring fed a chow diet. Western blot images are shown in the order of antibody probing. A red asterisk (*) indicates the protein of interest. The corresponding Ponceau stained membrane for each detected protein (or series of detected proteins) is shown below the Western blot images and indicates loading for each sample.

The full Western blot images of the PI3K pathway and lipid metabolic pathways in skeletal muscle from adult female control and Jz-ICR1Δ offspring fed a HSHF diet are shown in Figure A1.3.2.4.

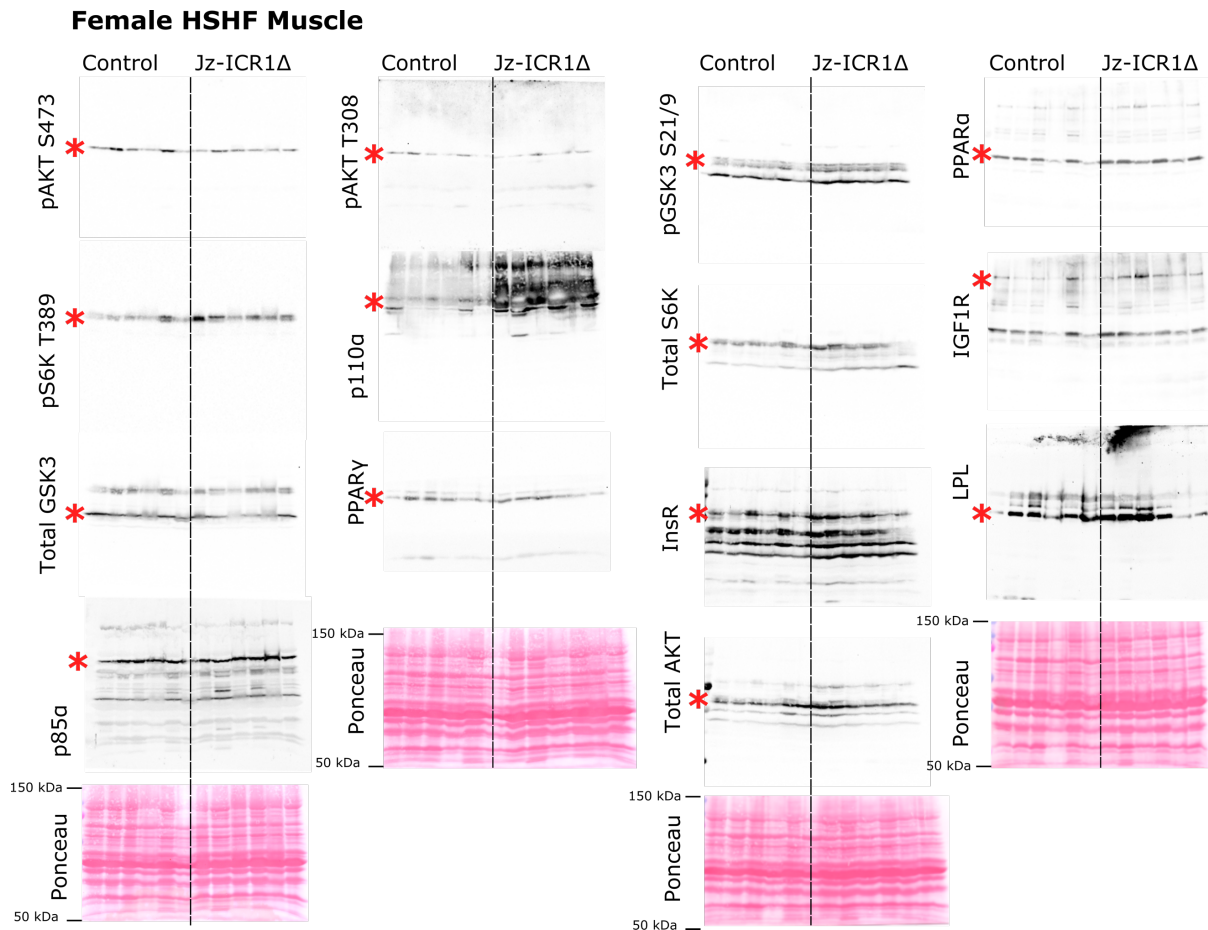


Figure A1.3.2.4. Full Western blot images and corresponding Ponceau staining in skeletal muscle from adult female control and Jz-ICR1Δ offspring fed a HSHF diet. Western blot images are shown in the order of antibody probing. A red asterisk (*) indicates the protein of interest. The corresponding Ponceau stained membrane for each detected protein (or series of detected proteins) is shown below the Western blot images and indicates loading for each sample. HSHF, high sugar high fat.

A1.3.3. Adipose western blot images

The full Western blot images of the PI3K pathway and lipid metabolic pathways in adipose tissue from adult male control and Jz-ICR1Δ offspring fed a chow diet are shown in Figure A1.3.3.1.

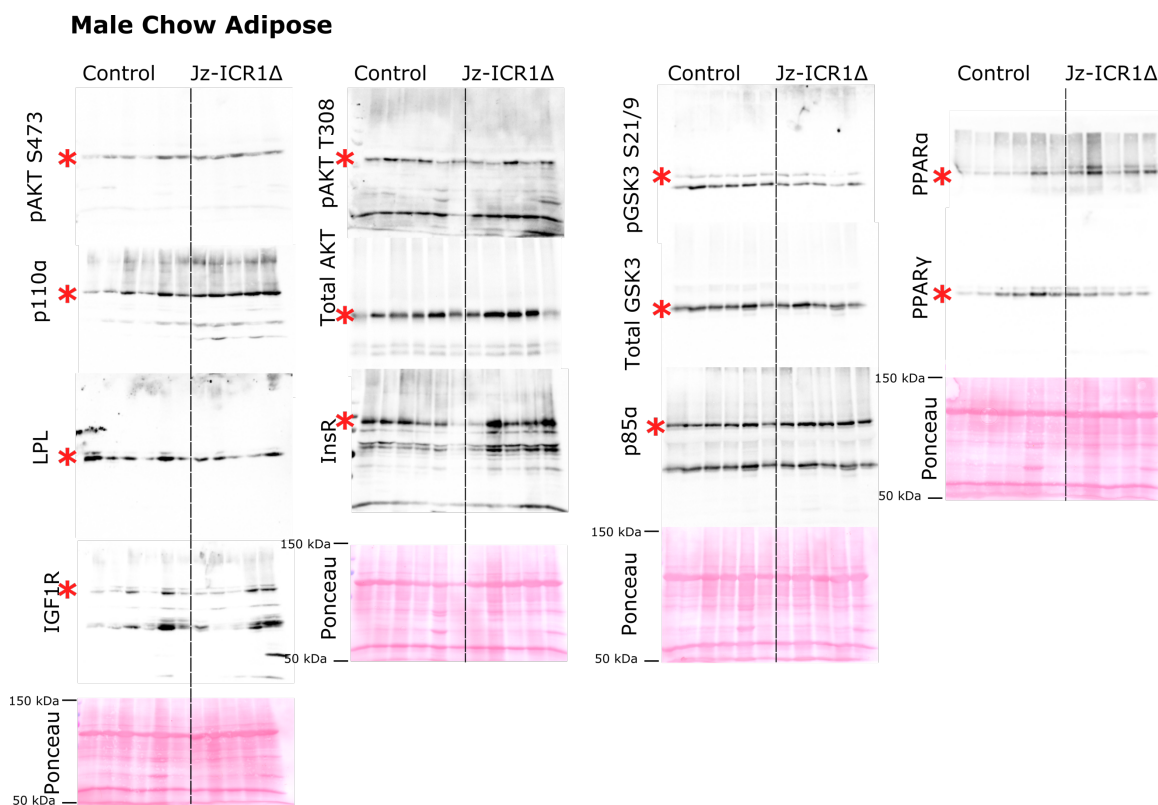


Figure A1.3.3.1. Full Western blot images and corresponding Ponceau staining in adipose tissue from adult male control and Jz-ICR1Δ offspring fed a chow diet. Western blot images are shown in the order of antibody probing. A red asterisk (*) indicates the protein of interest. The corresponding Ponceau stained membrane for each detected protein (or series of detected proteins) is shown below the Western blot images and indicates loading for each sample.

The full Western blot images of the PI3K pathway and lipid metabolic pathways in adipose tissue from adult male control and Jz-ICR1Δ offspring fed a HSHF diet are shown in Figure A1.3.3.2.

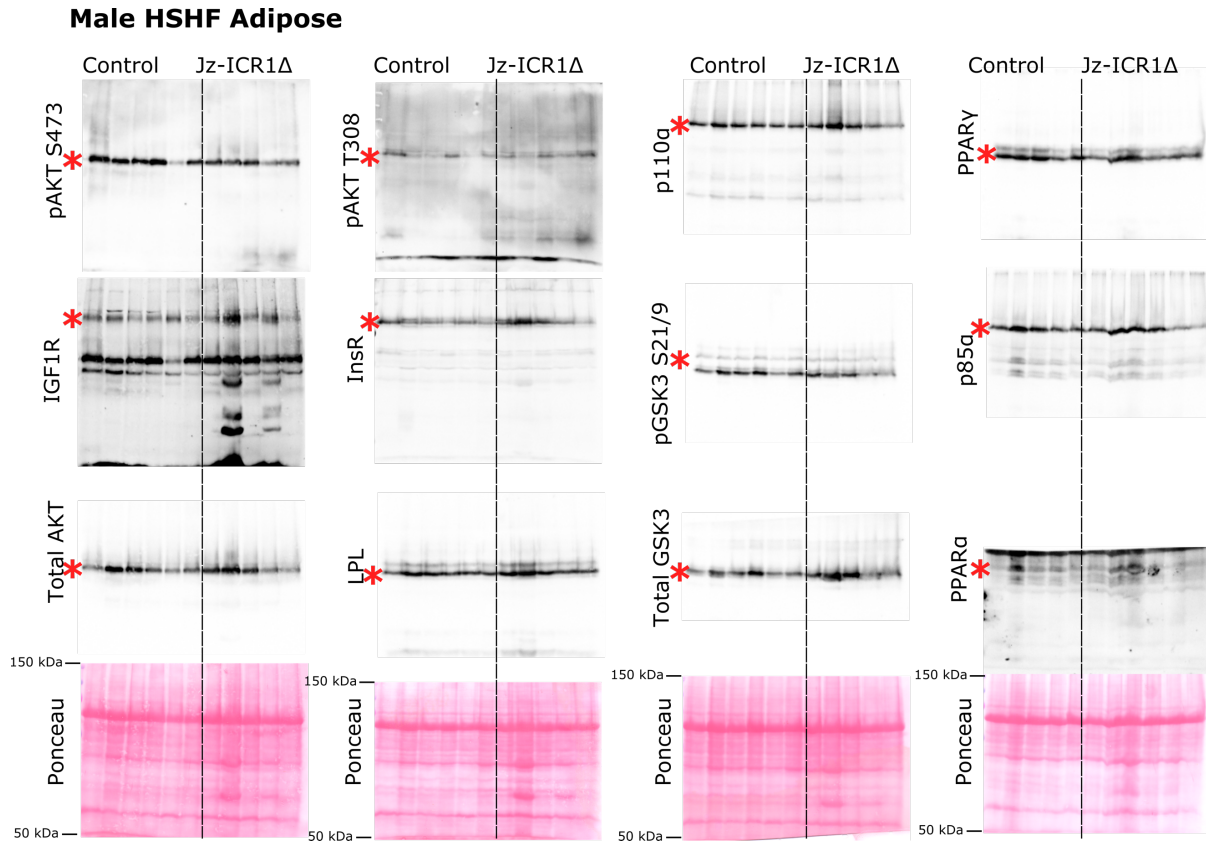


Figure A1.3.3.2. Full Western blot images and corresponding Ponceau staining in adipose tissue from adult male control and Jz-ICR1Δ offspring fed a HSHF diet. Western blot images are shown in the order of antibody probing. A red asterisk (*) indicates the protein of interest. The corresponding Ponceau stained membrane for each detected protein (or series of detected proteins) is shown below the Western blot images and indicates loading for each sample. HSHF, high sugar high fat.

The full Western blot images of the PI3K pathway and lipid metabolic pathways in adipose tissue from adult female control and Jz-ICR1Δ offspring fed a chow diet are shown in Figure A1.3.3.3.

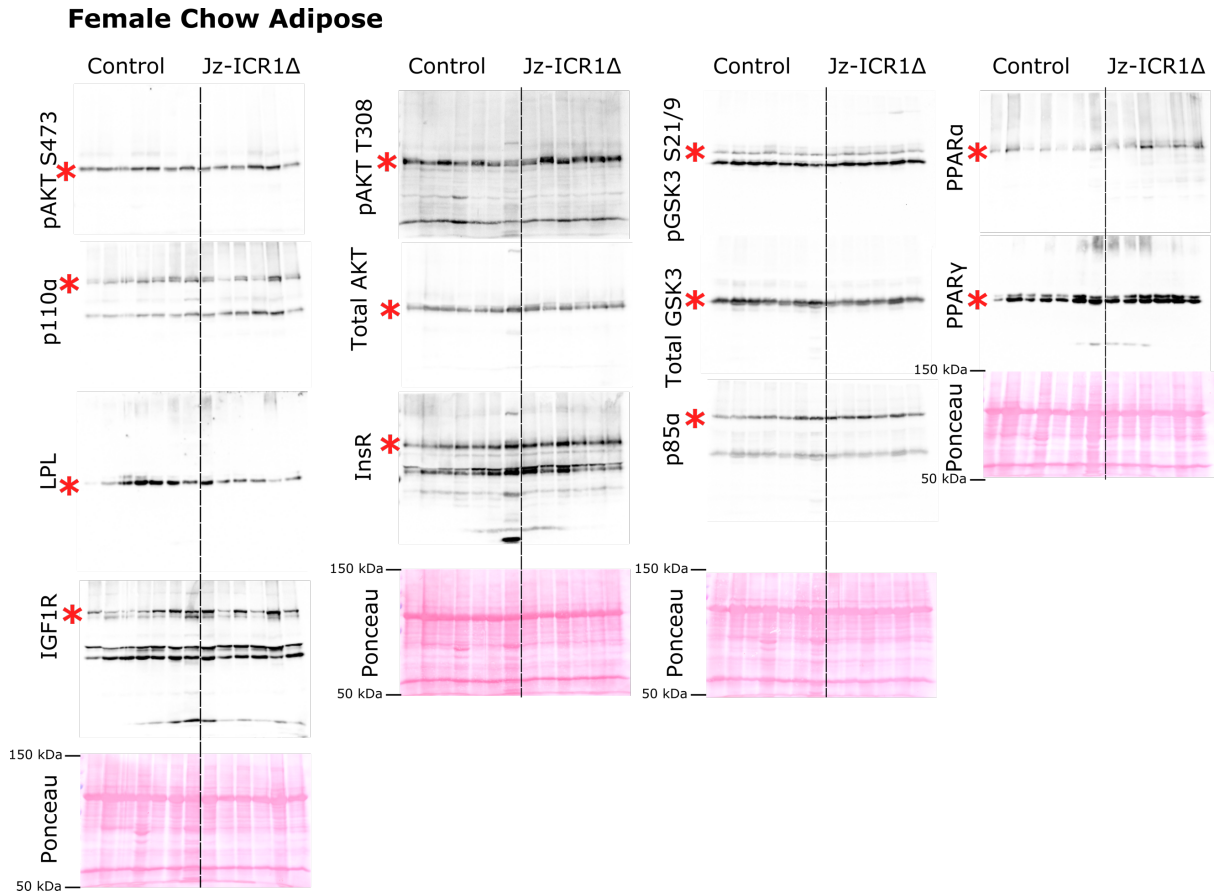


Figure A1.3.3.3. Full Western blot images and corresponding Ponceau staining in adipose tissue from adult female control and Jz-ICR1Δ offspring fed a chow diet. Western blot images are shown in the order of antibody probing. A red asterisk (*) indicates the protein of interest. The corresponding Ponceau stained membrane for each detected protein (or series of detected proteins) is shown below the Western blot images and indicates loading for each sample.

The full Western blot images of the PI3K pathway and lipid metabolic pathways in adipose tissue from adult female control and Jz-ICR1Δ offspring fed a HSHF diet are shown in Figure A1.3.3.4.

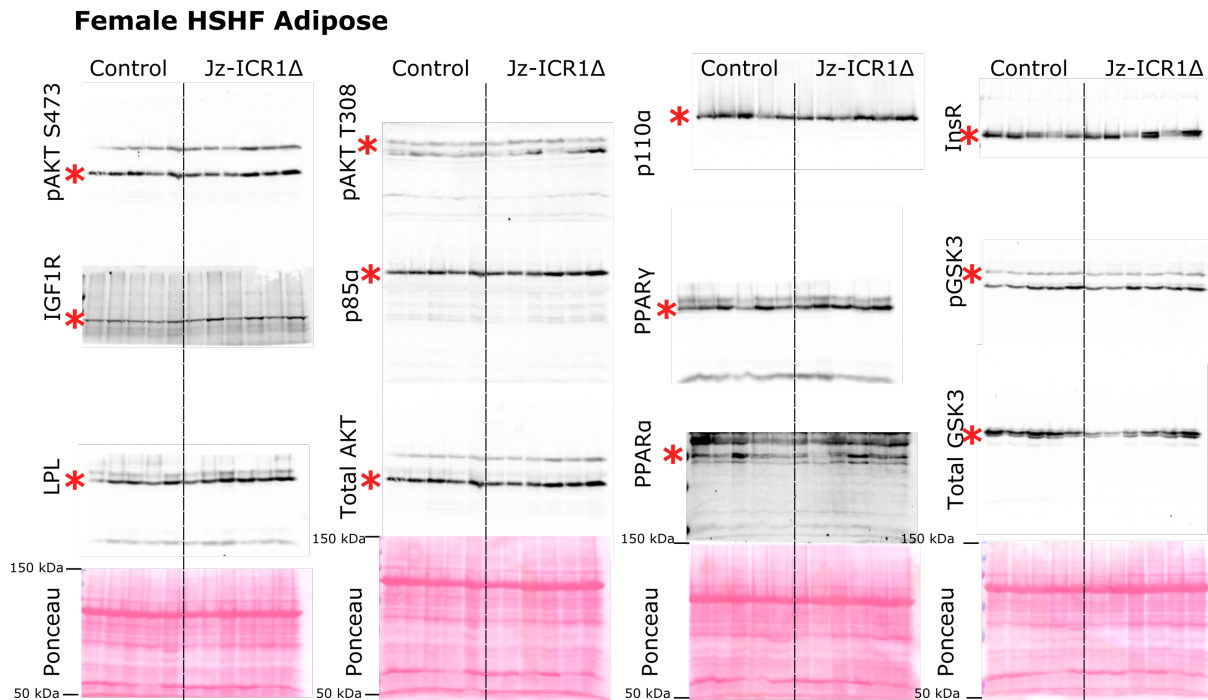


Figure A1.3.3.4. Full Western blot images and corresponding Ponceau staining in adipose tissue from adult female control and Jz-ICR1Δ offspring fed a HSHF diet. Western blot images are shown in the order of antibody probing. A red asterisk (*) indicates the protein of interest. The corresponding Ponceau stained membrane for each detected protein (or series of detected proteins) is shown below the Western blot images and indicates loading for each sample. HSHF, high sugar high fat.

A1.4: Supplementary RNA sequencing data

A1.4.1. Enrichment analyses

Enrichment analysis of DEGs between control and Jz-ICR1 Δ fetal livers irrespective of sex are shown in Figure A1.4.1. Molecular signatures that were enriched in response to Jz-ICR1 Δ in the fetal liver included those involved in TNF α signalling via NF- κ B and hypoxia (adjusted p value <0.05).

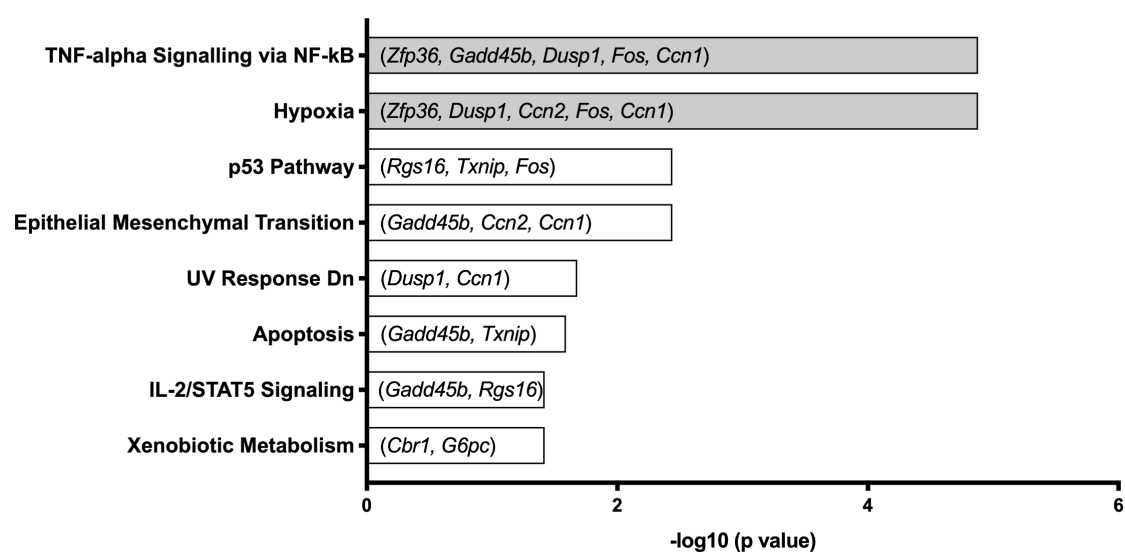


Figure A1.4.1. Enrichment analysis of DEGs in fetal livers between control and Jz-ICR1 Δ offspring, irrespective of sex. Enrichment analysis from the Molecular Signatures Database (MSigDB) is shown. Grey bars represent pathways with an adjusted p value < 0.05.

A1.4.2. The effect of sex on fetal liver DEGs

Lists of DEGs between male and female fetal livers on E19 irrespective of genotype (Table A1.4.2.1) between controls (Table A1.4.2.2) and between Jz-ICR1Δ (Table A1.4.2.3) are shown.

Table A1.4.2.1. List of DEGs between male and female fetal livers on E19 of pregnancy, irrespective of genotype

Gene	Fold change	Adjusted p value	Chromosome
DEAD (Asp-Glu-Ala-Asp) box polypeptide 3, Y-linked (<i>Ddx3y</i>)	-11.34	4.50E-51	Y
Eukaryotic translation initiation factor 2, subunit 3, structural gene Y-linked (<i>Eif2s3y</i>)	-10.82	1.51E-52	Y
Lysine (K)-specific demethylase 5D (<i>Kdm5d</i>)	-5.85	6.55E-34	Y
Ubiquitously transcribed tetratricopeptide repeat gene, Y chromosome (<i>Uty</i>)	-3.71	4.02E-27	Y
Inactive X specific transcripts (<i>Xist</i>)	1.90	2.32E-91	X
Lysine (K)-specific demethylase 6A (<i>Kdm6a</i>)	1.56	3.44E-11	X
Eukaryotic translation initiation factor 2, subunit 3, structural gene X-linked (<i>Eif2s3x</i>)	1.42	8.75E-11	X

Table A1.4.2.2. List of DEGs between control male and control female fetal livers on E19 of pregnancy

Gene	Fold change	Adjusted p value	Chromosome
Inactive X specific transcripts (<i>Xist</i>)	17.68	1.25E-56	X
DEAD (Asp-Glu-Ala-Asp) box polypeptide 3, Y-linked (<i>Ddx3y</i>)	-9.78	1.55E-17	Y
Eukaryotic translation initiation factor 2, subunit 3, structural gene Y-linked (<i>Eif2s3y</i>)	-9.29	9.32E-29	Y
Lysine (K)-specific demethylase 5D (<i>Kdm5d</i>)	-5.06	4.07E-13	Y
Ubiquitously transcribed tetratricopeptide repeat gene, Y chromosome (<i>Uty</i>)	-3.24	7.01E-09	Y
Ribosomal protein L23A (<i>Rpl23a</i>)	2.50	1.13E-12	11
Mesothelin (<i>Msln</i>)	1.60	0.00079	17
Lysine (K)-specific demethylase 6A (<i>Kdm6a</i>)	1.60	0.00017	X
Uroplakin 3B (<i>Upk3b</i>)	1.59	0.0013	5
Eukaryotic translation initiation factor 2, subunit 3, structural gene X-linked (<i>Eif2s3x</i>)	1.51	1.26E-05	X
Integral membrane protein 2A (<i>Itm2a</i>)	1.46	0.036	X
Insulin-like growth factor binding protein 5 (<i>Igfbp5</i>)	1.44	0.047	1

Table A1.4.2.3. List of DEGs between Jz-ICR1Δ male and Jz-ICR1Δ female fetal livers on E19 of pregnancy

Gene	Fold change	Adjusted p value	Chromosome
Inactive X specific transcripts (<i>Xist</i>)	18.85	1.6E-12	X
Eukaryotic translation initiation factor 2, subunit 3, structural gene Y-linked (<i>Eif2s3y</i>)	-12.30	8.62E-21	Y
DEAD (Asp-Glu-Ala-Asp) box polypeptide 3, Y-linked (<i>Ddx3y</i>)	-12.28	1.21E-30	Y
Lysine (K)-specific demethylase 5D (<i>Kdm5d</i>)	-6.32	2.91E-18	Y
Ubiquitously transcribed tetratricopeptide repeat gene, Y chromosome (<i>Uty</i>)	-4.15	6.00E-16	Y
Lysine (K)-specific demethylase 6A (<i>Kdm6a</i>)	1.51	0.0012	X

Appendix 2: Reagents

A2.1. Reagents

Reagent	Manufacturer	Catalogue number
¹⁴ C MeAIB	PerkinElmer	NEN NEC-671
2-Mercaptoethanol (B-ME)	Merck	8057400250
³ H MeG	PerkinElmer	NEN NEC-377
β-glycerophosphate	Sigma-Aldrich	G9422-10G
Acrylamide	Bio Rad	1610158
Agarose	Bioline	B10-41025
Ammonium nickel (II) sulphate hexahydrate	Aldrich Chemistry	09885-250G
Ammonium persulphate (APS)	Sigma Life Science	A3678-35G
Amyloglucosidase enzyme	Sigma Life Science	10115-IG-F
Barium hydroxide	Sigma Life Science	B4059
Bicinchoninic (BCA) protein assay	Thermoscientific	Reagent A: 23228 Reagent B: 23224
Bovine serum albumin (BSA)	Sigma Life Science	A2153-100G
Bromophenol blue	Sigma-Aldrich	B8026-5G
Chloroform	Fisher Chemical	C/4960/PB08
Complete mini protease cocktail inhibitor	Roche	11836170001
Corticosterone ELISA kit	Invitrogen	EIACORT
DAB substrate kit	Abcam	Ab64238
DL-Dithiothreitol	Sigma Life Science	D9779-5G
DNA ladder	New England BioLabs	N3232S
DPX	Sigma Life Science	06522
ECL	Thermo Scientific	32109 (Pierce) 34094 (Femto)
EGTA	Sigma-Aldrich	E4378-25G
Eosin Y solution	Sigma-Aldrich	HT110116-500 ml
Ethanol	Sigma-Aldrich	459836-1L
Ethylenediaminetetraacetic acid (EDTA)	Sigma Life Science	E5134-500g
Glucose	Dechra, POM-VPS,	Vm 10434/4047
Glycerol	Sigma	65516-1L
Glycine	Sigma Life Science	67126-1KG
Goat serum	Abcam	Ab7481
Haematoxylin Solution Gill no.2	Sigma-Aldrich	GHS232-1L
High-Capacity cDNA Reverse Transcription Kit	ThermoFisher Scientific	4368814
Histoclear II	Geneflow	HS-202
Hydrogen Peroxide	Fisher Chemical	H/1800/15
Insulin	Actrapid (100 IU/mL)	AS62205
Insulin ELISA kit	Mercodia	10-1247-01

Isobutanol	Sigma-Aldrich	1009841000
Methanol	Sigma-Aldrich	322415
Nuclear Fast red	Vector Laboratories, INC	H-3403
Nuclease free water	Thermo Fisher Scientific	AM9938
Paraformaldehyde (PFA)	Sigma-Aldrich	158127-500G
Phosphate buffered saline (PBS)	Oxoid	BR0014G
Ponceau S	Sigma Life Science	P7170-1L Batch 010M4350
Precision Plus Protein Dual Colour Standards	BioRad	161-0374
Radioimmunoprecipitation assay (RIPA) buffer	Sigma Life Science	R0278-50M
RedTaq ReadyMix PCR Reaction Mix	Sigma-Aldrich	R2523-20RXN
Restore Western blot Stripping buffer	Thermo Fisher	21059
RNeasy plus mini kit	Qiagen	74134
Safeview	NBS Biologicals Ltd	NBS-SV
Sodium azide	Sigma-Aldrich	S2002-25G
Sodium chloride (NaCl)	Fisher	S/3160/60
Sodium dodecyl sulphate (SDS)	Sigma	75746-250G
Sodium orthovanadate	Sigma Life Science	S6508-10G
Streptavidin-Peroxidase	Rockland	S000-30
Sodium pyrophosphate	Sigma-Aldrich	P80-10
SYBR Green	Applied Biosystems, Thermofisher	A25742
Tetramethylethylenediamine (TEMED)	Sigma-Aldrich	T2,250-0
Tris base	Sigma Life Science	T6066
TrisHCl (Trizma hydrochloride)	Sigma Life Science	T5941
Trisodium citrate dihydrate	Sigma-Aldrich	S1804-500G
Triton	Acros Organics	215680010
Tween 20	Acros Organics	233360010
Xylene	Fisher Chemical	X/0250/17
Zinc sulphate	Sigma Life Science	Z2876

Appendix 3: Stock solutions and reagents

A3.1. Solutions and primers for SRY sexing

Table A3.1.1. Lysis buffer for DNA isolation recipe

Compound	Final concentration	Amount
KCl	50 mM	0.187 g
1M Tris HCl (pH 8.3)	10 mM	0.5 mL
1M MgCl ₂	2 mM	0.1 mL
Gelatin	0.1 mg/mL	5 mg
Tween-20	0.45%	225 µL
Nonidet P-40	0.45%	225 µL

Made in a total of 50 mL of distilled water. The buffer was autoclaved and 0.25 mL of 20 mg/mL Proteinase K (Roche, 03-115-828-001) for a final concentration of 0.1 mg/mL.

Lysis buffer was stored in aliquots at -20 °C.

Table A3.1.2. SRY and housekeeping gene primers

Primer	Sequence
<i>Sry</i> F	GTGGGTTCCCTGTCCCACTGC
<i>Sry</i> R	GGCCATGTCAAGCGCCCCAT
<i>Ercc8</i> F	TGGTTGGCATT TTTATCCCTAGAAC
<i>Ercc8</i> R	GCAACATGGCAACTGGAAACA

Sry, sex-determining region Y; *Ercc8*, Excision Repair Cross-Complementation Group 8

Table A3.1.3. 10x Tris-borate-EDTA (TBE) buffer recipe

Compound	Amount
Tris base	109 g
Boric acid	55 g
EDTA	4.65 g
Distilled water	0.9 L

pH 8.3, stored at room temperature. 10x TBE was diluted with distilled water to make a 0.5x TBE buffer solution.

2% agarose gel recipe

To make 2% agarose gel, 2.4 g of agarose (Bioline, B10-41025) was combined with 120 mL of 0.5x TBE buffer and heated in a microwave until dissolved. The solution was cooled and 10 μ L of Safe View DNA stain (NBS Biologicals Ltd, NBS-SV) was added.

A3.2. Solutions for Immunohistochemistry and insulin content assay

Table A3.2.1. Sodium Citrate Buffer recipe

Compound	Amount
Tris-sodium citrate (dihydrate)	2.94 g
Distilled water	1000 mL
Tween-20	0.5 mL

pH 6.0, stored at 4 °C.

Table A3.2.2. Acid ethanol recipe

Compound	Amount
95% EtOH	87.5 mL
HCl (37%)	2.5 mL
Distilled water	10 mL

A3.3. Solutions for Western blots

Table A3.3.1. Lysis buffer recipe

Compound	Final concentration
Tris HCl (pH7.5)	20 mM
NaCl	150 mM
Na ₂ EDTA	1 mM
EGTA	1 mM
Triton	1%
Sodium pyrophosphate	2.5 mM
β-glycerophosphate	1 mM
Sodium orthovanadate	1 mM

Made in a total volume of 50 mL with distilled water and 5 tablets of mini protease cocktail inhibitor (Roche, 11836170001) added.

Radioimmunoprecipitation assay (RIPA) lysis buffer

1 tablet of complete mini protease cocktail inhibitor (Roche, 11836170001) was added to every 10 mL of RIPA buffer (Sigma Life Science, R0278-50M) and stored at 4 °C.

Table A3.3.2. SDS Gel Loading buffer recipe

Compound	Final Concentration	Amount
Tris-HCl (pH6.8)	200 mM	2 mL
Dithiothreitol	400 mM	0.6 g
SDS	8%	0.8 g
Glycerol	40%	4 mL
Bromophenol blue		30 mg

Made in a total volume of 10 mL with distilled water. Stored in 1 mL aliquots at -20 °C.

Table A3.3.3. Separating and stacking gel recipes

Compound	10% Separating gel	4% Stacking gel
30% Acrylamide	2.33 mL	400 µL
1.5M Tris Base (pH8.5)	1.75 mL	-
1 M Tris Base (pH6.5)	-	365 µL
5% SDS	140 µL	60 µL
Distilled water	2.723 mL	2.215 mL
TEMED	3.5 µL	2.5 µL
10% _(w/v) APS	53.5 µL	25 µL

Table A3.3.4. 10x Electrophoresis buffer recipe

Compound	Final concentration	Amount
Tris Base	25 mM	30.2 g
Glycine	250 mM	188 g
SDS	0.5%	5 g

Diluted 1:10 for a working 1x solution, stored at room temperature.

Table A3.3.5. Transfer Buffer recipe

Compound	Final concentration	Amount
Tris Base	48 mM	5.82 g
Glycine	39 mM	2.94 g
SDS	0.037%	0.38 g
Distilled water		800 mL
Methanol		200 mL

Stored at 4 °C.

Table A3.3.6. 10x Tris buffered saline (TBS) Washing Buffer recipe

Compound	Amount
Tris base	12.2 g
NaCl	58.4 g
Distilled water	To make 1 L

Diluted 1:10 for a working 1x solution, stored at room temperature. To make Tris buffered saline with Tween-20 (TBST) 1 mL of Tween-20 was added to 1L of 1x TBS.

Bibliography

- ABEL, E. D., PERONI, O., KIM, J. K., KIM, Y. B., BOSS, O., HADRO, E., MINNEMANN, T., SHULMAN, G. I. & KAHN, B. B. 2001. Adipose-selective targeting of the GLUT4 gene impairs insulin action in muscle and liver. *Nature*, 409, 729-33.
- ABUMRAD, N. A., EL-MAGHRABI, M. R., AMRI, E. Z., LOPEZ, E. & GRIMALDI, P. A. 1993. Cloning of a rat adipocyte membrane protein implicated in binding or transport of long-chain fatty acids that is induced during preadipocyte differentiation. Homology with human CD36. *J Biol Chem*, 268, 17665-8.
- ACCILI, D., DRAGO, J., LEE, E. J., JOHNSON, M. D., COOL, M. H., SALVATORE, P., ASICO, L. D., JOSÉ, P. A., TAYLOR, S. I. & WESTPHAL, H. 1996. Early neonatal death in mice homozygous for a null allele of the insulin receptor gene. *Nat Genet*, 12, 106-9.
- ACKERMANN, A. M. & GANNON, M. 2007. Molecular regulation of pancreatic beta-cell mass development, maintenance, and expansion. *J Mol Endocrinol*, 38, 193-206.
- ACOSTA, O., RAMIREZ, V. I., LAGER, S., GACCIOLI, F., DUDLEY, D. J., POWELL, T. L. & JANSSON, T. 2015. Increased glucose and placental GLUT-1 in large infants of obese nondiabetic mothers. *Am J Obstet Gynecol*, 212, 227.e1-7.
- ADAMSON, S. L., LU, Y., WHITELEY, K. J., HOLMYARD, D., HEMBERGER, M., PFARRER, C. & CROSS, J. C. 2002. Interactions between Trophoblast Cells and the Maternal and Fetal Circulation in the Mouse Placenta. *Developmental Biology*, 250, 358-373.
- AGARWAL, P., BRAR, N., MORRISEAU, T. S., KERELIUK, S. M., FONSECA, M. A., COLE, L. K., JHA, A., XIANG, B., HUNT, K. L., SESHADRI, N., HATCH, G. M., DOUCETTE, C. A. & DOLINSKY, V. W. 2019. Gestational Diabetes Adversely Affects Pancreatic Islet Architecture and Function in the Male Rat Offspring. *Endocrinology*, 160, 1907-1925.
- AHMED-SOROOR, H. & BAILEY, C. J. 1981. Role of ovarian hormones in the long-term control of glucose homeostasis, glycogen formation and gluconeogenesis. *Ann Nutr Metab*, 25, 208-12.
- AIKEN, C. E. & OZANNE, S. E. 2013. Sex differences in developmental programming models. *Reproduction*, 145, R1-13.
- AL-JEFOUT, M., ALNAWAISEH, N. & AL-QTAITAT, A. 2017. Insulin resistance and obesity among infertile women with different polycystic ovary syndrome phenotypes. *Sci Rep*, 7, 5339.
- ALBERTI, G., ZIMMET, P., SHAW, J., BLOOMGARDEN, Z., KAUFMAN, F. & SILINK, M. 2004. Type 2 diabetes in the young: the evolving epidemic: the international diabetes federation consensus workshop. *Diabetes Care*, 27, 1798-811.
- ALBERTI, K. G. & ZIMMET, P. Z. 1998. Definition, diagnosis and classification of diabetes mellitus and its complications. Part 1: diagnosis and classification of diabetes mellitus provisional report of a WHO consultation. *Diabet Med*, 15, 539-53.
- ALESSI, D. R., JAMES, S. R., DOWNES, C. P., HOLMES, A. B., GAFFNEY, P. R., REESE, C. B. & COHEN, P. 1997. Characterization of a 3-phosphoinositide-

- dependent protein kinase which phosphorylates and activates protein kinase Balpha. *Curr Biol*, 7, 261-9.
- ALTOBELLI, G., BOGDARINA, I. G., STUPKA, E., CLARK, A. J. & LANGLEY-EVANS, S. 2013. Genome-wide methylation and gene expression changes in newborn rats following maternal protein restriction and reversal by folic acid. *PLoS One*, 8, e82989.
- ANGIOLINI, E., COAN, P. M., SANDOVICI, I., IWAJOMO, O. H., PECK, G., BURTON, G. J., SIBLEY, C. P., REIK, W., FOWDEN, A. L. & CONSTANCIA, M. 2011. Developmental adaptations to increased fetal nutrient demand in mouse genetic models of Igf2-mediated overgrowth. *FASEB J*, 25, 1737-45.
- ANTHONY, T. G. & WEK, R. C. 2012. TXNIP switches tracks toward a terminal UPR. *Cell Metab*, 16, 135-7.
- APPEL, S., GROTHE, J., STORCK, S., JANOSCHEK, R., BAE-GARTZ, I., WOHLFARTH, M., HANDWERK, M., HUCKLENBRUCH-ROTHER, E., GELLHAUS, A. & DÖTSCH, J. 2019. A Potential Role for GSK3 β in Glucose-Driven Intrauterine Catch-Up Growth in Maternal Obesity. *Endocrinology*, 160, 377-386.
- ARAKANE, F., KALLEN, C. B., WATARI, H., FOSTER, J. A., SEPURI, N. B., PAIN, D., STAYROOK, S. E., LEWIS, M., GERTON, G. L. & STRAUSS, J. F., 3RD 1998. The mechanism of action of steroidogenic acute regulatory protein (StAR). StAR acts on the outside of mitochondria to stimulate steroidogenesis. *J Biol Chem*, 273, 16339-45.
- ARENSBURG, J., PAYNE, A. H. & ORLY, J. 1999. Expression of steroidogenic genes in maternal and extraembryonic cells during early pregnancy in mice. *Endocrinology*, 140, 5220-32.
- ARMANI, A., CINTI, F., MARZOLLA, V., MORGAN, J., CRANSTON, G. A., ANTELMINI, A., CARPINELLI, G., CANESE, R., PAGOTTO, U., QUARTA, C., MALORNI, W., MATARRESE, P., MARCONI, M., FABBRI, A., ROSANO, G., CINTI, S., YOUNG, M. J. & CAPRIO, M. 2014. Mineralocorticoid receptor antagonism induces browning of white adipose tissue through impairment of autophagy and prevents adipocyte dysfunction in high-fat-diet-fed mice. *Faseb j*, 28, 3745-57.
- ASAI, M., RAMACHANDRAPPA, S., JOACHIM, M., SHEN, Y., ZHANG, R., NUTHALAPATI, N., RAMANATHAN, V., STROCHLIC, D. E., FERKET, P., LINHART, K., HO, C., NOVOSELOVA, T. V., GARG, S., RIDDERSTRÅLE, M., MARCUS, C., HIRSCHHORN, J. N., KEOGH, J. M., O'RAHILLY, S., CHAN, L. F., CLARK, A. J., FAROOQI, I. S. & MAJZOUB, J. A. 2013. Loss of function of the melanocortin 2 receptor accessory protein 2 is associated with mammalian obesity. *Science*, 341, 275-8.
- AWAD, W. M., JR., WHITNEY, P. L., SKIBA, W. E., MANGUM, J. H. & WELLS, M. S. 1983. Evidence for direct methyl transfer in betaine: homocysteine S-methyltransferase. *J Biol Chem*, 258, 12790-2.
- AYE, I. L., ROSARIO, F. J., POWELL, T. L. & JANSSON, T. 2015. Adiponectin supplementation in pregnant mice prevents the adverse effects of maternal obesity on placental function and fetal growth. *Proc Natl Acad Sci U S A*, 112, 12858-63.
- AYKROYD, B. R. L., TUNSTER, S. J. & SFERRUZZI-PERRI, A. N. 2020. Igf2 deletion alters mouse placenta endocrine capacity in a sexually dimorphic manner. *J Endocrinol*, 246, 93-108.
- AYKROYD, B. R. L., TUNSTER, S. J. & SFERRUZZI-PERRI, A. N. 2021. Loss of imprinting of the Igf2-H19 ICR1 enhances placental endocrine capacity via sex-

- specific alterations in signalling pathways in the mouse. *bioRxiv*, 2021.05.14.444241.
- AYUK, P. T., THEOPHANOUS, D., D'SOUZA, S. W., SIBLEY, C. P. & GLAZIER, J. D. 2002. L-arginine transport by the microvillous plasma membrane of the syncytiotrophoblast from human placenta in relation to nitric oxide production: effects of gestation, preeclampsia, and intrauterine growth restriction. *J Clin Endocrinol Metab*, 87, 747-51.
- BAIN, M. D., COPAS, D. K., LANDON, M. J. & STACEY, T. E. 1988. In vivo permeability of the human placenta to inulin and mannitol. *J Physiol*, 399, 313-9.
- BAKER, J., LIU, J. P., ROBERTSON, E. J. & EFSTRATIADIS, A. 1993. Role of insulin-like growth factors in embryonic and postnatal growth. *Cell*, 75, 73-82.
- BANNON, A. W., SEDA, J., CARMOUCHE, M., FRANCIS, J. M., NORMAN, M. H., KARBON, B. & MCCALEB, M. L. 2000. Behavioral characterization of neuropeptide Y knockout mice. *Brain Res*, 868, 79-87.
- BAO, W., DAR, S., ZHU, Y., WU, J., RAWAL, S., LI, S., WEIR, N. L., TSAI, M. Y. & ZHANG, C. 2018. Plasma concentrations of lipids during pregnancy and the risk of gestational diabetes mellitus: A longitudinal study. *J Diabetes*, 10, 487-495.
- BARAK, Y., NELSON, M. C., ONG, E. S., JONES, Y. Z., RUIZ-LOZANO, P., CHIEN, K. R., KODER, A. & EVANS, R. M. 1999. PPAR gamma is required for placental, cardiac, and adipose tissue development. *Mol Cell*, 4, 585-95.
- BARBOUR, L. A., SHAO, J., QIAO, L., LEITNER, W., ANDERSON, M., FRIEDMAN, J. E. & DRAZNIN, B. 2004. Human placental growth hormone increases expression of the p85 regulatory unit of phosphatidylinositol 3-kinase and triggers severe insulin resistance in skeletal muscle. *Endocrinology*, 145, 1144-50.
- BARKER, D. J. & OSMOND, C. 1986. Infant mortality, childhood nutrition, and ischaemic heart disease in England and Wales. *Lancet*, 1, 1077-81.
- BARTHEL, A. & SCHMOLL, D. 2003. Novel concepts in insulin regulation of hepatic gluconeogenesis. *Am J Physiol Endocrinol Metab*, 285, E685-92.
- BARTOLOMEI, M. S., WEBBER, A. L., BRUNKOW, M. E. & TILGHMAN, S. M. 1993. Epigenetic mechanisms underlying the imprinting of the mouse H19 gene. *Genes Dev*, 7, 1663-73.
- BARTOLOMEI, M. S., ZEMEL, S. & TILGHMAN, S. M. 1991. Parental imprinting of the mouse H19 gene. *Nature*, 351, 153-5.
- BASU-MODAK, S., BRAISSANT, O., ESCHER, P., DESVERGNE, B., HONEGGER, P. & WAHLI, W. 1999. Peroxisome proliferator-activated receptor beta regulates acyl-CoA synthetase 2 in reaggregated rat brain cell cultures. *J Biol Chem*, 274, 35881-8.
- BÉGAY, V., SMINK, J. & LEUTZ, A. 2004. Essential requirement of CCAAT/enhancer binding proteins in embryogenesis. *Mol Cell Biol*, 24, 9744-51.
- BELFIORE, A., FRASCA, F., PANDINI, G., SCIACCA, L. & VIGNERI, R. 2009. Insulin receptor isoforms and insulin receptor/insulin-like growth factor receptor hybrids in physiology and disease. *Endocr Rev*, 30, 586-623.
- BEN-ZIMRA, M., KOLER, M., MELAMED-BOOK, N., ARENSBURG, J., PAYNE, A. H. & ORLY, J. 2002. Uterine and placental expression of steroidogenic genes during rodent pregnancy. *Mol Cell Endocrinol*, 187, 223-31.
- BENATTI, R. O., MELO, A. M., BORGES, F. O., IGNACIO-SOUZA, L. M., SIMINO, L. A., MILANSKI, M., VELLOSO, L. A., TORSONI, M. A. & TORSONI, A. S. 2014. Maternal high-fat diet consumption modulates hepatic lipid metabolism and microRNA-122 (miR-122) and microRNA-370 (miR-370) expression in offspring. *Br J Nutr*, 111, 2112-22.

- BERGHAUS, T. M., DEMMELMAIR, H. & KOLETZKO, B. 2000. Essential fatty acids and their long-chain polyunsaturated metabolites in maternal and cord plasma triglycerides during late gestation. *Biol Neonate*, 77, 96-100.
- BERLINER, C. L., JONES, J. E. & SALHANICK, H. A. 1956. The isolation of adrenal-like steroids from the human placenta. *J Biol Chem*, 223, 1043-53.
- BHADHPRASIT, W., SAKUMA, T., HATAKEYAMA, N., FUWA, M., KITAJIMA, K. & NEMOTO, N. 2007. Involvement of glucocorticoid receptor and pregnane X receptor in the regulation of mouse CYP3A44 female-predominant expression by glucocorticoid hormone. *Drug Metab Dispos*, 35, 1880-5.
- BIRD, A. 2007. Perceptions of epigenetics. *Nature*, 447, 396-8.
- BIRON-SHENTAL, T., SCHAIFF, W. T., RATAJCZAK, C. K., BILDIRICI, I., NELSON, D. M. & SADOVSKY, Y. 2007. Hypoxia regulates the expression of fatty acid-binding proteins in primary term human trophoblasts. *Am J Obstet Gynecol*, 197, 516.e1-6.
- BLASCO, M. J., LÓPEZ BERNAL, A. & TURNBULL, A. C. 1986. 11 beta-Hydroxysteroid dehydrogenase activity of the human placenta during pregnancy. *Horm Metab Res*, 18, 638-41.
- BOILEAU, P., MREJEN, C., GIRARD, J. & HAUGUEL-DE MOUZON, S. 1995. Overexpression of GLUT3 placental glucose transporter in diabetic rats. *J Clin Invest*, 96, 309-17.
- BOOMSMA, C. M., FAUSER, B. C. & MACKLON, N. S. 2008. Pregnancy complications in women with polycystic ovary syndrome. *Semin Reprod Med*, 26, 72-84.
- BOUILLOT, S., RAMPON, C., TILLET, E. & HUBER, P. 2006. Tracing the glycogen cells with protocadherin 12 during mouse placenta development. *Placenta*, 27, 882-8.
- BOULANGÉ, C. L., CLAUS, S. P., CHOU, C. J., COLLINO, S., MONTOLIU, I., KOCHHAR, S., HOLMES, E., REZZI, S., NICHOLSON, J. K., DUMAS, M. E. & MARTIN, F. P. 2013. Early metabolic adaptation in C57BL/6 mice resistant to high fat diet induced weight gain involves an activation of mitochondrial oxidative pathways. *J Proteome Res*, 12, 1956-68.
- BOWMAN, C. E., SELEN ALPERGIN, E. S., CAVAGNINI, K., SMITH, D. M., SCAFIDI, S. & WOLFGANG, M. J. 2019. Maternal Lipid Metabolism Directs Fetal Liver Programming following Nutrient Stress. *Cell Rep*, 29, 1299-1310.e3.
- BRASS, E., HANSON, E. & O'TIERNEY-GINN, P. F. 2013. Placental oleic acid uptake is lower in male offspring of obese women. *Placenta*, 34, 503-9.
- BRAZ, G. R. F., EMILIANO, A. S., SOUSA, S. M., PEDROZA, A. A. S., SANTANA, D. F., FERNANDES, M. P., DA SILVA, A. I. & LAGRANHA, C. J. 2017. Maternal low-protein diet in female rat heart: possible protective effect of estradiol. *J Dev Orig Health Dis*, 8, 322-330.
- BRELJE, T. C., SHARP, D. W., LACY, P. E., OGREN, L., TALAMANTES, F., ROBERTSON, M., FRIESEN, H. G. & SORENSON, R. L. 1993. Effect of homologous placental lactogens, prolactins, and growth hormones on islet B-cell division and insulin secretion in rat, mouse, and human islets: implication for placental lactogen regulation of islet function during pregnancy. *Endocrinology*, 132, 879-87.
- BRIFFA, J. F., O'DOWD, R., ROMANO, T., MUHLHAUSLER, B. S., MORITZ, K. M. & WLODEK, M. E. 2019. Reducing Pup Litter Size Alters Early Postnatal Calcium Homeostasis and Programs Adverse Adult Cardiovascular and Bone Health in Male Rats. *Nutrients*, 11.

- BRINGHENTI, I., ORNELLAS, F., MANDARIM-DE-LACERDA, C. A. & AGUILA, M. B. 2016. The insulin-signaling pathway of the pancreatic islet is impaired in adult mice offspring of mothers fed a high-fat diet. *Nutrition*, 32, 1138-43.
- BROWN, J. M., BETTERS, J. L., LORD, C., MA, Y., HAN, X., YANG, K., ALGER, H. M., MELCHIOR, J., SAWYER, J., SHAH, R., WILSON, M. D., LIU, X., GRAHAM, M. J., LEE, R., CROOKE, R., SHULMAN, G. I., XUE, B., SHI, H. & YU, L. 2010. CGI-58 knockdown in mice causes hepatic steatosis but prevents diet-induced obesity and glucose intolerance. *J Lipid Res*, 51, 3306-15.
- BRUNING, J. C., MICHAEL, M. D., WINNAY, J. N., HAYASHI, T., HORSCH, D., ACCILI, D., GOODYEAR, L. J. & KAHN, C. R. 1998. A muscle-specific insulin receptor knockout exhibits features of the metabolic syndrome of NIDDM without altering glucose tolerance. *Mol Cell*, 2, 559-69.
- BRYZGALOVA, G., GAO, H., AHREN, B., ZIERATH, J. R., GALUSKA, D., STEILER, T. L., DAHLMAN-WRIGHT, K., NILSSON, S., GUSTAFSSON, J. A., EFENDIC, S. & KHAN, A. 2006. Evidence that oestrogen receptor-alpha plays an important role in the regulation of glucose homeostasis in mice: insulin sensitivity in the liver. *Diabetologia*, 49, 588-97.
- BUCKLEY, A. J., KESERU, B., BRIODY, J., THOMPSON, M., OZANNE, S. E. & THOMPSON, C. H. 2005. Altered body composition and metabolism in the male offspring of high fat-fed rats. *Metabolism*, 54, 500-7.
- BURTON, G. J. & FOWDEN, A. L. 2015. The placenta: a multifaceted, transient organ. *Philos Trans R Soc Lond B Biol Sci*, 370, 20140066.
- BURTON, G. J., FOWDEN, A. L. & THORNBURG, K. L. 2016. Placental Origins of Chronic Disease. *Physiol Rev*, 96, 1509-65.
- BURTON, P. J., SMITH, R. E., KROZOWSKI, Z. S. & WADDELL, B. J. 1996. Zonal distribution of 11 beta-hydroxysteroid dehydrogenase types 1 and 2 messenger ribonucleic acid expression in the rat placenta and decidua during late pregnancy. *Biol Reprod*, 55, 1023-8.
- BUSTAMANTE, J. J., COPPLE, B. L., SOARES, M. J. & DAI, G. 2010. Gene profiling of maternal hepatic adaptations to pregnancy. *Liver Int*, 30, 406-15.
- CAI, D., YUAN, M., FRANTZ, D. F., MELENDEZ, P. A., HANSEN, L., LEE, J. & SHOELSON, S. E. 2005. Local and systemic insulin resistance resulting from hepatic activation of IKK-beta and NF-kappaB. *Nat Med*, 11, 183-90.
- CAI, X. & CULLEN, B. R. 2007. The imprinted H19 noncoding RNA is a primary microRNA precursor. *Rna*, 13, 313-6.
- CALATAYUD, M., KOREN, O. & COLLADO, M. C. 2019. Maternal Microbiome and Metabolic Health Program Microbiome Development and Health of the Offspring. *Trends Endocrinol Metab*, 30, 735-744.
- CAMPBELL, F. M., BUSH, P. G., VEERKAMP, J. H. & DUTTA-ROY, A. K. 1998. Detection and cellular localization of plasma membrane-associated and cytoplasmic fatty acid-binding proteins in human placenta. *Placenta*, 19, 409-15.
- CAMPISANO, S. E., ECHARTE, S. M., PODAZA, E. & CHISARI, A. N. 2017. Protein malnutrition during fetal programming induces fatty liver in adult male offspring rats. *J Physiol Biochem*, 73, 275-285.
- CARNEY, E. W., PRIDEAUX, V., LYE, S. J. & ROSSANT, J. 1993. Progressive expression of trophoblast-specific genes during formation of mouse trophoblast giant cells in vitro. *Mol Reprod Dev*, 34, 357-68.
- CARPENTER, C. L. & CANTLEY, L. C. 1996. Phosphoinositide kinases. *Curr Opin Cell Biol*, 8, 153-8.

- CARPENTER, M. W. & COUSTAN, D. R. 1982. Criteria for screening tests for gestational diabetes. *Am J Obstet Gynecol*, 144, 768-73.
- CARVALHO, E., KOTANI, K., PERONI, O. D. & KAHN, B. B. 2005. Adipose-specific overexpression of GLUT4 reverses insulin resistance and diabetes in mice lacking GLUT4 selectively in muscle. *Am J Physiol Endocrinol Metab*, 289, E551-61.
- CATALANO, P. M., MCINTYRE, H. D., CRUICKSHANK, J. K., MCCANCE, D. R., DYER, A. R., METZGER, B. E., LOWE, L. P., TRIMBLE, E. R., COUSTAN, D. R., HADDEN, D. R., PERSSON, B., HOD, M. & OATS, J. J. 2012. The hyperglycemia and adverse pregnancy outcome study: associations of GDM and obesity with pregnancy outcomes. *Diabetes Care*, 35, 780-6.
- CATALANO, P. M., TYZBIR, E. D., WOLFE, R. R., ROMAN, N. M., AMINI, S. B. & SIMS, E. A. 1992. Longitudinal changes in basal hepatic glucose production and suppression during insulin infusion in normal pregnant women. *Am J Obstet Gynecol*, 167, 913-9.
- CHAMBAZ, J., RAVEL, D., MANIER, M. C., PEPIN, D., MULLIEZ, N. & BEREZIAT, G. 1985. Essential fatty acids interconversion in the human fetal liver. *Biol Neonate*, 47, 136-40.
- CHANDLER-LANEY, P. C., BUSH, N. C., GRANGER, W. M., ROUSE, D. J., MANCUSO, M. S. & GOWER, B. A. 2012. Overweight status and intrauterine exposure to gestational diabetes are associated with children's metabolic health. *Pediatr Obes*, 7, 44-52.
- CHAPMAN, K., HOLMES, M. & SECKL, J. 2013. 11 β -hydroxysteroid dehydrogenases: intracellular gate-keepers of tissue glucocorticoid action. *Physiol Rev*, 93, 1139-206.
- CHEN, C., HOSOKAWA, H., BUMBALO, L. M. & LEAHY, J. L. 1994. Mechanism of compensatory hyperinsulinemia in normoglycemic insulin-resistant spontaneously hypertensive rats. Augmented enzymatic activity of glucokinase in beta-cells. *J Clin Invest*, 94, 399-404.
- CHEN, E. Y., TAN, C. M., KOU, Y., DUAN, Q., WANG, Z., MEIRELLES, G. V., CLARK, N. R. & MA'AYAN, A. 2013. Enrichr: interactive and collaborative HTML5 gene list enrichment analysis tool. *BMC Bioinformatics*, 14, 128.
- CHEN, H., LI, Y., SHI, J. & SONG, W. 2016. Role and mechanism of insulin-like growth factor 2 on the proliferation of human trophoblasts in vitro. *J Obstet Gynaecol Res*, 42, 44-51.
- CHEN, S., SUN, F. Z., HUANG, X., WANG, X., TANG, N., ZHU, B. & LI, B. 2015. Assisted reproduction causes placental maldevelopment and dysfunction linked to reduced fetal weight in mice. *Sci Rep*, 5, 10596.
- CHENG, Z., TSENG, Y. & WHITE, M. F. 2010. Insulin signaling meets mitochondria in metabolism. *Trends Endocrinol Metab*, 21, 589-98.
- CHIEN, P. F., SMITH, K., WATT, P. W., SCRIMGEOUR, C. M., TAYLOR, D. J. & RENNIE, M. J. 1993. Protein turnover in the human fetus studied at term using stable isotope tracer amino acids. *Am J Physiol*, 265, E31-5.
- CHIN, E. H., SCHMIDT, K. L., MARTEL, K. M., WONG, C. K., HAMDEN, J. E., GIBSON, W. T., SOMA, K. K. & CHRISTIANS, J. K. 2017. A maternal high-fat, high-sucrose diet has sex-specific effects on fetal glucocorticoids with little consequence for offspring metabolism and voluntary locomotor activity in mice. *PLoS One*, 12, e0174030.
- CHOI, S. B., JANG, J. S. & PARK, S. 2005. Estrogen and exercise may enhance beta-cell function and mass via insulin receptor substrate 2 induction in ovariectomized diabetic rats. *Endocrinology*, 146, 4786-94.

- CHOI, W.-I., JEON, B.-N., PARK, H., YOO, J.-Y., KIM, Y.-S., KOH, D.-I., KIM, M.-H., KIM, Y.-R., LEE, C.-E. & KIM, K.-S. 2008. Proto-oncogene FBI-1 (Pokemon) and SREBP-1 synergistically activate transcription of fatty-acid synthase gene (FASN). *Journal of Biological Chemistry*, 283, 29341-29354.
- CHOWEN, J. A., FRAGO, L. M. & ARGENTE, J. 2004. The regulation of GH secretion by sex steroids. *Eur J Endocrinol*, 151 Suppl 3, U95-100.
- CHRISTOFOROU, E. R. & SFERRUZZI-PERRI, A. N. 2020. Molecular mechanisms governing offspring metabolic programming in rodent models of in utero stress. *Cell Mol Life Sci*, 77, 4861-4898.
- CHUTKOW, W. A., BIRKENFELD, A. L., BROWN, J. D., LEE, H. Y., FREDERICK, D. W., YOSHIOKA, J., PATWARI, P., KURSAWE, R., CUSHMAN, S. W., PLUTZKY, J., SHULMAN, G. I., SAMUEL, V. T. & LEE, R. T. 2010. Deletion of the alpha-arrestin protein Txnip in mice promotes adiposity and adipogenesis while preserving insulin sensitivity. *Diabetes*, 59, 1424-34.
- CHUTKOW, W. A., PATWARI, P., YOSHIOKA, J. & LEE, R. T. 2008. Thioredoxin-interacting protein (Txnip) is a critical regulator of hepatic glucose production. *J Biol Chem*, 283, 2397-406.
- CINDROVA-DAVIES, T., JAUNIAUX, E., ELLIOT, M. G., GONG, S., BURTON, G. J. & CHARNOCK-JONES, D. S. 2017. RNA-seq reveals conservation of function among the yolk sacs of human, mouse, and chicken. *Proc Natl Acad Sci U S A*, 114, E4753-e4761.
- CLEAL, J. K., GLAZIER, J. D., NTANI, G., CROZIER, S. R., DAY, P. E., HARVEY, N. C., ROBINSON, S. M., COOPER, C., GODFREY, K. M., HANSON, M. A. & LEWIS, R. M. 2011. Facilitated transporters mediate net efflux of amino acids to the fetus across the basal membrane of the placental syncytiotrophoblast. *J Physiol*, 589, 987-97.
- CLIFTON, V. L., BISITS, A. & ZARZYCKI, P. K. 2007. Characterization of human fetal cord blood steroid profiles in relation to fetal sex and mode of delivery using temperature-dependent inclusion chromatography and principal component analysis (PCA). *J Chromatogr B Analyt Technol Biomed Life Sci*, 855, 249-54.
- COAN, P. M., ANGIOLINI, E., SANDOVICI, I., BURTON, G. J., CONSTANCIA, M. & FOWDEN, A. L. 2008a. Adaptations in placental nutrient transfer capacity to meet fetal growth demands depend on placental size in mice. *J Physiol*, 586, 4567-76.
- COAN, P. M., BURTON, G. J. & FERGUSON-SMITH, A. C. 2005. Imprinted genes in the placenta--a review. *Placenta*, 26 Suppl A, S10-20.
- COAN, P. M., CONROY, N., BURTON, G. J. & FERGUSON-SMITH, A. C. 2006. Origin and characteristics of glycogen cells in the developing murine placenta. *Dev Dyn*, 235, 3280-94.
- COAN, P. M., FERGUSON-SMITH, A. C. & BURTON, G. J. 2004. Developmental dynamics of the definitive mouse placenta assessed by stereology. *Biol Reprod*, 70, 1806-13.
- COAN, P. M., FOWDEN, A. L., CONSTANCIA, M., FERGUSON-SMITH, A. C., BURTON, G. J. & SIBLEY, C. P. 2008b. Disproportional effects of Igf2 knockout on placental morphology and diffusional exchange characteristics in the mouse. *J Physiol*, 586, 5023-32.
- COLE, T. J., BLENDY, J. A., MONAGHAN, A. P., KRIEGLSTEIN, K., SCHMID, W., AGUZZI, A., FANTUZZI, G., HUMMLER, E., UNSICKER, K. & SCHÜTZ, G. 1995. Targeted disruption of the glucocorticoid receptor gene blocks adrenergic

- chromaffin cell development and severely retards lung maturation. *Genes Dev*, 9, 1608-21.
- CONNOR, K. L., KIBSCHULL, M., MATYSIAK-ZABLOCKI, E., NGUYEN, T. T. N., MATTHEWS, S. G., LYE, S. J. & BLOISE, E. 2020. Maternal malnutrition impacts placental morphology and transporter expression: an origin for poor offspring growth. *J Nutr Biochem*, 78, 108329.
- CONSTANCIA, M., ANGIOLINI, E., SANDOVICI, I., SMITH, P., SMITH, R., KELSEY, G., DEAN, W., FERGUSON-SMITH, A., SIBLEY, C. P., REIK, W. & FOWDEN, A. 2005. Adaptation of nutrient supply to fetal demand in the mouse involves interaction between the Igf2 gene and placental transporter systems. *Proc Natl Acad Sci U S A*, 102, 19219-24.
- CONSTÂNCIA, M., DEAN, W., LOPES, S., MOORE, T., KELSEY, G. & REIK, W. 2000. Deletion of a silencer element in Igf2 results in loss of imprinting independent of H19. *Nat Genet*, 26, 203-6.
- CONSTANCIA, M., HEMBERGER, M., HUGHES, J., DEAN, W., FERGUSON-SMITH, A., FUNDELE, R., STEWART, F., KELSEY, G., FOWDEN, A., SIBLEY, C. & REIK, W. 2002. Placental-specific IGF-II is a major modulator of placental and fetal growth. *Nature*, 417, 945-8.
- COSTEA, D. M., GUNN, L. K., HARGREAVES, C., HOWELL, R. J. & CHARD, T. 2000. Delayed luteo-placental shift of progesterone production in IVF pregnancy. *Int J Gynaecol Obstet*, 68, 123-9.
- COSTRINI, N. V. & KALKHOFF, R. K. 1971. Relative effects of pregnancy, estradiol, and progesterone on plasma insulin and pancreatic islet insulin secretion. *J Clin Invest*, 50, 992-9.
- COULOMBE, P. A. & OMARY, M. B. 2002. 'Hard' and 'soft' principles defining the structure, function and regulation of keratin intermediate filaments. *Curr Opin Cell Biol*, 14, 110-22.
- CRAMER, S., BEVERIDGE, M., KILBERG, M. & NOVAK, D. 2002. Physiological importance of system A-mediated amino acid transport to rat fetal development. *Am J Physiol Cell Physiol*, 282, C153-60.
- CRAWFORD, L. W., FOLEY, J. F. & ELMORE, S. A. 2010. Histology atlas of the developing mouse hepatobiliary system with emphasis on embryonic days 9.5-18.5. *Toxicol Pathol*, 38, 872-906.
- CROSS, D. A., ALESSI, D. R., COHEN, P., ANDJELKOVICH, M. & HEMMINGS, B. A. 1995. Inhibition of glycogen synthase kinase-3 by insulin mediated by protein kinase B. *Nature*, 378, 785-9.
- CROSSON, S. M., KHAN, A., PRINTEN, J., PESSIN, J. E. & SALTIEL, A. R. 2003. PTG gene deletion causes impaired glycogen synthesis and developmental insulin resistance. *J Clin Invest*, 111, 1423-32.
- CSAPO, A. I., PULKKINEN, M. O., RUTTNER, B., SAUVAGE, J. P. & WIEST, W. G. 1972. The significance of the human corpus luteum in pregnancy maintenance. I. Preliminary studies. *Am J Obstet Gynecol*, 112, 1061-7.
- CSAPO, A. I., PULKKINEN, M. O. & WIEST, W. G. 1973. Effects of luteectomy and progesterone replacement therapy in early pregnant patients. *Am J Obstet Gynecol*, 115, 759-65.
- CSAPO, A. I. & WIEST, W. G. 1973. Plasma steroid levels and ovariectomy-induced placental hypertrophy in rats. *Endocrinology*, 93, 1173-7.
- CUSIN, I., TERRETTAZ, J., ROHNER-JEANRENAUD, F. & JEANRENAUD, B. 1990. Metabolic consequences of hyperinsulinaemia imposed on normal rats on

- glucose handling by white adipose tissue, muscles and liver. *Biochem J*, 267, 99-103.
- DABELEA, D. 2007. The predisposition to obesity and diabetes in offspring of diabetic mothers. *Diabetes Care*, 30 Suppl 2, S169-74.
- DAHLHOFF, M., PFISTER, S., BLUTKE, A., ROZMAN, J., KLINGENSPOR, M., DEUTSCH, M. J., RATHKOLB, B., FINK, B., GIMPFL, M., HRABĚ DE ANGELIS, M., ROSCHER, A. A., WOLF, E. & ENSENAUER, R. 2014. Periconceptional obesogenic exposure induces sex-specific programming of disease susceptibilities in adult mouse offspring. *Biochim Biophys Acta*, 1842, 304-17.
- DAHRI, S., SNOECK, A., REUSENS-BILLEN, B., REMACLE, C. & HOET, J. J. 1991. Islet function in offspring of mothers on low-protein diet during gestation. *Diabetes*, 40 Suppl 2, 115-20.
- DAYA, S. 1989. Efficacy of progesterone support for pregnancy in women with recurrent miscarriage. A meta-analysis of controlled trials. *Br J Obstet Gynaecol*, 96, 275-80.
- DE COURCY, C., GRAY, C. H. & LUNNON, J. B. 1952. Adrenal cortical hormones in human placenta. *Nature*, 170, 494.
- DE PAULA SIMINO, L. A., DE FANTE, T., FIGUEIREDO FONTANA, M., OLIVEIRA BORGES, F., TORSONI, M. A., MILANSKI, M., VELLOSO, L. A. & SOUZA TORSONI, A. 2017. Lipid overload during gestation and lactation can independently alter lipid homeostasis in offspring and promote metabolic impairment after new challenge to high-fat diet. *Nutr Metab (Lond)*, 14, 16.
- DECHIARA, T. M., ROBERTSON, E. J. & EFSTRATIADIS, A. 1991. Parental imprinting of the mouse insulin-like growth factor II gene. *Cell*, 64, 849-59.
- DEL RINCON, J. P., IIDA, K., GAYLINN, B. D., MCCURDY, C. E., LEITNER, J. W., BARBOUR, L. A., KOPCHICK, J. J., FRIEDMAN, J. E., DRAZNIN, B. & THORNER, M. O. 2007. Growth hormone regulation of p85alpha expression and phosphoinositide 3-kinase activity in adipose tissue: mechanism for growth hormone-mediated insulin resistance. *Diabetes*, 56, 1638-46.
- DELAHAYE, F., LUKASZEWSKI, M. A., WATTEZ, J. S., CISSE, O., DUTRIEZ-CASTELOOT, I., FAJARDY, I., MONTEL, V., DICKES-COOPMAN, A., LABORIE, C., LESAGE, J., BRETON, C. & VIEAU, D. 2010. Maternal perinatal undernutrition programs a "brown-like" phenotype of gonadal white fat in male rat at weaning. *Am J Physiol Regul Integr Comp Physiol*, 299, R101-10.
- DENG, S., VATAMANIUK, M., HUANG, X., DOLIBA, N., LIAN, M. M., FRANK, A., VELIDEDEOGLU, E., DESAI, N. M., KOEBERLEIN, B., WOLF, B., BARKER, C. F., NAJI, A., MATSCHINSKY, F. M. & MARKMANN, J. F. 2004. Structural and functional abnormalities in the islets isolated from type 2 diabetic subjects. *Diabetes*, 53, 624-32.
- DENG, X., ZHANG, W., I, O. S., WILLIAMS, J. B., DONG, Q., PARK, E. A., RAGHOW, R., UNTERMAN, T. G. & ELAM, M. B. 2012. FoxO1 inhibits sterol regulatory element-binding protein-1c (SREBP-1c) gene expression via transcription factors Sp1 and SREBP-1c. *J Biol Chem*, 287, 20132-43.
- DENISOVA, E. I., KOZHEVNIKOVA, V. V., BAZHAN, N. M. & MAKAROVA, E. N. 2020. Sex-specific effects of leptin administration to pregnant mice on the placentae and the metabolic phenotypes of offspring. *FEBS Open Bio*, 10, 96-106.
- DESAI, M., GAYLE, D., BABU, J. & ROSS, M. G. 2005a. Permanent reduction in heart and kidney organ growth in offspring of undernourished rat dams. *Am J Obstet Gynecol*, 193, 1224-32.

- DESAI, M., GAYLE, D., BABU, J. & ROSS, M. G. 2005b. Programmed obesity in intrauterine growth-restricted newborns: modulation by newborn nutrition. *Am J Physiol Regul Integr Comp Physiol*, 288, R91-6.
- DESAI, M., JELLYMAN, J. K., HAN, G., LANE, R. H. & ROSS, M. G. 2015. Programmed regulation of rat offspring adipogenic transcription factor (PPAR γ) by maternal nutrition. *J Dev Orig Health Dis*, 6, 530-8.
- DESERGNE, B. & WAHLI, W. 1999. Peroxisome proliferator-activated receptors: nuclear control of metabolism. *Endocr Rev*, 20, 649-88.
- DI SIMONE, N., DI NICUOLO, F., MARZIONI, D., CASTELLUCCI, M., SANGUINETTI, M., D'LEPOLITO, S. & CARUSO, A. 2009. Resistin modulates glucose uptake and glucose transporter-1 (GLUT-1) expression in trophoblast cells. *Journal of cellular and molecular medicine*, 13, 388-397.
- DIAZ, R., BROWN, R. W. & SECKL, J. R. 1998. Distinct ontogeny of glucocorticoid and mineralocorticoid receptor and 11 β -hydroxysteroid dehydrogenase types I and II mRNAs in the fetal rat brain suggest a complex control of glucocorticoid actions. *J Neurosci*, 18, 2570-80.
- DILWORTH, M. R., KUSINSKI, L. C., COWLEY, E., WARD, B. S., HUSAIN, S. M., CONSTÂNCIA, M., SIBLEY, C. P. & GLAZIER, J. D. 2010. Placental-specific Igf2 knockout mice exhibit hypocalcemia and adaptive changes in placental calcium transport. *Proc Natl Acad Sci U S A*, 107, 3894-9.
- DIMASUAY, K. G., BOEUF, P., POWELL, T. L. & JANSSON, T. 2016. Placental Responses to Changes in the Maternal Environment Determine Fetal Growth. *Front Physiol*, 7, 12.
- DING, W. G., KITASATO, H. & KIMURA, H. 1997. Development of neuropeptide Y innervation in the liver. *Microsc Res Tech*, 39, 365-71.
- DOMINICI, F. P., CIFONE, D., BARTKE, A. & TURYN, D. 1999. Loss of sensitivity to insulin at early events of the insulin signaling pathway in the liver of growth hormone-transgenic mice. *J Endocrinol*, 161, 383-92.
- DONG, H. P., TAN, M. Z., LIU, Q. J., WANG, J. & ZHONG, S. B. 2017. The study on the effect of hyperglycemia on offspring fatty tissue metabolism during pregnancy. *Eur Rev Med Pharmacol Sci*, 21, 3658-3664.
- DONG, X. C., COPPS, K. D., GUO, S., LI, Y., KOLLIPARA, R., DEPINHO, R. A. & WHITE, M. F. 2008. Inactivation of hepatic Foxo1 by insulin signaling is required for adaptive nutrient homeostasis and endocrine growth regulation. *Cell Metab*, 8, 65-76.
- DOR, Y., BROWN, J., MARTINEZ, O. I. & MELTON, D. A. 2004. Adult pancreatic beta-cells are formed by self-duplication rather than stem-cell differentiation. *Nature*, 429, 41-6.
- DUBÉ, E., GRAVEL, A., MARTIN, C., DESPAROIS, G., MOUSSA, I., ETHIER-CHIASSE, M., FOREST, J. C., GIGUÈRE, Y., MASSE, A. & LAFOND, J. 2012. Modulation of fatty acid transport and metabolism by maternal obesity in the human full-term placenta. *Biol Reprod*, 87, 14, 1-11.
- DUDLEY, D. J., BRANCH, D. W., EDWIN, S. S. & MITCHELL, M. D. 1996. Induction of preterm birth in mice by RU486. *Biol Reprod*, 55, 992-5.
- DUDLEY, K. J., SLOBODA, D. M., CONNOR, K. L., BELTRAND, J. & VICKERS, M. H. 2011. Offspring of mothers fed a high fat diet display hepatic cell cycle inhibition and associated changes in gene expression and DNA methylation. *PLoS One*, 6, e21662.
- DUMOLT, J. H., MA, M., MATHEW, J., PATEL, M. S. & RIDEOUT, T. C. 2019. Gestational hypercholesterolemia alters fetal hepatic lipid metabolism and

- microRNA expression in Apo-E-deficient mice. *Am J Physiol Endocrinol Metab*, 317, E831-e838.
- DUMORTIER, O., ROGER, E., PISANI, D. F., CASAMENTO, V., GAUTIER, N., LEBRUN, P., JOHNSTON, H., LOPEZ, P., AMRI, E. Z., JOUSSE, C., FAFOURNOUX, P., PRENTKI, M., HINAULT, C. & VAN OBERGHEN, E. 2017. Age-Dependent Control of Energy Homeostasis by Brown Adipose Tissue in Progeny Subjected to Maternal Diet-Induced Fetal Programming. *Diabetes*, 66, 627-639.
- DUVAL, F., SANTOS, E. D., POIDATZ, D., SERAZIN, V., GRONIER, H., VIALARD, F. & DIEUDONNE, M. N. 2016. Adiponectin Inhibits Nutrient Transporters and Promotes Apoptosis in Human Villous Cytotrophoblasts: Involvement in the Control of Fetal Growth. *Biol Reprod*, 94, 111.
- ECK, M. J., SHOELSON, S. E. & HARRISON, S. C. 1993. Recognition of a high-affinity phosphotyrosyl peptide by the Src homology-2 domain of p56lck. *Nature*, 362, 87-91.
- EHRENBERG, H. M., MERCER, B. M. & CATALANO, P. M. 2004. The influence of obesity and diabetes on the prevalence of macrosomia. *Am J Obstet Gynecol*, 191, 964-8.
- EISENSTEIN, A. B., STRACK, I. & STEINER, A. 1974. Increased hepatic gluconeogenesis without a rise of glucagon secretion in rats fed a high fat diet. *Diabetes*, 23, 869-75.
- EMILSSON, V., LIU, Y. L., CAWTHORNE, M. A., MORTON, N. M. & DAVENPORT, M. 1997. Expression of the functional leptin receptor mRNA in pancreatic islets and direct inhibitory action of leptin on insulin secretion. *Diabetes*, 46, 313-6.
- ENERBACK, S. & GIMBLE, J. M. 1993. Lipoprotein lipase gene expression: physiological regulators at the transcriptional and post-transcriptional level. *Biochim Biophys Acta*, 1169, 107-25.
- ESAKOFF, T. F., CHENG, Y. W., SPARKS, T. N. & CAUGHEY, A. B. 2009. The association between birthweight 4000 g or greater and perinatal outcomes in patients with and without gestational diabetes mellitus. *Am J Obstet Gynecol*, 200, 672.e1-4.
- ESQUILIANO, D. R., GUO, W., LIANG, L., DIKES, P. & LOPEZ, M. F. 2009. Placental glycogen stores are increased in mice with H19 null mutations but not in those with insulin or IGF type 1 receptor mutations. *Placenta*, 30, 693-9.
- EVANS, R. M., BARISH, G. D. & WANG, Y. X. 2004. PPARs and the complex journey to obesity. *Nat Med*, 10, 355-61.
- FANTE, T., SIMINO, L. A., REGINATO, A., PAYOLLA, T. B., VITORELI, D. C., SOUZA, M., TORSONI, M. A., MILANSKI, M. & TORSONI, A. S. 2016. Diet-Induced Maternal Obesity Alters Insulin Signalling in Male Mice Offspring Rechallenged with a High-Fat Diet in Adulthood. *PLoS One*, 11, e0160184.
- FERLAND-MCCOLLOUGH, D., FERNANDEZ-TWINN, D. S., CANNELL, I. G., DAVID, H., WARNER, M., VAAG, A. A., BORK-JENSEN, J., BRONS, C., GANT, T. W., WILLIS, A. E., SIDDLE, K., BUSHHELL, M. & OZANNE, S. E. 2012. Programming of adipose tissue miR-483-3p and GDF-3 expression by maternal diet in type 2 diabetes. *Cell Death Differ*, 19, 1003-12.
- FERNANDEZ-TWINN, D. S., ALFARADHI, M. Z., MARTIN-GRONERT, M. S., DUQUE-GUIMARAES, D. E., PIEKARZ, A., FERLAND-MCCOLLOUGH, D., BUSHHELL, M. & OZANNE, S. E. 2014. Downregulation of IRS-1 in adipose

- tissue of offspring of obese mice is programmed cell-autonomously through post-transcriptional mechanisms. *Mol Metab*, 3, 325-33.
- FERNANDEZ-TWINN, D. S., HJORT, L., NOVAKOVIC, B., OZANNE, S. E. & SAFFERY, R. 2019. Intrauterine programming of obesity and type 2 diabetes. *Diabetologia*, 62, 1789-1801.
- FERRE, P., PEGORIER, J. P., WILLIAMSON, D. H. & GIRARD, J. 1979. Interactions in vivo between oxidation of non-esterified fatty acids and gluconeogenesis in the newborn rat. *Biochem J*, 182, 593-8.
- FICKERT, P., ZOLLNER, G., FUCHSBICHLER, A., STUMPTNER, C., POJER, C., ZENZ, R., LAMMERT, F., STIEGER, B., MEIER, P. J., ZATLOUKAL, K., DENK, H. & TRAUNER, M. 2001. Effects of ursodeoxycholic and cholic acid feeding on hepatocellular transporter expression in mouse liver. *Gastroenterology*, 121, 170-83.
- FISHER, J. J., VANDERPEET, C. L., BARTHO, L. A., MCKEATING, D. R., CUFFE, J. S. M., HOLLAND, O. J. & PERKINS, A. V. 2020. Mitochondrial dysfunction in placental trophoblast cells experiencing gestational diabetes mellitus. *J Physiol*.
- FOLCH, J., LEES, M. & SLOANE STANLEY, G. H. 1957. A simple method for the isolation and purification of total lipides from animal tissues. *J Biol Chem*, 226, 497-509.
- FORBES, K., WESTWOOD, M., BAKER, P. N. & APLIN, J. D. 2008. Insulin-like growth factor I and II regulate the life cycle of trophoblast in the developing human placenta. *Am J Physiol Cell Physiol*, 294, C1313-22.
- FORNES, D., WHITE, V., HIGA, R., HEINECKE, F., CAPOBIANCO, E. & JAWERBAUM, A. 2018. Sex-dependent changes in lipid metabolism, PPAR pathways and microRNAs that target PPARs in the fetal liver of rats with gestational diabetes. *Mol Cell Endocrinol*, 461, 12-21.
- FOWDEN, A. L., COAN, P. M., ANGIOLINI, E., BURTON, G. J. & CONSTANCIA, M. 2011. Imprinted genes and the epigenetic regulation of placental phenotype. *Prog Biophys Mol Biol*, 106, 281-8.
- FOWDEN, A. L. & FORHEAD, A. J. 2004. Endocrine mechanisms of intrauterine programming. *Reproduction*, 127, 515-26.
- FOWDEN, A. L., FORHEAD, A. J., SFERRUZZI-PERRI, A. N., BURTON, G. J. & VAUGHAN, O. R. 2015. Review: Endocrine regulation of placental phenotype. *Placenta*, 36 Suppl 1, S50-9.
- FOWDEN, A. L., GIUSSANI, D. A. & FORHEAD, A. J. 2006. Intrauterine programming of physiological systems: causes and consequences. *Physiology (Bethesda)*, 21, 29-37.
- FOWDEN, A. L. & MOORE, T. 2012. Maternal-fetal resource allocation: co-operation and conflict. *Placenta*, 33 Suppl 2, e11-5.
- FRAENKEL-CONRAT, H. L., HERRING, V. V., SIMPSON, M. E. & EVANS, H. M. 1941. Mechanism of Action of Estrogens on Insulin Content of the Rat's Pancreas. *Proceedings of the Society for Experimental Biology and Medicine*, 48, 333-337.
- FRANKO, K. L., FORHEAD, A. J. & FOWDEN, A. L. 2010. Differential effects of prenatal stress and glucocorticoid administration on postnatal growth and glucose metabolism in rats. *J Endocrinol*, 204, 319-29.
- FRANKO, K. L., FORHEAD, A. J. & FOWDEN, A. L. 2017. Effects of stress during pregnancy on hepatic glucogenic capacity in rat dams and their fetuses. *Physiol Rep*, 5.

- FRATTALI, A. L. & PESSIN, J. E. 1993. Relationship between alpha subunit ligand occupancy and beta subunit autophosphorylation in insulin/insulin-like growth factor-1 hybrid receptors. *J Biol Chem*, 268, 7393-400.
- FRIEDMAN, Z., DANON, A., LAMBERTH, E. L., JR. & MANN, W. J. 1978. Cord blood fatty acid composition in infants and in their mothers during the third trimester. *J Pediatr*, 92, 461-6.
- FU, Q., YU, X., CALLAWAY, C. W., LANE, R. H. & MCKNIGHT, R. A. 2009. Epigenetics: intrauterine growth retardation (IUGR) modifies the histone code along the rat hepatic IGF-1 gene. *Faseb j*, 23, 2438-49.
- FUKASAWA, Y., SEGAWA, H., KIM, J. Y., CHAIROUNGDU, A., KIM, D. K., MATSUO, H., CHA, S. H., ENDOU, H. & KANAI, Y. 2000. Identification and characterization of a Na(+)-independent neutral amino acid transporter that associates with the 4F2 heavy chain and exhibits substrate selectivity for small neutral D- and L-amino acids. *J Biol Chem*, 275, 9690-8.
- GACCIOLI, F., AYE, I. L., ROOS, S., LAGER, S., RAMIREZ, V. I., KANAI, Y., POWELL, T. L. & JANSSON, T. 2015. Expression and functional characterisation of System L amino acid transporters in the human term placenta. *Reprod Biol Endocrinol*, 13, 57.
- GAITHER, K., QURAIISHI, A. N. & ILLSLEY, N. P. 1999. Diabetes alters the expression and activity of the human placental GLUT1 glucose transporter. *J Clin Endocrinol Metab*, 84, 695-701.
- GALLOU-KABANI, C., GABORY, A., TOST, J., KARIMI, M., MAYEUR, S., LESAGE, J., BOUDADI, E., GROSS, M. S., TAURELLE, J., VIGÉ, A., BRETON, C., REUSENS, B., REMACLE, C., VIEAU, D., EKSTRÖM, T. J., JAIS, J. P. & JUNIEN, C. 2010. Sex- and diet-specific changes of imprinted gene expression and DNA methylation in mouse placenta under a high-fat diet. *PLoS One*, 5, e14398.
- GALYON, K. D., FARSHIDI, F., HAN, G., ROSS, M. G., DESAI, M. & JELLYMAN, J. K. 2017. Maternal bisphenol A exposure alters rat offspring hepatic and skeletal muscle insulin signaling protein abundance. *Am J Obstet Gynecol*, 216, 290.e1-290.e9.
- GARDNER, M. O., GOLDENBERG, R. L., CLIVER, S. P., BOOTS, L. R. & HOFFMAN, H. J. 1997. Maternal serum concentrations of human placental lactogen, estradiol and pregnancy specific beta 1-glycoprotein and fetal growth retardation. *Acta Obstet Gynecol Scand Suppl*, 165, 56-8.
- GASPARINI, S. J., SWARBRICK, M. M., KIM, S., THAI, L. J., HENNEICKE, H., CAVANAGH, L. L., TU, J., WEBER, M. C., ZHOU, H. & SEIBEL, M. J. 2019. Androgens sensitise mice to glucocorticoid-induced insulin resistance and fat accumulation. *Diabetologia*, 62, 1463-1477.
- GE, Z. J., LIANG, Q. X., HOU, Y., HAN, Z. M., SCHATTE, H., SUN, Q. Y. & ZHANG, C. L. 2014a. Maternal obesity and diabetes may cause DNA methylation alteration in the spermatozoa of offspring in mice. *Reprod Biol Endocrinol*, 12, 29.
- GE, Z. J., LUO, S. M., LIN, F., LIANG, Q. X., HUANG, L., WEI, Y. C., HOU, Y., HAN, Z. M., SCHATTE, H. & SUN, Q. Y. 2014b. DNA methylation in oocytes and liver of female mice and their offspring: effects of high-fat-diet-induced obesity. *Environ Health Perspect*, 122, 159-64.
- GEORGE, G., DRAYCOTT, S. A. V., MUIR, R., CLIFFORD, B., ELMES, M. J. & LANGLEY-EVANS, S. C. 2019. Exposure to maternal obesity during suckling

- outweighs in utero exposure in programming for post-weaning adiposity and insulin resistance in rats. *Sci Rep*, 9, 10134.
- GEORGIA, S. & BHUSHAN, A. 2004. Beta cell replication is the primary mechanism for maintaining postnatal beta cell mass. *J Clin Invest*, 114, 963-8.
- GEORGIADES, P., FERGUSON-SMITH, A. C. & BURTON, G. J. 2002. Comparative developmental anatomy of the murine and human definitive placentae. *Placenta*, 23, 3-19.
- GIBB, F. W., HOMER, N. Z., FAQEHI, A. M., UPRETI, R., LIVINGSTONE, D. E., MCINNES, K. J., ANDREW, R. & WALKER, B. R. 2016. Aromatase Inhibition Reduces Insulin Sensitivity in Healthy Men. *J Clin Endocrinol Metab*, 101, 2040-6.
- GIBNEY, E. R. & NOLAN, C. M. 2010. Epigenetics and gene expression. *Heredity (Edinb)*, 105, 4-13.
- GICQUEL, C., ROSSIGNOL, S., CABROL, S., HOUANG, M., STEUNOU, V., BARBU, V., DANTON, F., THIBAUD, N., LE MERRER, M. & BURGLIN, L. 2005. Epimutation of the telomeric imprinting center region on chromosome 11p15 in Silver-Russell syndrome. *Nature genetics*, 37, 1003-1007.
- GINGRICH, J., TICIANI, E. & VEIGA-LOPEZ, A. 2020. Placenta Disrupted: Endocrine Disrupting Chemicals and Pregnancy. *Trends Endocrinol Metab*, 31, 508-524.
- GLAZIER, J. D., CETIN, I., PERUGINO, G., RONZONI, S., GREY, A. M., MAHENDRAN, D., MARCONI, A. M., PARDI, G. & SIBLEY, C. P. 1997. Association between the activity of the system A amino acid transporter in the microvillous plasma membrane of the human placenta and severity of fetal compromise in intrauterine growth restriction. *Pediatr Res*, 42, 514-9.
- GOHIR, W., KENNEDY, K. M., WALLACE, J. G., SAOI, M., BELLISSIMO, C. J., BRITZ-MCKIBBIN, P., PETRIK, J. J., SURETTE, M. G. & SLOBODA, D. M. 2019. High-fat diet intake modulates maternal intestinal adaptations to pregnancy and results in placental hypoxia, as well as altered fetal gut barrier proteins and immune markers. *J Physiol*, 597, 3029-3051.
- GOLDBERG, I. J., LE, N.-A., GINSBERG, H. N., KRAUSS, R. M. & LINDGREN, F. 1988. Lipoprotein metabolism during acute inhibition of lipoprotein lipase in the cynomolgus monkey. *The Journal of clinical investigation*, 81, 561-568.
- GONZÁLEZ, C., ALONSO, A., GRUESO, N. A., DÍAZ, F., ESTEBAN, M. M., FERNÁNDEZ, S. & PATTERSON, A. M. 2002. Role of 17beta-estradiol administration on insulin sensitivity in the rat: implications for the insulin receptor. *Steroids*, 67, 993-1005.
- GOSHEN, R., RACHMILEWITZ, J., SCHNEIDER, T., DE-GROOT, N., ARIEL, I., PALTI, Z. & HOCHBERG, A. A. 1993. The expression of the H-19 and IGF-2 genes during human embryogenesis and placental development. *Mol Reprod Dev*, 34, 374-9.
- GROENEWEG, F. L., KARST, H., DE KLOET, E. R. & JOELS, M. 2012. Mineralocorticoid and glucocorticoid receptors at the neuronal membrane, regulators of nongenomic corticosteroid signalling. *Mol Cell Endocrinol*, 350, 299-309.
- GROSS, D. N., VAN DEN HEUVEL, A. P. & BIRNBAUM, M. J. 2008. The role of FoxO in the regulation of metabolism. *Oncogene*, 27, 2320-36.
- GUILLAUME, M., HANDGRAAF, S., FABRE, A., RAYMOND-LETRON, I., RIAN, E., MONTAGNER, A., VINEL, A., BUSCATO, M., SMIRNOVA, N., FONTAINE, C., GUILLOU, H., ARNAL, J. F. & GOURDY, P. 2017. Selective Activation of Estrogen Receptor alpha Activation Function-1 Is Sufficient to

- Prevent Obesity, Steatosis, and Insulin Resistance in Mouse. *Am J Pathol*, 187, 1273-1287.
- GUILLAUME, M., RIAN, E., FABRE, A., RAYMOND-LETRON, I., BUSCATO, M., DAVEZAC, M., TRAMUNT, B., MONTAGNER, A., SMATI, S., ZAHREDDINE, R., PALIERNE, G., VALERA, M. C., GUILLOU, H., LENFANT, F., UNSICKER, K., METIVIER, R., FONTAINE, C., ARNAL, J. F. & GOURDY, P. 2019. Selective Liver Estrogen Receptor alpha Modulation Prevents Steatosis, Diabetes, and Obesity Through the Anorectic Growth Differentiation Factor 15 Hepatokine in Mice. *Hepatology*, 3, 908-924.
- GUO, J., FANG, M., ZHUANG, S., QIAO, Y., HUANG, W., GONG, Q., XU, D., ZHANG, Y. & WANG, H. 2020. Prenatal dexamethasone exposure exerts sex-specific effect on placental oxygen and nutrient transport ascribed to the differential expression of IGF2. *Annals of Translational Medicine*, 8.
- GUPTA, M., GUPTA, S. K., BALLIET, A. G., HOLLANDER, M. C., FORNACE, A. J., HOFFMAN, B. & LIEBERMANN, D. A. 2005. Hematopoietic cells from Gadd45a- and Gadd45b-deficient mice are sensitized to genotoxic-stress-induced apoptosis. *Oncogene*, 24, 7170-9.
- GUZELOGLU-KAYISLI, O., KAYISLI, U. A. & TAYLOR, H. S. 2009. The role of growth factors and cytokines during implantation: endocrine and paracrine interactions. *Semin Reprod Med*, 27, 62-79.
- GWYNNE, J. T. & STRAUSS, J. F., 3RD 1982. The role of lipoproteins in steroidogenesis and cholesterol metabolism in steroidogenic glands. *Endocr Rev*, 3, 299-329.
- HAGGARTY, P., ASHTON, J., JOYNSON, M., ABRAMOVICH, D. R. & PAGE, K. 1999. Effect of maternal polyunsaturated fatty acid concentration on transport by the human placenta. *Biol Neonate*, 75, 350-9.
- HAGGARTY, P., PAGE, K., ABRAMOVICH, D. R., ASHTON, J. & BROWN, D. 1997. Long-chain polyunsaturated fatty acid transport across the perfused human placenta. *Placenta*, 18, 635-42.
- HALES, C. N. & BARKER, D. J. 1992. Type 2 (non-insulin-dependent) diabetes mellitus: the thrifty phenotype hypothesis. *Diabetologia*, 35, 595-601.
- HALES, C. N., BARKER, D. J., CLARK, P. M., COX, L. J., FALL, C., OSMOND, C. & WINTER, P. D. 1991. Fetal and infant growth and impaired glucose tolerance at age 64. *Bmj*, 303, 1019-22.
- HALES, C. N., DESAI, M., OZANNE, S. E. & CROWTHER, N. J. 1996. Fishing in the stream of diabetes: from measuring insulin to the control of fetal organogenesis. *Biochem Soc Trans*, 24, 341-50.
- HALES, C. N. & OZANNE, S. E. 2003. The dangerous road of catch-up growth. *The Journal of physiology*, 547, 5-10.
- HANDA, R. J., BURGESS, L. H., KERR, J. E. & O'KEEFE, J. A. 1994. Gonadal Steroid Hormone Receptors and Sex Differences in the Hypothalamo-Pituitary-Adrenal Axis. *Hormones and Behavior*, 28, 464-476.
- HANDWERGER, S. & FREEMARK, M. 2000. The roles of placental growth hormone and placental lactogen in the regulation of human fetal growth and development. *J Pediatr Endocrinol Metab*, 13, 343-56.
- HARDT, P. D. & EWALD, N. 2011. Exocrine pancreatic insufficiency in diabetes mellitus: a complication of diabetic neuropathy or a different type of diabetes? *Exp Diabetes Res*, 2011, 761950.
- HARRINGTON, L. S., FINDLAY, G. M., GRAY, A., TOLKACHEVA, T., WIGFIELD, S., REBHOLZ, H., BARNETT, J., LESLIE, N. R., CHENG, S., SHEPHERD, P.

- R., GOUT, I., DOWNES, C. P. & LAMB, R. F. 2004. The TSC1-2 tumor suppressor controls insulin-PI3K signaling via regulation of IRS proteins. *J Cell Biol*, 166, 213-23.
- HARRIS, L. K., CROCKER, I. P., BAKER, P. N., APLIN, J. D. & WESTWOOD, M. 2011. IGF2 actions on trophoblast in human placenta are regulated by the insulin-like growth factor 2 receptor, which can function as both a signaling and clearance receptor. *Biol Reprod*, 84, 440-6.
- HARRIS, S. E., DE BLASIO, M. J., ZHAO, X., MA, M., DAVIES, K., WOODING, F. B. P., HAMILTON, R. S., BLACHE, D., MEREDITH, D., MURRAY, A. J., FOWDEN, A. L. & FORHEAD, A. J. 2020. Thyroid Deficiency Before Birth Alters the Adipose Transcriptome to Promote Overgrowth of White Adipose Tissue and Impair Thermogenic Capacity. *Thyroid*, 30, 794-805.
- HASAN, M. Z., IKAWATI, M., TOCHARUS, J., KAWAICHI, M. & OKA, C. 2015. Abnormal development of placenta in HtrA1-deficient mice. *Dev Biol*, 397, 89-102.
- HASHIMOTO, M., KOBAYASHI, K., WATANABE, M., KAZUKI, Y., TAKEHARA, S., INABA, A., NITTA, S., SENDA, N., OSHIMURA, M. & CHIBA, K. 2013. Knockout of mouse Cyp3a gene enhances synthesis of cholesterol and bile acid in the liver. *J Lipid Res*, 54, 2060-8.
- HAWKES, C. & KAR, S. 2004. The insulin-like growth factor-II/mannose-6-phosphate receptor: structure, distribution and function in the central nervous system. *Brain Res Brain Res Rev*, 44, 117-40.
- HAY, W. W., JR., SPARKS, J. W., WILKENING, R. B., BATTAGLIA, F. C. & MESCHIA, G. 1984. Fetal glucose uptake and utilization as functions of maternal glucose concentration. *Am J Physiol*, 246, E237-42.
- HE, W., BARAK, Y., HEVENER, A., OLSON, P., LIAO, D., LE, J., NELSON, M., ONG, E., OLEFSKY, J. M. & EVANS, R. M. 2003. Adipose-specific peroxisome proliferator-activated receptor gamma knockout causes insulin resistance in fat and liver but not in muscle. *Proc Natl Acad Sci U S A*, 100, 15712-7.
- HE, X. J., QIN, F. Y., HU, C. L., ZHU, M., TIAN, C. Q. & LI, L. 2015. Is gestational diabetes mellitus an independent risk factor for macrosomia: a meta-analysis? *Arch Gynecol Obstet*, 291, 729-35.
- HERRING, S. J., OKEN, E., RIFAS-SHIMAN, S. L., RICH-EDWARDS, J. W., STUEBE, A. M., KLEINMAN, K. P. & GILLMAN, M. W. 2009. Weight gain in pregnancy and risk of maternal hyperglycemia. *Am J Obstet Gynecol*, 201, 61.e1-7.
- HIGGINS, J. S., VAUGHAN, O. R., FERNANDEZ DE LIGER, E., FOWDEN, A. L. & SFERRUZZI-PERRI, A. N. 2016. Placental phenotype and resource allocation to fetal growth are modified by the timing and degree of hypoxia during mouse pregnancy. *J Physiol*, 594, 1341-56.
- HIGGINS, L., MILLS, T. A., GREENWOOD, S. L., COWLEY, E. J., SIBLEY, C. P. & JONES, R. L. 2013. Maternal obesity and its effect on placental cell turnover. *J Matern Fetal Neonatal Med*, 26, 783-8.
- HOLMAN, R. R. 1998. Assessing the potential for alpha-glucosidase inhibitors in prediabetic states. *Diabetes Res Clin Pract*, 40 Suppl, S21-5.
- HOLT, R. I. 2002. Fetal programming of the growth hormone-insulin-like growth factor axis. *Trends Endocrinol Metab*, 13, 392-7.
- HORTON, J. D., GOLDSTEIN, J. L. & BROWN, M. S. 2002. SREBPs: activators of the complete program of cholesterol and fatty acid synthesis in the liver. *J Clin Invest*, 109, 1125-31.

- HORTON, J. D., SHIMOMURA, I., IKEMOTO, S., BASHMAKOV, Y. & HAMMER, R. E. 2003. Overexpression of sterol regulatory element-binding protein-1a in mouse adipose tissue produces adipocyte hypertrophy, increased fatty acid secretion, and fatty liver. *J Biol Chem*, 278, 36652-60.
- HOWERTON, C. L., MORGAN, C. P., FISCHER, D. B. & BALE, T. L. 2013. O-GlcNAc transferase (OGT) as a placental biomarker of maternal stress and reprogramming of CNS gene transcription in development. *Proc Natl Acad Sci U S A*, 110, 5169-74.
- HU, D. & CROSS, J. C. 2011. Ablation of Tpbpa-positive trophoblast precursors leads to defects in maternal spiral artery remodeling in the mouse placenta. *Dev Biol*, 358, 231-9.
- HU, L., LYTRAS, A., BOCK, M. E., YUEN, C. K., DODD, J. G. & CATTINI, P. A. 1999. Detection of placental growth hormone variant and chorionic somatomammotropin-L RNA expression in normal and diabetic pregnancy by reverse transcriptase-polymerase chain reaction. *Mol Cell Endocrinol*, 157, 131-42.
- HUANG, B. W., CHIANG, M. T., YAO, H. T. & CHIANG, W. 2004. The effect of high-fat and high-fructose diets on glucose tolerance and plasma lipid and leptin levels in rats. *Diabetes Obes Metab*, 6, 120-6.
- HUANG, C., SNIDER, F. & CROSS, J. C. 2009. Prolactin receptor is required for normal glucose homeostasis and modulation of beta-cell mass during pregnancy. *Endocrinology*, 150, 1618-26.
- HUANG, J., PASHKOV, V., KURRASCH, D. M., YU, K., GOLD, S. J. & WILKIE, T. M. 2006. Feeding and fasting controls liver expression of a regulator of G protein signaling (Rgs16) in periportal hepatocytes. *Comp Hepatol*, 5, 8.
- HUANG, X., LIU, G., GUO, J. & SU, Z. 2018. The PI3K/AKT pathway in obesity and type 2 diabetes. *Int J Biol Sci*, 14, 1483-1496.
- ILAGAN, Y., MAMILLAPALLI, R., GOETZ, L. G., KAYANI, J. & TAYLOR, H. S. 2017. Bisphenol-A exposure in utero programs a sexually dimorphic estrogenic state of hepatic metabolic gene expression. *Reprod Toxicol*, 71, 84-94.
- INOUCHI, Y., ICHIYANAGI, K., OHISHI, H., MAEDA, Y., SONODA, N., OGAWA, Y., INOUCHI, T. & SASAKI, H. 2019. Poorly controlled diabetes during pregnancy and lactation activates the Foxo1 pathway and causes glucose intolerance in adult offspring. *Sci Rep*, 9, 10181.
- INUKAI, K., FUNAKI, M., OGIHARA, T., KATAGIRI, H., KANDA, A., ANAI, M., FUKUSHIMA, Y., HOSAKA, T., SUZUKI, M., SHIN, B. C., TAKATA, K., YAZAKI, Y., KIKUCHI, M., OKA, Y. & ASANO, T. 1997. p85alpha gene generates three isoforms of regulatory subunit for phosphatidylinositol 3-kinase (PI 3-Kinase), p50alpha, p55alpha, and p85alpha, with different PI 3-kinase activity elevating responses to insulin. *J Biol Chem*, 272, 7873-82.
- IRWIN, R. D., PARKER, J. S., LOBENHOFER, E. K., BURKA, L. T., BLACKSHEAR, P. E., VALLANT, M. K., LEBETKIN, E. H., GERKEN, D. F. & BOORMAN, G. A. 2005. Transcriptional profiling of the left and median liver lobes of male f344/n rats following exposure to acetaminophen. *Toxicol Pathol*, 33, 111-7.
- ISHIDA, M., OHASHI, S., KIZAKI, Y., NAITO, J., HORIGUCHI, K. & HARIGAYA, T. 2007. Expression profiling of mouse placental lactogen II and its correlative genes using a cDNA microarray analysis in the developmental mouse placenta. *J Reprod Dev*, 53, 69-76.
- ISHIHARA, K., HATANO, N., FURUUMI, H., KATO, R., IWAKI, T., MIURA, K., JINNO, Y. & SASAKI, H. 2000. Comparative genomic sequencing identifies

- novel tissue-specific enhancers and sequence elements for methylation-sensitive factors implicated in Igf2/H19 imprinting. *Genome Res*, 10, 664-71.
- ISLAM, A., KAGAWA, Y., SHARIFI, K., EBRAHIMI, M., MIYAZAKI, H., YASUMOTO, Y., KAWAMURA, S., YAMAMOTO, Y., SAKAGUTI, S., SAWADA, T., TOKUDA, N., SUGINO, N., SUZUKI, R. & OWADA, Y. 2014. Fatty Acid Binding Protein 3 Is Involved in n-3 and n-6 PUFA transport in mouse trophoblasts. *J Nutr*, 144, 1509-16.
- JACKSON, J. A. & ALBRECHT, E. D. 1985. The development of placental androstenedione and testosterone production and their utilization by the ovary for aromatization to estrogen during rat pregnancy. *Biol Reprod*, 33, 451-7.
- JANSSON, N., GREENWOOD, S. L., JOHANSSON, B. R., POWELL, T. L. & JANSSON, T. 2003. Leptin stimulates the activity of the system A amino acid transporter in human placental villous fragments. *J Clin Endocrinol Metab*, 88, 1205-11.
- JANSSON, N., ROSARIO, F. J., GACCIOLI, F., LAGER, S., JONES, H. N., ROOS, S., JANSSON, T. & POWELL, T. L. 2013. Activation of placental mTOR signaling and amino acid transporters in obese women giving birth to large babies. *J Clin Endocrinol Metab*, 98, 105-13.
- JANSSON, T. 2001. Amino acid transporters in the human placenta. *Pediatr Res*, 49, 141-7.
- JANSSON, T., COWLEY, E. A. & ILLSLEY, N. P. 1995. Cellular localization of glucose transporter messenger RNA in human placenta. *Reprod Fertil Dev*, 7, 1425-30.
- JANSSON, T., EKSTRAND, Y., BJORN, C., WENNERGREN, M. & POWELL, T. L. 2002. Alterations in the activity of placental amino acid transporters in pregnancies complicated by diabetes. *Diabetes*, 51, 2214-9.
- JANSSON, T. & POWELL, T. L. 2013. Role of placental nutrient sensing in developmental programming. *Clin Obstet Gynecol*, 56, 591-601.
- JANSSON, T., WENNERGREN, M. & ILLSLEY, N. P. 1993. Glucose transporter protein expression in human placenta throughout gestation and in intrauterine growth retardation. *J Clin Endocrinol Metab*, 77, 1554-62.
- JANZEN, C., LEI, M. Y., CHO, J., SULLIVAN, P., SHIN, B. C. & DEVASKAR, S. U. 2013. Placental glucose transporter 3 (GLUT3) is up-regulated in human pregnancies complicated by late-onset intrauterine growth restriction. *Placenta*, 34, 1072-8.
- JAUNIAUX, E. & BURTON, G. J. 2007. Morphological and biological effects of maternal exposure to tobacco smoke on the fetoplacental unit. *Early Hum Dev*, 83, 699-706.
- JAYABALAN, N., NAIR, S., NUZHAT, Z., RICE, G. E., ZUÑIGA, F. A., SOBREVIA, L., LEIVA, A., SANHUEZA, C., GUTIÉRREZ, J. A., LAPPAS, M., FREEMAN, D. J. & SALOMON, C. 2017. Cross Talk between Adipose Tissue and Placenta in Obese and Gestational Diabetes Mellitus Pregnancies via Exosomes. *Front Endocrinol (Lausanne)*, 8, 239.
- JETTON, T. L., LAUSIER, J., LAROCK, K., TROTMAN, W. E., LARMIE, B., HABIBOVIC, A., PESHAVARIA, M. & LEAHY, J. L. 2005. Mechanisms of compensatory beta-cell growth in insulin-resistant rats: roles of Akt kinase. *Diabetes*, 54, 2294-304.
- JIA, Y., LI, R., CONG, R., YANG, X., SUN, Q., PARVIZI, N. & ZHAO, R. 2013. Maternal low-protein diet affects epigenetic regulation of hepatic mitochondrial

- DNA transcription in a sex-specific manner in newborn piglets associated with GR binding to its promoter. *PLoS One*, 8, e63855.
- JIA, Z., PEI, Z., MAIGUEL, D., TOOMER, C. J. & WATKINS, P. A. 2007. The fatty acid transport protein (FATP) family: very long chain acyl-CoA synthetases or solute carriers? *J Mol Neurosci*, 33, 25-31.
- JIAO, F., YAN, X., YU, Y., ZHU, X., MA, Y., YUE, Z., OU, H. & YAN, Z. 2016. Protective effects of maternal methyl donor supplementation on adult offspring of high fat diet-fed dams. *J Nutr Biochem*, 34, 42-51.
- JOHNSON, D. C. & SEN, M. 1990. The cytochrome P450(17) alpha (17 alpha-hydroxylase/C17,20-lyase) activity of the junctional zone of the rat placenta. *J Endocrinol*, 125, 217-24.
- JOHNSON, L. W. & SMITH, C. H. 1980. Monosaccharide transport across microvillous membrane of human placenta. *Am J Physiol*, 238, C160-8.
- JOHNSON, L. W. & SMITH, C. H. 1985. Glucose transport across the basal plasma membrane of human placental syncytiotrophoblast. *Biochim Biophys Acta*, 815, 44-50.
- JONES, B. K., LEVORSE, J. M. & TILGHMAN, S. M. 1998. Igf2 imprinting does not require its own DNA methylation or H19 RNA. *Genes Dev*, 12, 2200-7.
- JONES, H. N., WOOLLETT, L. A., BARBOUR, N., PRASAD, P. D., POWELL, T. L. & JANSSON, T. 2009. High-fat diet before and during pregnancy causes marked up-regulation of placental nutrient transport and fetal overgrowth in C57/BL6 mice. *FASEB J*, 23, 271-8.
- JOOST, H. G., BELL, G. I., BEST, J. D., BIRNBAUM, M. J., CHARRON, M. J., CHEN, Y. T., DOEGE, H., JAMES, D. E., LODISH, H. F., MOLEY, K. H., MOLEY, J. F., MUECKLER, M., ROGERS, S., SCHURMANN, A., SEINO, S. & THORENS, B. 2002. Nomenclature of the GLUT/SLC2A family of sugar/polyol transport facilitators. *Am J Physiol Endocrinol Metab*, 282, E974-6.
- JOOST, H. G. & THORENS, B. 2001. The extended GLUT-family of sugar/polyol transport facilitators: nomenclature, sequence characteristics, and potential function of its novel members (review). *Mol Membr Biol*, 18, 247-56.
- JOSHI, A. A., VAIDYA, S. S., ST-PIERRE, M. V., MIKHEEV, A. M., DESINO, K. E., NYANDEGE, A. N., AUDUS, K. L., UNADKAT, J. D. & GERK, P. M. 2016. Placental ABC Transporters: Biological Impact and Pharmaceutical Significance. *Pharm Res*, 33, 2847-2878.
- KADAKIA, R., MA, M. & JOSEFSON, J. L. 2016. Neonatal adiposity increases with rising cord blood IGF-1 levels. *Clin Endocrinol (Oxf)*, 85, 70-5.
- KAGAWA, N., SAITO, Y. & NAGAO, T. 2014. Early to middle gestational exposure to diethylstilbestrol impairs the development of labyrinth zone in mouse placenta. *Congenit Anom (Kyoto)*, 54, 116-9.
- KAIKAEW, K., STEENBERGEN, J., VAN DIJK, T. H., GREFHORST, A. & VISSER, J. A. 2019. Sex Difference in Corticosterone-Induced Insulin Resistance in Mice. *Endocrinology*, 160, 2367-2387.
- KALHAN, S., ROSSI, K., GRUCA, L., BURKETT, E. & O'BRIEN, A. 1997. Glucose turnover and gluconeogenesis in human pregnancy. *J Clin Invest*, 100, 1775-81.
- KALIMAN, P., CANICIO, J., TESTAR, X., PALACÍN, M. & ZORZANO, A. 1999. Insulin-like growth factor-II, phosphatidylinositol 3-kinase, nuclear factor-kappaB and inducible nitric-oxide synthase define a common myogenic signaling pathway. *J Biol Chem*, 274, 17437-44.

- KAMEL, M. A., HELMY, M. H., HANAFI, M. Y., MAHMOUD, S. A. & ABO ELFETOOH, H. 2014. Impaired peripheral glucose sensing in F1 offspring of diabetic pregnancy. *J Physiol Biochem*, 70, 685-99.
- KANAI-AZUMA, M., KANAI, Y., KUROHMARU, M., SAKAI, S. & HAYASHI, Y. 1993. Insulin-like growth factor (IGF)-I stimulates proliferation and migration of mouse ectoplacental cone cells, while IGF-II transforms them into trophoblastic giant cells in vitro. *Biol Reprod*, 48, 252-61.
- KARL, P. I., ALPY, K. L. & FISHER, S. E. 1992. Amino acid transport by the cultured human placental trophoblast: effect of insulin on AIB transport. *Am J Physiol*, 262, C834-9.
- KAUTZKY-WILLER, A., PACINI, G., TURA, A., BIEGLMAYER, C., SCHNEIDER, B., LUDVIK, B., PRAGER, R. & WALDHAUSL, W. 2001. Increased plasma leptin in gestational diabetes. *Diabetologia*, 44, 164-72.
- KAWAHARA, M., WU, Q. & KONO, T. 2010. Involvement of insulin-like growth factor 2 in angiogenic factor transcription in Bi-maternal mouse conceptuses. *J Reprod Dev*, 56, 79-85.
- KEELAN, J. A., MATTES, E., TAN, H., DINAN, A., NEWNHAM, J. P., WHITEHOUSE, A. J., JACOBY, P. & HICKEY, M. 2012. Androgen concentrations in umbilical cord blood and their association with maternal, fetal and obstetric factors. *PLoS One*, 7, e42827.
- KELLY, P. A., DJIANE, J., POSTEL-VINAY, M. C. & EDERY, M. 1991. The prolactin/growth hormone receptor family. *Endocr Rev*, 12, 235-51.
- KENIRY, A., OXLEY, D., MONNIER, P., KYBA, M., DANDOLO, L., SMITS, G. & REIK, W. 2012. The H19 lincRNA is a developmental reservoir of miR-675 that suppresses growth and Igf1r. *Nat Cell Biol*, 14, 659-65.
- KERSTEN, S. 2001. Mechanisms of nutritional and hormonal regulation of lipogenesis. *EMBO Rep*, 2, 282-6.
- KERSTEN, S., SEYDOUX, J., PETERS, J. M., GONZALEZ, F. J., DESVERGNE, B. & WAHLI, W. 1999. Peroxisome proliferator-activated receptor alpha mediates the adaptive response to fasting. *J Clin Invest*, 103, 1489-98.
- KHALYFA, A., CARRERAS, A., HAKIM, F., CUNNINGHAM, J. M., WANG, Y. & GOZAL, D. 2013. Effects of late gestational high-fat diet on body weight, metabolic regulation and adipokine expression in offspring. *Int J Obes (Lond)*, 37, 1481-9.
- KIM, J. K. 2009. Hyperinsulinemic-euglycemic clamp to assess insulin sensitivity in vivo. *Methods Mol Biol*, 560, 221-38.
- KIM, J. K., FILLMORE, J. J., CHEN, Y., YU, C., MOORE, I. K., PYPAERT, M., LUTZ, E. P., KAKO, Y., VELEZ-CARRASCO, W., GOLDBERG, I. J., BRESLOW, J. L. & SHULMAN, G. I. 2001. Tissue-specific overexpression of lipoprotein lipase causes tissue-specific insulin resistance. *Proc Natl Acad Sci U S A*, 98, 7522-7.
- KIM, K.-H., CHEN, C.-C., MONZON, R. I. & LAU, L. F. 2013. Matricellular protein CCN1 promotes regression of liver fibrosis through induction of cellular senescence in hepatic myofibroblasts. *Molecular and cellular biology*, 33, 2078-2090.
- KIM, K. H., CHEN, C. C., ALPINI, G. & LAU, L. F. 2015. CCN1 induces hepatic ductular reaction through integrin $\alpha\beta_5$ -mediated activation of NF- κ B. *J Clin Invest*, 125, 1886-900.

- KING, B. F. & HASTINGS, R. A., 2ND 1977. The comparative fine structure of the interhemal membrane of chorioallantoic placentas from six genera of myomorph rodents. *Am J Anat*, 149, 165-79.
- KING, B. R., NICHOLSON, R. C. & SMITH, R. 2001. Placental corticotrophin-releasing hormone, local effects and fetomaternal endocrinology. *Stress*, 4, 219-33.
- KNIPP, G. T., LIU, B., AUDUS, K. L., FUJII, H., ONO, T. & SOARES, M. J. 2000. Fatty acid transport regulatory proteins in the developing rat placenta and in trophoblast cell culture models. *Placenta*, 21, 367-75.
- KNOPP, R. H., SAUDEK, C. D., ARKY, R. A. & O'SULLIVAN, J. B. 1973. 2 phases of adipose tissue metabolism in pregnancy: maternal adaptations for fetal growth. *Endocrinology*, 92, 984-8.
- KOH, P. O., KIM, Y. S., CHEON, E. W., KANG, S. S., CHO, G. J. & CHOI, W. S. 2002. Expression of steroidogenic acute regulatory protein mRNA in rat placenta during mid-late pregnancy. *Mol Cells*, 14, 355-60.
- KOHJIMA, M., SUN, Y. & CHAN, L. 2010. Increased food intake leads to obesity and insulin resistance in the tg2576 Alzheimer's disease mouse model. *Endocrinology*, 151, 1532-1540.
- KOMINE, H., KUHN, L., MATSUSHITA, N., MULÉ, J. J. & PILON-THOMAS, S. 2013. Examination of MARCO activity on dendritic cell phenotype and function using a gene knockout mouse. *PLoS One*, 8, e67795.
- KOTOKORPI, P., GARDMO, C., NYSTRÖM, C. S. & MODE, A. 2004. Activation of the glucocorticoid receptor or liver X receptors interferes with growth hormone-induced akr1b7 gene expression in rat hepatocytes. *Endocrinology*, 145, 5704-13.
- KRAEGEN, E. W., CLARK, P. W., JENKINS, A. B., DALEY, E. A., CHISHOLM, D. J. & STORLIEN, L. H. 1991. Development of muscle insulin resistance after liver insulin resistance in high-fat-fed rats. *Diabetes*, 40, 1397-403.
- KRAUSE, B. J., HANSON, M. A. & CASANELLO, P. 2011. Role of nitric oxide in placental vascular development and function. *Placenta*, 32, 797-805.
- KREY, G., BRAISSANT, O., L'HORSET, F., KALKHOVEN, E., PERROUD, M., PARKER, M. G. & WAHLI, W. 1997. Fatty acids, eicosanoids, and hypolipidemic agents identified as ligands of peroxisome proliferator-activated receptors by coactivator-dependent receptor ligand assay. *Molecular Endocrinology*, 11, 779-791.
- KROZOWSKI, Z., MAGUIRE, J. A., STEIN-OAKLEY, A. N., DOWLING, J., SMITH, R. E. & ANDREWS, R. K. 1995. Immunohistochemical localization of the 11 beta-hydroxysteroid dehydrogenase type II enzyme in human kidney and placenta. *J Clin Endocrinol Metab*, 80, 2203-9.
- KUBOTA, N., KUBOTA, T., KAJIWARA, E., IWAMURA, T., KUMAGAI, H., WATANABE, T., INOUE, M., TAKAMOTO, I., SASAKO, T., KUMAGAI, K., KOHJIMA, M., NAKAMUTA, M., MOROI, M., SUGI, K., NODA, T., TERAUCHI, Y., UEKI, K. & KADOWAKI, T. 2016. Differential hepatic distribution of insulin receptor substrates causes selective insulin resistance in diabetes and obesity. *Nat Commun*, 7, 12977.
- KULESHOV, M. V., JONES, M. R., ROUILLARD, A. D., FERNANDEZ, N. F., DUAN, Q., WANG, Z., KOPLEV, S., JENKINS, S. L., JAGODNIK, K. M., LACHMANN, A., MCDERMOTT, M. G., MONTEIRO, C. D., GUNDERSEN, G. W. & MA'AYAN, A. 2016. Enrichr: a comprehensive gene set enrichment analysis web server 2016 update. *Nucleic Acids Res*, 44, W90-7.
- KURUKUTI, S., TIWARI, V. K., TAVOOSIDANA, G., PUGACHEVA, E., MURRELL, A., ZHAO, Z., LOBANENKOV, V., REIK, W. & OHLSSON, R.

2006. CTCF binding at the H19 imprinting control region mediates maternally inherited higher-order chromatin conformation to restrict enhancer access to Igf2. *Proc Natl Acad Sci U S A*, 103, 10684-9.
- KWONG, W. Y., MILLER, D. J., WILKINS, A. P., DEAR, M. S., WRIGHT, J. N., OSMOND, C., ZHANG, J. & FLEMING, T. P. 2007. Maternal low protein diet restricted to the preimplantation period induces a gender-specific change on hepatic gene expression in rat fetuses. *Mol Reprod Dev*, 74, 48-56.
- LAGER, S. & POWELL, T. L. 2012. Regulation of nutrient transport across the placenta. *J Pregnancy*, 2012, 179827.
- LAN, X. F., ZHANG, X. J., LIN, Y. N., WANG, Q., XU, H. J., ZHOU, L. N., CHEN, P. L. & LI, Q. Y. 2017. Estradiol Regulates Txnip and Prevents Intermittent Hypoxia-Induced Vascular Injury. *Sci Rep*, 7, 10318.
- LANG, P., HASSELWANDER, S., LI, H. & XIA, N. 2019. Effects of different diets used in diet-induced obesity models on insulin resistance and vascular dysfunction in C57BL/6 mice. *Sci Rep*, 9, 19556.
- LARQUE, E., DEMMELMAIR, H., KLINGLER, M., DE JONGE, S., BONDY, B. & KOLETZKO, B. 2006a. Expression pattern of fatty acid transport protein-1 (FATP-1), FATP-4 and heart-fatty acid binding protein (H-FABP) genes in human term placenta. *Early Hum Dev*, 82, 697-701.
- LARQUE, E., KRAUSS-ETSCHMANN, S., CAMPOY, C., HARTL, D., LINDE, J., KLINGLER, M., DEMMELMAIR, H., CANO, A., GIL, A., BONDY, B. & KOLETZKO, B. 2006b. Docosahexaenoic acid supply in pregnancy affects placental expression of fatty acid transport proteins. *Am J Clin Nutr*, 84, 853-61.
- LATOUCHE, C., HEYWOOD, S. E., HENRY, S. L., ZIEMANN, M., LAZARUS, R., EL-OSTA, A., ARMITAGE, J. A. & KINGWELL, B. A. 2014. Maternal overnutrition programs changes in the expression of skeletal muscle genes that are associated with insulin resistance and defects of oxidative phosphorylation in adult male rat offspring. *J Nutr*, 144, 237-44.
- LAW, C. M., BARKER, D. J., OSMOND, C., FALL, C. H. & SIMMONDS, S. J. 1992. Early growth and abdominal fatness in adult life. *Journal of epidemiology and community health*, 46, 184-186.
- LE MOULLEC, N., FIANU, A., MAILLARD, O., CHAZELLE, E., NATY, N., SCHNEEBELI, C., GERARDIN, P., HUIART, L., CHARLES, M. A. & FAVIER, F. 2018. Sexual dimorphism in the association between gestational diabetes mellitus and overweight in offspring at 5-7 years: The OBEGEST cohort study. *PLoS One*, 13, e0195531.
- LEA, R. G., HOWE, D., HANNAH, L. T., BONNEAU, O., HUNTER, L. & HOGGARD, N. 2000. Placental leptin in normal, diabetic and fetal growth-retarded pregnancies. *Mol Hum Reprod*, 6, 763-9.
- LECOUTRE, S., DERACINOIS, B., LABORIE, C., EBERLE, D., GUINEZ, C., PANCHENKO, P. E., LESAGE, J., VIEAU, D., JUNIEN, C., GABORY, A. & BRETON, C. 2016. Depot- and sex-specific effects of maternal obesity in offspring's adipose tissue. *J Endocrinol*, 230, 39-53.
- LECOUTRE, S., POURPE, C., BUTRUILLE, L., MAROUSEZ, L., LABORIE, C., GUINEZ, C., LESAGE, J., VIEAU, D., ECKHOUTE, J., GABORY, A., OGER, F., EBERLE, D. & BRETON, C. 2018. Reduced PPARgamma2 expression in adipose tissue of male rat offspring from obese dams is associated with epigenetic modifications. *Faseb j*, 32, 2768-2778.

- LEE, J. E., PINTAR, J. & EFSTRATIADIS, A. 1990. Pattern of the insulin-like growth factor II gene expression during early mouse embryogenesis. *Development*, 110, 151-9.
- LEI, K. J., CHEN, H., PAN, C. J., WARD, J. M., MOSINGER, B., JR., LEE, E. J., WESTPHAL, H., MANSFIELD, B. C. & CHOU, J. Y. 1996. Glucose-6-phosphatase dependent substrate transport in the glycogen storage disease type-1a mouse. *Nat Genet*, 13, 203-9.
- LEIGHTON, P. A., INGRAM, R. S., EGGENSCHWILER, J., EFSTRATIADIS, A. & TILGHMAN, S. M. 1995. Disruption of imprinting caused by deletion of the H19 gene region in mice. *Nature*, 375, 34-9.
- LEISER, R. & KAUFMANN, P. 1994. Placental structure: in a comparative aspect. *Exp Clin Endocrinol*, 102, 122-34.
- LERNER, A. G., UPTON, J. P., PRAVEEN, P. V., GHOSH, R., NAKAGAWA, Y., IGBARIA, A., SHEN, S., NGUYEN, V., BACKES, B. J., HEIMAN, M., HEINTZ, N., GREENGARD, P., HUI, S., TANG, Q., TRUSINA, A., OAKES, S. A. & PAPA, F. R. 2012. IRE1 α induces thioredoxin-interacting protein to activate the NLRP3 inflammasome and promote programmed cell death under irremediable ER stress. *Cell Metab*, 16, 250-64.
- LESCAR, J., LORIS, R., MITCHELL, E., GAUTIER, C., CHAZALET, V., COX, V., WYNS, L., PEREZ, S., BRETON, C. & IMBERTY, A. 2002. Isolectins I-A and I-B of Griffonia (Bandeiraea) simplicifolia. Crystal structure of metal-free GS I-B(4) and molecular basis for metal binding and monosaccharide specificity. *J Biol Chem*, 277, 6608-14.
- LETURQUE, A., FERRE, P., BURNOL, A. F., KANDE, J., MAULARD, P. & GIRARD, J. 1986. Glucose utilization rates and insulin sensitivity in vivo in tissues of virgin and pregnant rats. *Diabetes*, 35, 172-7.
- LI, J., FU, Z., JIANG, H., CHEN, L., WU, X., DING, H., XIA, Y., WANG, X., TANG, Q. & WU, W. 2018. IGF2-derived miR-483-3p contributes to macrosomia through regulating trophoblast proliferation by targeting RB1CC1. *Mol Hum Reprod*, 24, 444-452.
- LI, J., YING, H., CAI, G., GUO, Q. & CHEN, L. 2015a. Impaired proliferation of pancreatic beta cells, by reduced placental growth factor in pre-eclampsia, as a cause for gestational diabetes mellitus. *Cell Prolif*, 48, 166-74.
- LI, S., LEE, J., ZHOU, Y., GORDON, W. C., HILL, J. M., BAZAN, N. G., MINER, J. H. & JIN, M. 2013. Fatty acid transport protein 4 (FATP4) prevents light-induced degeneration of cone and rod photoreceptors by inhibiting RPE65 isomerase. *J Neurosci*, 33, 3178-89.
- LI, S., ZHU, Y., YEUNG, E., CHAVARRO, J. E., YUAN, C., FIELD, A. E., MISSMER, S. A., MILLS, J. L., HU, F. B. & ZHANG, C. 2017. Offspring risk of obesity in childhood, adolescence and adulthood in relation to gestational diabetes mellitus: a sex-specific association. *Int J Epidemiol*, 46, 1533-1541.
- LI, T., HU, J. F., QIU, X., LING, J., CHEN, H., WANG, S., HOU, A., VU, T. H. & HOFFMAN, A. R. 2008. CTCF regulates allelic expression of Igf2 by orchestrating a promoter-polycomb repressive complex 2 intrachromosomal loop. *Mol Cell Biol*, 28, 6473-82.
- LI, Y., LEY, S. H., TOBIAS, D. K., CHIUVE, S. E., VANDERWEELE, T. J., RICH-EDWARDS, J. W., CURHAN, G. C., WILLETT, W. C., MANSON, J. E., HU, F. B. & QI, L. 2015b. Birth weight and later life adherence to unhealthy lifestyles in predicting type 2 diabetes: prospective cohort study. *Bmj*, 351, h3672.

- LI, Y., LEY, S. H., VANDERWEELE, T. J., CURHAN, G. C., RICH-EDWARDS, J. W., WILLETT, W. C., FORMAN, J. P., HU, F. B. & QI, L. 2015c. Joint association between birth weight at term and later life adherence to a healthy lifestyle with risk of hypertension: a prospective cohort study. *BMC Med*, 13, 175.
- LIAN, J., WATTS, R., QUIROGA, A. D., BEGGS, M. R., ALEXANDER, R. T. & LEHNER, R. 2019. Cers1d deficiency protects against high-sucrose diet-induced hepatic triacylglycerol accumulation. *J Lipid Res*, 60, 880-891.
- LIAO, S., VICKERS, M. H., TAYLOR, R. S., FRASER, M., MCCOWAN, L. M. E., BAKER, P. N. & PERRY, J. K. 2017. Maternal serum placental growth hormone, insulin-like growth factors and their binding proteins at 20 weeks' gestation in pregnancies complicated by gestational diabetes mellitus. *Hormones (Athens)*, 16, 282-290.
- LILLYCROP, K. A., PHILLIPS, E. S., JACKSON, A. A., HANSON, M. A. & BURDGE, G. C. 2005. Dietary protein restriction of pregnant rats induces and folic acid supplementation prevents epigenetic modification of hepatic gene expression in the offspring. *J Nutr*, 135, 1382-6.
- LIM, K., LOMBARDO, P., SCHNEIDER-KOLSKY, M., HILLIARD, L., DENTON, K. M. & BLACK, M. J. 2011. Induction of hyperglycemia in adult intrauterine growth-restricted rats: effects on renal function. *Am J Physiol Renal Physiol*, 301, F288-94.
- LIN, J., TARR, P. T., YANG, R., RHEE, J., PUIGSERVER, P., NEWGARD, C. B. & SPIEGELMAN, B. M. 2003. PGC-1beta in the regulation of hepatic glucose and energy metabolism. *J Biol Chem*, 278, 30843-8.
- LIN, Y., HAN, X. F., FANG, Z. F., CHE, L. Q., NELSON, J., YAN, T. H. & WU, D. 2011. Beneficial effects of dietary fibre supplementation of a high-fat diet on fetal development in rats. *Br J Nutr*, 106, 510-8.
- LINDSAY, R., LINDSAY, R., WADDELL, B. & SECKL, J. 1996. Prenatal glucocorticoid exposure leads to offspring hyperglycaemia in the rat: studies with the 11 b-hydroxysteroid dehydrogenase inhibitor carbenoxolone. *Diabetologia*, 39, 1299-1305.
- LIU, M. J., TAKAHASHI, Y., WADA, T., HE, J., GAO, J., TIAN, Y., LI, S. & XIE, W. 2009a. The aldo-keto reductase Akr1b7 gene is a common transcriptional target of xenobiotic receptors pregnane X receptor and constitutive androstane receptor. *Mol Pharmacol*, 76, 604-11.
- LIU, X., QI, Y., TIAN, B., CHEN, D., GAO, H., XI, C., XING, Y. & YUAN, Z. 2014. Maternal protein restriction induces alterations in hepatic tumor necrosis factor-alpha/CYP7A1 signaling and disorders regulation of cholesterol metabolism in the adult rat offspring. *J Clin Biochem Nutr*, 55, 40-7.
- LIU, X., RAMJIGANESH, T., CHEN, Y. H., CHUNG, S. W., HALL, S. R., SCHISSEL, S. L., PADERA, R. F., JR., LIAO, R., ACKERMAN, K. G., KAJSTURA, J., LERI, A., ANVERSA, P., YET, S. F., LAYNE, M. D. & PERRELLA, M. A. 2009b. Disruption of striated preferentially expressed gene locus leads to dilated cardiomyopathy in mice. *Circulation*, 119, 261-8.
- LIVAK, K. J. & SCHMITTGEN, T. D. 2001. Analysis of relative gene expression data using real-time quantitative PCR and the 2(-Delta Delta C(T)) Method. *Methods*, 25, 402-8.
- LOGUE, J., WALKER, J. J., COLHOUN, H. M., LEESE, G. P., LINDSAY, R. S., MCKNIGHT, J. A., MORRIS, A. D., PEARSON, D. W., PETRIE, J. R., PHILIP, S., WILD, S. H. & SATTAR, N. 2011. Do men develop type 2 diabetes at lower body mass indices than women? *Diabetologia*, 54, 3003-6.

- LOPEZ, M. F., DIKES, P., ZURAKOWSKI, D. & VILLA-KOMAROFF, L. 1996. Insulin-like growth factor II affects the appearance and glycogen content of glycogen cells in the murine placenta. *Endocrinology*, 137, 2100-8.
- LOPEZ, M. F., ZHENG, L., MIAO, J., GALI, R., GORSKI, G. & HIRSCHHORN, J. N. 2018. Disruption of the Igf2 gene alters hepatic lipid homeostasis and gene expression in the newborn mouse. *Am J Physiol Endocrinol Metab*, 315, E735-e744.
- LÓPEZ-TELLO, J., PÉREZ-GARCÍA, V., KHAIRA, J., KUSINSKI, L. C., COOPER, W. N., ANDREANI, A., GRANT, I., FERNÁNDEZ DE LIGER, E., LAM, B. Y., HEMBERGER, M., SANDOVICI, I., CONSTANCIA, M. & SFERRUZZI-PERRI, A. N. 2019. Fetal and trophoblast PI3K p110 α have distinct roles in regulating resource supply to the growing fetus in mice. *eLife*, 8, e45282.
- LOUWAGIE, E. J., LARSEN, T. D., WACHAL, A. L. & BAACK, M. L. 2018. Placental lipid processing in response to a maternal high-fat diet and diabetes in rats. *Pediatr Res*, 83, 712-722.
- LOWE, R., GEMMA, C., RAKYAN, V. K. & HOLLAND, M. L. 2015. Sexually dimorphic gene expression emerges with embryonic genome activation and is dynamic throughout development. *BMC Genomics*, 16, 295.
- LU, H., CHOUDHURI, S., OGURA, K., CSANAKY, I. L., LEI, X., CHENG, X., SONG, P. Z. & KLAASSEN, C. D. 2008. Characterization of organic anion transporting polypeptide 1b2-null mice: essential role in hepatic uptake/toxicity of phalloidin and microcystin-LR. *Toxicol Sci*, 103, 35-45.
- LUCAS, M. J., LEVENO, K. J., WILLIAMS, M. L., RASKIN, P. & WHALLEY, P. J. 1989. Early pregnancy glycosylated hemoglobin, severity of diabetes, and fetal malformations. *Am J Obstet Gynecol*, 161, 426-31.
- LUO, J., FIELD, S. J., LEE, J. Y., ENGELMAN, J. A. & CANTLEY, L. C. 2005. The p85 regulatory subunit of phosphoinositide 3-kinase down-regulates IRS-1 signaling via the formation of a sequestration complex. *J Cell Biol*, 170, 455-64.
- MA, G. T., ROTH, M. E., GROSKOPF, J. C., TSAI, F. Y., ORKIN, S. H., GROSVELD, F., ENGEL, J. D. & LINZER, D. I. 1997. GATA-2 and GATA-3 regulate trophoblast-specific gene expression in vivo. *Development*, 124, 907-14.
- MA, L., ROBINSON, L. N. & TOWLE, H. C. 2006. ChREBP* Mlx is the principal mediator of glucose-induced gene expression in the liver. *J Biol Chem*, 281, 28721-30.
- MACKENZIE, B. & ERICKSON, J. D. 2004. Sodium-coupled neutral amino acid (System N/A) transporters of the SLC38 gene family. *Pflugers Arch*, 447, 784-95.
- MAGNUSON, B., EKIM, B. & FINGAR, D. C. 2012. Regulation and function of ribosomal protein S6 kinase (S6K) within mTOR signalling networks. *Biochemical Journal*, 441, 1-21.
- MAGNUSSON, A. L., WATERMAN, I. J., WENNERGREN, M., JANSSON, T. & POWELL, T. L. 2004. Triglyceride hydrolase activities and expression of fatty acid binding proteins in the human placenta in pregnancies complicated by intrauterine growth restriction and diabetes. *J Clin Endocrinol Metab*, 89, 4607-14.
- MAHENDRAN, D., DONNAI, P., GLAZIER, J. D., D'SOUZA, S. W., BOYD, R. D. & SIBLEY, C. P. 1993. Amino acid (system A) transporter activity in microvillous membrane vesicles from the placentas of appropriate and small for gestational age babies. *Pediatr Res*, 34, 661-5.
- MAKKAR, A., MISHIMA, T., CHANG, G., SCIFRES, C. & SADOVSKY, Y. 2014. Fatty acid binding protein-4 is expressed in the mouse placental labyrinth, yet is

- dispensable for placental triglyceride accumulation and fetal growth. *Placenta*, 35, 802-7.
- MALANDRO, M. S., BEVERIDGE, M. J., KILBERG, M. S. & NOVAK, D. A. 1996. Effect of low-protein diet-induced intrauterine growth retardation on rat placental amino acid transport. *Am J Physiol*, 271, C295-303.
- MALASSINÉ, A., FRENDON, J. L. & EVAÏN-BRION, D. 2003. A comparison of placental development and endocrine functions between the human and mouse model. *Hum Reprod Update*, 9, 531-9.
- MALIK, N. M., CARTER, N. D., WILSON, C. A., SCARAMUZZI, R. J., STOCK, M. J. & MURRAY, J. F. 2005. Leptin expression in the fetus and placenta during mouse pregnancy. *Placenta*, 26, 47-52.
- MAMANE, Y., PETROULAKIS, E., RONG, L., YOSHIDA, K., LER, L. W. & SONENBERG, N. 2004. eIF4E--from translation to transformation. *Oncogene*, 23, 3172-9.
- MANDOUR, T., KISSEBAH, A. H. & WYNN, V. 1977. Mechanism of oestrogen and progesterone effects on lipid and carbohydrate metabolism: alteration in the insulin: glucagon molar ratio and hepatic enzyme activity. *Eur J Clin Invest*, 7, 181-7.
- MANIKKAM, M., CRESPI, E. J., DOOP, D. D., HERKIMER, C., LEE, J. S., YU, S., BROWN, M. B., FOSTER, D. L. & PADMANABHAN, V. 2004. Fetal programming: prenatal testosterone excess leads to fetal growth retardation and postnatal catch-up growth in sheep. *Endocrinology*, 145, 790-8.
- MANNING, B. D. & CANTLEY, L. C. 2007. AKT/PKB signaling: navigating downstream. *Cell*, 129, 1261-74.
- MANSELL, T., NOVAKOVIC, B., MEYER, B., RZEHA, P., VUILLERMIN, P., PONSONBY, A. L., COLLIER, F., BURGNER, D., SAFFERY, R. & RYAN, J. 2016. The effects of maternal anxiety during pregnancy on IGF2/H19 methylation in cord blood. *Transl Psychiatry*, 6, e765.
- MAO, J., ZHANG, X., SIELI, P. T., FALDUTO, M. T., TORRES, K. E. & ROSENFELD, C. S. 2010. Contrasting effects of different maternal diets on sexually dimorphic gene expression in the murine placenta. *Proc Natl Acad Sci U S A*, 107, 5557-62.
- MARGARETO, J., AGUADO, M., OSÉS-PRIETO, J. A., RIVERO, I., MONGE, A., ALDANA, I., MARTI, A. & MARTÍNEZ, J. A. 2000. A new NPY-antagonist strongly stimulates apoptosis and lipolysis on white adipocytes in an obesity model. *Life Sci*, 68, 99-107.
- MARGARETO, J., RIVERO, I., MONGE, A., ALDANA, I., MARTI, A. & MARTÍNEZ, J. A. 2002. Changes in UCP2, PPARgamma2, and c/EBPalpha gene expression induced by a neuropeptide Y (NPY) related receptor antagonist in overweight rats. *Nutr Neurosci*, 5, 13-7.
- MARK, P. J., SMITH, J. T. & WADDELL, B. J. 2006. Placental and fetal growth retardation following partial progesterone withdrawal in rat pregnancy. *Placenta*, 27, 208-14.
- MARTIN, G., POIRIER, H., HENNUYER, N., CROMBIE, D., FRUCHART, J. C., HEYMAN, R. A., BESNARD, P. & AUWERX, J. 2000. Induction of the fatty acid transport protein 1 and acyl-CoA synthase genes by dimer-selective rexinoids suggests that the peroxisome proliferator-activated receptor-retinoid X receptor heterodimer is their molecular target. *J Biol Chem*, 275, 12612-8.
- MASOUE, I., HAGENS, G., VAN KUPPEVELT, T. H., MADSEN, P., SAURAT, J. H., VEERKAMP, J. H., PEPPER, M. S. & SIEGENTHALER, G. 1997.

- Endothelial cells of the human microvasculature express epidermal fatty acid-binding protein. *Circ Res*, 81, 297-303.
- MASUYAMA, H., MITSUI, T., NOBUMOTO, E. & HIRAMATSU, Y. 2015. The Effects of High-Fat Diet Exposure In Utero on the Obesogenic and Diabetogenic Traits Through Epigenetic Changes in Adiponectin and Leptin Gene Expression for Multiple Generations in Female Mice. *Endocrinology*, 156, 2482-91.
- MAYER, C. M. & BELSHAM, D. D. 2009. Insulin directly regulates NPY and AgRP gene expression via the MAPK MEK/ERK signal transduction pathway in mHypoE-46 hypothalamic neurons. *Mol Cell Endocrinol*, 307, 99-108.
- MAYHEW, T. M. 2006. Stereology and the placenta: where's the point? -- a review. *Placenta*, 27 Suppl A, S17-25.
- MIKAELSSON, M. A., CONSTANCIA, M., DENT, C. L., WILKINSON, L. S. & HUMBY, T. 2013. Placental programming of anxiety in adulthood revealed by Igf2-null models. *Nat Commun*, 4, 2311.
- MINN, A. H., HAFELE, C. & SHALEV, A. 2005. Thioredoxin-interacting protein is stimulated by glucose through a carbohydrate response element and induces beta-cell apoptosis. *Endocrinology*, 146, 2397-405.
- MISHIMA, T., MINER, J. H., MORIZANE, M., STAHL, A. & SADOVSKY, Y. 2011. The expression and function of fatty acid transport protein-2 and -4 in the murine placenta. *PLoS One*, 6, e25865.
- MO, F. E. & LAU, L. F. 2006. The matricellular protein CCN1 is essential for cardiac development. *Circ Res*, 99, 961-9.
- MODI, H., JACOVETTI, C., TARUSSIO, D., METREF, S., MADSEN, O. D., ZHANG, F. P., RANTAKARI, P., POUTANEN, M., NEF, S., GORMAN, T., REGAZZI, R. & THORENS, B. 2015. Autocrine Action of IGF2 Regulates Adult β -Cell Mass and Function. *Diabetes*, 64, 4148-57.
- MOGENSEN, C. E. & ANDERSEN, M. J. 1973. Increased kidney size and glomerular filtration rate in early juvenile diabetes. *Diabetes*, 22, 706-12.
- MOITRA, J., MASON, M. M., OLIVE, M., KRYLOV, D., GAVRILOVA, O., MARCUS-SAMUELS, B., FEIGENBAUM, L., LEE, E., AOYAMA, T., ECKHAUS, M., REITMAN, M. L. & VINSON, C. 1998. Life without white fat: a transgenic mouse. *Genes Dev*, 12, 3168-81.
- MONDER, C. & SHACKLETON, C. H. 1984. 11 beta-Hydroxysteroid dehydrogenase: fact or fancy? *Steroids*, 44, 383-417.
- MONTANO, M. M., WANG, M. H. & VOM SAAL, F. S. 1993. Sex differences in plasma corticosterone in mouse fetuses are mediated by differential placental transport from the mother and eliminated by maternal adrenalectomy or stress. *J Reprod Fertil*, 99, 283-90.
- MOORE, L. G., CHARLES, S. M. & JULIAN, C. G. 2011. Humans at high altitude: hypoxia and fetal growth. *Respir Physiol Neurobiol*, 178, 181-90.
- MOORE, T. 2001. Genetic conflict, genomic imprinting and establishment of the epigenotype in relation to growth. *Reproduction*, 122, 185-93.
- MORGAN, R. A., BECK, K. R., NIXON, M., HOMER, N. Z. M., CRAWFORD, A. A., MELCHERS, D., HOUTMAN, R., MEIJER, O. C., STOMBY, A., ANDERSON, A. J., UPRETI, R., STIMSON, R. H., OLSSON, T., MICHOEL, T., COHAIN, A., RUUSALEPP, A., SCHADT, E. E., BJÖRKEGREN, J. L. M., ANDREW, R., KENYON, C. J., HADOKÉ, P. W. F., ODERMATT, A., KEEN, J. A. & WALKER, B. R. 2017. Carbonyl reductase 1 catalyzes 20 β -reduction of glucocorticoids, modulating receptor activation and metabolic complications of obesity. *Sci Rep*, 7, 10633.

- MOUSIOLIS, A. V., KOLLIA, P., SKENTOU, C. & MESSINIS, I. E. 2012. Effects of leptin on the expression of fatty acid-binding proteins in human placental cell cultures. *Mol Med Rep*, 5, 497-502.
- MUNIYAPPA, R., LEE, S., CHEN, H. & QUON, M. J. 2008. Current approaches for assessing insulin sensitivity and resistance in vivo: advantages, limitations, and appropriate usage. *Am J Physiol Endocrinol Metab*, 294, E15-26.
- MUNTENER, M. & HSU, Y. C. 1977. Development of trophoblast and placenta of the mouse. A reinvestigation with regard to the in vitro culture of mouse trophoblast and placenta. *Acta Anat (Basel)*, 98, 241-52.
- MÜNTENER, M. & HSU, Y. C. 1977. Development of trophoblast and placenta of the mouse. A reinvestigation with regard to the in vitro culture of mouse trophoblast and placenta. *Acta Anat (Basel)*, 98, 241-52.
- MURR, S. M., BRADFORD, G. E. & GESCHWIND, II 1974. Plasma luteinizing hormone, follicle-stimulating hormone and prolactin during pregnancy in the mouse. *Endocrinology*, 94, 112-6.
- MUSIAL, B., FERNANDEZ-TWINN, D. S., VAUGHAN, O. R., OZANNE, S. E., VOSHOL, P., SFERRUZZI-PERRI, A. N. & FOWDEN, A. L. 2016. Proximity to Delivery Alters Insulin Sensitivity and Glucose Metabolism in Pregnant Mice. *Diabetes*, 65, 851-60.
- MUSIAL, B., VAUGHAN, O. R., FERNANDEZ-TWINN, D. S., VOSHOL, P., OZANNE, S. E., FOWDEN, A. L. & SFERRUZZI-PERRI, A. N. 2017. A Western-style obesogenic diet alters maternal metabolic physiology with consequences for fetal nutrient acquisition in mice. *J Physiol*, 595, 4875-4892.
- MYATT, L. & THORNBURG, K. L. 2018. Effects of Prenatal Nutrition and the Role of the Placenta in Health and Disease. *Methods Mol Biol*, 1735, 19-46.
- NAPSO, T., YONG, H. E. J., LOPEZ-TELLO, J. & SFERRUZZI-PERRI, A. N. 2018. The Role of Placental Hormones in Mediating Maternal Adaptations to Support Pregnancy and Lactation. *Front Physiol*, 9, 1091.
- NAPSO, T., ZHAO, X., IBAÑEZ LLIGONA, M., SANDOVICI, I., KAY, R., GRIBBLE, F., REIMANN, F., MEEK, C., HAMILTON, R. & SFERRUZZI-PERRI, A. 2020. Unbiased placental secretome characterization identifies candidates for pregnancy complications. *bioRxiv*, 2020.07.12.198366.
- NAZARI, Z., NABIUNI, M., SAEIDI, M. & GOLALIPOUR, M. J. 2017. Gestational diabetes leads to down-regulation of CDK4-pRB-E2F1 pathway genes in pancreatic islets of rat offspring. *Iran J Basic Med Sci*, 20, 150-154.
- NEWBERN, D. & FREEMARK, M. 2011. Placental hormones and the control of maternal metabolism and fetal growth. *Curr Opin Endocrinol Diabetes Obes*, 18, 409-16.
- NGALA, R. A., FONDJO, L. A., GMAGNA, P., GHARTEY, F. N. & AWE, M. A. 2017. Placental peptides metabolism and maternal factors as predictors of risk of gestational diabetes in pregnant women. A case-control study. *PLoS One*, 12, e0181613.
- NILSSON, C., SWOLIN-EIDE, D., OHLSSON, C., ERIKSSON, E., HO, H. P., BJÖRNTORP, P. & HOLMÄNG, A. 2003. Reductions in adipose tissue and skeletal growth in rat adult offspring after prenatal leptin exposure. *J Endocrinol*, 176, 13-21.
- NOGUES, P., DOS SANTOS, E., JAMMES, H., BERVEILLER, P., ARNOULD, L., VIALARD, F. & DIEUDONNÉ, M. N. 2019. Maternal obesity influences expression and DNA methylation of the adiponectin and leptin systems in human third-trimester placenta. *Clin Epigenetics*, 11, 20.

- NOORLANDER, C. W., DE GRAAN, P. N., NIKKELS, P. G., SCHRAMA, L. H. & VISSER, G. H. 2004. Distribution of glutamate transporters in the human placenta. *Placenta*, 25, 489-95.
- NTEEBBA, J., VARBERG, K. M., SCOTT, R. L., SIMON, M. E., IQBAL, K. & SOARES, M. J. 2020. Poorly controlled diabetes mellitus alters placental structure, efficiency, and plasticity. *BMJ Open Diabetes Res Care*, 8.
- NUGENT, B. M., O'DONNELL, C. M., EPPERSON, C. N. & BALE, T. L. 2018. Placental H3K27me3 establishes female resilience to prenatal insults. *Nat Commun*, 9, 2555.
- O'DOWD, R., KENT, J. C., MOSELEY, J. M. & WLODEK, M. E. 2008. Effects of uteroplacental insufficiency and reducing litter size on maternal mammary function and postnatal offspring growth. *Am J Physiol Regul Integr Comp Physiol*, 294, R539-48.
- O'NEILL, S. & O'DRISCOLL, L. 2015. Metabolic syndrome: a closer look at the growing epidemic and its associated pathologies. *Obes Rev*, 16, 1-12.
- OKAMOTO, T., KATADA, T., MURAYAMA, Y., UI, M., OGATA, E. & NISHIMOTO, I. 1990. A simple structure encodes G protein-activating function of the IGF-II/mannose 6-phosphate receptor. *Cell*, 62, 709-17.
- OLA, M. S., NAWAZ, M. & AHSAN, H. 2011. Role of Bcl-2 family proteins and caspases in the regulation of apoptosis. *Mol Cell Biochem*, 351, 41-58.
- OLIVEIRA, A. C., ANDREOTTI, S., CHIMIN, P., SERTIE, R. A., FARIAS TDA, S., TORRES-LEAL, F. L., DE PROENCA, A. R., CAMPANA, A. B., D'AVILA, L. S., OLIVEIRA, K. A. & LIMA, F. B. 2015. Neonatal streptozotocin-induced diabetes in mothers promotes metabolic programming of adipose tissue in male rat offspring. *Life Sci*, 136, 151-6.
- OLSON, L. E., BEDJA, D., ALVEY, S. J., CARDOUNEL, A. J., GABRIELSON, K. L. & REEVES, R. H. 2003. Protection from doxorubicin-induced cardiac toxicity in mice with a null allele of carbonyl reductase 1. *Cancer Res*, 63, 6602-6.
- OPHERK, C., TRONCHE, F., KELLENDONK, C., KOHLMÜLLER, D., SCHULZE, A., SCHMID, W. & SCHÜTZ, G. 2004. Inactivation of the glucocorticoid receptor in hepatocytes leads to fasting hypoglycemia and ameliorates hyperglycemia in streptozotocin-induced diabetes mellitus. *Mol Endocrinol*, 18, 1346-53.
- ORNELLAS, F., MELLO, V. S., MANDARIM-DE-LACERDA, C. A. & AGUILA, M. B. 2013. Sexual dimorphism in fat distribution and metabolic profile in mice offspring from diet-induced obese mothers. *Life Sci*, 93, 454-63.
- OSINSKI, P. A. 1960. Steroid 11beta-ol dehydrogenase in human placenta. *Nature*, 187, 777.
- PALACIN, M., ESTEVEZ, R., BERTRAN, J. & ZORZANO, A. 1998. Molecular biology of mammalian plasma membrane amino acid transporters. *Physiol Rev*, 78, 969-1054.
- PANCHENKO, P. E., VOISIN, S., JOUIN, M., JOUNEAU, L., PREZELIN, A., LECOUTRE, S., BRETON, C., JAMMES, H., JUNIEN, C. & GABORY, A. 2016. Expression of epigenetic machinery genes is sensitive to maternal obesity and weight loss in relation to fetal growth in mice. *Clin Epigenetics*, 8, 22.
- PARIKH, R. M., JOSHI, S. R., MENON, P. S. & SHAH, N. S. 2007. Intensive glycemic control in diabetic pregnancy with intrauterine growth restriction is detrimental to fetus. *Med Hypotheses*, 69, 203-5.

- PARRA-VARGAS, M., RAMON-KRAUEL, M., LERIN, C. & JIMENEZ-CHILLARON, J. C. 2020. Size Does Matter: Litter Size Strongly Determines Adult Metabolism in Rodents. *Cell Metab*, 32, 334-340.
- PASHKOV, V., HUANG, J., PARAMESWARA, V. K., KEDZIERSKI, W., KURRASCH, D. M., TALL, G. G., ESSER, V., GERARD, R. D., UYEDA, K., TOWLE, H. C. & WILKIE, T. M. 2011. Regulator of G protein signaling (RGS16) inhibits hepatic fatty acid oxidation in a carbohydrate response element-binding protein (ChREBP)-dependent manner. *J Biol Chem*, 286, 15116-25.
- PAYNE, A. H. & HALES, D. B. 2004. Overview of steroidogenic enzymes in the pathway from cholesterol to active steroid hormones. *Endocr Rev*, 25, 947-70.
- PAYOLLA, T. B., LEMES, S. F., DE FANTE, T., REGINATO, A., MENDES DA SILVA, C., DE OLIVEIRA MICHELETTI, T., RODRIGUES, H. G., TORSONI, A. S., MILANSKI, M. & TORSONI, M. A. 2016. High-fat diet during pregnancy and lactation impairs the cholinergic anti-inflammatory pathway in the liver and white adipose tissue of mouse offspring. *Mol Cell Endocrinol*, 422, 192-202.
- PEDERSEN, K. B., ZHANG, P., DOUMEN, C., CHARBONNET, M., LU, D., NEWGARD, C. B., HAYCOCK, J. W., LANGE, A. J. & SCOTT, D. K. 2007. The promoter for the gene encoding the catalytic subunit of rat glucose-6-phosphatase contains two distinct glucose-responsive regions. *Am J Physiol Endocrinol Metab*, 292, E788-801.
- PENG, L. & PAYNE, A. H. 2002. AP-2 gamma and the homeodomain protein distal-less 3 are required for placental-specific expression of the murine 3 beta-hydroxysteroid dehydrogenase VI gene, Hsd3b6. *J Biol Chem*, 277, 7945-54.
- PÉNICAUD, L., ROHNER-JEANRENAUD, F. & JEANRENAUD, B. 1986. In vivo metabolic changes as studied longitudinally after ventromedial hypothalamic lesions. *Am J Physiol*, 250, E662-8.
- PENNO, C. A., MORGAN, S. A., ROSE, A. J., HERZIG, S., LAVERY, G. G. & ODERMATT, A. 2014. 11 β -Hydroxysteroid dehydrogenase-1 is involved in bile acid homeostasis by modulating fatty acid transport protein-5 in the liver of mice. *Mol Metab*, 3, 554-64.
- PEREIRA, T. J., FONSECA, M. A., CAMPBELL, K. E., MOYCE, B. L., COLE, L. K., HATCH, G. M., DOUCETTE, C. A., KLEIN, J., ALIANI, M. & DOLINSKY, V. W. 2015. Maternal obesity characterized by gestational diabetes increases the susceptibility of rat offspring to hepatic steatosis via a disrupted liver metabolome. *J Physiol*, 593, 3181-97.
- PETITT, D. J., BENNETT, P. H., KNOWLER, W. C., BAIRD, H. R. & ALECK, K. A. 1985. Gestational diabetes mellitus and impaired glucose tolerance during pregnancy. Long-term effects on obesity and glucose tolerance in the offspring. *Diabetes*, 34 Suppl 2, 119-22.
- PHILLIPS, K., KEDERSHA, N., SHEN, L., BLACKSHEAR, P. J. & ANDERSON, P. 2004. Arthritis suppressor genes TIA-1 and TTP dampen the expression of tumor necrosis factor alpha, cyclooxygenase 2, and inflammatory arthritis. *Proc Natl Acad Sci U S A*, 101, 2011-6.
- PICARD, F., WANATABE, M., SCHOONJANS, K., LYDON, J., O'MALLEY, B. W. & AUWERX, J. 2002. Progesterone receptor knockout mice have an improved glucose homeostasis secondary to beta -cell proliferation. *Proc Natl Acad Sci U S A*, 99, 15644-8.
- PICK, A., CLARK, J., KUBSTRUP, C., LEVISETTI, M., PUGH, W., BONNER-WEIR, S. & POLONSKY, K. S. 1998. Role of apoptosis in failure of beta-cell mass

- compensation for insulin resistance and beta-cell defects in the male Zucker diabetic fatty rat. *Diabetes*, 47, 358-64.
- PLOWS, J. F., STANLEY, J. L., BAKER, P. N., REYNOLDS, C. M. & VICKERS, M. H. 2018. The Pathophysiology of Gestational Diabetes Mellitus. *Int J Mol Sci*, 19.
- POLLOCK, K. E., STEVENS, D., PENNINGTON, K. A., THAISRIVONGS, R., KAISER, J., ELLERSIECK, M. R., MILLER, D. K. & SCHULZ, L. C. 2015. Hyperleptinemia During Pregnancy Decreases Adult Weight of Offspring and Is Associated With Increased Offspring Locomotor Activity in Mice. *Endocrinology*, 156, 3777-90.
- PREVIS, S. F., WITHERS, D. J., REN, J. M., WHITE, M. F. & SHULMAN, G. I. 2000. Contrasting effects of IRS-1 versus IRS-2 gene disruption on carbohydrate and lipid metabolism in vivo. *J Biol Chem*, 275, 38990-4.
- PRINGLE, K. G. & ROBERTS, C. T. 2007. New light on early post-implantation pregnancy in the mouse: roles for insulin-like growth factor-II (IGF-II)? *Placenta*, 28, 286-97.
- QIU, X., VU, T. H., LU, Q., LING, J. Q., LI, T., HOU, A., WANG, S. K., CHEN, H. L., HU, J. F. & HOFFMAN, A. R. 2008. A complex deoxyribonucleic acid looping configuration associated with the silencing of the maternal Igf2 allele. *Mol Endocrinol*, 22, 1476-88.
- RADAELLI, T., CETIN, I., AYUK, P. T., GLAZIER, J. D., PARDI, G. & SIBLEY, C. P. 2002. Cationic amino acid transporter activity in the syncytiotrophoblast microvillous plasma membrane and oxygenation of the uteroplacental unit. *Placenta*, 23 Suppl A, S69-74.
- RADAELLI, T., LEPERCQ, J., VARASTEHPOUR, A., BASU, S., CATALANO, P. M. & HAUGUEL-DE MOUZON, S. 2009. Differential regulation of genes for fetoplacental lipid pathways in pregnancy with gestational and type 1 diabetes mellitus. *Am J Obstet Gynecol*, 201, 209.e1-209.e10.
- RADULESCU, L., MUNTEANU, O., POPA, F. & CIRSTOIU, M. 2013. The implications and consequences of maternal obesity on fetal intrauterine growth restriction. *J Med Life*, 6, 292-8.
- RAMATHAL, C. Y., BAGCHI, I. C., TAYLOR, R. N. & BAGCHI, M. K. 2010. Endometrial decidualization: of mice and men. *Semin Reprod Med*, 28, 17-26.
- RAMOS, M. P., CRESPO-SOLANS, M. D., DEL CAMPO, S., CACHO, J. & HERRERA, E. 2003. Fat accumulation in the rat during early pregnancy is modulated by enhanced insulin responsiveness. *Am J Physiol Endocrinol Metab*, 285, E318-28.
- RANDO, G., TAN, C. K., KHALED, N., MONTAGNER, A., LEUENBERGER, N., BERTRAND-MICHEL, J., PARAMALINGAM, E., GUILLOU, H. & WAHLI, W. 2016. Glucocorticoid receptor-PPAR α axis in fetal mouse liver prepares neonates for milk lipid catabolism. *Elife*, 5.
- RAO, P. N., SHASHIDHAR, A. & ASHOK, C. 2013. In utero fuel homeostasis: Lessons for a clinician. *Indian J Endocrinol Metab*, 17, 60-8.
- RAPPOLEE, D. A., STURM, K. S., BEHRENDTSEN, O., SCHULTZ, G. A., PEDERSEN, R. A. & WERB, Z. 1992. Insulin-like growth factor II acts through an endogenous growth pathway regulated by imprinting in early mouse embryos. *Genes Dev*, 6, 939-52.
- RAVELLI, A. C. J., VAN DER MEULEN, J. H. P., MICHELS, R. P. J., OSMOND, C., BARKER, D. J. P., HALES, C. N. & BLEKER, O. P. 1998. Glucose tolerance in adults after prenatal exposure to famine. *The Lancet*, 351, 173-177.

- RAVELLI, G. P., STEIN, Z. A. & SUSSER, M. W. 1976. Obesity in young men after famine exposure in utero and early infancy. *N Engl J Med*, 295, 349-53.
- REBUFFÉ-SCRIVE, M., KROTKIEWSKI, M., ELFVERSON, J. & BJÖRNTORP, P. 1988. Muscle and adipose tissue morphology and metabolism in Cushing's syndrome. *J Clin Endocrinol Metab*, 67, 1122-8.
- REBUFFÉ-SCRIVE, M., WALSH, U. A., MCEWEN, B. & RODIN, J. 1992. Effect of chronic stress and exogenous glucocorticoids on regional fat distribution and metabolism. *Physiol Behav*, 52, 583-90.
- REDLINE, R. W., CHERNICKY, C. L., TAN, H. Q., ILAN, J. & ILAN, J. 1993. Differential expression of insulin-like growth factor-II in specific regions of the late (post day 9.5) murine placenta. *Mol Reprod Dev*, 36, 121-9.
- REGNAULT, T. R., DE VRIJER, B. & BATTAGLIA, F. C. 2002. Transport and metabolism of amino acids in placenta. *Endocrine*, 19, 23-41.
- REIK, W., CONSTÂNCIA, M., FOWDEN, A., ANDERSON, N., DEAN, W., FERGUSON-SMITH, A., TYCKO, B. & SIBLEY, C. 2003. Regulation of supply and demand for maternal nutrients in mammals by imprinted genes. *J Physiol*, 547, 35-44.
- REIK, W. & WALTER, J. 2001. Genomic imprinting: parental influence on the genome. *Nat Rev Genet*, 2, 21-32.
- REYNOLDS, C. M., LI, M., GRAY, C. & VICKERS, M. H. 2013. Prewaning growth hormone treatment ameliorates adipose tissue insulin resistance and inflammation in adult male offspring following maternal undernutrition. *Endocrinology*, 154, 2676-86.
- RICH, D. Q., DEMISSIE, K., LU, S. E., KAMAT, L., WARTENBERG, D. & RHOADS, G. G. 2009. Ambient air pollutant concentrations during pregnancy and the risk of fetal growth restriction. *J Epidemiol Community Health*, 63, 488-96.
- RIECK, S. & KAESTNER, K. H. 2010. Expansion of beta-cell mass in response to pregnancy. *Trends Endocrinol Metab*, 21, 151-8.
- RINKENBERGER, J. & WERB, Z. 2000. The labyrinthine placenta. *Nat Genet*, 25, 248-50.
- RINNINGER, F., KAISER, T., MANN, W. A., MEYER, N., GRETEN, H. & BEISIEGEL, U. 1998. Lipoprotein lipase mediates an increase in the selective uptake of high density lipoprotein-associated cholesteryl esters by hepatic cells in culture. *J Lipid Res*, 39, 1335-48.
- RISKIN-MASHIAH, S., DAMTI, A., YOUNES, G. & AUSLENDER, R. 2010. First trimester fasting hyperglycemia as a predictor for the development of gestational diabetes mellitus. *Eur J Obstet Gynecol Reprod Biol*, 152, 163-7.
- ROBERTS, K. A., RILEY, S. C., REYNOLDS, R. M., BARR, S., EVANS, M., STATHAM, A., HOR, K., JABBOUR, H. N., NORMAN, J. E. & DENISON, F. C. 2011. Placental structure and inflammation in pregnancies associated with obesity. *Placenta*, 32, 247-54.
- RODER, P. V., WU, B., LIU, Y. & HAN, W. 2016. Pancreatic regulation of glucose homeostasis. *Exp Mol Med*, 48, e219.
- RODRÍGUEZ-GONZÁLEZ, G. L., REYES-CASTRO, L. A., BAUTISTA, C. J., BELTRÁN, A. A., IBÁÑEZ, C. A., VEGA, C. C., LOMAS-SORIA, C., CASTRO-RODRÍGUEZ, D. C., ELÍAS-LÓPEZ, A. L., NATHANIELSZ, P. W. & ZAMBRANO, E. 2019. Maternal obesity accelerates rat offspring metabolic ageing in a sex-dependent manner. *J Physiol*, 597, 5549-5563.
- RODRIK-OUTMEZGUINE, V. S., CHANDARLAPATY, S., PAGANO, N. C., POULIKAKOS, P. I., SCALTRITI, M., MOSKATEL, E., BASELGA, J.,

- GUICHARD, S. & ROSEN, N. 2011. mTOR kinase inhibition causes feedback-dependent biphasic regulation of AKT signaling. *Cancer Discov*, 1, 248-59.
- RODUIT, R. & THORENS, B. 1997. Inhibition of glucose-induced insulin secretion by long-term preexposure of pancreatic islets to leptin. *FEBS Lett*, 415, 179-82.
- ROG-ZIELINSKA, E. A., THOMSON, A., KENYON, C. J., BROWNSTEIN, D. G., MORAN, C. M., SZUMSKA, D., MICHAILIDOU, Z., RICHARDSON, J., OWEN, E., WATT, A., MORRISON, H., FORRESTER, L. M., BHATTACHARYA, S., HOLMES, M. C. & CHAPMAN, K. E. 2013. Glucocorticoid receptor is required for foetal heart maturation. *Hum Mol Genet*, 22, 3269-82.
- ROLAND, B. L. & FUNDER, J. W. 1996. Localization of 11beta-hydroxysteroid dehydrogenase type 2 in rat tissues: in situ studies. *Endocrinology*, 137, 1123-8.
- ROSARIO, F. J., KANAI, Y., POWELL, T. L. & JANSSON, T. 2015. Increased placental nutrient transport in a novel mouse model of maternal obesity with fetal overgrowth. *Obesity (Silver Spring)*, 23, 1663-70.
- ROSEBOOM, T. J., VAN DER MEULEN, J. H., RAVELLI, A. C., OSMOND, C., BARKER, D. J. & BLEKER, O. P. 2001. Effects of prenatal exposure to the Dutch famine on adult disease in later life: an overview. *Mol Cell Endocrinol*, 185, 93-8.
- ROSEN, E. D., SARRAF, P., TROY, A. E., BRADWIN, G., MOORE, K., MILSTONE, D. S., SPIEGELMAN, B. M. & MORTENSEN, R. M. 1999. PPAR gamma is required for the differentiation of adipose tissue in vivo and in vitro. *Mol Cell*, 4, 611-7.
- ROSEN, O. M. 1987. After insulin binds. *Science*, 237, 1452-8.
- ROSSANT, J. & CROSS, J. C. 2001. Placental development: lessons from mouse mutants. *Nat Rev Genet*, 2, 538-48.
- ROWAN, J. A., HAGUE, W. M., GAO, W., BATTIN, M. R. & MOORE, M. P. 2008. Metformin versus insulin for the treatment of gestational diabetes. *N Engl J Med*, 358, 2003-15.
- RUEDA-CLAUSEN, C. F., DOLINSKY, V. W., MORTON, J. S., PROCTOR, S. D., DYCK, J. R. & DAVIDGE, S. T. 2011. Hypoxia-induced intrauterine growth restriction increases the susceptibility of rats to high-fat diet-induced metabolic syndrome. *Diabetes*, 60, 507-16.
- RUI, L. 2014. Energy metabolism in the liver. *Compr Physiol*, 4, 177-97.
- RUIZ-PALACIOS, M., PRIETO-SÁNCHEZ, M. T., RUIZ-ALCARAZ, A. J., BLANCO-CARNERO, J. E., SANCHEZ-CAMPILLO, M., PARRILLA, J. J. & LARQUÉ, E. 2017. Insulin Treatment May Alter Fatty Acid Carriers in Placentas from Gestational Diabetes Subjects. *Int J Mol Sci*, 18.
- RYAN, E. A. & ENNS, L. 1988. Role of gestational hormones in the induction of insulin resistance. *J Clin Endocrinol Metab*, 67, 341-7.
- SAEGUSA, H., NAKAGAWA, Y., LIU, Y.-J. & OHZEKI, T. 1999. Influence of placental 11β-hydroxysteroid dehydrogenase (11β-HSD) inhibition on glucose metabolism and 11β-HSD regulation in adult offspring of rats. *Metabolism-Clinical and Experimental*, 48, 1584-1588.
- SAITO, T., OKUMURA, A., WATANABE, H., ASANO, M., ISHIDA-OKAWARA, A., SAKAGAMI, J., SUDO, K., HATANO-YOKOE, Y., BEZBRADICA, J. S., JOYCE, S., ABO, T., IWAKURA, Y., SUZUKI, K. & YAMAGOE, S. 2004. Increase in hepatic NKT cells in leukocyte cell-derived chemotaxin 2-deficient mice contributes to severe concanavalin A-induced hepatitis. *J Immunol*, 173, 579-85.

- SAKLAYEN, M. G. 2018. The Global Epidemic of the Metabolic Syndrome. *Curr Hypertens Rep*, 20, 12.
- SAKUMA, T., BHADHPRASIT, W., HASHITA, T. & NEMOTO, N. 2008. Synergism of glucocorticoid hormone with growth hormone for female-specific mouse Cyp3a44 gene expression. *Drug Metab Dispos*, 36, 878-84.
- SAKUMA, T., ENDO, Y., MASHINO, M., KUROIWA, M., OHARA, A., JARUKAMJORN, K. & NEMOTO, N. 2002. Regulation of the expression of two female-predominant CYP3A mRNAs (CYP3A41 and CYP3A44) in mouse liver by sex and growth hormones. *Arch Biochem Biophys*, 404, 234-42.
- SALMON, W. D., JR. & DAUGHADAY, W. H. 1957. A hormonally controlled serum factor which stimulates sulfate incorporation by cartilage in vitro. *J Lab Clin Med*, 49, 825-36.
- SALOMÄKI, H., HEINÄNIEMI, M., VÄHÄTALO, L. H., AILANEN, L., EEROLA, K., RUOHONEN, S. T., PESONEN, U. & KOULU, M. 2014. Prenatal metformin exposure in a maternal high fat diet mouse model alters the transcriptome and modifies the metabolic responses of the offspring. *PLoS One*, 9, e115778.
- SANDOVAL-RODRIGUEZ, A., MONROY-RAMIREZ, H. C., MEZA-RIOS, A., GARCIA-BAÑUELOS, J., VERA-CRUZ, J., GUTIÉRREZ-CUEVAS, J., SILVA-GOMEZ, J., STAELS, B., DOMINGUEZ-ROSALES, J., GALICIA-MORENO, M., VAZQUEZ-DEL MERCADO, M., NAVARRO-PARTIDA, J., SANTOS-GARCIA, A. & ARMENDARIZ-BORUNDA, J. 2020. Pirfenidone Is an Agonistic Ligand for PPAR α and Improves NASH by Activation of SIRT1/LKB1/pAMPK. *Hepatology Commun*, 4, 434-449.
- SANDOVICI, I., GEORGOPOULOU, A., HUFNAGEL, A. S., SCHIEFER, S. N., SANTOS, F., HOELLE, K., LAM, B. Y. H., YEO, G. S. H., BURLING, K., LÓPEZ-TELLO, J., REITERER, M., FOWDEN, A. L., BURTON, G. J., SFERRUZZI-PERRI, A. N., BRANCO, C. M. & CONSTÂNCIA, M. 2019. Fetus-derived IGF2 matches placental development to fetal demand. *bioRxiv*, 520536.
- SANO, H., KANE, S., SANO, E., MIINEA, C. P., ASARA, J. M., LANE, W. S., GARNER, C. W. & LIENHARD, G. E. 2003. Insulin-stimulated phosphorylation of a Rab GTPase-activating protein regulates GLUT4 translocation. *J Biol Chem*, 278, 14599-602.
- SARBASSOV, D. D., GUERTIN, D. A., ALI, S. M. & SABATINI, D. M. 2005. Phosphorylation and regulation of Akt/PKB by the rictor-mTOR complex. *Science*, 307, 1098-101.
- SASSON, I. E., VITINS, A. P., MAINIGI, M. A., MOLEY, K. H. & SIMMONS, R. A. 2015. Pre-gestational vs gestational exposure to maternal obesity differentially programs the offspring in mice. *Diabetologia*, 58, 615-24.
- SAWATZKY, D. A., WILLOUGHBY, D. A., COLVILLE-NASH, P. R. & ROSSI, A. G. 2006. The involvement of the apoptosis-modulating proteins ERK 1/2, Bcl-xL and Bax in the resolution of acute inflammation in vivo. *Am J Pathol*, 168, 33-41.
- SCHADINGER, S. E., BUCHER, N. L., SCHREIBER, B. M. & FARMER, S. R. 2005. PPAR γ 2 regulates lipogenesis and lipid accumulation in steatotic hepatocytes. *Am J Physiol Endocrinol Metab*, 288, E1195-205.
- SCHAFFER, J. E. & LODISH, H. F. 1994. Expression cloning and characterization of a novel adipocyte long chain fatty acid transport protein. *Cell*, 79, 427-36.
- SCHAIFF, W. T., KNAPP, F. F., JR., BARAK, Y., BIRON-SHENTAL, T., NELSON, D. M. & SADOVSKY, Y. 2007. Ligand-activated peroxisome proliferator

- activated receptor gamma alters placental morphology and placental fatty acid uptake in mice. *Endocrinology*, 148, 3625-34.
- SCHIFF, R., ARENSBURG, J., ITIN, A., KESHET, E. & ORLY, J. 1993. Expression and cellular localization of uterine side-chain cleavage cytochrome P450 messenger ribonucleic acid during early pregnancy in mice. *Endocrinology*, 133, 529-37.
- SCHLESSINGER, J. 1994. SH2/SH3 signaling proteins. *Curr Opin Genet Dev*, 4, 25-30.
- SCHMELZLE, K., KANE, S., GRIDLEY, S., LIENHARD, G. E. & WHITE, F. M. 2006. Temporal dynamics of tyrosine phosphorylation in insulin signaling. *Diabetes*, 55, 2171-9.
- SCHMIDT, D. R., SCHMIDT, S., HOLMSTROM, S. R., MAKISHIMA, M., YU, R. T., CUMMINS, C. L., MANGELSDORF, D. J. & KLIEWER, S. A. 2011. AKR1B7 is induced by the farnesoid X receptor and metabolizes bile acids. *J Biol Chem*, 286, 2425-32.
- SCHMIDT-SUPPRIAN, M. & RAJEWSKY, K. 2007. Vagaries of conditional gene targeting. *Nat Immunol*, 8, 665-8.
- SCHOONJANS, K., PEINADO-ONSURBE, J., LEFEBVRE, A. M., HEYMAN, R. A., BRIGGS, M., DEEB, S., STAELS, B. & AUWERX, J. 1996a. PPARalpha and PPARgamma activators direct a distinct tissue-specific transcriptional response via a PPRE in the lipoprotein lipase gene. *Embo j*, 15, 5336-48.
- SCHOONJANS, K., STAELS, B. & AUWERX, J. 1996b. The peroxisome proliferator activated receptors (PPARS) and their effects on lipid metabolism and adipocyte differentiation. *Biochimica et Biophysica Acta (BBA)-Lipids and Lipid Metabolism*, 1302, 93-109.
- SCHURCH, N. J., SCHOFIELD, P., GIERLIŃSKI, M., COLE, C., SHERSTNEV, A., SINGH, V., WROBEL, N., GHARBI, K., SIMPSON, G. G., OWEN-HUGHES, T., BLAXTER, M. & BARTON, G. J. 2016. How many biological replicates are needed in an RNA-seq experiment and which differential expression tool should you use? *RNA (New York, N.Y.)*, 22, 839-851.
- SCIFRES, C. M., CHEN, B., NELSON, D. M. & SADOVSKY, Y. 2011. Fatty acid binding protein 4 regulates intracellular lipid accumulation in human trophoblasts. *J Clin Endocrinol Metab*, 96, E1083-91.
- SECKL, J. R. & HOLMES, M. C. 2007. Mechanisms of disease: glucocorticoids, their placental metabolism and fetal 'programming' of adult pathophysiology. *Nat Clin Pract Endocrinol Metab*, 3, 479-88.
- SEET, E. L., YEE, J. K., JELLYMAN, J. K., HAN, G., ROSS, M. G. & DESAI, M. 2015. Maternal high-fat-diet programs rat offspring liver fatty acid metabolism. *Lipids*, 50, 565-73.
- SEINO, S., SEINO, M., NISHI, S. & BELL, G. I. 1989. Structure of the human insulin receptor gene and characterization of its promoter. *Proc Natl Acad Sci U S A*, 86, 114-8.
- SFERRUZZI-PERRI, A. N. 2018a. Assessment of Placental Transport Function in Studies of Disease Programming. *Methods Mol Biol*, 1735, 239-250.
- SFERRUZZI-PERRI, A. N. 2018b. Regulating needs: Exploring the role of insulin-like growth factor-2 signalling in materno-fetal resource allocation. *Placenta*, 64 Suppl 1, S16-s22.
- SFERRUZZI-PERRI, A. N. & CAMM, E. J. 2016. The Programming Power of the Placenta. *Front Physiol*, 7, 33.

- SFERRUZZI-PERRI, A. N., LOPEZ-TELLO, J., NAPSO, T. & YONG, H. E. J. 2020. Exploring the causes and consequences of maternal metabolic maladaptations during pregnancy: Lessons from animal models. *Placenta*.
- SFERRUZZI-PERRI, A. N., OWENS, J. A., STANDEN, P. & ROBERTS, C. T. 2008. Maternal insulin-like growth factor-II promotes placental functional development via the type 2 IGF receptor in the guinea pig. *Placenta*, 29, 347-55.
- SFERRUZZI-PERRI, A. N., OWENS, J. A., STANDEN, P., TAYLOR, R. L., HEINEMANN, G. K., ROBINSON, J. S. & ROBERTS, C. T. 2007. Early treatment of the pregnant guinea pig with IGFs promotes placental transport and nutrient partitioning near term. *Am J Physiol Endocrinol Metab*, 292, E668-76.
- SFERRUZZI-PERRI, A. N., SANDOVICI, I., CONSTANCIA, M. & FOWDEN, A. L. 2017. Placental phenotype and the insulin-like growth factors: resource allocation to fetal growth. *J Physiol*, 595, 5057-5093.
- SFERRUZZI-PERRI, A. N., VAUGHAN, O. R., COAN, P. M., SUCIU, M. C., DARBYSHIRE, R., CONSTANCIA, M., BURTON, G. J. & FOWDEN, A. L. 2011. Placental-specific IGF2 deficiency alters developmental adaptations to undernutrition in mice. *Endocrinology*, 152, 3202-12.
- SFERRUZZI-PERRI, A. N., VAUGHAN, O. R., FORHEAD, A. J. & FOWDEN, A. L. 2013a. Hormonal and nutritional drivers of intrauterine growth. *Curr Opin Clin Nutr Metab Care*, 16, 298-309.
- SFERRUZZI-PERRI, A. N., VAUGHAN, O. R., HARO, M., COOPER, W. N., MUSIAL, B., CHARALAMBOUS, M., PESTANA, D., AYYAR, S., FERGUSON-SMITH, A. C., BURTON, G. J., CONSTANCIA, M. & FOWDEN, A. L. 2013b. An obesogenic diet during mouse pregnancy modifies maternal nutrient partitioning and the fetal growth trajectory. *FASEB J*, 27, 3928-37.
- SHAMS, M., KILBY, M. D., SOMERSET, D. A., HOWIE, A. J., GUPTA, A., WOOD, P. J., AFNAN, M. & STEWART, P. M. 1998. 11Beta-hydroxysteroid dehydrogenase type 2 in human pregnancy and reduced expression in intrauterine growth restriction. *Hum Reprod*, 13, 799-804.
- SHEN, L., LIU, Z., GONG, J., ZHANG, L., WANG, L., MAGDALOU, J., CHEN, L. & WANG, H. 2014. Prenatal ethanol exposure programs an increased susceptibility of non-alcoholic fatty liver disease in female adult offspring rats. *Toxicol Appl Pharmacol*, 274, 263-73.
- SHIMOMURA, I., HAMMER, R. E., RICHARDSON, J. A., IKEMOTO, S., BASHMAKOV, Y., GOLDSTEIN, J. L. & BROWN, M. S. 1998. Insulin resistance and diabetes mellitus in transgenic mice expressing nuclear SREBP-1c in adipose tissue: model for congenital generalized lipodystrophy. *Genes Dev*, 12, 3182-94.
- SHIN, B. C., FUJIKURA, K., SUZUKI, T., TANAKA, S. & TAKATA, K. 1997. Glucose transporter GLUT3 in the rat placental barrier: a possible machinery for the transplacental transfer of glucose. *Endocrinology*, 138, 3997-4004.
- SIBLEY, C. P., COAN, P. M., FERGUSON-SMITH, A. C., DEAN, W., HUGHES, J., SMITH, P., REIK, W., BURTON, G. J., FOWDEN, A. L. & CONSTANCIA, M. 2004. Placental-specific insulin-like growth factor 2 (Igf2) regulates the diffusional exchange characteristics of the mouse placenta. *Proc Natl Acad Sci U S A*, 101, 8204-8.
- SIGURDSSON, V., HAGA, Y., TAKEI, H., MANSELL, E., OKAMATSU-HAGA, C., SUZUKI, M., RADULOVIC, V., VAN DER GARDE, M., KOIDE, S., SOBOLEVA, S., GÅFVELS, M., NITTONO, H., OHARA, A. & MIHARADA,

- K. 2020. Induction of blood-circulating bile acids supports recovery from myelosuppressive chemotherapy. *Blood advances*, 4, 1833-1843.
- SIGURDSSON, V., TAKEI, H., SOBOLEVA, S., RADULOVIC, V., GALEEV, R., SIVA, K., LEEB-LUNDBERG, L. M., IIDA, T., NITTONO, H. & MIHARADA, K. 2016. Bile Acids Protect Expanding Hematopoietic Stem Cells from Unfolded Protein Stress in Fetal Liver. *Cell Stem Cell*, 18, 522-32.
- SIMI, B., SEMPORE, B., MAYET, M. H. & FAVIER, R. J. 1991. Additive effects of training and high-fat diet on energy metabolism during exercise. *J Appl Physiol (1985)*, 71, 197-203.
- SIMMONS, D. G. & CROSS, J. C. 2005. Determinants of trophoblast lineage and cell subtype specification in the mouse placenta. *Dev Biol*, 284, 12-24.
- SIMMONS, D. G., FORTIER, A. L. & CROSS, J. C. 2007. Diverse subtypes and developmental origins of trophoblast giant cells in the mouse placenta. *Dev Biol*, 304, 567-78.
- SIMMONS, D. G., RAWN, S., DAVIES, A., HUGHES, M. & CROSS, J. C. 2008. Spatial and temporal expression of the 23 murine Prolactin/Placental Lactogen-related genes is not associated with their position in the locus. *BMC Genomics*, 9, 352.
- SIMMONS, R. A., SUPONITSKY-KROYTER, I. & SELAK, M. A. 2005. Progressive accumulation of mitochondrial DNA mutations and decline in mitochondrial function lead to beta-cell failure. *J Biol Chem*, 280, 28785-91.
- SIMONČIČ, M., REŽEN, T., JUVAN, P., ROZMAN, D., FAZARINC, G., FIEVET, C., STAELS, B. & HORVAT, S. 2011. Obesity resistant mechanisms in the Lean polygenic mouse model as indicated by liver transcriptome and expression of selected genes in skeletal muscle. *BMC Genomics*, 12, 96.
- SINCLAIR, K. D., ALLEGRUCCI, C., SINGH, R., GARDNER, D. S., SEBASTIAN, S., BISPHAM, J., THURSTON, A., HUNTLEY, J. F., REES, W. D., MALONEY, C. A., LEA, R. G., CRAIGON, J., MCEVOY, T. G. & YOUNG, L. E. 2007. DNA methylation, insulin resistance, and blood pressure in offspring determined by maternal periconceptional B vitamin and methionine status. *Proc Natl Acad Sci U S A*, 104, 19351-6.
- SKARRA, D. V., HERNANDEZ-CARRETERO, A., RIVERA, A. J., ANVAR, A. R. & THACKRAY, V. G. 2017. Hyperandrogenemia Induced by Letrozole Treatment of Pubertal Female Mice Results in Hyperinsulinemia Prior to Weight Gain and Insulin Resistance. *Endocrinology*, 158, 2988-3003.
- SKARZINSKI, G., KHAMAISI, M., BURSZTYN, M., MEKLER, J., LAN, D., EVDOKIMOV, P. & ARIEL, I. 2009. Intrauterine growth restriction and shallower implantation site in rats with maternal hyperinsulinemia are associated with altered NOS expression. *Placenta*, 30, 898-906.
- SLOBODA, D. M., NEWNHAM, J. P. & CHALLIS, J. R. 2000. Effects of repeated maternal betamethasone administration on growth and hypothalamic-pituitary-adrenal function of the ovine fetus at term. *J Endocrinol*, 165, 79-91.
- SMITH, P. K., KROHN, R. I., HERMANSON, G. T., MALLIA, A. K., GARTNER, F. H., PROVENZANO, M. D., FUJIMOTO, E. K., GOEKE, N. M., OLSON, B. J. & KLENK, D. C. 1985. Measurement of protein using bicinchoninic acid. *Anal Biochem*, 150, 76-85.
- SMITH, T., SLOBODA, D. M., SAFFERY, R., JOO, E. & VICKERS, M. H. 2014. Maternal nutritional history modulates the hepatic IGF-IGFBP axis in adult male rat offspring. *Endocrine*, 46, 70-82.

- SMOAK, K. & CIDLOWSKI, J. A. 2006. Glucocorticoids regulate tristetraprolin synthesis and posttranscriptionally regulate tumor necrosis factor alpha inflammatory signaling. *Molecular and cellular biology*, 26, 9126-9135.
- SOARES, M. J. 2004. The prolactin and growth hormone families: pregnancy-specific hormones/cytokines at the maternal-fetal interface. *Reprod Biol Endocrinol*, 2, 51.
- SOARES, M. J., CHAPMAN, B. M., RASMUSSEN, C. A., DAI, G., KAMEI, T. & ORWIG, K. E. 1996. Differentiation of trophoblast endocrine cells. *Placenta*, 17, 277-89.
- SOMM, E., VAUTHAY, D. M., GUERARDEL, A., TOULOTTE, A., CETTOUR-ROSE, P., KLEE, P., MEDA, P., AUBERT, M. L., HUPPI, P. S. & SCHWITZGEBEL, V. M. 2012. Early metabolic defects in dexamethasone-exposed and undernourished intrauterine growth restricted rats. *PLoS One*, 7, e50131.
- SONG, Y. P., CHEN, Y. H., GAO, L., WANG, P., WANG, X. L., LUO, B., LI, J. & XU, D. X. 2018. Differential effects of high-fat diets before pregnancy and/or during pregnancy on fetal growth development. *Life Sci*, 212, 241-250.
- SORENSEN, R. L. & BRELJE, T. C. 1997. Adaptation of islets of Langerhans to pregnancy: beta-cell growth, enhanced insulin secretion and the role of lactogenic hormones. *Horm Metab Res*, 29, 301-7.
- SOWTON, A. P., PADMANABHAN, N., TUNSTER, S. J., MCNALLY, B. D., MURGIA, A., YUSUF, A., GRIFFIN, J. L., MURRAY, A. J. & WATSON, E. D. 2020. Mtrr hypomorphic mutation alters liver morphology, metabolism and fuel storage in mice. *Mol Genet Metab Rep*, 23, 100580.
- SRIVASTAVA, M., HSIEH, S., GRINBERG, A., WILLIAMS-SIMONS, L., HUANG, S. P. & PFEIFER, K. 2000. H19 and Igf2 monoallelic expression is regulated in two distinct ways by a shared cis acting regulatory region upstream of H19. *Genes Dev*, 14, 1186-95.
- ST-PIERRE, J., HIVERT, M. F., PERRON, P., POIRIER, P., GUAY, S. P., BRISSON, D. & BOUCHARD, L. 2012. IGF2 DNA methylation is a modulator of newborn's fetal growth and development. *Epigenetics*, 7, 1125-32.
- STARK, M. J., WRIGHT, I. M. & CLIFTON, V. L. 2009. Sex-specific alterations in placental 11beta-hydroxysteroid dehydrogenase 2 activity and early postnatal clinical course following antenatal betamethasone. *Am J Physiol Regul Integr Comp Physiol*, 297, R510-4.
- STEIL, G. M., TRIVEDI, N., JONAS, J. C., HASENKAMP, W. M., SHARMA, A., BONNER-WEIR, S. & WEIR, G. C. 2001. Adaptation of beta-cell mass to substrate oversupply: enhanced function with normal gene expression. *Am J Physiol Endocrinol Metab*, 280, E788-96.
- STERN, M. P., WILLIAMS, K. & HAFFNER, S. M. 2002. Identification of persons at high risk for type 2 diabetes mellitus: do we need the oral glucose tolerance test? *Ann Intern Med*, 136, 575-81.
- STEWART, I. & PEEL, S. 1978. The differentiation of the decidua and the distribution of metrial gland cells in the pregnant mouse uterus. *Cell Tissue Res*, 187, 167-79.
- STRAKOVSKY, R. S., ZHANG, X., ZHOU, D. & PAN, Y. X. 2011. Gestational high fat diet programs hepatic phosphoenolpyruvate carboxykinase gene expression and histone modification in neonatal offspring rats. *J Physiol*, 589, 2707-17.
- STRAUSS, J. F., 3RD, KISHIDA, T., CHRISTENSON, L. K., FUJIMOTO, T. & HIROI, H. 2003. START domain proteins and the intracellular trafficking of cholesterol in steroidogenic cells. *Mol Cell Endocrinol*, 202, 59-65.

- STRAUSS, J. F., 3RD, MARTINEZ, F. & KIRIAKIDOU, M. 1996. Placental steroid hormone synthesis: unique features and unanswered questions. *Biol Reprod*, 54, 303-11.
- STRAZZABOSCO, M. & FABRIS, L. 2012. Development of the bile ducts: essentials for the clinical hepatologist. *J Hepatol*, 56, 1159-70.
- SU, R., WANG, C., FENG, H., LIN, L., LIU, X., WEI, Y. & YANG, H. 2016a. Alteration in Expression and Methylation of IGF2/H19 in Placenta and Umbilical Cord Blood Are Associated with Macrosomia Exposed to Intrauterine Hyperglycemia. *PLoS One*, 11, e0148399.
- SU, R., YAN, J. & YANG, H. 2016b. Transgenerational Glucose Intolerance of Tumor Necrosis Factor with Epigenetic Alteration in Rat Perirenal Adipose Tissue Induced by Intrauterine Hyperglycemia. *J Diabetes Res*, 2016, 4952801.
- SUMIYOSHI, M., SAKANAKA, M. & KIMURA, Y. 2006. Chronic intake of high-fat and high-sucrose diets differentially affects glucose intolerance in mice. *J Nutr*, 136, 582-7.
- SUN, X. J., CRIMMINS, D. L., MYERS, M. G., JR., MIRALPEIX, M. & WHITE, M. F. 1993. Pleiotropic insulin signals are engaged by multisite phosphorylation of IRS-1. *Mol Cell Biol*, 13, 7418-28.
- SUSIARJO, M., XIN, F., BANSAL, A., STEFANIAK, M., LI, C., SIMMONS, R. A. & BARTOLOMEI, M. S. 2015. Bisphenol a exposure disrupts metabolic health across multiple generations in the mouse. *Endocrinology*, 156, 2049-58.
- SUTTER-DUB, M. T., DAZEY, B., VERGNAUD, M. T. & MADEC, A. M. 1981. Progesterone and insulin-resistance in the pregnant rat. I. In vivo and in vitro studies. *Diabete Metab*, 7, 97-104.
- SZKLARCZYK, D., FRANCESCHINI, A., WYDER, S., FORSLUND, K., HELLER, D., HUERTA-CEPAS, J., SIMONOVIC, M., ROTH, A., SANTOS, A., TSAFOU, K. P., KUHN, M., BORK, P., JENSEN, L. J. & VON MERING, C. 2015. STRING v10: protein-protein interaction networks, integrated over the tree of life. *Nucleic Acids Res*, 43, D447-52.
- TAKAHASHI, Y., NISHIMURA, T., MARUYAMA, T., TOMI, M. & NAKASHIMA, E. 2017. Contributions of system A subtypes to α -methylaminoisobutyric acid uptake by placental microvillous membranes of human and rat. *Amino Acids*, 49, 795-803.
- TAKATA, K., KASAHARA, T., KASAHARA, M., EZAKI, O. & HIRANO, H. 1994. Immunolocalization of glucose transporter GLUT1 in the rat placental barrier: possible role of GLUT1 and the gap junction in the transport of glucose across the placental barrier. *Cell Tissue Res*, 276, 411-8.
- TAKEDA, K., TODA, K., SAIBARA, T., NAKAGAWA, M., SAIKA, K., ONISHI, T., SUGIURA, T. & SHIZUTA, Y. 2003. Progressive development of insulin resistance phenotype in male mice with complete aromatase (CYP19) deficiency. *J Endocrinol*, 176, 237-46.
- TAKEKAWA, M. & SAITO, H. 1998. A family of stress-inducible GADD45-like proteins mediate activation of the stress-responsive MTK1/MEKK4 MAPKKK. *Cell*, 95, 521-30.
- TAN, H. C., ROBERTS, J., CATOV, J., KRISHNAMURTHY, R., SHYPAILO, R. & BACHA, F. 2015. Mother's pre-pregnancy BMI is an important determinant of adverse cardiometabolic risk in childhood. *Pediatr Diabetes*, 16, 419-26.
- TANG, L., LI, P. & LI, L. 2020. Whole transcriptome expression profiles in placenta samples from women with gestational diabetes mellitus. *J Diabetes Investig*.

- TANG, T., ZHANG, J., YIN, J., STASZKIEWICZ, J., GAWRONSKA-KOZAK, B., JUNG, D. Y., KO, H. J., ONG, H., KIM, J. K., MYNATT, R., MARTIN, R. J., KEENAN, M., GAO, Z. & YE, J. 2010. Uncoupling of inflammation and insulin resistance by NF-kappaB in transgenic mice through elevated energy expenditure. *J Biol Chem*, 285, 4637-44.
- TARRY-ADKINS, J. L. & OZANNE, S. E. 2018. Telomere Length Analysis: A Tool for Dissecting Aging Mechanisms in Developmental Programming. *Methods Mol Biol*, 1735, 351-363.
- TATULIAN, S. A. 2015. Structural Dynamics of Insulin Receptor and Transmembrane Signaling. *Biochemistry*, 54, 5523-32.
- TAYLOR, S. I. 1992. Lilly Lecture: molecular mechanisms of insulin resistance. Lessons from patients with mutations in the insulin-receptor gene. *Diabetes*, 41, 1473-90.
- TENG, Y. W., ELLIS, J. M., COLEMAN, R. A. & ZEISEL, S. H. 2012. Mouse betaine-homocysteine S-methyltransferase deficiency reduces body fat via increasing energy expenditure and impairing lipid synthesis and enhancing glucose oxidation in white adipose tissue. *J Biol Chem*, 287, 16187-98.
- TENG, Y. W., MEHEDINT, M. G., GARROW, T. A. & ZEISEL, S. H. 2011. Deletion of betaine-homocysteine S-methyltransferase in mice perturbs choline and 1-carbon metabolism, resulting in fatty liver and hepatocellular carcinomas. *J Biol Chem*, 286, 36258-67.
- THEYS, N., AHN, M. T., BOUCKENOOGHE, T., REUSENS, B. & REMACLE, C. 2011. Maternal malnutrition programs pancreatic islet mitochondrial dysfunction in the adult offspring. *J Nutr Biochem*, 22, 985-94.
- THOMAS, C. R., ERIKSSON, G. L. & ERIKSSON, U. J. 1990. Effects of maternal diabetes on placental transfer of glucose in rats. *Diabetes*, 39, 276-282.
- THOMPSON, A., HAN, V. K. & YANG, K. 2002. Spatial and temporal patterns of expression of 11beta-hydroxysteroid dehydrogenase types 1 and 2 messenger RNA and glucocorticoid receptor protein in the murine placenta and uterus during late pregnancy. *Biol Reprod*, 67, 1708-18.
- THORPE, L. M., YUZUGULLU, H. & ZHAO, J. J. 2015. PI3K in cancer: divergent roles of isoforms, modes of activation and therapeutic targeting. *Nat Rev Cancer*, 15, 7-24.
- THORVALDSEN, J. L., DURAN, K. L. & BARTOLOMEI, M. S. 1998. Deletion of the H19 differentially methylated domain results in loss of imprinted expression of H19 and Igf2. *Genes Dev*, 12, 3693-702.
- THORVALDSEN, J. L., FEDORIW, A. M., NGUYEN, S. & BARTOLOMEI, M. S. 2006. Developmental profile of H19 differentially methylated domain (DMD) deletion alleles reveals multiple roles of the DMD in regulating allelic expression and DNA methylation at the imprinted H19/Igf2 locus. *Mol Cell Biol*, 26, 1245-58.
- TIANO, J. P. & MAUVAIS-JARVIS, F. 2012. Molecular mechanisms of estrogen receptors' suppression of lipogenesis in pancreatic β -cells. *Endocrinology*, 153, 2997-3005.
- TONTONOZ, P., GRAVES, R. A., BUDAVARI, A. I., ERDJUMENT-BROMAGE, H., LUI, M., HU, E., TEMPST, P. & SPIEGELMAN, B. M. 1994. Adipocyte-specific transcription factor ARF6 is a heterodimeric complex of two nuclear hormone receptors, PPAR gamma and RXR alpha. *Nucleic Acids Res*, 22, 5628-34.
- TRUJILLO, M. L., SPUCH, C., CARRO, E. & SENARIS, R. 2011. Hyperphagia and central mechanisms for leptin resistance during pregnancy. *Endocrinology*, 152, 1355-65.

- TSUNODA, Y., TOKUNAGA, T. & SUGIE, T. 1985. Altered sex ratio of live young after transfer of fast-and slow-developing mouse embryos. *Gamete Research*, 12, 301-304.
- TUNSTER, S. J., WATSON, E. D., FOWDEN, A. L. & BURTON, G. J. 2020. Placental glycogen stores and fetal growth: insights from genetic mouse models. *Reproduction*, 159, R213-r235.
- TURNER, N. & ROBKER, R. L. 2015. Developmental programming of obesity and insulin resistance: does mitochondrial dysfunction in oocytes play a role? *Mol Hum Reprod*, 21, 23-30.
- UEKI, K., ALGENSTAEDT, P., MAUVAIS-JARVIS, F. & KAHN, C. R. 2000. Positive and negative regulation of phosphoinositide 3-kinase-dependent signaling pathways by three different gene products of the p85alpha regulatory subunit. *Mol Cell Biol*, 20, 8035-46.
- UM, S. H., FRIGERIO, F., WATANABE, M., PICARD, F., JOAQUIN, M., STICKER, M., FUMAGALLI, S., ALLEGRINI, P. R., KOZMA, S. C., AUWERX, J. & THOMAS, G. 2004. Absence of S6K1 protects against age- and diet-induced obesity while enhancing insulin sensitivity. *Nature*, 431, 200-5.
- VACCA, P., CHIOSSONE, L., MINGARI, M. C. & MORETTA, L. 2019. Heterogeneity of NK Cells and Other Innate Lymphoid Cells in Human and Murine Decidua. *Front Immunol*, 10, 170.
- VALDIVIA, R. P., KUNIEDA, T., AZUMA, S. & TOYODA, Y. 1993. PCR sexing and developmental rate differences in preimplantation mouse embryos fertilized and cultured in vitro. *Mol Reprod Dev*, 35, 121-6.
- VALTAT, B., DUPUIS, C., ZENATY, D., SINGH-ESTIVALET, A., TRONCHE, F., BRÉANT, B. & BLONDEAU, B. 2011. Genetic evidence of the programming of beta cell mass and function by glucocorticoids in mice. *Diabetologia*, 54, 350-9.
- VAN HERWAARDEN, A. E., WAGENAAR, E., VAN DER KRUIJSSSEN, C. M., VAN WATERSCHOOT, R. A., SMIT, J. W., SONG, J. Y., VAN DER VALK, M. A., VAN TELLINGEN, O., VAN DER HOORN, J. W., ROSING, H., BEIJNEN, J. H. & SCHINKEL, A. H. 2007. Knockout of cytochrome P450 3A yields new mouse models for understanding xenobiotic metabolism. *J Clin Invest*, 117, 3583-92.
- VASAVADA, R. C., CAVALIERE, C., D'ERCOLE, A. J., DANN, P., BURTIS, W. J., MADLENER, A. L., ZAWALICH, K., ZAWALICH, W., PHILBRICK, W. & STEWART, A. F. 1996. Overexpression of parathyroid hormone-related protein in the pancreatic islets of transgenic mice causes islet hyperplasia, hyperinsulinemia, and hypoglycemia. *J Biol Chem*, 271, 1200-8.
- VATNER, D. F., MAJUMDAR, S. K., KUMASHIRO, N., PETERSEN, M. C., RAHIMI, Y., GATTU, A. K., BEARS, M., CAMPOREZ, J. P., CLINE, G. W., JURCZAK, M. J., SAMUEL, V. T. & SHULMAN, G. I. 2015. Insulin-independent regulation of hepatic triglyceride synthesis by fatty acids. *Proc Natl Acad Sci U S A*, 112, 1143-8.
- VAUGHAN, O. R., FISHER, H. M., DIONELIS, K. N., JEFFREYS, E. C., HIGGINS, J. S., MUSIAL, B., SFERRUZZI-PERRI, A. N. & FOWDEN, A. L. 2015. Corticosterone alters materno-fetal glucose partitioning and insulin signalling in pregnant mice. *J Physiol*, 593, 1307-21.
- VAUGHAN, O. R., POWELL, T. L. & JANSSON, T. 2019. Apelin is a novel regulator of human trophoblast amino acid transport. *Am J Physiol Endocrinol Metab*, 316, E810-e816.

- VAUGHAN, O. R., SFERRUZZI-PERRI, A. N., COAN, P. M. & FOWDEN, A. L. 2013. Adaptations in placental phenotype depend on route and timing of maternal dexamethasone administration in mice. *Biol Reprod*, 89, 80.
- VAUGHAN, O. R., SFERRUZZI-PERRI, A. N. & FOWDEN, A. L. 2012. Maternal corticosterone regulates nutrient allocation to fetal growth in mice. *J Physiol*, 590, 5529-40.
- VICKERS, M. H., BREIER, B. H., CUTFIELD, W. S., HOFMAN, P. L. & GLUCKMAN, P. D. 2000. Fetal origins of hyperphagia, obesity, and hypertension and postnatal amplification by hypercaloric nutrition. *Am J Physiol Endocrinol Metab*, 279, E83-7.
- VOLAT, F. E., POINTUD, J. C., PASTEL, E., MORIO, B., SION, B., HAMARD, G., GUICHARDANT, M., COLAS, R., LEFRANÇOIS-MARTINEZ, A. M. & MARTINEZ, A. 2012. Depressed levels of prostaglandin F2 α in mice lacking Akr1b7 increase basal adiposity and predispose to diet-induced obesity. *Diabetes*, 61, 2796-806.
- VOM SAAL, F. S. 1989. Sexual differentiation in litter-bearing mammals: influence of sex of adjacent fetuses in utero. *J Anim Sci*, 67, 1824-40.
- VOM SAAL, F. S., GRANT, W. M., MCMULLEN, C. W. & LAVES, K. S. 1983. High fetal estrogen concentrations: correlation with increased adult sexual activity and decreased aggression in male mice. *Science*, 220, 1306-9.
- VON MERING, C., JENSEN, L. J., SNEL, B., HOOPER, S. D., KRUPP, M., FOGlierINI, M., JOUFFRE, N., HUYNEN, M. A. & BORK, P. 2005. STRING: known and predicted protein-protein associations, integrated and transferred across organisms. *Nucleic Acids Res*, 33, D433-7.
- VON WILAMOWITZ-MOELLENDORFF, A., HUNTER, R. W., GARCIA-ROCHA, M., KANG, L., LOPEZ-SOLDADO, I., LANTIER, L., PATEL, K., PEGGIE, M. W., MARTINEZ-PONS, C., VOSS, M., CALBO, J., COHEN, P. T., WASSERMAN, D. H., GUINOVART, J. J. & SAKAMOTO, K. 2013. Glucose-6-phosphate-mediated activation of liver glycogen synthase plays a key role in hepatic glycogen synthesis. *Diabetes*, 62, 4070-82.
- VOUTILAINEN, R. & MILLER, W. L. 1986. Developmental expression of genes for the steroidogenic enzymes P450scc (20,22-desmolase), P450c17 (17 α -hydroxylase/17,20-lyase), and P450c21 (21-hydroxylase) in the human fetus. *J Clin Endocrinol Metab*, 63, 1145-50.
- WADA, T., HORI, S., SUGIYAMA, M., FUJISAWA, E., NAKANO, T., TSUNEKI, H., NAGIRA, K., SAITO, S. & SASAOKA, T. 2010. Progesterone inhibits glucose uptake by affecting diverse steps of insulin signaling in 3T3-L1 adipocytes. *Am J Physiol Endocrinol Metab*, 298, E881-8.
- WADLEY, G. D., SIEBEL, A. L., COONEY, G. J., MCCONELL, G. K., WLODEK, M. E. & OWENS, J. A. 2008. Uteroplacental insufficiency and reducing litter size alters skeletal muscle mitochondrial biogenesis in a sex-specific manner in the adult rat. *Am J Physiol Endocrinol Metab*, 294, E861-9.
- WAHAB, R. J., SCHOLING, J. M. & GAILLARD, R. 2020. Maternal early pregnancy dietary glycemic index and load, fetal growth, and the risk of adverse birth outcomes. *Eur J Nutr*.
- WAN, M., LEAVENS, K. F., HUNTER, R. W., KOREN, S., VON WILAMOWITZ-MOELLENDORFF, A., LU, M., SATAPATI, S., CHU, Q., SAKAMOTO, K., BURGESS, S. C. & BIRNBAUM, M. J. 2013. A noncanonical, GSK3-independent pathway controls postprandial hepatic glycogen deposition. *Cell Metab*, 18, 99-105.

- WANG, H., CHEN, Y., MAO, X. & DU, M. 2019a. Maternal obesity impairs fetal mitochondriogenesis and brown adipose tissue development partially via upregulation of miR-204-5p. *Biochim Biophys Acta Mol Basis Dis*, 1865, 2706-2715.
- WANG, H., WILLERSHÄUSER, M., KARLAS, A., GORPAS, D., REBER, J., NTZIACHRISTOS, V., MAURER, S., FROMME, T., LI, Y. & KLINGENSPOR, M. 2019b. A dual Ucp1 reporter mouse model for imaging and quantitation of brown and brite fat recruitment. *Mol Metab*, 20, 14-27.
- WARNES, D. M., SEAMARK, R. F. & BALLARD, F. J. 1977. The appearance of gluconeogenesis at birth in sheep. Activation of the pathway associated with blood oxygenation. *Biochem J*, 162, 627-34.
- WATANABE, M., HOUTEN, S. M., MATAKI, C., CHRISTOFFOLETE, M. A., KIM, B. W., SATO, H., MESSADDEQ, N., HARNEY, J. W., EZAKI, O., KODAMA, T., SCHOONJANS, K., BIANCO, A. C. & AUWERX, J. 2006. Bile acids induce energy expenditure by promoting intracellular thyroid hormone activation. *Nature*, 439, 484-9.
- WATKINS, A. J., DIAS, I., TSURO, H., ALLEN, D., EMES, R. D., MORETON, J., WILSON, R., INGRAM, R. J. M. & SINCLAIR, K. D. 2018. Paternal diet programs offspring health through sperm- and seminal plasma-specific pathways in mice. *Proc Natl Acad Sci U S A*, 115, 10064-10069.
- WATSON, E. D. & CROSS, J. C. 2005. Development of structures and transport functions in the mouse placenta. *Physiology (Bethesda)*, 20, 180-93.
- WEKSBERG, R., SHUMAN, C. & BECKWITH, J. B. 2010. Beckwith–Wiedemann syndrome. *European journal of human genetics*, 18, 8-14.
- WHITE, M. F. & KAHN, C. R. 1994. The insulin signaling system. *J Biol Chem*, 269, 1-4.
- WIECZOREK, A., PERANI, C. V., NIXON, M., CONSTANCIA, M., SANDOVICI, I., ZAZARA, D. E., LEONE, G., ZHANG, M. Z., ARCK, P. C. & SOLANO, M. E. 2019. Sex-specific regulation of stress-induced fetal glucocorticoid surge by the mouse placenta. *Am J Physiol Endocrinol Metab*, 317, E109-e120.
- WILCOX, G. 2005. Insulin and insulin resistance. *Clin Biochem Rev*, 26, 19-39.
- WINTERHAGER, E. & GELLHAUS, A. 2017. Transplacental Nutrient Transport Mechanisms of Intrauterine Growth Restriction in Rodent Models and Humans. *Front Physiol*, 8, 951.
- WITHERS, D. J., BURKS, D. J., TOWERY, H. H., ALTAMURO, S. L., FLINT, C. L. & WHITE, M. F. 1999. Irs-2 coordinates Igf-1 receptor-mediated beta-cell development and peripheral insulin signalling. *Nat Genet*, 23, 32-40.
- WLODEK, M. E., WESTCOTT, K., SIEBEL, A. L., OWENS, J. A. & MORITZ, K. M. 2008. Growth restriction before or after birth reduces nephron number and increases blood pressure in male rats. *Kidney Int*, 74, 187-95.
- WOOD, C., KABAT, E. A., MURPHY, L. A. & GOLDSTEIN, I. J. 1979. Immunochemical studies of the combining sites of the two isolectins, A4 and B4, isolated from *Bandeiraea simplicifolia*. *Arch Biochem Biophys*, 198, 1-11.
- WOODGETT, J. R. 1990. Molecular cloning and expression of glycogen synthase kinase-3/factor A. *Embo j*, 9, 2431-8.
- WRIGHT, J., BARRISON, I., LEWIS, I., MACRAE, K., WATERSON, E., TOPLIS, P., GORDON, M., MORRIS, N. & MURRAY-LYON, I. 1983. Alcohol consumption, pregnancy, and low birthweight. *The Lancet*, 321, 663-665.
- WU, G., BAZER, F. W., CUDD, T. A., MEININGER, C. J. & SPENCER, T. E. 2004. Maternal nutrition and fetal development. *J Nutr*, 134, 2169-72.

- WU, Z., ROSEN, E. D., BRUN, R., HAUSER, S., ADELMANT, G., TROY, A. E., MCKEON, C., DARLINGTON, G. J. & SPIEGELMAN, B. M. 1999. Cross-regulation of C/EBP alpha and PPAR gamma controls the transcriptional pathway of adipogenesis and insulin sensitivity. *Mol Cell*, 3, 151-8.
- WULLSCHLEGER, S., LOEWITH, R. & HALL, M. N. 2006. TOR signaling in growth and metabolism. *Cell*, 124, 471-84.
- YAMAGATA, K., DAITOKU, H., SHIMAMOTO, Y., MATSUZAKI, H., HIROTA, K., ISHIDA, J. & FUKAMIZU, A. 2004. Bile acids regulate gluconeogenic gene expression via small heterodimer partner-mediated repression of hepatocyte nuclear factor 4 and Foxo1. *J Biol Chem*, 279, 23158-65.
- YAMAGUCHI, Y., TAYAMA, C., TOMIKAWA, J., AKAISHI, R., KAMURA, H., MATSUOKA, K., WAKE, N., MINAKAMI, H., KATO, K., YAMADA, T., NAKABAYASHI, K. & HATA, K. 2019. Placenta-specific epimutation at H19-DMR among common pregnancy complications: its frequency and effect on the expression patterns of H19 and IGF2. *Clin Epigenetics*, 11, 113.
- YAMASHITA, H., TAKENOSHITA, M., SAKURAI, M., BRUICK, R. K., HENZEL, W. J., SHILLINGLAW, W., ARNOT, D. & UYEDA, K. 2001. A glucose-responsive transcription factor that regulates carbohydrate metabolism in the liver. *Proc Natl Acad Sci U S A*, 98, 9116-21.
- YAMAUCHI, T., KAMON, J., WAKI, H., MURAKAMI, K., MOTOJIMA, K., KOMEDA, K., IDE, T., KUBOTA, N., TERAUCHI, Y., TOBE, K., MIKI, H., TSUCHIDA, A., AKANUMA, Y., NAGAI, R., KIMURA, S. & KADOWAKI, T. 2001. The mechanisms by which both heterozygous peroxisome proliferator-activated receptor gamma (PPARgamma) deficiency and PPARgamma agonist improve insulin resistance. *J Biol Chem*, 276, 41245-54.
- YANG, K. F., CAI, W., XU, J. L. & SHI, W. 2012. Maternal high-fat diet programs Wnt genes through histone modification in the liver of neonatal rats. *J Mol Endocrinol*, 49, 107-14.
- YANG, Q. Y., LIANG, J. F., ROGERS, C. J., ZHAO, J. X., ZHU, M. J. & DU, M. 2013. Maternal obesity induces epigenetic modifications to facilitate Zfp423 expression and enhance adipogenic differentiation in fetal mice. *Diabetes*, 62, 3727-35.
- YANG, X., SCHADT, E. E., WANG, S., WANG, H., ARNOLD, A. P., INGRAM-DRAKE, L., DRAKE, T. A. & LUSIS, A. J. 2006. Tissue-specific expression and regulation of sexually dimorphic genes in mice. *Genome Res*, 16, 995-1004.
- YOKOMIZO, H., INOBUCHI, T., SONODA, N., SAKAKI, Y., MAEDA, Y., INOUE, T., HIRATA, E., TAKEI, R., IKEDA, N., FUJII, M., FUKUDA, K., SASAKI, H. & TAKAYANAGI, R. 2014. Maternal high-fat diet induces insulin resistance and deterioration of pancreatic beta-cell function in adult offspring with sex differences in mice. *Am J Physiol Endocrinol Metab*, 306, E1163-75.
- YOSHIMATSU, M., TERASAKI, Y., SAKASHITA, N., KIYOTA, E., SATO, H., VAN DER LAAN, L. J. & TAKEYA, M. 2004. Induction of macrophage scavenger receptor MARCO in nonalcoholic steatohepatitis indicates possible involvement of endotoxin in its pathogenic process. *Int J Exp Pathol*, 85, 335-43.
- ZAVALZA-GOMEZ, A. B., ANAYA-PRADO, R., RINCON-SANCHEZ, A. R. & MORA-MARTINEZ, J. M. 2008. Adipokines and insulin resistance during pregnancy. *Diabetes Res Clin Pract*, 80, 8-15.
- ZHANG, H., NIU, B., HU, J. F., GE, S., WANG, H., LI, T., LING, J., STEELMAN, B. N., QIAN, G. & HOFFMAN, A. R. 2011a. Interruption of intrachromosomal looping by CCCTC binding factor decoy proteins abrogates genomic imprinting of human insulin-like growth factor II. *J Cell Biol*, 193, 475-87.

- ZHANG, W., PATIL, S., CHAUHAN, B., GUO, S., POWELL, D. R., LE, J., KLOTSAS, A., MATIKA, R., XIAO, X., FRANKS, R., HEIDENREICH, K. A., SAJAN, M. P., FARESE, R. V., STOLZ, D. B., TSO, P., KOO, S. H., MONTMINY, M. & UNTERMAN, T. G. 2006. FoxO1 regulates multiple metabolic pathways in the liver: effects on gluconeogenic, glycolytic, and lipogenic gene expression. *J Biol Chem*, 281, 10105-17.
- ZHANG, X., STRAKOVSKY, R., ZHOU, D., ZHANG, Y. & PAN, Y. X. 2011b. A maternal high-fat diet represses the expression of antioxidant defense genes and induces the cellular senescence pathway in the liver of male offspring rats. *J Nutr*, 141, 1254-9.
- ZHANG, Y., HU, J. F., WANG, H., CUI, J., GAO, S., HOFFMAN, A. R. & LI, W. 2017. CRISPR Cas9-guided chromatin immunoprecipitation identifies miR483 as an epigenetic modulator of IGF2 imprinting in tumors. *Oncotarget*, 8, 34177-34190.
- ZHANG, Y., ZHAO, W., XU, H., HU, M., GUO, X., JIA, W., LIU, G., LI, J., CUI, P., LAGER, S., SFERRUZZI-PERRI, A. N., LI, W., WU, X. K., HAN, Y., BRÄNNSTRÖM, M., SHAO, L. R. & BILLIG, H. 2019. Hyperandrogenism and insulin resistance-induced fetal loss: evidence for placental mitochondrial abnormalities and elevated reactive oxygen species production in pregnant rats that mimic the clinical features of polycystic ovary syndrome. *J Physiol*, 597, 3927-3950.
- ZHENG, J., XIAO, X., ZHANG, Q., YU, M., XU, J. & WANG, Z. 2014. Maternal high-fat diet modulates hepatic glucose, lipid homeostasis and gene expression in the PPAR pathway in the early life of offspring. *Int J Mol Sci*, 15, 14967-83.
- ZHENG, J., ZHANG, Q., MUL, J. D., YU, M., XU, J., QI, C., WANG, T. & XIAO, X. 2016. Maternal high-calorie diet is associated with altered hepatic microRNA expression and impaired metabolic health in offspring at weaning age. *Endocrine*, 54, 70-80.
- ZHOU, D., WANG, H., CUI, H., CHEN, H. & PAN, Y. X. 2015a. Early-life exposure to high-fat diet may predispose rats to gender-specific hepatic fat accumulation by programming Pepck expression. *J Nutr Biochem*, 26, 433-40.
- ZHOU, Y. Y., LI, Y., JIANG, W. Q. & ZHOU, L. F. 2015b. MAPK/JNK signalling: a potential autophagy regulation pathway. *Biosci Rep*, 35.
- ZHOU, Z., RIBAS, V., RAJBHANDARI, P., DREW, B. G., MOORE, T. M., FLUITT, A. H., REDDISH, B. R., WHITNEY, K. A., GEORGIA, S., VERGNES, L., REUE, K., LIESA, M., SHIRIHAI, O., VAN DER BLIEK, A. M., CHI, N. W., MAHATA, S. K., TIANO, J. P., HEWITT, S. C., TONTONOZ, P., KORACH, K. S., MAUVAIS-JARVIS, F. & HEVENER, A. L. 2018. Estrogen receptor α protects pancreatic β -cells from apoptosis by preserving mitochondrial function and suppressing endoplasmic reticulum stress. *J Biol Chem*, 293, 4735-4751.
- ZHU, H., CHEN, B., CHENG, Y., ZHOU, Y., YAN, Y. S., LUO, Q., JIANG, Y., SHENG, J. Z., DING, G. L. & HUANG, H. F. 2019. Insulin Therapy for Gestational Diabetes Mellitus Does Not Fully Protect Offspring From Diet-Induced Metabolic Disorders. *Diabetes*, 68, 696-708.